SHRP-C/FR-91-103

High Performance Concretes

A State-of-the-Art Report

Strategic Highway Research Program
National Research Council

Strategic Highway Research Program Executive Committee

SHRP-C/FR-91-103

High Performance Concretes

A State-of-the-Art Report

Paul Zia
Michael L. Leming
Shuaib H. Ahmad

North Carolina State University
Raleigh, NC

Strategic Highway Research Program
National Research Council
Washington, D.C. 1991

SHRP-C/FR-91-103
Contract C-205

January 1991

key words:
creep
durability
early strength
fiber reinforced concrete
fatigue
high early strength
high performance concrete
high strength
mechanical behavior
mechanical properties
mix proportioning
pavement
shrinkage
very early strength
very high strength

Strategic Highway Research Program
2101 Constitution Avenue, N.W.
Washington, D.C. 20418

(202) 334-3774

TO

Robert E. Philleo

Acknowledgments

The research described herein was supported by the Strategic Highway Research Program (SHRP). SHRP is a unit of the National Research Council that was authorized by section 128 of the Surface Transportation and Uniform Relocation Assistance Act of 1987.

The preparation of this report is a joint effort of the research team engaged in the investigation of the mechanical behavior of high performance concretes under contract C-205 with SHRP. The team includes the three authors at North Carolina State University, A. E. Naaman and M. H. Harajli at the University of Michigan, and Robert P. Elliott and John J. Schemmel at the University of Arkansas.

Chapter 4 was written initially by Naaman and Harajli whose research focus is on fiber-reinforced concrete. It is an abbreviated version of a separate state-of-the-art report on fiber-reinforced concrete prepared by them as a working document of the project. Likewise, the initial draft of Chapter 5 was prepared by Elliott and Schemmel whose research focus is on pavement applications. Both contributions were integrated into this report with revisions and editing performed by the authors who should be held accountable for any errors and omissions.

During the past year, the late Robert E. Philleo served as project consultant. The research team benefitted greatly from his many stimulating discussions and guidance for which the team is forever grateful.

The authors would also like to thank Andrea Hardison, Juliet Leigh, and Rakesh Garg who helped type and edit the report.

Comments and inquiries regarding this publication should be directed to:

Inam Jawed
Manager, Concrete Program
Strategic Highway Research Program
818 Connecticut Ave., NW
Suite 400
Washington, DC 20006
(202) 334-3774

Contents

Abstract

This state-of-the-art report summarizes the results of an extensive search and review of available literature on mechanical properties of concrete, with particular reference to high performance concrete for highway applications. For the purpose of this report, high performance concrete is defined in terms of minimum requirements for both strength and durability.

Included in the review and discussion are the behavior of plastic concrete as well as the strength and deformation characteristics of hardened concrete. Both short-term and long-term effects are considered.

Based on the review of the available information, research needs are identified. It is concluded that much research is needed to develop data on the strength and durability properties of concrete which develops high strength, particularly very early strength.

Executive Summary

This state-of-the-art report is the first interim report of SHRP Contract C-205 which is concerned with investigating the mechanical behavior of high performance concrete. The principal focus of the research is on high performance concrete for highway applications.

There is no unique definition of high performance concrete. It can be defined only with reference to the performance requirements of the intended use of the concrete. In highway construction projects, speed of construction and safety are of the utmost importance. Rapid repair and construction will minimize traffic interruptions and reduce safety hazards, both resulting in overall long-term economic benefits. Improved durability can also contribute to a reduction in long-term life costs. For the purpose of this study, high performance concrete is defined by the following three requirements:

(1) A maximum W/C ratio of 0.35
(2) A minimum durability factor of 80% as determined by ASTM C 666, Method A, (AASHTO T161, Method A)
(3) A minimum strength criteria of either
  (a) 3,000 psi (21 MPa) within 4 hours after placement
    - Very Early Strength (VES), or
  (b) 5,000 psi (34 MPa) within 24 hours
    - High Early Strength (HES), or
  (c) 10,000 psi (69 MPa) within 28 days
    - Very High Strength (VHS)

From the above definition, it is clear that one should not confuse high performance with high strength. There are many aspects of performance other than high strength that often may be more important in a given application.

One of the first objectives of this research was to conduct an extensive literature search and review so that current knowledge about the mechanical properties of high performance

concrete could be summarized and significant gaps in knowledge identified. As a result of the literature search, an annotated bibliography containing 830 references published in the period of 1974-1989 has been compiled and published as a reference document. From this reference source, about 150 references were selected for critical review. The results of the review are summarized in this state-of-the-art report.

Included in this report are discussions regarding selection of raw materials and manufacture of high performance concrete, behavior of hardened concrete, behavior of fiber reinforced concrete, and applications of high performance concrete. Based on the results of the literature review, several major observations can be made as follows:

It is crucial that criteria for the selection of raw materials for the manufacture of high performance concrete are carefully established. In general, there are more varieties of materials available for VHS concrete production, but in terms of cementitious materials and admixtures, only limited choices for VES and HES concretes are possible.

More information is needed on all aspects of short-term and long-term mechanical properties of VES concrete. These include modulus of elasticity, strength and strain capacity, creep, shrinkage, and fatigue.

Much is already known about the various mechanical properties of concrete with a strength range comparable to that of HES concrete. However, most of the existing data are based on tests at 28 days. Since HES concrete achieves its expected strength in only 24 hours, there is a need to confirm the mechanical properties of HES with the existing data.

For VHS concrete, more information on its mechanical properties at 28 days is needed since most of the existing data are based on tests conducted at older ages such as 56 or 90 days. In addition, data on durability, fatigue, and brittleness of VHS concrete is needed.

With respect to fiber reinforced concrete, there is ample information on the mechanical properties under short-time loading except for thermal expansion and Poisson's ratio after cracking. However, more research is needed for different aspects of long-term effects.

In pavement applications, steel fibers have been used almost exclusively. Use of other types of fibers is practically nonexistent. Mixed fibers such as a combination of steel and polypropylene fibers may enhance both strength and ductility of concrete. Virtually no research has been conducted in this area.

There is little evidence that high performance concrete is used in current pavement applications. However, for such applications, one can anticipate significant potential benefit. The use of VES and HES concretes will permit rapid repair and construction of pavements so that the interruption of traffic can be minimized, while at the same time providing adequate long-term performance at a reasonable cost.

Most rigid pavement design methods rely heavily on empirically developed relationships. The data on which these empirical formulas were based do not include any of the high performance concretes. Therefore, research data on durability, shrinkage, thermal properties, fatigue, and long-term strength gain of the high performance concrete are critically needed. Field trials will also be required to establish their performance record.

1

Introduction

1.1 General

"High performance concrete" (HPC) may be broadly defined as any concrete which satisfies the criteria proposed to overcome limitations of conventional concretes. This includes concrete which provides either substantially improved resistance to environmental influences (durability in service) or substantially increased structural capacity while maintaining adequate durability. An additional definition would be any concrete which significantly reduces construction time to permit rapid opening or reopening of roads to traffic, without compromising long-term serviceability.

Regardless of interpretation, high performance concretes are typified by low water-cementitious materials ratios (W/C), low permeability, high early strengths and, frequently, high ultimate strengths. They are generally higher in initial cost but should be more economical in life cycle cost. Relatively little information is available on the behavior of high performance concretes which are appropriate to paving or bridge construction, where frequently high salt or frost durability is required.

1.2 Purpose

This report is intended to summarize what is currently known about the mechanical properties of high performance concretes, and identify gaps in knowledge which are critical to understanding the behavior of high performance concrete. Based on the findings of this report, plans for additional research will be developed.

1.3 Background

1.3.1 Historical Perspective

By the mid-1950s, many of the major problems with the use of concrete in pavements and bridge structures were thought to have been identified. Construction procedures, design guidelines and mix proportion criteria were developed and seemed to provide a consistent, useful product of acceptable durability.

The ingredients in concrete were usually limited to cement, sand, stone, water and air. The use of an admixture, other than air entraining agents, was rare. Aggregates of acceptable quality were generally in adequate supply.

Structural design procedures and criteria for reinforced concrete and concrete pavements were beginning to change significantly, however. Design was becoming more rational and more complex. Even so, compressive strength of concrete did not typically exceed 4,000 psi (28 MPa) other than for prestressed concrete.

The mechanical properties of concrete were generally estimated from the compressive strength of 6 x 12 in. (150 x 300 mm) cylinders tested after moist curing for 28 days. The mechanical behavior of a structural component was analyzed using empirical relations which were based on concretes of relatively low strength.

Structural and durability requirements were rarely linked in an explicit form, except to note that the reduction in W/C ratio necessary for higher strengths also improved durability under most service conditions. Requirements for these two factors were generally determined independently.

Determination of durability requirements of concrete in a specific application was relatively straightforward. Decisions regarding selection of air contents, maximum W/C ratios and cement types, for example, were rule based; the desired attributes could be selected from a list or table coupled with prescriptions for mix proportions which were based on anticipated service conditions. Compared with what must be considered today, relatively few options existed in the mix proportioning process. Relationships among many of the concrete properties were rarely completely understood.

With time, more fundamental research into concrete response to both structural loads and environmental influences has brought about a greatly improved, though still incomplete, understanding of concrete behavior.

Mineral admixtures have become more widely available, as improvements in quality and manufacturing control have occurred. Use of mineral admixtures has become routine in many locations.

Class F fly ash has a long history of successful applications especially where sulfate durability and alkali-aggregate durability are concerned. Class C fly ashes frequently contribute to an earlier strength gain than Class F fly ashes. Ground granulated blast furnace slag (GGBFS) may be intermediate in strength gain. Durability of concretes containing GGBFS or Class C fly ash subjected to certain types of chemical attack, may be reduced, particularly when compared with Class F fly ash. Prediction of long term concrete properties has become more complex.

Use of chemical admixtures, particularly the use of water reducers and high-range water reducers (superplasticizers), has also increased significantly. These admixtures permit the practical use of concrete with low or very low water contents and water-cement ratios. The use of chemical admixtures that provide set acceleration without promoting corrosion or that inhibit corrosion has become more common in practice.

1.3.2 Concrete in Transportation

Concrete may be used in a pavement or overlay (both fast-track or conventional construction), or in a bridge (superstructure or substructure). The mechanical properties which must be considered in either application are somewhat different.

Complex stresses in pavements are created by temperature or moisture-induced volumetric changes, with restraint provided by a subgrade or base course of substantially different modulus; by volume change of the subgrade or base course itself; by continuity of the subgrade support; and by externally applied loads.

Time dependent factors such as creep and shrinkage will also influence volumetric changes while repeated traffic loadings (fatigue) will change the effective stiffness of the pavement. When dowels or reinforcement are used, steel bond, corrosion and stresses associated with the presence of the reinforcement must also be considered. These effects on pavement performance are related to the mechanical properties of the concrete and also influence effective service life.

Concrete durability in a pavement is a function of the permeability and chemical stability of both the cement paste and the aggregate, the wear resistance, and the crack resistance of the concrete. The crack resistance is related to the chemical stability of both the paste and the aggregate, the strength properties and dimensional stability of the concrete, and the freeze-thaw resistance. It is also related to moisture and temperature values and gradients in the pavement. For bridge decks, concrete strengths may be higher than required for structural purposes in order to attain desired durability through low W/C ratio specifications.

Bridge substructures are frequently subjected to abrasion by water and debris, to attack by salts in groundwater, deicing chemicals or seawater, and to other effects common to all exposed concrete elements. Concrete superstructures frequently suffer from a high exposure to deicer salts and marine sea spray, more extreme temperature gradients (pavements may have temperature gradients of up to 3^0F per inch or 0.7^0C per cm, while a bridge deck may exceed 5^0F per inch or 1^0C per cm), a greater tendency to saturation, and higher concentrated stresses.

1.3.3 High Strength Concrete

High strength concrete (commonly defined as having a 28-day 6 x 12 in. or 150 x 300 mm cylinder strength of at least 6,000 psi or 42 MPa) has become commercially available in many locations. Since high strength concrete does not behave precisely like conventional strength concrete, the prediction of long-term performance has been somewhat complicated.

Little, if any high strength concrete has been used as such in pavements, although low W/C ratio concretes are fairly common. Fast-track paving applications have used high early strength concrete, which may have many of the same long-term properties as high strength concrete.

ACI Committee 363, State-of-the-Art-Report [1.1] offers many suggestions and guidelines for the use of high strength concrete for structural applications. This report and one entitled "Research Need for High Strength Concrete", also by ACI Committee 363 [1.2], explicitly mention many of the gaps which exist in the technology. Significant among these are the response to fatigue loads, determination of the complete stress strain curve, and strain capacity. The relationships of strength and permeability to freeze-thaw durability and entrained air contents of high strength concretes have not been clearly established.

A survey of the pertinent literature addressing the characteristics of high performance concrete indicate that while there has been a significant amount of research conducted, the research is spotty and lacks coherence. There are many gaps in the body of knowledge.

1.4 Definition of High Performance Concrete

It is not possible to provide a unique definition of high performance concrete. To define such a term, one must consider the performance requirements of the intended use of the concrete. For concrete used in pavement and bridge projects, both strength and durability criteria must be established. The following definitions have been developed for the purpose of this report.

1.4.1 Strength Criteria

Considering the essential performance of pavements and bridges, one may designate three categories of high performance concrete on the basis of strength.

1.4.1.1 Very Early Strength

Very Early Strength (VES) concrete will have a compressive strength of at least 3,000 psi (21 MPa) within 4 hours after placement. No curing of the concrete is expected after the first 4 hours although continued curing would be beneficial. This type of concrete would be most likely used in a full-depth pavement patch or possibly in a small-size overlay. Its potential use in structural applications is limited except for precast members.

This material would be used primarily in situations where early opening or reopening of the pavement to traffic is critical and unit costs of the material are relatively less important. Placement by hand is a likely construction method, although placement by machine is possible. When longer curing periods are available, it is unlikely that this type of material would be used for new pavement due to cost.

1.4.1.2 High Early Strength

High Early Strength (HES) concrete will have a compressive strength of at least 5,000 psi (34 MPa) within 24 hours. This type of concrete would have potential applications in many aspects of transportation construction. It could be used in new paving, although its most likely applications would be in full-depth pavement or in overlays where reopening the pavement to traffic would be important, but the time constraint is not as critical as those situations requiring VES concrete. HES concrete may also be considered in structural applications where accelerated construction schedules are needed.

This type of concrete, when used in a pavement, would be placed by machine and receive little or no curing after 24 hours. It would be expected to provide very-long term serviceability.

1.4.1.3 Very High Strength

Very High Strength (VHS) concrete will have a compressive strength of 10,000 psi (69 MPa) at 28 days. This concrete would have primary applications in bridge construction where time for long-term curing is available and structural efficiency is at a premium.

1.4.2 Durability Criteria

Durability cannot be sacrificed to attain high strength. Although high ultimate strength is generally accompanied by a low W/C ratio, this is not, in itself, adequate to satisfy all durability-related requirements. All types of high performance concrete used in paving applications must provide acceptable frost resistance, sufficient fatigue life and adequate serviceability.

There are, however, problems insuring adequate durability. Many important concrete durability characteristics cannot be conveniently quantified. Acceptance testing methodology and criteria for high performance concrete are not universally established in all cases, and can be extremely time consuming. Specifications are not explicitly interrelated, and in many cases the concrete is simply considered either "durable" or "nondurable".

For example, evaluation of frost durability of concrete with very low W/C ratios, based on results from the current freeze-thaw test procedure may not be valid [1.4]. Specifications for aggregate may classify the material as acceptable or not acceptable. Certain aspects of durability which depend on chemical stability, such as durability related to marine environments, salt or brackish water and deicing salts, sulfates, corrosion protection, chloride permeability, carbonation, and other aggressive agents may take long periods of testing to determine response.

Therefore, additional requirements in our definition of high performance concrete are necessary. As a minimum, standard requirements for durability will be required for all high performance concretes based on portland cement. In the absence of appropriate standards, as with some blended cements, a demonstrated level of acceptable durability will be required.

1.4.2.1 Freeze-Thaw Durability

Freeze-thaw requirements for high performance concrete to be used in transportation structures must necessarily be more stringent than those generally required for standard commercial concrete. For that reason a minimum freeze-thaw durability factor of 80%, as measured by AASHTO T 161 (Method A), will be required.

1.4.2.1 Water to Cementitious Material Ratio

Concrete with a W/C ratio of 0.35 will produce a discontinuous capillary system in about a day of moist curing, which will provide improved durability to chemical attack, freeze-thaw cycling and wetting and drying. Therefore, all high performance concrete will have a maximum W/C ratio of 0.35.

1.4.3 Definition Summary

In summary, High Performance Concrete may be defined as concrete with

(1) a maximum W/C ratio of 0.35,

(2) a minimum Durability Factor of 80%, as determined by ASTM C 666, Method A,

and

(3) a minimum strength criteria of either

(a) 3000 psi (21 MPa) within 4 hours after placement (VES),
(b) 5000 psi (34 MPa) within 24 hours (HES),
(c) 10,000 psi (69 MPa) within 28 days (VHS).

1.4.4 Other Considerations and Requirements

1.4.4.1 Fiber Reinforced Concrete

Concrete is inherently a brittle material with little toughness, as measured by the area under the stress-strain curve. Reinforcement is necessary to provide ductility after cracking. Fiber reinforcement incorporated in the plastic concrete will typically increase the flexural and tensile strength of plain concrete although there is little substantial increase in compressive strength.

Fiber reinforcement concrete (FRC) has been used in paving applications to increase the flexural capacity of the concrete. Steel fibers have been the primary type of fiber used in practice, although carbon fibers and polypropylene fibers have also been investigated.

The primary use of FRC in transportation has been in airport pavements, rather than highways. The high impact of takeoffs and landings and high point loads make FRC pavements a viable alternative for airports. The extra cost in materials and the substantially higher handling costs of FRC have not proven to be economically justifiable under most, if not all circumstances, in highways, which have lower point loads, less impact loading, a higher number of load applications and less channelized traffic flow.

The minimum desirable ductility or fracture toughness of FRC concrete using steel fibers has been established as five times the area under the stress-strain curve compared to the same concrete without reinforcement. This is frequently referred to as the I_5 criteria. For fiber reinforced, high performance concrete, the definitions given in section 1.4 must be amended so that VES FRC, HES FRC or VHS FRC additionally meet the I_5 criteria.

1.4.4.2 Abrasion Resistance

Abrasion resistance refers to the ability of a concrete surface to resist wear due to the abrasive action of tires. Adequate abrasion resistance is important for pavements and bridge decks from the standpoint of safety. Excessive abrasion leads to an increase in accidents as the pavement becomes polished, reducing its skid resistance.

No generally accepted criteria for evaluating the abrasion resistance of conventional concrete pavements exists. The lack of an abrasion resistance criterion is probably due to the fact that surface wear is normally not a controlling factor in pavement performance. If the surface is provided an adequate texture depth during construction, other problems require treatment before surface wear becomes a problem. An exception to this is in areas that permit the use of studded tires. See Chapter 3 for additional information concerning abrasion resistance.

1.5 Exclusions

This report excludes detailed examination of the properties of several types of materials. These exclusions are based on several considerations, including cost effectiveness and status of technology.

1.5.1 Cost-Related Exclusions

Even with limited data, it is appropriate to exclude many materials from further consideration since they are unlikely to produce significant improvement in performance on a cost-effective basis.

1.5.1.1 Extremely High Strength Concrete

Even though it is possible to attain concrete compressive strengths much higher than 10,000 psi (69 MPa) (although the use of entrained air may place a practical limit at about this level), exceptionally high strength concretes such as those with compressive strengths greater than 20,000 psi (138 MPa), are excluded from consideration at this point. Such concretes can be produced only from select raw materials and at a high premium. It is difficult at this time to justify economically the use of such materials in most transportation structures.

1.5.1.2 Rapid Setting Patching Compounds

Patching compounds, particularly materials based on magnesium oxide or other similar materials, will not be examined in this report. These types of materials are specifically intended for use in small patches. Their high unit cost, extremely rapid set and rapid heat evolution make them poorly suited for large-scale applications.

1.5.2 Technology-Related Exclusions

There are technologies and materials which may appear promising for applications in the transportation field, but are excluded from further consideration since it is the intent of this report to examine high performance concretes as defined above without relying excessively on exotic materials and or processes.

1.5.2.1 Roller Compacted Concrete

Roller compacted concrete is a promising material/construction technology. However, it is sufficiently different from the high performance concretes defined above to be excluded from this report.

1.5.2.2 Fast-Track Paving

Fast track paving is primarily a construction technique, utilizing warm concrete, heated or insulated curing, Type I or Type III cement, and, at least some of the time, calcium chloride. It may not be a high performance concrete material although high performance concrete could be used to advantage. Additionally, calcium chloride is known to contribute to reductions in freeze-thaw durability, reductions in sulfate durability and an increased corrosion potential of the reinforcement. Fast-track paving, per se, is therefore outside the scope of this report, although many of the aspects of high performance concrete may be utilized in fast-track paving operations.

1.5.2.3 Lightweight Concrete

Lightweight concretes, produced from expanded clay, shale or slate aggregates, offer reductions of 20% to 25% in weight over conventional concretes at the same strength. Some of these aggregates can be used to produce concrete with strengths in excess of 10,000 psi (69 MPa). The cost of lightweight concrete is higher than that of normal weight concrete, creep and shrinkage are higher, and elastic modulus is lower.

There are no proven advantages to the use of lightweight concrete in paving applications. There are many potential applications for bridge members where dead load is a sizeable portion of the total load. However, the properties of lightweight concrete are so strongly influenced by the specific type and brand of aggregate used that it is appropriate to exclude lightweight concrete from further consideration in this report.

1.5.2.4 Sulfur Concrete

Sulfur concrete is a specialty concrete suitable for industrial slab applications where acid and salt attack are severe. It is not suitable to the applications being considered here, due to, among other things, reported difficulties in obtaining high freeze-thaw durability factors [1.3]. Therefore, sulfur concrete is not examined in this report.

1.5.2.5 High Alumina Cement

High alumina cement based concretes are not considered because of the conversion of the hydrated aluminate compounds that occur over time, resulting in dramatic increases in porosity and permeability and significant strength loss.

1.5.2.6 Polymer Concretes

Polymer concretes, especially epoxy concretes, are excluded from this report. They are inappropriate for large-scale, full-depth patches, new paving construction and major structural components. In addition, they are extremely expensive.

1.5.2.7 Polymer Impregnated Concretes

Polymer impregnated concretes are also excluded from consideration in this report since this is a construction or repair method. Additionally, this technique has not proven entirely reliable in all cases.

1.5.2.8 Sealed Concrete

The use of external sealers, in addition to polymer impregnation, is not reviewed in this report. While these materials may improve concrete performance, they are not required for high performance, as defined above, and do not necessarily produce a high performance concrete.

Internally sealed concrete, using wax beads or other integrally mixed chemical compounds (such as calcium stearate), cannot be considered as high performance concrete. Heating of the concrete is required when using wax beads mixed with the plastic concrete. The liquid wax flows into capillaries and substantially reduces permeability. However, excessive cracking from the heat makes this process impractical in the field. Integral waterproofing type compounds are not suited for high scour or frequent wetting and drying environments.

1.5.3 Related Research

Other research conducted for the Strategic Highway Research Program, although it may have a decided impact on the mechanical properties of high performance concrete, will not, in general, be discussed here. Reports from other contracts may be expected on several subject areas, including microstructure, sulfate durability, alkali-aggregate durability, corrosion of steel, and freeze-thaw durability of concrete.

1.6 Economic Factors

Initial costs of high performance concrete will be higher than that of commodity grade concrete. Raw materials costs, quality assurance and quality control costs, supplier profit margins and risk, and handling costs will all be moderately or substantially higher with high performance concretes. Project cost differences resulting from changes in design criteria, substantially improved life cycle costs and, in particular, reduction of costs related to traffic delays, must offset these higher material and construction costs. Since only moderate cost differences at best are likely due to changes in design of pavements or bridges, much of the cost offset must come in the form of improved durability and extended service life or in reduction of traffic delays and slowdowns.

1.6.1 Cost of Materials and Construction

Cost of materials per cubic yard will be higher for high performance concrete than for commodity grade concrete due to higher cement and admixture contents. The delivered or bid price per unit volume of high performance concrete may also increase as risk (both real and perceived) and costs of other factors increase, such as quality control and management and supervision of the contractor and concrete supplier.

Constructibility considerations will effect the bid price of high performance concrete. For HES concretes based on Type III cement and an accelerator, job site addition of one or more chemical admixtures will create extra costs in terms of supervision and time. VES and HES concretes will be more sensitive to delays in placing.

Contract costs will also increase. Funding agencies should anticipate more involvement and therefore higher management costs in these projects. Contract prices will therefore increase faster than the cost of materials alone.

1.6.2 Cost Offsets

Substantial improvements in durability, which lead to reduced life cycle costs through increased useful life and reduced maintenance, can offset initial construction costs somewhat. Savings due to reduced pavement downtime and traffic rerouting during construction or maintenance operations can be substantial. The difference in initial cost may be insignificant compared to reductions in traffic-related costs.

Cost trade-offs must be determined on a project-by-project basis, based on the time and budget constraints of the funding agency, the urgency of the construction, and a thorough knowledge and understanding of the mechanical properties of any proposed concretes. That knowledge and understanding is not currently available. This state-of-the-art Report is intended to address many of the problems and concerns of using high performance concrete in pavements and bridges, and will establish a starting point for continued research in this area.

2

Materials and Manufacture of High Performance Concrete

The quality of high performance concrete is, like all concretes, ultimately limited by the quality of the raw materials used, the level of quality management exercised in production, and the care maintained in handling and curing.

An excellent discussion of raw materials and methods of production suitable for high strength concrete may be found in ACI Committee 363 State-of-the-Art Report on High Strength Concrete [2.6]. The same criteria will, in many cases, also apply to high performance concrete used in pavements and bridges.

Discussion in this section will concentrate on the concretes defined in section 1.4.1 and those materials and handling or production methods distinctive to them.

2.1 Raw Materials

2.1.1 Cements

The cements used in high performance concrete must minimally be any of the portland cements which meet the requirements of ASTM C 150 or AASHTO M 85, or any of the blended cements meeting the requirements of ASTM C 595 or AASHTO M 240, appropriately selected for sulfate exposure, high early strength requirements or other service conditions. More stringent requirements may be imposed concerning variability (ASTM C 911) or durability-related issues such as alkali limits (optional specifications).

Many Type I or Type II portland cements and many blended cements may be successfully used, in combination with both mineral and chemical admixtures, to produce Very High Strength (VHS) concretes. The strength level of the cements used in VHS concretes should be higher than the minimums required by standard specifications.

High Early Strength (HES) concretes may be obtained with either specialty cements or Type III portland cement. Even when using Type III cement, the use of an accelerator will generally be required to attain the strength levels of HES concretes at 24 hours, in the absence of applied heat and without using excessive cement.

Both HES and VHS types of high performance concrete can have sizeable heat evolution due to the high cement content and the rapid reactions occurring. In situations where the mass effect of the concrete may be important, such as large or thick structural components, a Type II, moderate heat of hydration portland cement, or LH (low heat) or MH (moderate heat) blended cement may be useful. It may be difficult or impossible to attain HES levels with those cements, however.

It is generally desirable to use the minimum cement quantity necessary to attain the required levels of concrete performance. This is done for economic reasons in order to limit the heat of hydration of rich mixes and to keep shrinkage and shrinkage-induced cracking to a minimum.

There is an optimum cement content, for ultimate strength, for any given set of raw materials. The addition of portland cement above a certain amount will result in additional water demand, and a lower ultimate strength. This optimum may be extended with the use of mineral or chemical admixtures. However, practical maximum cement contents exist for any given set of raw materials and may be determined by trial batch testing.

Compressive strength requirements of the Very Early Strength (VES) concretes will be possible, in conventional practice, only with specialty cements. As noted in Chapter 1, cements which are commonly used as patching materials will not be considered in this report. Such materials have unit cost or heat evolution characteristics which make them unsuitable for use in large-scale applications. Two other specialty cements may be investigated.

Regulated set cements are capable of producing very early strengths. There is generally a trade-off between the set time and the ultimate strength attained. The set time must typically be kept very short in order to attain the very early strength levels desired. Further, there are durability concerns which may affect the use of these cements. Most regulated cements are susceptible to sulfate attack, due to high calcium aluminate contents. The manufacturer of at least one regulated set cement has claimed to have overcome this limitation by the use of a pozzolanic additive.

Another type of blended cement, Pyrament, has been reported to have both excellent early strength and ultimate strength with low permeability, as well as excellent resistance to deicer scaling and excellent frost durability. Three types of this material are available. One is a patching material with extremely rapid set times and the other two are materials developed for ready mixed types of application, with longer working times.

Typical properties of this material, as reported by the manufacturer, for a W/C ratio of 0.27, include a 1-day strength of almost 4,500 psi (31 MPa), a 28-day compressive strength of just over 9,200 psi (63 MPa), and a relative dynamic modulus of 114% after more than 300 cycles of freezing and thawing begun at 1 day, without the use of an air-entraining agent [2.15].

This material is designed to work without additional admixtures. Even at W/C ratios less than 0.30, high slumps have been obtained. The use of additional admixtures will give unpredictable results. Performance of Pyrament-based mixes is therefore somewhat more sensitive to the properties and water demand of the aggregates than portland cement-based mixes, in which admixtures can be used to mitigate these effects.

Two problems have been noted by the manufacturer with this material. Although it has excellent strength gain even in cold weather, the materials should be mixed warm to prevent excessively rapid set in the faster setting compositions. The material also has a high alkaline content which might render it unsuitable for use with alkali-sensitive aggregates.

In addition to its ability to provide very rapid strength gain, concretes made with Pyrament for VES applications can also be used to meet the requirements for HES and VHS concretes.

2.1.2 Chemical Admixtures

Chemical admixtures may be used to modify the setting characteristics of concrete, the water required for a given workability, or the corrosion potential of the reinforcing steel. Air-entraining agents may be used to provide an air-void system capable of providing frost-resistant concrete. Some admixtures may perform more than one function at the same time.

A more complete discussion of chemical admixtures may be found in ACI Committee 212 report entitled Chemical Admixtures for Concrete [2.1]. The following discussion concentrates on the use of chemical admixtures in high performance concretes.

2.1.2.1 Entrained Air

Entrained air improves frost resistance of concrete in different degrees depending on the bubble size, bubble spacing and concrete permeability. Environmental conditions, particularly moisture condition at time of freezing, number of freeze-thaw cycles, rate of freezing and thawing, presence of salts, and salt gradients, also play a key role in the rate of deterioration of the concrete.

Resistance to freezing and thawing is also a function of the pore sizes and pore size distribution. The air-void system considered optimal for commodity grade concrete may not be needed for low permeability concrete. Osmotic and pore solution gradients can still exert damaging pressures, even without the formation of ice, however. At W/C ratios below about 0.35, the pores will become discontinuous at very early ages (typically about 1 day under standard conditions) and the average size will therefore be reduced substantially. At these W/C ratios, the freezing point of water in the pores, which is depressed as pore size is reduced, may drop below practical minimums. The effects of solution gradients may also be altered with a noncontinuous pore system.

Frost susceptibility is determined in laboratory testing by reduction in the dynamic modulus of the concrete under controlled freezing conditions. A 40% reduction in dynamic modulus (60% durability factor) is considered failing. If failure occurs prior to 300 cycles of either freezing and thawing in water (the more severe method), or freezing in air and thawing in water, the concrete is not considered durable; otherwise the concrete is considered acceptably frost resistant.

Test results are only generally correlated with frost resistance in the field due to the wide variety of actual in-service environmental conditions and the severity of the freeze-thaw test itself. The rate of freezing in the standard test method is extremely, and generally unrealistically, high. For very low W/C ratio concretes with discontinuous pore systems, the test may be unduly prejudicial [2.34]. The standard test method does provide a means of identifying sound materials which will perform well in the field.

A high performance concrete has been previously defined as one with a durability factor of not less than 80%. At this time, some quantity of entrained air is required for portland cement-based concretes, at least for those with compressive strength not appreciably exceeding 10,000 psi (69 MPa), to provide acceptable frost resistance, using currently accepted test methodologies and constraints.

2.1.2.2 Set modifiers

Chemical admixtures may be used to modify the setting characteristics of concrete. Accelerators may be used in cool weather to speed up the setting process and retarders may be used in hot weather to prevent excessively rapid set. Many commercially available retarders also provide some water-reducing capability and provide an increase in strength at all ages.

A common accelerator for many years has been calcium chloride. This material provides not only decreased setting time, but an increase in strength at virtually all ages. Calcium chloride is an efficient and relatively inexpensive accelerating admixture. However, it is severely limited in many applications where the concrete will be saturated in service while subjected to freezing and thawing, deicing salts, sulfates, or when the concrete contains reinforcing steel.

The use of nonchloride accelerators has become more prevalent as it has become more common to limit the use of calcium chloride. Some nonchloride accelerators have suffered problems with erratic set times and efficiencies.

Accelerators based on calcium nitrite and calcium nitrate have proven generally effective although they are substantially more expensive than calcium chloride and may not provide the same level of efficiency. Other nonchloride accelerators are available, and all should be tested prior to use to determine suitability.

Additional portland cement can also result in decreased setting time and increased strength at all ages. Cement contents are typically already very high in high performance concretes, and the use of additional cement may not be acceptable from the standpoint of heat of hydration or water demand.

High performance concretes will frequently require the use of a retarding admixture to control rapid stiffening in even moderate temperatures, due to high cement contents. Retarding admixtures must be used with care in early strength mixes. Excessive retardation in setting time will cause strength development to be delayed and early strength (one day or less) targets may not be attained, although later strengths will typically be enhanced and ultimate strength almost certainly so.

A retarded, high-cement content mix may also be more susceptible to plastic shrinkage cracking. Bleeding is reduced for high-cement content mixes and, if retarded, there is more time available for plastic shrinkage cracking to develop. A concrete which sets and gains strength rapidly will be less susceptible to plastic shrinkage cracking.

2.1.2.3 Water-Reducing Admixtures and High-Range Water Reducers

Water-reducing admixtures (WRA) and high-range water reducers (HRWR, or superplasticizers) are chemical admixtures which provide increased workability for concretes without increasing the water content. High-range water-reducing admixtures will generally be required for all low W/C ratio concrete based on portland cement. HRWR's may be used either alone or in combination with water reducing admixtures.

Many water reducing or high range water-reducing admixtures, even those which are nominally nonretarding, contribute to increased setting times. If used in very high dosages, very early strengths can be reduced.

For large surfaces requiring a hard trowel finish, the use of a HRWR, especially with a retarding admixture, an air entraining admixture or both, may lead to problems in timing of finishing operations and satisfactory surface characteristics of the hardened concrete. This is not a problem with pavements however, since a smooth, troweled surface is undesirable.

The durability of any concrete containing a HRWR subjected to freezing and thawing has been questioned. Bubble size seems to be increased in mixes with a HRWR, so at equal total air contents, air-void spacing may exceed that recommended for good frost resistance. Some of these concretes have shown acceptable freeze-thaw resistance in laboratory testing, however, while some have not.

Very low porosity concretes may not require the same air-void system as conventional strength concrete for acceptable frost resistance (see section 2.1.2.1, Entrained Air). Pore size is reduced and the water in the pores cannot freeze at service temperatures. The permeability is reduced so the time to critical saturation will certainly be longer and the member may, in fact, never reach critical saturation in service. Unrealistically high rates of freezing during tests may unfairly penalize low permeability concretes. The effect of loading induced microcracking on frost resistance has not been established. Preliminary results of ongoing research by Hoover at Cornell (private communication) suggests that permeability is increased when concrete is subjected to compressive stress in excess of 50% of ultimate strength.

Field data for concrete with low W/C ratios, minimal air contents and high-range water reducers is limited except for some precast, prestressed members. There is no evidence which suggests that these members are not durable with respect to freezing and thawing in service, although few, if any, may be critically saturated prior to freezing.

Mixes which contain HRWRs are prone to rapid slump loss. In many situations, this requires the addition of the HRWR at the job site or the use of a retarding admixture in conjunction with the HRWR. Additional dosages of HRWR may be required if the rate of placement is not fast enough. The effect of redosing on entrained air content, however, can vary dramatically with different raw materials and mixes. In one study [2.40], using one particular HRWR with concretes ranging from about 4,000 psi (28 MPa) to over 6,000 psi (42 MPa), Smutzer and Zander found that redosing a mix already containing HRWR was detrimental to the air-void system and resulted in a significant reduction in durability as determined by ASTM C 666, Method B (freezing in air and thawing in water).

Redosing presents other additional quality control and management problems. Delayed addition will have an effect on admixture efficiency and setting characteristics. Because it is difficult to precisely determine quantities remaining in the truck, actual dosage rates may vary considerably. The chances of an accidental misdose of the admixture are increased. Due to the rapid slump loss, the effects of a minor overdose on slump can frequently be overcome simply by additional time in the truck at agitate speed, if all other characteristics remain acceptable and there is no appreciable segregation or excessive bleeding. In large-scale paving applications, a second redosing of HRWR will generally not be required due to the rate of placement.

2.1.2.4 Corrosion Inhibitors

The most common commercially available corrosion inhibitor is probably calcium nitrite. This material has been reported to increase the corrosion resistance of steel in the presence of chloride ions [2.22].

The high pH of concrete pore solution will normally prevent corrosion of the reinforcing steel, even in moist concrete, by creating a stable, passivated layer which protects the steel from continued oxidation. However, the presence of chloride ions will increase the pH necessary to provide passivation of the steel to levels which cannot be practically attained in portland cement concrete. The calcium nitrite is reported to provide the passivation needed to keep the steel from actively corroding even in the presence of chloride ions [2.22, 2.41].

Calcium nitrite is also an accelerating admixture. In the quantity recommended by one manufacturer to inhibit corrosion (5.4 gallons of a nominal 30% solution per cubic yard of concrete), the admixture is a very powerful accelerator. Where both accelerated setting times and enhanced corrosion protection are required, calcium nitrite may be useful. If significantly reduced setting times are not desirable, either addition of a retarding admixture or delayed addition of the calcium nitrite solution may be used to permit longer working time. If addition of the calcium nitrite solution is delayed, care must be taken to insure adequate mixing.

Because of the large quantity of admixture added, the effect on W/C ratio will be significant. Therefore, delayed addition of the calcium nitrite can lead to problems in initial mixing due to lack of adequate workability. The dosage of any high-range water reducer used initially may need to be increased to overcome this difficulty. Any increase in setting time provided by additional HRWR is usually beneficial in this case.

2.1.2.5 Latex-Modified Concrete

Latex-modified concrete (LMC) has been successfully used in highway and bridge work, primarily in overlays. The advantage is an improvement in durability which is related to substantial reductions in permeability of a properly cured and dried concrete. The most common type of latex in use in concrete is probably styrene butadiene polymer in an aqueous colloidal suspension. Other types of latex, such as those based on polyacrylic esters, have also been investigated. Latex-modified concretes based on polyvinyl acetate or polyvinylidene chloride are not appropriate for highway and bridge work due to wet strength and corrosion concerns.

Typical polymer contents in concrete are between 10% and 25% of cement weight. Use of latex in these quantities provides only a slight increase in compressive strength but a significant increase in tensile, flexural and impact strength.

The latex forms a film on the capillary pores on drying which reduces the permeability of the concrete to water and chlorides by sealing the pores, thereby improving durability considerably. Adhesion of LMC, provided by the latex film, to other concrete and to reinforcing steel is excellent. The adhesive qualities of the dry latex film, combined with its high extensibility, probably account for the improvement in tensile and flexural strength by acting as crack arresters for microcrack propagation. Latex will also increase both entrained and entrapped air contents, although the air-void system formed may not be satisfactory.

The cost of LMC is considerably higher due to the cost of the latex itself. Its use has been limited primarily to thin (less than 2 in. or 50 mm thick) overlays. The permeability of LMC and silica fume concretes has been reported to be similar [2.32, 2.10].

2.1.3 Mineral Admixtures

Mineral admixtures are frequently critical to the performance of high strength concrete, and can be used to improve durability or strength characteristics.

2.1.3.1 Fly Ash

Commercially useful fly ashes may be either Class F or Class C. Class F fly ashes are composed primarily of silicious and aluminous compounds with very limited quantities of calcium, are not cementitious in themselves and have a pozzolanic reaction. Class C fly ashes usually contain substantially more calcium than Class F ashes, and are derived from different types of coal. Class C fly ashes are generally cementitious in themselves; however, when mixed with portland cement, Class C fly ashes also undergo a pozzolanic reaction.

Class F fly ashes have been shown to improve durability of concrete to sulfates attack, to play a role in reduction of alkali-aggregate reactivity, to reduce permeability and porosity of the paste when properly cured, and to reduce heat of hydration when used as a partial cement replacement. Fly ashes have also been shown to reduce water demand somewhat for a given workability in many concretes.

Concrete containing fly ash will have satisfactory freeze-thaw durability if the air-void system is adequate. Generally, adequate air-void systems can be successfully developed and maintained in low residual carbon content (low loss on ignition) ashes. It has been reported that fly ash concretes requiring a high initial dosage of air-entraining agent are more susceptible to loss of entrained air [2.30, 2.23]. Class F fly ash has, under some conditions, contributed to slightly increased scaling in the presence of deicing salts [2.33]. Use of fly ash in pavements has generally been successful and has led, in one case in Kansas, to a reduction in map-cracking [2.4].

Class F fly ash will contribute to strength gain in concretes at later ages, with minimal strength effects prior to 7 days age. Class C fly ashes are typically somewhat more reactive and provide an earlier contribution to strength than most Class F fly ashes.

Certain Class C fly ashes have been reported to decrease sulfate durability, depending on quantity used [2.20]. Due to the lower silicate content of Class C fly ash, it does not provide the same level of mitigation of alkali-aggregate reactivity as an otherwise equivalent Class F ash.

Quantity of fly ash used will vary with type of ash, purpose in using the ash and desired concrete properties. In mass concrete structures, quantities as high as 60% to 100% of the cement weight may be successfully used. For most commercial work, 15% to 30% by weight of the total cementitious or binder material (cement plus mineral admixture), is more common. Fly ash is not generally used with blended cements since these cements already contain slag or ash.

ACI Committee 226 report on Fly Ash in Concrete [2.4], AASHTO M 295 and ASTM C 618 provide additional guidance for the use of fly ash in concrete.

2.1.3.2 Ground Granulated Blast-Furnace Slag

Ground granulated blast-furnace slag (GGBFS), is a high calcium mineral admixture, available in certain parts of the United States. GGBFS is classified as Grade 80, Grade 100, or Grade 120, depending on the slag-activity index, with the higher grades indicating generally higher cementitious potential. The grade is approximately the relative efficiency of the slag compared to an equal weight of portland cement, although this will vary with cement used, slag used, and concrete temperature and proportions.

Addition of GGBFS may vary from 25% to 70% of total cementitious material, although 40% to 60% is more common in commercial work. If sulfate resistance is desired, a minimum of 50% GGBFS should be used [2.25]. Alkali-silica expansion potential can be reduced with sufficient quantities of GGBFS [2.25]. Freezing and thawing resistance is adequate, as long as a proper air-void system has been developed. As with other pozzolanic admixtures, use of GGBFS, as an addition, can reduce permeability in a properly cured paste.

Early strength gain of concretes with substantial quantities of GGBFS may be relatively low, if cured at normal or low temperatures. At higher temperatures, rapid strength gain may be obtained.

ACI Committee 226 report on Granulated Blast-Furnace Slag as a Concrete Constituent [2.3], AASHTO M 302 and ASTM C 989 provide additional information and guidance on use of GGBFS in concrete.

2.1.3.3 Silica Fume

Silica fume, also known as condensed silica fume or microsilica, is a mineral admixture composed primarily of extremely small particles of glassy silica, which provide a strong pozzolanic reaction in portland cement paste. Silica fume is used in cast in place applications in the United States primarily to either attain very high strengths or significantly improve durability.

A. Production and Handling Silica fume can be purchased in dry bulk form or in a slurry. In dry, loose form, the bulk density is typically low, about a quarter of that of portland cement, resulting in a large volume per weight shipped. Due to silica fume's fine size, dust control and handling of the dry material, particularly with an air slide, can be a problem. "Densified" dry bulk products developed to overcome these problems are available.

The most common silica fume product used in commercial work in the United States is probably a slurry of approximately 50% water with stabilizing admixtures. The slurry form can be handled easily in production facilities as long as the material remains in suspension. Some products have shown a thixotropic tendency over long periods of storage. As long as the product has remained in suspension, fluidity of the product can be restored by agitation prior to batching.

Whereas other types of mineral admixtures may be 20% to 40% of the cost of portland cement, silica fume will typically be at least twice, and easily up to 10 times the cost of portland cement, depending on location, source and form of silica fume used. This cost can be offset to some extent because silica fume can replace portland cement on as much as a 3- or 4-to-1 basis with no loss in strength, depending on the level of strength sought and percent replacement. However, on a purely economic basis, other mineral admixtures are generally more efficient. If a high-range water reducer is additionally required, as it frequently is, further costs are incurred.

The specific surface of silica fume is very high--on the order of 50 times that of portland cement. The high surface area can cause a dramatic increase in water demand. In particular, if silica fume is used in very low W/C ratio concretes, it is necessary to use a high range water reducer to maintain adequate workability at low W/C ratios. The FIP State of the Art Report [2.21] recommends that concrete containing silica fume have a slump about 1 in. (25 mm) higher for the same workability as concrete without silica fume.

The high surface area of the silica fume reduces bleeding. In lower W/C ratio concrete, bleeding may be nonexistent, thus creating potential plastic shrinkage cracking of slabs or pavement, requiring additional attention during construction.

B. Durability Silica fume is exceptionally effective at improving durability against many types of chemical attack of regular portland cement concretes. The highly pozzolanic nature of the material contributes significantly to improvements in durability against sulfate attack and alkali-aggregate reactivity.

It has been reported that the permeability of concrete containing silica fume is lower than that of concrete without silica fume at the same compressive strength. Although total porosity may remain similar, a finer pore system is developed with silica fume [2.29]. This can further improve durability against aggressive or harmful chemicals.

Silica fume concrete with an adequate air-void system will have adequate or superior freeze-thaw durability, at least as long as the silica fume content is relatively low. For high silica fume contents, the results are mixed and inconclusive. Concretes which contain silica fume may require somewhat higher dosages of air-entraining agent to provide acceptable air content, but the air-void system so produced is stable in most cases [2.21].

The air-void system required for durability with respect to frost for commodity-grade concrete may not be attainable with low W/C ratio concrete containing significant quantities of silica fume. For concretes with more than about 5% silica fume, the use of a high-range water reducer is a practical requirement. The air-void system in these cases is found to be coarser, with lower spacing factor [2.31]. It may be difficult to attain a conventional air-void system in concretes with high silica fume contents requiring the use of high range water reducers [2.35, 2.32]. This is related to the use of high-range water reducers rather than the silica fume, however (see section 2.1.3.3).

Due to the dramatic change in pore refinement in concretes containing silica fume, very low W/C ratio, silica fume concretes may be frost resistant, under practical conditions, without entrained air. Concrete with a W/C ratio equal to 0.35, containing a 5% silica fume replacement of cement and a high-range water reducer, was found to be frost resistant even with spacing factors higher than .008 and a specific surface much less than 600 in^{-1} [2.34]. This area is undergoing further research.

C. Strength Another consequence of the extremely high surface area of silica fume is a rapid pozzolanic reaction. Silica fume contributes to strength at an earlier age than other pozzolans.

Strength contributions of the silica fume as early as 1 day cannot be attributed to pozzolanic reaction alone, however. Early strength may result from silica fume particles acting as nucleation sites for the formation of hydration products [2.19, 2.28]. Silica fume not only has an accelerating effect and a pozzolanic effect, but has a densifying, or filler, effect, as well [2.21, 2.20, 2.14, 2.15]. Strength improvement in the transition zone between paste and aggregate can be significant due to both pozzolanic and filler effects [2.24, 2.12, 2.21].

In one study, for concretes with W/C ratios of 0.34 and 0.28, silica fume contents higher than 15% of total cementitious material were found to reduce compressive strength for mixes at the same slump and W/C ratio. For the same concretes, silica fume contents higher than 10% were found to reduce flexural strength [2.42]. The reduction in strength at higher percentages of silica fume was due to the difficulty of properly compacting the mixes. This may be due to increases in stickiness associated with higher fines content. At higher slumps or with reproportioning of the mix, these limits may no longer apply.

Carette and Malhotra [2.14] report that replacements of cement by silica fume greater than 10% reduce compressive, strength and greater than 5% reduce flexural strengths, for mixes with a W/C ratio of 0.64. ACI Committee 226, Silica Fume in Concrete [2.2], notes that Malhotra and Carette found an increase in compressive strength for concrete with a 0.40 W/C ratio, using silica fume up to 30% cement replacement. The use of a high-range water reducer, even at moderate W/C ratios, may be a practical necessity for concretes containing more than 5% silica fume. The FIP State of the Art Report [2.21] indicates that silica fume content is rarely more than 10% in normal usage. Much of the research to date has focused on concrete with a maximum silica fume content of 10%.

The optimum silica fume content for high strength concrete may be between 5% and 10% of total cementitious material, although data are somewhat conflicting due to the sensitivity of the mix to proper proportioning, especially high-range water reducer content. For pavements, it may be best to use a silica fume content not substantially more than 5%. At least minimal air contents are recommended at this time for structures which may become critically saturated prior to freezing.

An ASTM standard does not currently exist for silica fume. For more information, see ACI Committee 226 report on Silica Fume in Concrete [2.2] and especially the FIP State-of-the-Art Report on Condensed Silica Fume in Concrete [2.21].

2.1.4 Aggregates

Aggregates play a key role in high performance concrete. Fine aggregate affects the finishing characteristics, the water demand and the coarse-aggregate content. Coarse aggregate affects the water demand, compressive and flexural strength, shrinkage and creep, elastic modulus, and wear resistance of concrete pavements.

Fine aggregates should be on the coarse side of the specifications with minimal amounts of No. 50 and finer material. A fineness modulus of 3.0 was reported in one study [2.13] to give the best results for high strength concrete. A coarser sand tends to reduce the stickiness of paste-rich mixes, improving the workability and increasing the compressive strength. The use of sand with rounded, smooth particle shape is recommended in ACI Committee 363 State-of-the-Art Report on High Strength Concrete [2.6] to reduce water demand.

Coarse aggregate plays the dominant role in most aggregate durability considerations. Alkali-silica reactivity is primarily a coarse aggregate phenomenon. "D" cracking is a function of the pore structure and size of the coarse aggregate. Wear resistance of a concrete pavement is dependent on both the paste quality and the polishing characteristics and abrasion resistance of the aggregate.

Coarse aggregate must be durable itself to be suitable for use in high performance concrete. Where high strength concrete is needed for structural components, the guidelines suggested in ACI Committee 363 State-of-the-Art Report on High Strength Concrete [2.6] should be followed.

In pavement applications, abrasion resistance, susceptibility to alkali-aggregate reactivity and "D" cracking must be considered. Although the quality and composition of the paste can mitigate marginal aggregate performance in these areas, high performance concrete should be produced with high performance aggregates where possible and at least with the best, economically available aggregates.

Aggregate strength will not be the limiting factor in a high strength concrete except in a few cases with relatively low-strength rock. Aggregate-paste bond strength is the limiting factor with most high strength concrete. Mineralogy, texture and paste composition significantly affect the aggregate-paste bond. Examination of the stress-strain curve during loading and unloading in the elastic range may provide additional insight into the nature of the aggregate-paste bond. A large hysteresis loop may indicate an inherent weakness in the aggregate particles or in the transition zone [2.9]

Increases in compressive strength due to smaller-sized aggregate have been attributed to reduction in average bond stress resulting from an increase in surface area per unit volume of aggregate, and to less stress concentration at the aggregate-paste interface due to smaller differences in elastic modulus of the paste and aggregate. Optimum cement content increases with decreasing nominal maximum size aggregate (NMSA) [2.18].

Reduction of the NMSA to 1/2 in or 3/8 in. (12 or 10 mm) has been suggested to attain optimum strength. However, this is contrary to normal practice for optimal flexural strength and, due to the reduction in aggregate quantity typically found with smaller-sized aggregate, may lead to increases in creep or shrinkage. Since these aspects are offset to some extent by the increase in paste stiffness, the overall changes in long-term volumetric change associated with reduction in NMSA may be minimal. Coarse aggregate with maximum sizes of 3/4 in and 1 in. (19 and 25 mm) have also been successfully used in high strength concrete.

The use of smaller-sized aggregate may be necessary in areas where "D" cracking is prevalent but for most other paving applications, the use of 3/4 or 1 in. (19 or 25 mm) or larger, aggregate should be considered. In any case, the quantity of aggregate in a paving mix will typically be higher than in standard construction mixes.

Crushed aggregate is generally recommended over rounded stone or gravel due to improvement in aggregate-paste bond strength.

2.1.5 Water

Mixing water quality standards are not changed for high performance concrete.

It is possible, given the variety and types of admixtures available, to produce concretes with very low-water contents. However, in many cases, the concretes so produced are very sticky and difficult to place, vibrate and, particularly, to finish properly. It has been reported [2.27] that a minimum water content of approximately 250 pounds per cubic yard (pcy) (148 kg/m^3), using angular sands, will mitigate many of the problems related to excessive stickiness found in high performance concrete. In mixes using a clean, rounded sand, water quantities of 220 pcy (131 kg/m^3) have been reported to produce acceptable high strength mixes [2.36].

2.2 Manufacturing Considerations

2.2.1 Proportioning

Proportioning of high performance concrete is not substantially different than for other concretes. Raw material properties and quantities must be selected to achieve the desired mix in terms of strength (at a particular age), durability, workability and economy. In the development of these mixes, determination of optimum cement and admixture quantities will typically involve more trial batches than for commodity grade concrete. Admixture-cement compatibility will need to be closely checked, particularly with the number of admixtures used in some high performance concretes.

Selection of an appropriate average strength level for VHS mixes may be somewhat different than for commodity concrete. Average strength level, for standard, structural, reinforced concrete, based on past strength records, is required by ACI 318 [2.5] to be such that a test result (the average strength of at least two cylinders) will fall below the design strength (f_c') no more than about once in ten times and a test result will fall below the design strength less 500 psi (3 MPa) no more than about once in a hundred times. The requirement given is

$$f_{cr}' = larger\ of \begin{cases} f_c' + 1.34\,s \\ f_c' + 2.33\,s - 500 \end{cases} \tag{2.1}$$

where s is the standard deviation, adjusted, if necessary for number of data points.

An alternate requirement has been suggested [2.17] for high strength concrete and is under consideration by ACI Committee 211. The alternative requirement provides an average strength so that test results will fall below 90% of the design strength no more than about once in a hundred times.

$$f'_{cr} = larger\ of \begin{cases} f'_c + 1.34\,s \\ .90\,f'_c + 2.33\,s \end{cases} \tag{2.2}$$

Rigorous control over added water, extra attention to quality control and proper testing procedures, and lack of entrained air can contribute to a reduction in standard deviation. However, due to the sensitivity of high strength concretes to relatively small changes in raw material quality or proportions, and non-standard testing procedures, standard deviations can increase. Reported values for standard deviation of high strength concrete at 56 days have ranged from about 270 psi (2 MPa) for concrete with an average compressive strength of over 18,000 psi (124 MPa) [2.36] to between 680 and 850 psi (5 and 6 MPa) for concrete with an average compressive strength of approximately 12,000 psi (83 MPa) [2.16].

Where the standard deviation is not known accurately, either

$$f'_{cr} = f'_c + 1400\ psi \quad (conventional) \tag{2.3}$$

or

$$f'_{cr} = \frac{(f'_c + 1400)}{.90}\ psi \quad (alternate) \tag{2.4}$$

may be used.

While these minimum requirements for average strength are acceptable for concrete strengths at 28 days (for reinforced concrete members designed on an ultimate strength basis) they may not be appropriate for pavements. Design of AASHTO pavements are based on average flexural strength, on an allowable stress basis, with overall variability explicitly considered in the design process itself.

Selection of an appropriate average strength level for VES and HES mixes is difficult. Variability is likely to be high at these ages and the effects of temperature more pronounced. The structural effects of a slight deficiency in strength will not be as severe in a pavement at these ages, since strength gain is very rapid for these concretes at design age and design strengths should be attained within a short time. Reopening of a pavement to traffic should be delayed however, if strength levels are too low. A minimally acceptable strength of 85% of f_c' for these mixes may be appropriate. At present, without further research, especially data correlating flexural and compressive strengths at these early ages, a firm recommendation for adequate average strength cannot be made.

2.2.2 Production

Batching and mixing criteria for high performance concrete include certification of plants and trucks, tight quality control by the producer and probably should include additional training of drivers regarding the properties of the plastic concrete they are to deliver.

Several differences in batch operations may be required for high performance concrete. When producing concrete at a "dry batch" plant, the mixing will be accomplished in the truck. Frequently the high performance concretes will be somewhat stickier and may be more difficult to mix due to the lower water content. In order to insure adequate mixing, the guidelines of ASTM C 94, Specifications for Ready Mixed-Concrete, should be followed regarding consistency within the batch or truck. This can be used to determine the rated capacity of the truck for high performance mixes. It may be necessary to batch somewhat less than the nominal maximum rated truck capacity to insure adequate mixing, including on site additions of chemical admixtures.

Holding out a given quantity of mix water for use by the driver in washing down the chute after loading has been suggested to improve control of delivered W/C ratio [2.36].

2.2.3 Delivery and Handling

Delivery and handling of high performance concrete will be more difficult and require additional management time by the concrete supplier, the contractor, and the owner. Rapid slump loss may require job site additions or redosing of HRWR's. If calcium nitrite is used to help inhibit corrosion of reinforcing steel, job site addition may also be required to control rapid slump loss.

Delayed addition of HRWR's may produce different effects at the same dosage. While this may not have an appreciable effect on production of flowable concrete, tightly controlled low-slump concrete, such as the concrete used with slip-form paving machines, may be more difficult to consistently attain.

Delayed addition of admixtures, rapid slump loss and stickier mixes may cause problems in maintaining an acceptable air content (see section 2.1.2.3).

Batching, delivery and handling procedures will need to be "proofed" by construction of a mock-up, shoulder construction or less critical section of pavement prior to acceptance of materials and methods for any high performance concrete project.

2.2.4 Placing, Consolidation and Curing

It has been reported that moist curing of low W/C ratio (0.3) concrete containing silica fume past seven days will not substantially increase the compressive strength since the concrete has become impervious [2.11]. This will not occur until much later with concretes containing a less-reactive mineral admixture, such as Class F fly ash. Concrete containing silica fume has been reported to be more susceptible to strength loss due to early drying than conventional concrete at the same W/C ratio. Concrete with silica fume has also been reported to be more sensitive to curing conditions, especially premature drying [2.11, 2.12].

The use of nonbleeding concrete in a slip form paving operation will require the immediate application of curing compound or other methods of reducing moisture loss. This will improve strength in place and reduce the potential for plastic shrinkage cracking.

Temperature of the concrete after casting should be controlled by the use of insulating blankets. Even in warm weather, the use of a blanket may reduce cracking by reducing the temperature differential between the surface and center or bottom of the pavement and therefore reducing stresses at early ages while the concrete has limited tensile strength. Joint construction techniques may need to be reviewed if blankets are used.

2.2.5 Testing

Requirements for the use of high performance concrete include certification of the testing agency, anticipation of and planning for a greater level of participation in quality control, quality management and adequate training at all levels. High performance concrete should require not only high performance materials, but high performance testing.

Certification of the testing agency, including certification of technicians on the job, a record of satisfactory performance on similar work, testing equipment of the required capacity, and adequate facilities are mandatory.

High strength concrete is more sensitive to testing than commodity grade concrete and testing requirements must be rigorously enforced. For most departments of transportation, this standard may be attained through additional training of technicians and staff in handling high strength concrete.

HES and VES concretes, while not technically high strength concretes, will still present many of the same problems in initial testing. Slump measurements, particularly if a HRWR has been added, may not be especially effective as quality control measures. Air contents may be difficult to accurately measure in low-slump, high-fines mixes and conventional guidelines for content may not be entirely reliable in insuring adequate frost protection in all mixes.

The HES and VES mixes will also be sensitive to handling until design age. Accurate strength measurements will be more difficult due to the strict controls on time.

Very high strength concrete test cylinders may be prepared for compressive strength testing by grinding the ends or by use of a high strength capping compound. It would be difficult or impossible to grind HES and VES concrete specimens in a timely fashion. The use of capping compounds would also present problems in early stripping or short curing times. The use of neoprene pads inserted in a flat steel cup as unbonded capping devices is widespread and should prove adequate for the VES and HES concretes. The use of these devices for Very High Strength concrete is probably acceptable when strengths are not much higher than 10,000 psi (69 MPa), but should be used with caution for strengths up to 15,000 psi (103 MPa).

The use of steel or sturdy plastic molds is recommended, as the member is cured until design age for HES and VES mixes or cured according to ASTM standards for VHS mixes. ASTM C 31, Standard Method of Making and Curing Concrete Test Specimens in the Field, calls for keeping test cylinders at 60 to 80^{0}F (16 to 27^{0}C) for the first 24 hours, protected from evaporation. For low W/C ratio concretes, protection from evaporation will be critical. Special precautions should be taken to insure no initial moisture loss.

Size, moisture condition, loading rate and other testing effects are covered in Chapter 3.

2.3 Special Considerations for Fiber Reinforced Concrete

Satisfactory performance of fiber reinforced concrete (FRC) depends mainly on adequate mix proportions. This is true of conventional concrete as well; however, it is considered more critical in FRC. There are two primary criteria to be considered in proportioning of FRC [2.38]: 1) meeting structural design requirements of strength, fatigue endurance, and the like, and 2) constructibility or ability to be mixed, transported, placed and finished.

For normal weight concretes, steel fiber contents have been used in experimental and actual pavement applications, including pavements, overlays, bridge decks, and airfields, from as low as 60 pcy (36 kg per cubic meter (kg/m^3)) to as high as 265 pcy (157 kg/m^3) with an average of about 175 pcy (100 kg/m^3). The high range limit is usually about 160 to 200 pcy (95 to 118 kg/m^3). In terms of volume percentage for normal weight concrete, 60, 175 and 265 pcy correspond to 0.45%, 1.3% and 2.0% of fiber respectively. The cementitious content varied between as low as 550 pcy (326 kg/m^3) to as high as 970 pcy (575 kg/m^3). Pozzolans such as fly ash were provided to partially replace the cement in amounts varying between 20% to 30% of the total weight of cement.

Compared to conventional concrete, FRC mixes are generally characterized by higher cement factors, higher fine aggregate content and smaller-sized coarse aggregate.

Steel fiber reinforced concrete (SFRC) pavements tend to have low slumps and low W/C ratios between 0.39 and 0.34 with no superplasticizer used. High cement contents result in higher drying shrinkage and heat release compared to conventional concrete. This often leads to the development of full-width transverse cracks and curl in most steel FRC pavement applications. The use of water-reducing admixtures, both regular and high-range (superplasticizer) to increase workability along with better attention to gradation and use of large aggregates are important remedies. As indicated by Schrader [2.38], aggregate sizes of 1-1/2 in. (38 mm) are suitable for pavement mixes with large fibers having lengths greater than the larger aggregate dimensions. This kind of mix could permit lower fiber content on a volume basis due to lower paste content.

Procedures for proportioning SFRC mixtures in paving and structural applications with emphasis on good workability have been proposed by Schrader and Munch [2.39]. With steel fibers, experience has shown that satisfying the overall aggregate gradation such as given in Table 2.1 will minimize fiber balling and enhance workability. Also, as indicated by ACI Committee 544 [2.7], trial mixes may be based on previous, proven mixes, such as shown in Table 2.2. ACI Committee 544 [2.7] presents typical mix proportions that have been used for airfield paving (Table 2.3).

Steel fiber reinforced concrete is usually specified by strength and fiber content. For paving applications, the static flexural strength at a given age is specified while for structural applications, the compressive strength is normally specified. Typical values used in practice are 700 to 1,000 psi (5 to 7 MPa) for flexural strengths and 5,000 to 7,000 psi (35 to 48 MPa) for compressive strengths [2.8]. Although increasing the fiber content does not significantly influence the compressive strength, it may result in a considerable increase in the flexural strength and toughness. However, increasing the fiber content decreases workability. Hence there is a limit on the fiber content that can be used beyond which workability and ease of constructibility are reduced. Ranges of optimum design mixes with recommended fiber contents are discussed earlier (see Tables 2.2 and 2.3).

Batching and mixing equipment for FRC can vary from sophisticated fully-automated on-site batch and mixing plants to adding the fibers on the job site and mixing in the transit trucks. One of the most important considerations in mixing FRC is good dispersion of the fibers and prevention of fiber balling or clumping. This is the primary difference between FRC mixing and conventional concrete mixing.

Segregation and balling of fibers during mixing depends mainly on the care with which fibers are added; the aspect ratio and volume percentage of fibers; the coarse aggregate size, gradation and quantity; the W/C ratio; and the method of mixing. Increasing the aspect ratio, fiber volume percentage and size or the quantity of aggregate increases the tendency for fiber balling. Fiber clumping primarily occurs before the fibers get in mix [2.8]. Once the fibers get into the mixture clump-free, they nearly always remain clump-free.

Fiber clumping can be minimized or eliminated by care in the sequence and rate of fiber addition; use of shorter fibers but with improved bond properties (such as deformed ends) to offset the loss of bond strength resulting from the shortened length; and use of collated fibers (about 30 fibers glued together with a water-soluble glue), which enables mixing without tangling, with subsequent fiber separation within the mix.

Adequate vibration is essential for the placement of fiber-reinforced concrete, particularly SFRC. High frequency-low amplitude vibration has been found to work best [2.38]. Properly controlled internal vibration is acceptable, but external vibration of the forms and exposed surface is preferable to prevent fiber segregation [2.7].

For pavement applications, thin placements of layers of about 4 in. (100 mm) or less can be consolidated by properly operating a surface screed vibrator with enough energy to fluidize the mass beneath it. Double-screed systems with closely spaced air-actuated vibrators have proven to work very well.

No special measures are required for placing SFRC around reinforcing steel except adequate vibration. In congested sections or where it is difficult to place FRC, ACI Committee 544 [2.8] recommends a 3/8 in. (10 mm) maximum size aggregate.

Finishing FRC requires minor refinements in the techniques and workmanship used in conventional concrete. The primary concern in finishing FRC surfaces is the prevention of loose or exposed fibers, particularly steel. Loose or exposed fibers represent a serious potential safety hazard and should be eliminated or minimized.

Conventional equipment such as metal trowels, tube floats and rotating power floats can be used to finish FRC surfaces [2.7, 2.39]. Proper use of this equipment with minor refinement can result in a smooth surface with no visible or exposed fibers.

3

Behavior of Hardened Concrete

Chapter 2 discussed the production of concrete and the effects of a large number of constituent materials - cement, water, fine aggregate, coarse aggregate (crushed stone or gravel), air, and other admixtures. In this chapter, the behavior of hardened concrete subjected to applied loads and environmentally induced stress is investigated.

Concrete must be proportioned and produced to carry imposed loads, resist deterioration and be dimensionally stable. The quality of concrete is characterized by its mechanical properties and ability to resist deterioration. The mechanical properties of concrete can be broadly classified as short-term (essentially instantaneous) and long-term properties. Short-term properties include strength in compression, tension, bond, and modulus of elasticity. The long-term properties include creep, shrinkage, behavior under fatigue, and durability characteristics such as porosity, permeability, freeze-thaw resistance, and abrasion resistance.

Information concerning the behavior of Very Early Strength and High Early Strength concrete, as defined in Chapter 1, is extremely limited. While data on Very High Strength concrete is insufficient, there is a substantial body of information on the mechanical properties of high strength concrete and additional information is being developed rapidly. Since high performance concretes all typically have low water-cementitious materials (W/C) ratios and high paste contents, characteristics will, in many cases, be similar to those of high strength concrete. Much of the discussion in this chapter will therefore concentrate on high strength concretes.

A significant difference in behavior between the early strength and the high strength concretes is in the relationship of compressive strength to mechanical properties. Strength gain in compression is typically much faster than strength gain in aggregate-paste bond, for instance. This will lead to relative differences in elastic modulus and tensile strength of early strength concretes and high strength concretes, expressed as a function of compressive strength. The relationships of mechanical properties to 28-day compressive strength developed in other studies cannot be expected to necessarily apply to VES and HES concretes. Further research in this area is needed.

3.1 Strength

The strength of concrete is perhaps the most important overall measure of the quality of concrete, although other characteristics may also be critical. Strength is an important indicator of quality because strength is directly related to the structure of hardened cement paste. Although strength is not a direct measure of concrete durability or dimensional stability, it has a strong relationship to the W/C ratio of the concrete. The W/C ratio, in turn, influences durability, dimensional stability and other properties of the concrete by controlling porosity. Concrete compressive strength, in particular, is widely used in specifying, controlling, and evaluating concrete quality.

The strength of concrete depends on a number of factors including the properties and proportions of the constituent materials, degree of hydration, rate of loading, method of testing and specimen geometry.

The properties of the constituent materials which affect the strength are the quality of fine and coarse aggregate, the cement paste and the paste-aggregate bond characteristics (properties of the interfacial, or transition, zone). These, in turn, depend on the macro- and microscopic structural features including total porosity, pore size and shape, pore distribution and morphology of the hydration products, plus the bond between individual solid components. A simplified view of the factors affecting the strength of concrete is shown in Fig. 3.1.

Testing conditions including age, rate of loading, method of testing, and specimen geometry significantly influence the measured strength. The strength of saturated specimens can be 15% to 20% lower than that of dry specimens. Under impact loading, strength may be as much as 25% to 35% higher than under a normal rate of loading (10 to 20 microstrains per second ($\mu\varepsilon$/sec)). Cube specimens generally exhibit 20% to 25% higher strengths than cylindrical specimens. Larger specimens exhibit lower average strengths.

3.1.1 Constituent Materials and Mix Proportions

Concrete composition limits the ultimate strength which can be obtained and significantly affects the levels of strength attained at early ages. A more complete discussion of the effects of constituent materials and mix proportions is given in Chapter 2. However, a review of the two dominant constituent materials on strength is useful at this point. Coarse aggregate and paste characteristics are typically considered to control maximum concrete strength.

3.1.1.1 Coarse Aggregate

The important parameters of coarse aggregate are its shape, texture and the maximum size. Since the aggregate is generally stronger than the paste, its strength is not a major factor for normal strength concrete, or in HES or VES concrete. However, the aggregate strength becomes important in the case of higher-strength concrete or lightweight aggregate concrete. Surface texture and mineralogy affect the bond between the aggregates and the paste and the stress level at which microcracking begins. The surface texture, therefore, may also affect the modulus of elasticity, the shape of the stress-strain curve and, to a lesser degree, the compressive strength of concrete. Since bond strength increases at a slower rate than compressive strength, these effects will be more pronounced in HES and VES concretes. Tensile strengths may be very sensitive to differences in aggregate surface texture and surface area per unit volume.

The effect of different types of coarse aggregate on concrete strength has been reported in numerous articles. A recent paper [3.17] reports results of four different types of coarse aggregates in a very high strength concrete mixture (W/C = 0.27). The results showed that the compressive strength was significantly influenced by the mineralogical characteristics of the aggregates. Crushed aggregates from fine-grained diabase and limestone gave the best results. Concretes made from a smooth river gravel and from crushed granite that contained inclusions of a soft mineral were found to be relatively weaker in strength.

The use of larger maximum size of aggregate affects the strength in several ways. Since larger aggregates have less specific surface area, the bond strength between aggregates and paste is less, thus reducing the compressive strength. Larger aggregate results in a smaller volume of paste thereby providing more restraint to volume changes of the paste. This may induce additional stresses in the paste, creating microcracks prior to application of load, which may be a critical factor in VHS concretes.

The effect of the coarse aggregate size on concrete strength was discussed by Cook et al.

[3.65]. Two sizes of aggregates were investigated: a 3/8 in. (10 mm) and a 1 in. (25 mm) limestone. A superplasticizer was used in all the mixes. In general, the smallest size of the coarse aggregate produces the highest strength for a given W/C ratio, see Figs. 3.2 - 3.6. It may be noted that compressive strengths in excess of 10,000 psi (69 MPa) can be produced using a 1 in. (25 mm) maximum size aggregate when the mixture is properly proportioned.

Although these studies [3.17,3.65] provide useful data and insight, much more research is needed on the effects of aggregate mineral properties and particle shape on the strength properties and durability of higher strength concrete. This was recognized as one of the research needs by the ACI 363 Committee [3.8].

3.1.1.2 Paste Characteristics

The most important parameter affecting concrete strength is the W/C ratio, sometimes referred to as the W/B (binder) ratio. Even though the strength of concrete is dependent largely on the capillary porosity or gel/space ratio, these are not easy quantities to measure or predict. The capillary porosity of a properly compacted concrete is determined by the W/C ratio and degree of hydration. The effect of W/C ratio on the compressive strength is shown in Fig. 3.7. The practical use of very low W/C ratio concretes has been made possible by use of both conventional and high range water reducers, which permit production of workable concrete with very low water contents.

Supplementary cementitious materials (fly ash, slag and silica fume) have been effective additions in the production of high strength concrete. Although fly ash is probably the most common mineral admixture, on a volume basis, silica fume (ultra-fine amorphous silica, derived from the production of silicon or ferrosilica alloys) in particular, used in combination with high-range water reducers, has increased achievable strength levels dramatically [Fig. 3.7] [3.15, 3.129, 3.130].

The effect of condensed silica fume on the strength of concrete was reported in a very comprehensive study [3.80]. The beneficial effect of using up to 16% (by weight of cement) condensed silica fume on the compressive strength is shown in Fig. 3.8. The data indicate that to achieve 10,000 psi (69 MPa) 28 day 4 x 4 x 4 in. (100 x 100 x 100 mm) cube strength, the W/C ratio required is about 0.35 if no silica fume is used; however, with 8% silica fume, the W/C needed is about 0.50, and with 16% silica fume content the W/C ratio requirement increases to about 0.65. This indicates that higher compressive strength can be very easily achieved with high silica fume content at relatively higher W/C ratios.

The efficiency of silica fume in producing concrete of higher strength depends on water/cement+silica fume ratio, dosage of silica fume, age and curing conditions. Yogendram and Langan [3.210] investigated the efficiency of silica fume at lower W/C ratio. Their results indicated that the efficiency is much lower at W/C ratio of 0.28 as compared to the efficiency at W/C ratio of 0.48.

The performance of chemical admixtures is influenced by the particular cement and other cementitious materials. Combinations which have been shown to be effective in many cases may not work in all situations, due to adverse cement and admixture interaction (see Fig. 3.9). Substantial testing should be conducted with any new combination of cements, and mineral or chemical admixtures prior to large scale use.

3.1.2 Strength Development and Curing Temperature

The strength development with time is a function of the constituent materials and curing techniques. An adequate amount of moisture is necessary to ensure that hydration is sufficient to reduce the porosity to a level necessary to attain the desired strength level. Although cement paste in practice will never completely hydrate, the aim of curing is to ensure sufficient hydration. In pastes with lower W/C ratios, self-desiccation can occur during hydration and thus prevent further hydration unless water is supplied externally.

The strength development with time up to 95 days for normal, medium and high strength concretes utilizing limestone aggregates and moist cured until testing are shown in Fig. 3.10. The results indicate a higher rate of strength gain for higher strength concrete at early ages. At later ages the difference is not significant. The compressive strength development of 9,000 psi, 11,000 psi, and 14,000 psi (62 Mpa, 76 Mpa, 97 MPa) concretes up to a period of 400 days is shown in Fig. 3.11. The results shown in the figure are for mixes containing cement only or cement and fly ash, with some mixes using high range water-reducing agents. The data indicate that for moist-cured specimens, strengths at 56 days are about 10% greater than 28 day strengths. Strengths at 90 days are about 15% greater than 28 day strengths. While it is inappropriate to generalize such results, they do indicate the potential for strength gain at later ages.

In a recent study [3.120] at North Carolina State University (NCSU), concretes utilizing a number of different aggregates and mineral admixtures, with strengths from 7,000 psi to 12,000 psi (48 MPa to 83 MPa) at 28 days and from 10,000 psi to almost 18,000 psi (69 MPa to 124 MPa) at one year were tested. On examining the absolute strength gain against the percentage strength gain with time, it was concluded that there appears to be no single, constant factor which can be used to accurately predict later strengths from early strengths except in a very general sense. This is no doubt due to the contributions of not only the ultimate strength of the aggregate and the mortar, but to the strength of the transition zone. The transition zone strength, or interfacial bond strength of the mortar to the aggregate, of concretes of higher strengths is typically affected by the binder composition as well as the ultimate strength of the mortar. Results for splitting tensile strength and modulus of rupture were similar.

The effect of condensed silica fume (CSF) on concrete strength development at 20^{0}C generally takes place from about 3 to 28 days after mixing [3.71]. It was found in this study that for a CSF and control concrete of equal 28 day strength, the strength of the CSF concrete is lower over the entire time period with 20^{0}C curing. Furthermore, the results indicate that at 7 days, the influence of silica fume on the compressive strength may be attributed mainly to physical effects. By the age of 28 days, both physical and chemical effects become significant. However, even at 7 days, there is a difference in the resistance to subcritical crack growth in the cement paste-aggregate transition zone between silica fume and carbon black (which is physically similar to silica fume but is not pozzolanic) mixes. This explains the differences observed in the shapes of the stress-strain curves. Another recent study [3.90] indicates that strength enhancement due to the inherent effect of silica fume is as important as the water-reducing effect. Johansen [3.106, 3.107] measured strength up to 3 years and concluded that there was little effect of CSF on either the strength gain between 28 days and 1 year or between 1 and 3 years for water-stored specimens.

The effect of cement types on the strength development is presented in Table 3.1. At ordinary temperatures, for different types of portland and blended cements, the degree of hydration at 90 days and above is usually similar; therefore, the influence of cement composition on the porosity of the matrix and strength is primarily a concern at early ages. The effect of condensed silica fume on the strength development of concretes with four different types of cement was investigated by Maage and Hammer [3.125]. The four cement types were ordinary portland cement, 10% and 25% pulverized fuel ash (fly ash) blends, and a 15% slag blend. Concrete mixes without CSF and with 0%, 5%, and 10% CSF were made at 5^{0}C, 20^{0}C and 35^{0}C and maintained at these temperatures in water for up to one year. The compressive strengths were measured from 16 hours up to a period of one year. Mixes in three strength classes were made: 2,000 psi, 3,500 psi and 6,500 psi (15 Mpa, 25 Mpa and 45 MPa). Fig. 3.12 shows the compressive strength development of concrete water-cured at 20^{0}C, with various CSF dosages and utilizing different cement types. In the figure each curve represents a mean value for four cement types and relative compressive strength of 100% represents 28 day strength for each mix type. From the figure, it can be seen that at 20^{0}C curing, regardless of the cement type, the CSF had the same influence on the strength-age relationship. Figures 13 and 14 show relative strength development at 5^{0}C with and without 10% CSF for the four cement types, and similar data for 35°C curing are shown in Figures 15 and 16. At 5°C curing, the blended cement lags behind OPC up to 28 days; with 10% CSF the lag increases which indicates that the pozzolanic reactions have not contributed much to the strength in the 28 day period. At 35°C the CSF mix is more strongly accelerated (in comparison with 20°C curing) than the reference mixes, particularly between the first and the seventh day.

Curing at elevated temperatures has a greater accelerating effect on condensed silica fume (CSF) concrete than on control concrete. Evidence [3.80] indicates that a curing temperature of roughly 50°C is necessary for CSF concrete to equal 1 day strength of an equivalent control mix. Curing at temperatures below 20°C retards strength development more for CSF concrete than for control concrete. CSF makes it possible to design low-heat concrete over a wide range of strength levels [3.80]. Therefore the condensed silica fume concrete is more sensitive to curing temperature than ordinary portland cement concrete [3.80]. The effect of curing on the condensed silica fume and fly ash concrete was studied in a recent investigation [3.170], in which concrete was exposed to six different curing conditions. It was concluded that concrete cured at 20°C continuously in water (reference) exhibited increasing strengths at all ages; concrete cured in water for 3 days before exposure to 50% RH showed higher initial strength, but the strength decreased after 2-4 months with respect to the reference; and concrete exposed to 50% RH showed lower strength after 28 days of curing than that cured in water.

Curing techniques have significant effects on the strength. The key concerns in curing, especially for concrete of higher strength, are maintaining adequate moisture and temperatures to permit continued cement hydration. Water curing of higher strength concrete is highly recommended [3.7] due to its low W/C ratio. At W/C ratio below 0.40, the ultimate degree of hydration is significantly reduced if free water is not provided. The effects of two different curing conditions on concrete strength were investigated [3.50]. The two conditions were moist curing for 7 days followed by drying at 50% relative humidity until testing at 28 days, and moist curing for 28 days followed by drying at 50% relative humidity until testing at 95 days. Higher strength concrete showed a larger reduction in compressive strength when allowed to dry before completion of curing. The results are shown in Table 3.2. It has been reported that the strength is higher with moist curing as compared to field curing [3.53].

3.1.3 Compressive Strength

Conventionally, in the US, concrete properties such as elastic modulus, tensile or flexural strength, shear strength, stress-strain relationships and bond strength are usually expressed in terms of uniaxial compressive strength of 6 x 12 in. (150 x 300 mm) cylinders, moist cured to 28 days. Compressive strength is the common basis for design for most structures, other than pavements, and even then is the common method of routine quality testing. The terms "strength" and "compressive strength" are used virtually interchangeably. The discussion above in sections 3.1.1 and 3.1.2 generally applies equally well to all measures of strength, although most results and conclusions were based either primarily or exclusively on compressive strength results.

Maximum, practically achievable, compressive strengths have increased steadily in the last decade. Presently, 28 day strengths of up to 12,000 psi (84 MPa) are routinely obtainable. The trend for the future has been examined in a recent ACI Committee 363 article [3.8] which identified development of concrete with compressive strength in excess of 20,000 psi (138 MPa) as one of the research needs.

Testing variables have a considerable influence on the measured compressive strength. The major testing variables are: mold type, specimen size, end conditions, and rate of loading. The sensitivity of measured compressive strength to testing variables varies with level of compressive strength.

Since the compressive strength of VES and HES concretes are at conventional levels, conventional testing procedures can be used for the most part, although curing during the first several hours can affect test results dramatically. Testing of VHS concretes is much more demanding. However, in all concretes, not just high performance concrete, competent testing is critical.

The effect of mold type on strength was reported in a recent paper by Carrasquillo et al. [3.53]. Their results indicated that use of 6 x 12 in. (150 x 300 mm) plastic molds gave strengths lower than steel molds and use of 4 x 8 in. (102 x 203 mm) plastic molds gave negligible difference with steel molds. They concluded that steel molds should be used for concrete with compressive strengths up to 15,000 psi (103 MPa). It seems appropriate that steel molds should also be used for concrete of higher strengths.

The specimen size effect on the strength is shown in Fig. 3.17, which shows the relationship between the compressive strength of 4 x 8 in. (102 x 203 mm) cylinders and 6 x 12 in. (150 x 300 mm) cylinders. The figure indicates that 4 x 8 in. (102 x 203 mm) cylinders exhibit approximately 5% higher strengths than 6 x 12 in. (150 x 300 mm) cylinders. Similar results were also obtained in a recent study at North Carolina State University [3.120]. A contradictory result [3.53] is reported, however, which indicates that the compressive strength of 4 x 8 in. (102 x 203 mm) cylinders is slightly lower than 6 x 12 in. (150 x 300 mm) cylinders, see Fig. 3.18. The strength gain for 17,000 psi (117 MPa) concrete as shown by 6 x 12 in. (150 x 300 mm) and 4 x 8 in. (102 x 203 mm) cylinders has been reported by Moreno [3.137] and the results are shown in Fig. 3.19. His study also showed that the specimen size effect on the compressive strength is negligible on the basis of 29 tests, see Table 3.3. Another study [3.50] concluded that the ratio of 6 x 12 in. (150 x 300 mm) cylinder to 4 x 8 in. (102 x 203 mm) cylinder was close to 0.90 regardless of the strength of concrete for the ranges tested between 3,000 and 11,000 psi (21 and 76 MPa).

The relationship between the compressive strength of 6 x 12 in. (150 x 300 mm) and cores from a column was studied for concrete with a strength of 10,000 psi (69 MPa), see Table 3.4. It was concluded that the 85% criterion specified in the ACI Building Code (ACI 318-89) [3.6] would be applicable to high strength concrete. This study also confirms the belief that job cured specimens do not give accurate measurements of the in-place strength. The reason for lower strength in the middle portion of the columns is probably due to temperature rise, i.e, 100^0F (38^0C) for high strength mixtures. In a recent study [3.16], it was shown that the strength of 4 in. (100 mm) cores taken from a mock column at two and four years after casting was nearly identical to that of specimens cured for 28 days in lime-saturated water at room temperature. The strength of the concrete tested was 12,300 psi (85 MPa).

The effect of end conditions on the compressive strength of concrete is summarized in a recent paper [3.52]. More than five hundred 6 x 12 in. (150 x 300 mm) cylinders from concretes having compressive strengths from 2,500 to 16,500 psi (17 Mpa to 114 MPa) were tested with either unbonded caps (two types) or sulfur mortar caps. It was concluded that use of unbonded caps (with a restraining ring and elastomeric insert) could provide a cleaner, safer and more cost-effective alternative to sulfur mortar for capping concrete cylinders. For concretes between 4,000 and 10,000 psi (28 and 69 MPa), the use of polyurethane inserts with aluminum restraining rings in testing concrete cylinders yielded average test results within 5% of those obtained using sulfur mortar. For concrete strengths below 11,000 psi (76 MPa), the use of neoprene inserts with steel restraining rings in testing concrete cylinders yielded average test results within 3% of those obtained using sulfur mortar. For higher strength concrete, the use of either unbonded capping system is questionable. Substantial differences in compressive strength test results were obtained when two sets of restraining rings obtained from the same manufacturer were used. It was recommended that prior to acceptance, each set should be tested for correlation to results obtained from cylinders capped according to ASTM C 617 for all strength levels of concrete for which the unbonded caps are to be used. (Equipment now exists for parallel grinding the ends of concrete cylinders prior to compression testing, thereby eliminating the need for any type of end cap.)

Measured compressive strength increases with higher rates of loading. This trend has been reported in a number of studies [3.23, 3.39, 3.75, 3.102, 3.126, 3.203] for concrete with strengths in the range of 2,000 to 5,500 psi (14 to 49 MPa). However, only one study [3.13] has reported the effect of strain rate on concretes with compressive strengths in excess of 6,000 psi (41 MPa). Based on their research and other reported data [3.23, 3.39, 3.75, 3.102, 3.126, 3.203], Ahmad and Shah [3.13] proposed an equation to estimate the strength under very fast loading conditions. The recommended equation is

$$(f_c')_{\dot{\varepsilon}} = f_c' \left[0.95 + 0.27 \log \frac{\dot{\varepsilon}}{f_c'} \right] \alpha \tag{3.1}$$

where ε is the strain rate in $\mu\varepsilon$/sec,
α is the shape factor.

The shape factor α accounts for the different sizes of the specimens tested by different researchers and is given by

$$\alpha = 0.85 + 0.09\,(d) - 0.02\,(h) \quad for\ \frac{h}{d} \leq 5 \tag{3.2}$$

where d = diameter or least lateral dimension (in.),
h = height (in.).

No information is available on the effect of rate of loading on the strength for concrete with strengths in excess of 10,000 psi (69 MPa).

3.1.4 Tensile Strength

The tensile strength governs the cracking behavior and affects other properties such as stiffness, damping action, bond to embedded steel, and durability of concrete. It is also of importance with regard to the behavior of concrete under shear loads. The tensile strength is determined either by direct tensile tests or by indirect tensile tests such as flexural or split cylinder tests.

3.1.4.1 Direct Tensile Strength

The direct tensile strength is difficult to obtain. Due to the difficulty in testing, only limited and often conflicting data is available. It is often assumed that direct tensile strength of concrete is about 10% of its compressive strength.

Two recent studies [3.66, 3.91] have reported the direct tensile strength of concrete. A study at Delft University [3.66] utilized 4.7 in. (120 mm) diameter cylinders having a length of 11.8 in. (300 mm). A study at Northwestern [3.91] employed 3 x 0.75 x 12 in. (76 x 19 x 304 mm) and 3 x 1.5 x 12 in. (76 x 38 x 304 mm) thin plates having a notch in the central region for creating a weak section for crack initiation and propagation, and used special wedge like frictional grips. The study at Delft tested concrete of one strength which had either been sealed for four weeks or moist-cured for two weeks and air-dried for two weeks. The results indicated 18% higher tensile strength for the sealed concrete compared to the air dried concrete. The investigation at Northwestern included different concrete strengths up to 7,000 psi (48 MPa) strength, and it was concluded that the uniaxial tensile strength can be estimated by the expression $6.5\sqrt{f_c'}$. Direct tensile strength data is not available for concrete with strengths in excess of 8,000 psi (55 MPa).

The effect of rate of loading on the tensile strength has been the focus of some recent studies by Hatano [3.95], Surias and Shah [3.193], and Zielinski et al. [3.213]. The effect of fast strain rate on the tensile strength of concrete as observed by these studies is shown in Fig. 3.20. Also shown in the figure is a comparison of the predictions per a constitutive theory for concrete subjected to static uniaxial tension [3.144] and the experimental results.

The effect of sustained and cyclic loading on the tensile properties of concrete was investigated by Cook and Chindaprasirt [3.64]. Their results indicate that prior loading of any form reduces the strength of concrete on reloading. Strain at peak stress and the modulus on reloading follows the same trend as strength. This behavior can be attributed to the cumulative damage induced by repetitive loadings. Saito [3.173] investigated the microcracking phenomenon of concrete under static and repeated tensile loads and concluded that cumulative damage occurs in concrete due to reloading beyond the stage at which interfacial cracks are formed.

The effect of uniaxial impact in tension was investigated by Zielinski and Reinhardt [3.213].

Their results indicated an increase in the tensile strength similar to the phenomenon generally observed under uniaxial impact in compression.

3.1.4.2 Indirect Tensile Strength

The most commonly used tests for estimating the indirect tensile strength of concrete are the splitting tension test (ASTM C 496) and the third-point flexural loading test (ASTM C 78).

A. Splitting tensile strength As recommended by ACI Committee 363 [3.7], the splitting tensile strength (f_{ct}) for normal weight concrete can be estimated by

$$f_{ct} = 7.4\sqrt{f_c'} \; psi \quad 3{,}000 \le f_c' \le 12{,}000 \; psi \qquad (3.3)$$

$$(21 \le f_c' \le 83 \; MPa)$$

In 1985, based on the available experimental data of split cylinder tests on concretes of low-, medium- [3.92, 3.101, 3.199], and high strengths [3.12, 3.49, 3.72], an empirical relationship was proposed by Ahmad et al. [3.9] as

$$f_{ct} = 4.34\,(f_c')^{0.55} \; psi \quad f_c' \le 12{,}000 \; psi \qquad (3.4)$$

$$(f_c' \le 83 \; MPa)$$

Fig. 3.21 shows the experimental data, with the predictions using the above equation and the recommendations of the ACI Committee 363. The latter appears to overestimate values of tensile strength. Recommendations of ACI Committee 363 were based on work performed at Cornell University [3.49].

Fig. 3.22 shows the aging effect on splitting tensile strength, which is similar to that under compressive loading. In an investigation by Ojdrovic on cracking modes [3.145], it was concluded that at early ages, tensile strength of concrete is the property of the matrix which governs the cracking mode.

The effect of prior compressive loading on the split tensile strength was investigated by Liniers [3.121] and the results are shown in Fig. 3.23. From this figure, he concluded that limiting the compressive stresses to 60% of the strength is essential if only tolerable damage is to be accepted.

The tensile strength of condensed silica fume (CSF) concrete is related to the compressive strength in a manner similar to that of normal concrete. However if CSF concrete is exposed to drying after one day of curing in the mold, the tensile strength is reduced more than the control concrete [3.80].

B. Flexural strength or modulus of rupture Flexural strength or modulus of rupture is measured by a beam flexural test and is generally taken to be a more reliable indicator of the tensile strength of concrete. The modulus of rupture is also used as the flexural strength of concrete in pavement design. It is often assumed that flexural strength of concrete is about 15% of the compressive strength.

In the absence of actual test data, the modulus of rupture may be estimated by

$$f_r = k\sqrt{f_c'} \tag{3.5}$$

with k typically in the range of 7.5 to 12. For high strength concrete, the ACI Committee 363 State-of-the-Art Report [3.7] recommends a value of k = 11.7 as appropriate for concrete with compressive strength in the range of 3,000 psi to 12,000 psi (21 MPa to 83 MPa).

Based on the available data of beam flexural tests on concretes of low, medium [3.92, 3.101, 3.199] and high strengths [3.12, 3.49, 3.72], an empirical equation to predict the flexural strength (modulus of rupture) was proposed [3.9] as

$$f_r = 2.30\,(f_c')^{\frac{2}{3}} \tag{3.6}$$

where f_c' is the compressive strength in psi.

The above equation is of the same form as proposed by Jerome [3.105], which was developed on the basis of data for concretes of strengths up to 8,000 psi (56 MPa). Fig. 3.24 shows the plot of the experimental data and the proposed equation [3.80] for predicting the modulus of rupture of concretes with strengths up to 12,000 psi (83 MPa). Also shown in the figure is the expression recommended by Carrasquillo and Nilson [3.49].

The results of uniaxial and biaxial flexural tests [3.212] indicated that the tensile strength was 38% higher in the uniaxial stress state than in the biaxial stress state.

Flexural strength is higher for moist-cured as compared to field cured specimens [3.53]. However, wet-cured specimens containing condensed silica fume (CSF) exhibit a lower ratio of tensile to compressive strength than dry-stored concrete specimens with silica fume [3.122]. For all concretes, allowing a moist cured beam to dry during testing will result in lowered measured strength, due to the addition of applied load and drying shrinkage stresses on the tensile face. The flexural strength of condensed silica fume (CSF) concrete is related to the compressive strength in a manner similar to that of concrete without silica fume; however, if CSF concrete is exposed to drying after only one day of curing in the mold, the flexural strength reduces more than the control concrete [3.80].

3.1.5 Bond

Two types of bond strength are of interest in pavement applications; bond strength of concrete to concrete and bond strength of concrete to reinforcing steel.

3.1.5.1 Concrete-Concrete Bond

New concrete is placed against existing concrete in many circumstances. Often an attempt is made to bond the two concretes together. The stress states that develop at the bonding surface will vary considerably depending on the type and the use of the structure. For example, the bond on a bridge deck overlay may be subject to shear stress in conjunction with tensile or compressive stresses induced by shrinkage or thermal effects, in addition to compression and shear from service loads.

Bonding agents are often used with the intention of producing a bond that is as strong as the components being joined. A wide variety of bonding agents have been used in practice, including epoxy resin, acrylic latex, styrene butadiene rubber (SBR) latex, copolymer polyvinyl acetate (PVA), and portland cement mortar. The latter two are used widely as inexpensive general purpose agents for bonding concretes.

No single method of test can replicate all in-service state of stresses in bond. Wall, Shrive and Gamble [3.200], assessed different tests that exposed bonded surfaces to various combinations of shear, compression, and tension. A slant shear, an indirect tension, and two flexural tests were evaluated by measuring sensitivity of strength and deformation to bond strength. The slant shear test was found to be the most appropriate and therefore used to assess the effect of various parameters on the bond strength. Experiments were conducted to evaluate factors such as environment and type of bonding agent.

Other researchers [3.76, 3.115, 3.201] have also used slant shear tests to evaluate bond strength. The results of experimental and analytical studies [3.201] concluded that bond materials with a modulus of elasticity higher than that of concrete cause higher compressive stresses at the bond line and lower tensile stresses in the adjacent concrete than bond materials with a modulus of elasticity lower than that of concrete. A bond material with a modulus of elasticity that is similar to that of the adjacent concrete is desirable. A small misalignment between the new and old concrete surfaces caused by the casting procedures does not produce significant errors in the results. The effect of adherent thickness in the bonding of fresh to hardened concrete has not been studied as extensively as with masonry. However, in both forms of construction, adherent thickness in the 1/8 in. (3 mm) to 1/4 in. (6 mm) range has a strong effect on bond strength. An excessively thick bond layer will cause a considerable reduction in bond strength. Therefore, the maximum bond layer thickness of 1/8 in. (3 mm) specified by many highway departments is justified. With portland cement mortars, prewetting the bond surface of the substrate concrete appears to have a small beneficial effect on bond strength; however the results indicate that the practice of prewetting the bond surface is not critical. Copolymer PVA is a poor bonding agent under a wide range of curing conditions and for different mix designs. Under the laboratory conditions, the use of PVA consistently produces weaker bonds than having no bonding agent at all. The bond produced with the paint form of copolymer PVA is particularly weak.

A method for determining the in-place concrete-concrete bond has been presented in a very recent paper [3.98]. The important advantages of the method are that the test can be performed in-situ and represents actual field conditions. It appears to be a useful tool for quality control during construction repairs.

3.1.5.2 Steel-Concrete Bond

Methods recommended by the current ACI Building Code (ACI 318-89) for estimating the development length and anchorage of tensile steel are based on bond tests generally using concrete with compressive strength not greater than about 4,000 psi (28 MPa). It is uncertain that these empirical equations for estimating the steel-concrete bond are applicable for higher strength concrete, and research on bond strength characteristics of higher strength concrete has been identified as one of the research needs [3.8].

The effect of loading rate on anchorage bond was investigated by Chung and Shah [3.61] and their results indicated that shear strength at the column face (a measure of the bond characteristics) deteriorated more quickly for specimens loaded at a faster loading rate.

Pull-out type bond tests are not considered to represent actual bond strength in a flexural member due to significant differences in the type of stresses induced at the reinforcement interface in flexure versus pull out load configurations. However, significant differences found in pull-out type tests are probably indicative of relative differences in bond. Chapman and Shah investigated age effect on bond strength [3.60] using pull-out bond tests conducted at various ages from 1 to 28 days of curing. Smooth bars did not show any age effect. However, the bond characteristics of deformed bars showed a significant age effect. It was observed that the equation for development length suggested by the ACI Building Code (ACI 318-89) [3.6] overestimated the test results at very early ages.

The effect of superplasticizer on the bond characteristics of normal weight concrete was investigated by Carrasquillo [3.51]. By comparing the results of pullout tests conducted on concrete mixtures containing either naphthalene or melamine with results of tests on non-plasticized concrete, it was concluded that addition of superplasticizer does not adversely affect the bond between steel and concrete.

Burge [3.46, 3.47] has reported improvement in bond strength to reinforcing steel by using condensed silica fume (CSF) for both high strength lightweight concrete and for high strength normal weight concrete. According to Elzedin and Balaguru [3.78], the presence of silica fume enhances the bond strength, but silica fume renders the concrete more brittle. A recent study [3.89] investigated interface structure and bond strength between concrete and reinforcing steel using pull-out tests. Concretes with varying strength levels and CSF dosages from 0 to 16% by weight of cement were tested. It was concluded that addition of CSF gave improved pull-out strength, see Fig. 3.25, particularly at high compressive strength levels of concrete. In addition, the interface zone was found to be "more densified", that is, to have reduced porosity and thickness.

3.2 Deformation

The deformation of concrete depends on short-term properties such as the static and dynamic modulus, as well as strain capacity. It is also affected by time dependent properties such as shrinkage and creep.

3.2.1 Static and Dynamic Elastic Modulus

The modulus of elasticity is generally related to the compressive strength of concrete. This relationship depends on the aggregate type, the mix proportions, curing conditions, rate of loading and method of measurement. More information is available on the static modulus than on the dynamic modulus since the measurement of elastic modulus can be routinely performed whereas the measurement of dynamic modulus is relatively more complex.

3.2.1.1 Static Modulus

The static modulus of elasticity can be expressed as secant, chord or tangent modulus. According to the ACI Building Code (ACI 318-89) [3.6], E_c, the static, secant modulus of elasticity, is defined as the ratio of the stress at 45% of the strength to the corresponding strain. Static, chord modulus of elasticity, as determined by ASTM C 469, is defined as the ratio of the difference of the stress at 40% of the ultimate strength and the stress at 50 millionths strain to the difference in strain corresponding to the stress at 40% of ultimate strength and 50 millionths strain.

At present there are two empirical relationships that can be used for design when the static modulus of elasticity has not been determined by tests. They are the ACI Code formula [3.6]

$$E_c = 33\, w^{1.5} \sqrt{f_c'} \quad psi \tag{3.7}$$

where w = unit weight in pounds per cubic foot (pcf) and the formula recommended by the ACI Committee 363 on High Strength Concrete [3.7] for concrete with unit weight of 145 pcf.

$$E_c = 1.0 \times 10^6 + 40{,}000 \sqrt{f_c'} \quad psi \tag{3.8}$$

This formula is based on work performed at Cornell University [3.5].

Fig. 3.26 shows the range of scatter of data with the predictions of ACI equation and the ACI Committee 363 equation. A third equation was recommended by Ahmad et al. [3.9] which seems to be more representative of the trend of the data. The equation is

$$E_c = w^{2.5} (\sqrt{f'_c})^{0.65} \quad psi \tag{3.9}$$

where w = unit weight of concrete in pcf.

Fig. 3.27 gives a comparison of experimental values of elastic modulus collected by Cook [3.65] with the predictions by the ACI 318-89 Code and the ACI Committee 363 equations. The concrete contained aggregates from South Carolina, Tennessee, Texas and Arizona. Aggregate sizes varied from 3/8 in. to 1 in. (10 to 25 mm) and consisted primarily of crushed limestones, granites and native gravels. Cook recommended the following equation which gives a better fit for the particular set of experimental data.

$$E_c = w^{2.5} (f'_c)^{0.315} \quad psi \tag{3.10}$$

where w = 151 pcf.

Fig. 3.28 summarizes test results of modulus of elasticity as a function of compressive strength. These results confirm the increased stiffness at higher strengths. Modulus of elasticity of very high strength concrete up to 17,000 psi (117 MPa) is shown in Fig. 3.29. According to Moreno [3.137], the results are generally closer to the predictions of the ACI Code (ACI 318-89) equation. However, at strength higher than 15,000 psi (105 MPa), the ACI Code equation overestimates the test results. Moreno also contends that ACI Committee 363 equation [3.7] always predicts results lower than the test data even for 17,000 psi (117 MPa) concrete and hence it was concluded that the equation recommended by the ACI committee 363 is more appropriate for higher-strength concrete.

In a recent study at NCSU [3.120] based on the results of 16 specimens with strengths varying between 8,000 psi (55 MPa) at 28 days and 18,000 psi (124 MPa) at one year, it was concluded that ACI Committee 363 [3.7] formula gave closer predictions of experimental results obtained from 6 x 12 in. (150 x 300 mm) cylinders.

The modulus of elasticity of concrete is affected by the properties of the coarse aggregate. The higher the modulus of elasticity of the aggregate the higher the modulus of the resulting concrete. The shape of the coarse aggregate particles and their surface characteristics may also influence the value of the modulus of elasticity of concrete. Figure 3.30 shows the effect of the coarse aggregate type and the mix proportions on the modulus of elasticity. From this figure it can be concluded that, in general, the larger the amount of coarse aggregate with a high elastic modulus, the higher would be the modulus of elasticity of concrete. The use of four different types of coarse aggregates in a very high strength concrete mixture (W/C = 0.27) showed that elastic modulus was significantly influenced by the mineralogical characteristics of the aggregates [3.17]. Limestone and crushed aggregates from fine-grained diabase gave higher modulus than a smooth river gravel and crushed granite that contained inclusions of a soft mineral.

It is generally accepted that regardless of the mix proportions or curing age, concrete specimens tested in wet conditions show about 15% higher elastic modulus than the corresponding specimens tested in dry conditions [3.134]. This is attributed to the effect of drying on the transition zone. Because of drying, there is microcracking in the transition zone due to shrinkage, which reduces the modulus of elasticity.

As strain rate is increased, the measured modulus of elasticity increases. Based on the available experimental data for concrete with strength up to 7,000 psi (48 MPa) [3.13, 3.23, 3.39, 3.75, 3.102, 3.126, 3.203], the following empirical equation was proposed for estimating the modulus of elasticity under very high strain rates.

$$(E_c)_{\dot{\varepsilon}} = E_c \left[0.96 + 0.038 \frac{\log \dot{\varepsilon}}{\log (\varepsilon_s)} \right] \qquad (3.11)$$

where $E_c = 27.5 \, w^{1.5} \sqrt{f_c'}$,
ε is the strain rate ($\mu\varepsilon$/sec),
$\varepsilon_s = 32 \, \mu\varepsilon$/sec.

A recent paper [3.113] has suggested that if internal strains are measured by means of embeddable strain gauges, the measured modulus is 50% higher than that from strain measurements made on the surface. The author concluded that the reason for this observation is the non-uniform strain field across the section of the cylinders.

3.2.1.2 Dynamic Modulus

The measurement of dynamic modulus corresponds to a very small instantaneous strain. Therefore the dynamic modulus is approximately equal to the initial tangent modulus. Dynamic modulus is appreciably higher than the static (secant) modulus. The difference between the two moduli is due in part to the fact that heterogeneity of concrete affects the two moduli in different ways. For low, medium, and high strength concretes, the dynamic modulus is generally 40%, 30% and 20% respectively higher than the static modulus of elasticity [3.134].

Popovics [3.162] has suggested that for both lightweight and normal weight concretes, the relation between the static and dynamic moduli is a function of density of concrete, just as is the case with relation between the static modulus and strength [3.162]. Popovics expressed E_c as a linear function of $E_d^{1.4}/\rho$, where ρ is the density of concrete.

The ratio of static to dynamic modulus is also affected by the age at testing as shown by Philleo [3.158] in Fig. 3.31. The figure indicates that at early ages (up to 6 months) the ratio of the two moduli increases from 0.4 to about 0.8 and becomes essentially constant thereafter.

A typical relationship between the dynamic modulus determined by the vibration of the cylinders and their compressive strength is shown in Fig. 3.32. It has been reported by Sharma [3.186] that the relationship between the strength and the dynamic modulus is unaffected by air entrainment, method of curing, condition at test, or type of cement.

It should also be noted that no information is available regarding the relationship between the static and dynamic modulus of elasticity for concrete with strength in excess of 8,000 psi (55 MPa).

3.2.2 Strain Capacity

The usable strain capacity of concrete can be measured either in compression or in tension. In the compression mode, it can be measured by either concentric or eccentric compression testing. In the tensile mode, the strain capacity can be either for direct tension or indirect tension. The behavior under multiaxial stress states is outside the scope of this report, and only the behavior under uniaxial stress condition will be discussed.

3.2.2.1 Stress-Strain Behavior in Compression

The stress-strain behavior is dependent on a number of parameters which include material variables such as aggregate type and testing variables such as age at testing, loading rate, strain gradient and others noted above.

The effect of the aggregate type on the stress-strain curve is shown in Fig. 3.37 which indicates that higher strength and corresponding strain are achieved for crushed aggregate from fine-grained diabase and limestone as compared to concretes made from smooth river gravel and from crushed granite that contained inclusions of a soft mineral.

A number of investigations [3.10, 3.96, 3.109, 3.142, 3.184, 3.185, 3.202, 3.207] have been undertaken to obtain the complete stress-strain curves in compression. Axial stress-strain curves for concretes with compressive strengths up to 14,000 psi (98 MPa) concrete as obtained by different researchers are shown in Fig. 3.38.

It is generally recognized that for concrete of higher strength, the shape of the ascending part of the curve becomes more linear and steeper, the strain at maximum stress is slightly higher, and the slope of the descending part becomes steeper. The existence of the postpeak descending part of the stress-strain curve has been the focus of a recent paper [3.190]. It was concluded that the postpeak behavior can be quantified for inclusion in finite element analysis and that it can have considerable influence on the predicted structural behavior and strength [3.166].

To obtain the descending part of the stress-strain curve, it is necessary to avoid specimen-testing machine interaction. One approach is to use a closed-loop system with a constant rate of axial strain as a feedback signal for closed-loop operation. The difficulties of experimentally obtaining the postpeak behavior and methods of overcoming these difficulties are described in a study by Ahmad and Shah [3.14]. For very high strength concretes it may be necessary to use the lateral strains as a feedback signal rather than the axial strains [3.183]. In a recent paper [3.114], it is argued that a more realistic description of the postpeak specimen behavior may be a complete and immediate loss of load-carrying capacity as soon as the peak load is exceeded. A different point of view is reflected in another recent paper [3.190] which suggests that there is usable strength for concrete after peak stress.

Based on the above mentioned experimental investigations, different analytical representations for the stress-strain curve have been proposed. They include use of a fractional equation [3.11, 3.175, 3.202], or a combined power and exponential equation [3.184] and serpentine curve. The fractional equation is a comprehensive, yet simple way of characterizing the stress-strain response of concrete in compression [3.9]. The fractional equation can be written as

$$f_\varepsilon = (f_c') \frac{A\left(\dfrac{\varepsilon}{\varepsilon_c'}\right) + (B - 1)\left(\dfrac{\varepsilon}{\varepsilon_c'}\right)^2}{1 + (A - 2)\left(\dfrac{\varepsilon}{\varepsilon_c'}\right) + B\left(\dfrac{\varepsilon}{\varepsilon_c'}\right)^2} \tag{3.12}$$

(for $f_\varepsilon > 0.1\, f_c'$, when $\varepsilon > \varepsilon_c'$)

where f_ε is the compressive stress at strain ε,
f_c' and ε_c' the maximum stress and corresponding strain,
A and B are parameters which determine the shape of the curve.

The values of the parameters A and B, which control the shape of the ascending and the descending parts, respectively, may be estimated by

$$A = E_c \frac{\varepsilon_c'}{f_c'} \tag{3.13}$$

$$B = 0.88087 - 0.57 \times 10^{-4}\, (f_c') \tag{3.14}$$

$$\varepsilon_c' = 0.001648 + 1.14 \times 10^{-7}\, (f_c') \tag{3.15}$$

$$E_c = 27.55\, w^{1.5} \sqrt{f_c'} \tag{3.16}$$

where f_c' is the compressive strength in psi and w is the unit weight in pcf. The parameters A, B, ε_c', and E_c are as recommended by Ahmad et al. [3.9] and were determined from the statistical analysis of the experimental results on 3 x 6 in. (75 x 152 mm) concrete cylinders [3.10, 3.184]. These cylinders were tested under strain controlled conditions in a closed-loop testing machine and had compressive strengths ranging from 3000 to 11,000 psi (20 to 75 MPa).

3.2.2.2 *Stress-Strain Behavior in Tension*

The direct tensile stress-strain curve is difficult to obtain. Due to difficulties in testing concrete in direct tension, only limited and often conflicting data are available.

Direct tensile tests were carried out on tapered cylindrical specimens of 4.7 in. diameter and 11.8 in. length (120 mm dia x 300 mm) [3.68]. For the application of the load, steel platens were glued to the top and bottom of the specimens. In order to provide plane-parallel and axial connection of these platens, a special gluing press was designed. Some 500 direct tensile tests, 300 compressive and 300 splitting tests were performed. A typical stress-strain curve with a 95% confidence region for concrete subjected to direct tension is shown in Fig. 3.39. The stress-strain curve shown in the figure is for dry specimens. The results may vary slightly for specimens tested in moist conditions.

A study at Northwestern by Gopalaratham [3.91] points out that due to the localized nature of the post-cracking deformations in tension, no unique tensile stress-strain relationship exists. According to this study, the uniaxial tensile strength can be estimated by the expression $6.5\sqrt{f_c'}$, the tangent modulus of elasticity is identical in tension and compression. The stress-strain relationship in tension before peak is less nonlinear than in compression.

Laser speckle interferometry was employed in a recent study [3.22], to investigate the behavior of concrete subjected to uniaxial tension. Unique post-peak stress-strain and stress-deformation behavior were not observed. The stress-strain response of concrete was found to be sensitive to gauge-length. Strains measured within a gauge length inside the microcracking zone were two orders of magnitude higher than values previously reported [3.79].

In a recent study [3.59], it was shown that while the use of strain gauges would lead to non-objective constitutive stress-strain relations, interferometric measurements on notched specimens allow an indirect determination of the local stress-strain and stress-separation (deformations) relations. Guo and Zhang [3.93] tested 29 specimens in direct tension and obtained complete stress-deformation curves. Based on the experimental results an equation was also derived for the stress-displacement curves.

3.2.2.3 Flexural Tension

While the information on the stress-strain behavior in tension is severely limited, virtually no data is available regarding the strain capacity in flexural tension. This is an area for which research is sorely needed to provide a basis for design where flexural cracking is an important consideration.

3.2.3 Poisson's Ratio

Poisson's ratio under uniaxial loading conditions is defined as the ratio of lateral strain to strain in the direction of loading. In the inelastic range, due to volume dilation resulting from internal microcracking, the apparent Poisson's ratio is not constant but is an increasing function of the axial strain.

Experimental data on the values of Poisson's ratio for high strength concrete is very limited [3.49, 3.155]. Based on the available experimental information, Poisson's ratio of higher strength concrete in the elastic range appears comparable to the expected range of values for lower-strength concrete. In the inelastic range, the relative increase in lateral strains is less for higher-strength concrete as compared to concrete of lower strength [3.11]. That is, higher-strength concrete exhibits less volume dilation than lower-strength concrete (see Fig. 3.44). This implies less internal microcracking for concrete of higher strength [3.50]. The lower relative expansion during the inelastic range may mean that the effects of triaxial stresses will be proportionately different for higher-strength concrete. For example, the effectiveness of hoop confinement is reported to be less for higher-strength concrete [3.11].

No data has been found for Poisson's ratio of concrete with strength greater than 12,000 psi (83 MPa).

3.2.4 Shrinkage and Creep

Shrinkage and creep are time-dependent deformations that, along with cracking, provide the greatest concern for designers because of the degree of uncertainty associated with their prediction. Concrete exhibits elastic deformations only under loads of short duration, and due to additional deformation with time, the effective behavior is that of an inelastic and time-dependent material.

3.2.4.1 Shrinkage

Shrinkage is the decrease of concrete volume with time. This decrease is due to changes in the moisture content of the concrete and physicochemical changes, which occur without stress attributable to actions external to the concrete. Swelling is the increase of concrete volume with time. Shrinkage and swelling are usually expressed as a dimensionless strain (in./in. or mm/mm) under given conditions of relative humidity and temperature.

Shrinkage of high performance concrete may be expected to differ from conventional concrete in three broad areas: plastic shrinkage, drying shrinkage, and autogenous shrinkage. Plastic shrinkage occurs during the first few hours after fresh concrete is placed. During this period, moisture may evaporate faster from the concrete surface than it is replaced by bleed water from lower layers of the concrete mass. Paste-rich mixes, such as high performance concretes, will be more susceptible to plastic shrinkage than conventional concretes. Drying shrinkage occurs after the concrete has already attained its final set and a good portion of the chemical hydration process in the cement gel has been accomplished. Drying shrinkage of high strength concretes, although perhaps potentially larger due to higher paste volumes, do not, in fact, appear to be appreciably larger than conventional concretes. This is probably due to the increase in stiffness of the stronger mixes. Data for VES and HES mixes is limited. Autogenous shrinkage due to self-desiccation is perhaps more likely with very low W/C ratio concretes, although there is little data outside indirect evidence with certain high strength concrete research [3.16].

Shrinkage is a function of the paste, but is significantly influenced by the stiffness of the coarse aggregate. The interdependence of many factors creates difficulty in isolating causes and effectively predicting shrinkage without extensive testing. The principal variables that affect shrinkage are summarized in Table 3.5 [3.3]. The key factors affecting the magnitude of shrinkage are:

A. Aggregate The aggregate acts to restrain the shrinkage of cement paste; hence concrete with higher aggregate content exhibits smaller shrinkage. In addition, concrete with aggregates of higher modulus of elasticity or of rougher surfaces is more resistant to the shrinkage process.

B. Water-cementitious material ratio The higher the W/C ratio is, the higher the shrinkage. This occurs due to two interrelated effects. As W/C increases, paste strength and stiffness decrease; and as water content increases, shrinkage potential increases.

C. Member size Both the rate and the total magnitude of shrinkage decrease with an increase in the volume of the concrete member. However, the duration of shrinkage is longer for larger members since more time is needed for shrinkage effects to reach the interior regions.

D. Medium ambient conditions The relative humidity greatly affects the magnitude of shrinkage; the rate of shrinkage is lower at higher values of relative humidity. Shrinkage becomes stabilized at low temperatures.

E. Admixtures Admixture effect varies from admixture to admixture. Any material which substantially changes the pore structure of the paste will affect the shrinkage characteristics of the concrete. In general, as pore refinement is enhanced shrinkage is increased.

Pozzolans typically increase the drying shrinkage, due to several factors. With adequate curing, pozzolans generally increase pore refinement. Use of a pozzolan results in an increase in the relative paste volume due to two mechanisms; pozzolans have a lower specific gravity than portland cement and, in practice, more slowly reacting pozzolans (such as Class F fly ash) are frequently added at better than one-to-one replacement factor, in order to attain specified strength at 28 days. Additionally, since pozzolans such as fly ash and slag do not contribute significantly to early strength, pastes containing pozzolans generally have a lower stiffness at earlier ages as well, making them more susceptible to increased shrinkage under standard testing conditions. Silica fume will contribute to strength at an earlier age than other pozzolans but may still increase shrinkage due to pore refinement.

Chemical admixtures will tend to increase shrinkage unless they are used in such a way as to reduce the evaporable water content of the mix, in which case the shrinkage will be reduced. Calcium chloride, used to accelerate the hardening and setting of concrete, increases the shrinkage. Air-entraining agents, however, seem to have little effect.

F. Cement Type The effects of cement type are generally negligible except as rate-of-strength-gain changes. Even here the interdependence of several factors make it difficult to isolate causes. Rapid hardening cement gains strength more rapdily than ordinary cement but shrinks somewhat more than other types, primarily due to an increase in the water demand with increasing fineness. Shrinkage compensating cements can be used to minimize or eliminate shrinkage cracking if they are used with restraining reinforcement.

G. Carbonation Carbonation shrinkage is caused by the reaction between carbon dioxide (CO_2) present in the atmosphere and calcium hydroxide ($CaOH_2$) present in the cement paste. The amount of combined shrinkage varies according to the sequence of occurrence of carbonation and drying process. If both phenomena take place simultaneously, less shrinkage develops. The process of carbonation, however, is dramatically reduced at relative humidities below 50 percent.

The effect of the aggregate content and the W/C ratio on the shrinkage deformations is shown in Fig. 3.33. The figure reinforces the generally recognized fact that shrinkage deformations decrease with a higher aggregate content and a lower W/C ratio.

For prediction of shrinkage strain (drying shrinkage) ε_{sh} after t days of drying, ACI Committee 209 [3.3] suggests that

$$(\varepsilon_{sh})_t = (\varepsilon_{sh})_u \frac{t^\alpha}{(f + t^\alpha)} \tag{3.17}$$

where f and α are considered to be constants for a given member shape and size,
$(\varepsilon_{sh})_u$ is the ultimate shrinkage strain.

Branson et al. [3.36, 3.37] found normal ranges of f = 20 to 130 days, α = 0.90 to 1.10 and $(\varepsilon_{sh})_u$ = 415 to 1070 microstrains. ACI Committee 209 [3.3] suggests that in the absence of specific data for local aggregates and conditions, shrinkage strain at any time t can be estimated by

$$(\varepsilon_{sh})_t = (\varepsilon_{sh})_u \frac{t}{(35 + t)} \tag{3.18}$$

after 7 days of moist curing and that

$$(\varepsilon_{sh})_u = 780\,\gamma_{sh} \tag{3.19}$$

where γ_{sh} = the product of applicable factors.

The parameter γ_{sh} is based on average thickness and values can be obtained from sections 2.5 and 2.6 of the ACI Committee 209 report [3.3].

If the usual laboratory-sized test specimens are used for determining the shrinkage properties of a concrete mix, then the predicted behavior of a concrete structure such as bridge, could well be in error unless correct allowances for size effect are used. Surface area to volume and shape effect correction factors are used to accommodate physical differences affecting drying rates. Humidity and composition effect parameters can also be applied, however, these corrections are necessarily broad. Differences in empirical data can be large. Effects in design due to these differences are usually not significant.

It should be noted that the parameter α in Equation 3.16 reflects the member shape and size effect. Experience indicated that Equation 3.16 overestimates the amount of shrinkage in an actual structure. However, there is also experimental evidence which indicates that Equation 3.16 can underestimate the shrinkage of relatively small specimens. The size effect on the prediction of the shrinkage strains by the ACI Committee 209 recommendations were investigated by Bryant and Vadhanavikkit [3.43]. The measured shrinkage strains were generally larger than predicted.

The shrinkage properties of concretes with higher compressive strengths are summarized in an ACI State-of-the-Art Report [3.7]. The basic conclusions were:

(1) Shrinkage is unaffected by the W/C ratio [3.85] but is approximately proportional to the percentage of water by volume in concrete,

(2) Laboratory [3.141] and field studies [3.97, 3.157] have shown that shrinkage of higher strength concrete is similar to that of lower-strength concrete,

(3) Shrinkage of high strength concrete containing high range water reducers is less than for lower strength concrete,

(4) Higher strength concrete exhibits relatively higher initial rate of shrinkage [3.151, 3.195], but after drying for 180 days, there is little difference between the shrinkage of high strength concrete and lower strength concrete made with dolomite or limestone.

There is conflicting information on the drying shrinkage for concrete with high range water reducers [3.40, 3.41, 3.108, 3.148]. Flowing concrete, for a given strength, is likely to require a slightly higher cement content and therefore will exhibit somewhat higher shrinkage [3.73]. Use of a HRWR to reduce water content can be expected to reduce shrinkage in most cases. Tests over a period of one year showed that the effect of naphthalene-based HRWR, with 840 to 1,000 pcy (500 to 600 kg/m^3 cement) was to reduce shrinkage [3.40].

However, there was an increase in swelling after a year of storage in water. The swelling of concrete with superplasticizer was approximately 50% greater than that of control concrete. Since swelling increases with an increase in cement content, it can be postulated that the higher swelling of the concrete with superplasticizer is due to a higher hydrated-cement paste content because of a rapid early-age development of strength. An alternative explanation is that the admixture modifies the paste structure so that its swelling capacity is increased.

In a recent study [3.62], it was shown that for five mixes with 28-day design strengths ranging from 8,700 psi to 9,300 psi (60 to 64 MPa), the shrinkage deformation was inversely proportional to the moist-curing time (the longer the curing time, the lower the shrinkage). It was also concluded that shrinkage was somewhat less for concrete mixtures with lower cement paste and larger (1.5 in. or 38 mm) aggregate size. In addition, the use of a high range water reducing admixture did not have a significant effect on the shrinkage deformation.

Observed shrinkage deformations of higher strength concrete (12,000 psi to 19,700 psi or 83 MPa to 136 MPa) were compared by Pentalla [3.153] to the predictions based on CEB Code recommendation [3.58]. It was concluded that shrinkage deformation of higher strength concrete took place much faster than predicted by the CEB formula.

In a study by Luther and Hansen [3.124], five high strength concrete mixtures were monitored for 400 days. The authors concluded that drying shrinkage in high strength concrete with silica fume is either equal to or somewhat less than that of concrete without silica fume but containing fly ash.

The use of high fly ash content (50% cement replacement by weight with low calcium, Class F fly ash) for 5,800 psi and 8,700 psi (40 MPa and 60 MPa) concretes [3.196], resulted in ultimate shrinkage values from 400 microstrains to 500 microstrains, with swelling amounting to 40% to 55% of the shrinkage value. The study also indicated the importance of continued water curing for full pozzolanic reaction of fly ash. The data [3.196] shows that shrinkage of concrete properly proportioned with high fly ash content compares favorably with that of portland cement concrete.

Field measurements of surface shrinkage strains on a mock column, fabricated with high strength concrete, after two and four years were made by Aitcin [3.16] and the measurements were compared with results on specimens under laboratory conditions. As shown in Fig. 3.34, the surface shrinkage strains under the field condition are considerably lower than those measured under the laboratory conditions.

The influence of drying and of sustained compressive stresses, at and in excess of normal working stress levels, on shrinkage properties of high, medium, and low strength concretes were investigated by Smadi, Slate and Nilson [3.189]. The 28 day compressive strength ranged from 3000 psi to 10,000 psi (21 to 69 MPa). The long-term shrinkage was found to be greater for low strength concrete and smaller for medium and high strength concretes. The study also indicated that the effect of aggregate content on the shrinkage of low strength and medium strength concrete is less significant than the effect of W/C ratio.

Based on a study period of 8 months, Bishra et al [3.34] concluded that shrinkage of latex-modified mortar was twice of the shrinkage of latex-modified concrete (LMC) and of air-entrained normal-weight concrete. Almost 95% of the total shrinkage of LMC occurred within the first 2 months, and after the third month the shrinkage deformations were of the same order of magnitude as those of air-entrained normal weight concrete.

In recent papers [3.27, 3.29] a large amount of data on carefully controlled shrinkage tests of concrete involving a large number of identical specimens was used to compare the predictive equations of ACI, CEB-FIP, and Bazant and Panula [3.30, 3.31, 3.32]. Bazant and Panula claimed that their equation (which has a large number of empirical constants) gave the best agreement with the experimental data. The validity of the Bazant and Panula equation for high strength concrete was explored by Bazant et al. [3.28], and it was reported that the equation could be made applicable to higher strength concrete with minor adjustments. Similar conclusions by Almudaiheem and Hansen [3.20] also showed good correlations with the experimental data.

3.2.4.2 Creep

Creep is the time-dependent increase in strain of hardened concrete subjected to sustained stress. It is usually determined by subtracting, from the total measured strain in a loaded specimen, the sum of the initial instantaneous strain (usually considered elastic) due to sustained stress, the shrinkage, and any thermal strain in an identical load-free specimen, subjected to the same history of relative humidity and temperature conditions. The principal variables that affect creep are summarized in Table 3.5.

Creep is closely related to shrinkage and both phenomena are related to the hydrated cement paste. As a rule, a concrete that is resistant to shrinkage also has a low creep potential. The principal parameter influencing creep is the load intensity as a function of time; however, creep is also influenced by the composition of the concrete, the environmental conditions, and the size of the specimen.

The composition of concrete can essentially be defined by the W/C ratio, aggregate and cement types and quantities. Therefore, as with shrinkage, an increase in W/C ratio and in cement content generally results in an increase in creep. Also, as with shrinkage, the aggregate induces a restraining effect so that an increase in aggregate content reduces creep.

Numerous tests have indicated that creep deformations are proportional to the applied stress at low stress levels. The valid upper limit of the relationship can vary between 0.2 and 0.5 of the compressive strength. This range of the proportionality is expected due to the large extent of microcracks in concrete at about 40 to 45% of the strength.

For prediction of creep coefficient, ν_t after t days of loading, ACI Committee 209 [3.3] suggests that

$$\nu_t = \nu_\mu \frac{t^\psi}{(d + t^\psi)} \tag{3.20}$$

where d and ψ are constants for a given member shape and size,
ν_μ is the ultimate creep coefficient.

For normal ranges, d = 6 to 30 days, ψ = 0.40 to 0.80 and ν_μ = 1.30 to 4.15 [3.36, 3.37]. ACI Committee 209 [3.3] recommends, in the absence of specific creep data for local aggregates and conditions, that

$$\nu_t = \nu_\mu \frac{t^{0.6}}{(10 + t^{0.6})} \tag{3.21}$$

for moist-cured concrete with a loading age of 7 days, and that

$$\nu_\mu = 2.35\ \gamma_c \tag{3.22}$$

where γ_c = product of applicable factors.

Values of γ_c are given in section 2.5 and 2.6 of the ACI Committee 209 report [3.3], with an average thickness as indicator of size.

As with shrinkage, use of standard-sized laboratory test specimens for determining creep properties of a concrete mix will require adjustment for size and shape effects to reasonably predict behavior of a concrete structure.

Very few data are reported on creep of concrete containing condensed silica fume. In one study [3.45], creep tests were performed on a concrete in which 25% of the cement was replaced by silica fume and a naphthalene-based high-range water reducer was added. The results showed that total deformation was reduced under drying conditions, with no significant reduction in basic creep.

Results of studies on creep of concrete containing fly ash [3.25, 3.88, 3.209] indicate that creep of sealed specimens can be reduced in the same proportions as the ratio of replacement of portland cement by fly ash, ranging between 0 and 30%, if water content is reduced substantially. However, fly ash mixes frequently show slightly higher creep under drying conditions than control mixes at the same 28-day strength, due to somewhat slower initial strength gain combined with early drying associated with standard test procedures.

Information on creep of concrete containing a high-range water reducer [3.41, 3.148] is restricted in scope. The creep of concrete with melamine-based high-range water reducer was reported to be 10% higher than control concrete [3.19]. Tests over a period of one year [3.40] showed that mixes with 840 lbs/cu yd (500 kg/m^3) cement containing a naphthalene-based high-range water reducer exhibited creep characteristics similar to control concrete; mixes with 1000 lbs/cu yd (600 kg/m^3) cement and the same high-range water reducer exhibited greater creep than control mixes. Flowing concrete for a given strength is likely to require a slightly higher cement content and it exhibits lower creep while its creep recovery and postcreep recovery elastic deformation are generally comparable to control concrete [3.73].

In a recent study by Luther and Hansen [3.124], the specific creep of five high strength concrete mixtures ($7{,}350 < f_c' < 10{,}000$ psi or $51 < f_c' < 69$ MPa) was monitored for 400 days. It was concluded that creep of the silica fume (SF) concrete was not significantly different from that of fly ash concrete. The relationship between the specific creep and compressive strength is shown in Fig. 3.35, which also includes other data from Wolsiefer [3.208], Perenchio and Klieger [3.155], Saucier [3.176], Ngab, Nilson and Slate [3.141], and Neville [3.140]. The Ngab, Nilson and Slate and Neville data have been adjusted to one year specific creep values using the equation 3.20 [3.3]. The data in the figure shows a hyperbolic relationship between specific creep and compressive strength. Also, these data [3.124] nestle between the Neville data (dashed curve on the left) and the Perenchio and Klieger data (dashed curve on the right), and they agree with the applicable Ngab, Nilson and Slate results. Furthermore, these data near high-strength levels are very close to Wolsiefer's and Saucier's results. Thus all of the concretes show similar specific creep to compressive strength relationships. Therefore, there is no apparent difference between the specific creep of silica fume (SF) concrete, portland cement concrete, or fly ash concrete.

It has been reported by Pentalla [3.153] that the creep deformation of higher-strength concrete with strengths from 12,000 psi to 19,700 psi (83 to 136 MPa) takes place much faster than the prediction by the CEB Code recommendations [3.58].

The influence of drying and of sustained compressive stresses, at and in excess of normal working stress levels, on creep properties of high, medium, and low strength concretes was investigated by Smadi, Slate and Nilson [3.189]. The 28 day compressive strength ranged from 3,000 psi to 10,000 psi (21 MPa to 69 MPa). Creep strains, creep coefficient, and specific creep were all smaller for high strength concrete than for concretes of medium and low strengths at different stress levels and at any time after loading. The creep-to-stress proportionality limit (as a percent of f_c') was higher for the high strength concrete than for the others by about 20% [3.189].

The effect of mix proportions on creep characteristics was investigated in a study [3.62], in which five mixes with 28-day design strengths ranging from 8,700 psi to 9,300 psi (60 MPa to 64 MPa) were used. The results indicated that creep is somewhat less for concrete mixtures with lower cement paste and larger aggregate size. It was also shown that the use of high-range water-reducing admixture did not show a significant effect on the creep deformations.

A very limited amount of work is reported on tensile creep tests [3.77]. Tensile creep test at 35% of the ultimate short-term strength show that specific creep increases with an increasing W/C ratio and decreasing aggregate-cement ratio. These trends are similar to those of compressive creep and the levels of specific creep are similar. Sealed concrete creeps less than immersed concrete [3.77]. Also, tensile creep generally increases with concurrent shrinkage and swelling. These effects are similar to those that occur in compression [3.77]. In another study [3.67], from uniaxial tensile creep tests, relations between the relative stress level and the time to failure were derived. These relations were not found to be affected by temperature, cement type or concrete quality. Fig. 3.36 shows the relative stress versus time to failure for the specimens subjected to uniaxial tensile creep tests.

A number of analytical models are available for estimating the creep behavior and are summarized in the ACI Committee 209 report [3.3]. In addition, there are other models such as the CEB-FIP Model Code [3.58], Bazant and Panula [3.31] and Bazant and Chern

[3.26]. The model of Bazant and Chern [3.26] based on log double-power law appears to be the most effective analytically.

3.2.5 Thermal Properties

The thermal properties of concrete are of special concern in structures where thermal differentials may occur from environmental effects, including solar heating of pavements and bridge decks. The thermal properties of concrete are more complex than for most other materials, because not only is concrete a composite material whose components have different thermal properties, but its properties also depend on moisture content and porosity.

Data on thermal properties of high performance concrete is limited, although the thermal properties of high strength concrete fall approximately within the same range as those of lower strength concrete [3.151, 3.177], for characteristics such as specific heat, diffusivity, thermal conductivity and coefficient of thermal expansion. Such other data as available involve ranges of temperature and conditions which are not pertinent to highway applications, but are included here for general interest.

Three types of tests are commonly used to study the effect of transient high temperature on the stress-strain properties of concrete under axial compression: (1) unstressed tests where specimens are heated under no initial stress and loaded to failure at the desired elevated temperature; (2) stressed tests, where a fraction of the compressive strength capacity at room temperature is applied and sustained during heating and, when the target temperature is reached, the specimens are loaded to failure; and (3) residual unstressed tests, where the specimens are heated without any load, cooled down to room temperature, and then loaded to failure.

Although fire protection of bridges and pavements is not typically a great concern, additional information on response of concrete to temperature extremes is included for completeness.

For normal strength concretes, exposed to temperatures above 450°C, the residual unstressed strength has been observed to drop sharply due to loss of bond between the aggregate and cement paste [3.117]. If concrete is stressed while being heated, the presence of compressive stresses retards the growth of cracks, resulting in a smaller loss of strength [3.1, 3.127].

The moisture content at the time of testing has a significant effect on the strength of concrete at elevated temperatures. Tests on sealed and unsealed specimens have shown that higher strength is obtained if the moisture is allowed to escape [3.94, 3.116].

For a given temperature, as the preload level is increased, the ultimate strength and the stiffness of normal strength concrete has been observed to decrease while the ultimate strain also decreases [3.178].

In a recent study, Castillo and Durrani [3.57] tested concrete with strengths from 4,500 psi to 12,900 psi (31 to 89 MPa) under temperatures ranging from 23°C to 800°C. The presence of loads in real structures were simulated by preloading the specimens before exposure to elevated temperatures. The strength of stressed and unstressed specimens of both normal and high strength concretes at different temperatures is shown in Fig. 3.40. Each point represents an average of at least three specimens normalized with respect to maximum compressive strength at room temperature. From this figure it can be seen that exposure to temperatures in the range of 100°C to 300°C decreased the compressive strength of high strength concrete by 15% to 20%. As the strength increased, the loss of strength from exposure to high temperature also increased. At temperatures above 400°C, the high strength concrete progressively lost its compressive strength which at 800 deg C dropped to about 30% of the room-temperature strength. The study also observed that none of the preloaded specimens were able to sustain the load beyond 700°C. About one third of these specimens failed in explosive manner in the temperature range of 320°C to 360°C while being heated under a constant preload. The variation of the modulus of elasticity of normal and high strength concretes with increasing temperature is shown in Fig. 3.41. The modulus decreases between 5% to 15% when exposed to temperatures in the range of 100°C to 300°C. This trend is similar for normal and high strength concretes. At 800°C, for both the normal and high strength concretes, the modulus of elasticity was only 20% to 25% of the value at room temperature.

In a recent study at Helsinki University [3.74], high temperature behavior of three high strength concretes made with different binder combinations was investigated. Ordinary cements, silica fume and class F fly ash with superplasticizers were used as binders. The aggregates were granite-based sand and crushed diabase. Compressive strengths of 4 in. (100 mm) cubes at 28 days were 12,300 psi to 16,000 psi (85 MPa to 111 MPa). The study consisted of investigations of mechanical properties at elevated temperatures, and attention was also given to the chemical and physical background of their alteration due to heating. The thermal stability and alterations were also investigated. The mechanical properties at high temperatures were studied by determining the stress-strain relationship. The risk of spalling was also studied primarily with small specimens. The three high strength concretes showed very similar high temperature behavior. They all show, in the temperature region from 100°C to 350°C, more loss of strength than normal strength concrete. This is caused by temperature-dependent destruction of cement paste. Its influence on the strength of high strength concrete is more decisive than on the normal strength concrete, because the cement paste matrix of high strength concrete must carry higher loads than in normal strength concrete (more homogeneous stress distribution between the aggregate and cement past). The denser cement paste and overall microstructure of the higher strength concrete result in slower drying. So the higher risk of destructive spalling must be taken into account in structures exposed to fire.

It is generally recognized that concrete cast and cured at low temperatures develops strengths at a significantly slower rate than similar concrete placed at room temperature. Lee [3.119] conducted a study on mechanical properties of high strength concrete in the temperature range between +20°C and -70°C (68°F and -94°F) without considering the effect of freezing cycles. Test results showed that the values of compressive and tensile strength, modulus of elasticity and Poisson's ratio increased as the temperature decreased. The ratio of bond strength at low temperature is generally larger under reversed cyclic loading than under monotonic or repeated cyclic loads. The rate of increase in compressive, splitting tensile strength, Young's modulus, local bond strength, and Poisson's ratio for high strength concrete at corresponding low temperature (-10°C, -30°C, -50°C, -70°C) is generally lower than for normal strength concrete. The effect of decreasing temperature on the compressive strength and the tensile strength is shown in Figs. 42 and 43 respectively. From these figures it can be seen that higher strength concrete shows less susceptibility to decreasing temperatures as compared to normal strength concrete.

Price [3.167], and Klieger [3.111] determined that concrete mixed and placed at 4°C had a 28-day compressive strength which was 22% lower than concrete cast and continuously cured at 21°C. However, recent work by Aitcin, Cheung, and Shah [3.18], and Gardener, Sau, and Cheung [3.87] indicated that expected slow strength development at low temperatures was not realized for cold cast and cured concretes.

3.3 Fatigue

Many theoretical and experimental studies on fatigue strength of concrete have been conducted in the past thirty years. A general discussion of the fatigue property of concrete can be found in a report of ACI Committee 215, first published in 1974 and revised in 1986 [3.5]. A report by Cornelissen [3.66] also presents a review of literature and some of the published research data.

Under repeated loads, concrete suffers damages resulting from progressive growth of internal microcracks. After a sufficient number of load repetitions, concrete fails at a load less than its static strength. The fatigue strength of concrete is therefore a fraction of its static strength that the concrete can support repeatedly for a given number of load cycles. At fatigue failure, concrete exhibits increased strains and reduced modulus (i.e. slope of its stress-strain curve) due to the progressive internal damages from microcracking.

As the static strength of concrete increases, it becomes increasingly more brittle and its ultimate strain capacity does not increase proportionately with the increase in strength. Therefore very high strength concrete could be vulnerable to fatigue loading. However, in high strength concrete, the elastic modulus of the paste and that of the aggregate are more similar, thereby reducing stress concentrations at the aggregate paste interface, which would make high strength concrete less susceptible to fatigue loading.

3.3.1 S-N Curve

The results of fatigue tests are generally expressed in a graphical form as a set of the stress-fatigue life curves, commonly referred to as S-N curves, shown in Fig. 3.45. It is noted that the S-N curves for concrete are approximately linear between 10^2 and 10^7 cycles. This means that there is no endurance limit for concrete up to 10 million cycles of loading. The S-N curve can be represented analytically by a general equation as

$$S = A - B(1 - R)\log N \tag{3.23}$$

where S = ratio of maximum stress to static strength,
R = ratio of minimum stress to maximum stress,
N = number of load repetitions,
A, B = coefficients determined experimentally.

Theoretically, the value of the coefficient A should be 1, but it is usually less than 1 as obtained from the test data.

It is generally accepted that the fatigue strength of concrete for a life of 10 million cycles is roughly 55% of its static strength. This result seems to be valid whether the loading is compression, tension, or flexure. In addition, variables such as water-cement ratio, cement content, type of aggregates, amount of entrained air, curing condition, and age of loading, affect the fatigue strength in a similar proportionate manner as they affect the static strength.

Consequently, the fatigue strength as a fraction of the corresponding static strength remains the same.

Figure 3.45 indicates the significant influence of stress range on the fatigue strength of concrete. For a given number of load cycles, a decrease of the range between the maximum and minimum stresses results in increased fatigue strength.

Fatigue test data usually show much larger scatter than that of static tests. Therefore, probabilistic procedures are used to account for the statistical nature of the test results. For a given maximum and minimum stresses and a given number of load cycles, the probability of failure can be estimated from the test data. By repeating the procedures for different numbers of load cycles, a relationship between probability of failure and number of load cycles is obtained for a given stress range. From such relationships, S-N curves for different probabilities of failure can be plotted as shown in Fig. 3.45. The fatigue curve is usually shown for a probability of failure of 50%. For design, it would be reasonable to use a lower probability of failure. Using a probabilistic approach to predict the fatigue reliability of concrete, Oh [3.143] found that the distribution of flexural fatigue life of concrete under a given stress level follows the Weibull distribution.

In a study of fatigue of concrete under biaxial compression, Su and Hsu [3.192] found that the S-N curves of concrete should be idealized by two straight lines with significantly different slopes as shown in Fig. 3.46. The slope for low-cycle fatigue is much greater than that for high-cycle fatigue. They also found that the fatigue strength of concrete under biaxial compression is greater than that under uniaxial compression.

3.3.2 Goodman Diagram

A convenient procedure for fatigue design is the modified Goodman diagram as shown in Fig. 3.47. For a zero minimum stress level, the maximum stress level which the concrete can support without failure after one million load cycles is taken conservatively as 50% of the static strength. As the minimum stress level is increased, the stress range that the concrete can support is decreased.

3.3.3 Miner's Rule

Nearly all fatigue data from laboratory tests are based on constant maximum and minimum stress values. To account for the effect of randomly varying loads on fatigue behavior of concrete, the Miner's hypothesis is widely used. According to this rule, fatigue failure occurs if

$$\sum \frac{n_i}{N_i} = 1 \qquad (3.24)$$

where n_i is the number of cycles applied at a particular stress level,
N_i is the number of cycles which will cause fatigue failure at that same stress level.

While Miner's rule has been substantiated by several recent fatigue studies [3.66, 3.174], Shah [3.182] pointed out that this rule may not be always conservative. He argued that all experimental evidence indicates that the increase of damage in concrete with cyclic loading is highly nonlinear, and thus the basic assumption of Miner's hypothesis is not valid for concrete. Based on a stress dependent nonlinear damage evolution concept, he developed a nonlinear cumulative damage law:

$$a\sum X_i^3 + b\sum X_i^2 + c\sum X_i = 1 \qquad (3.25)$$

where $X_i = N_i / N_{fi}$,
N_i = Number of load cycles applied at stress level S,
N_{fi} = Number of load cycles to failure at stress S,
a, b, c = coefficients depending on materials parameters.

3.3.4 Effect of Variation in Load Configuration

Variations in the stress field, load rate and frequency, and other factors can have a profound effect on the measured fatigue resistance of a concrete specimen. Additionally, fatigue testing frequently results in substantial experimental variability, making interpretation difficult.

3.3.4.1 Effect of Resting

The effect of rest periods between repeated load cycles is to cause a slight increase in fatigue strength of concrete. This effect is probably due to some stress relaxation during the rest period.

3.3.4.2 *Effect of Loading Rate*

Most fatigue tests have been conducted with a loading rate of at least several hertz. Under such a high rate of loading, the fatigue strength is not affected unless the stress level exceeds 75% of the static strength. For higher levels of stress with decreasing loading rate, creep effects may become more important, thus leading to a reduction in fatigue strength.

3.3.4.3 *Effect of Stress Gradient*

Fatigue strength of concrete may be influenced also by stress gradient since it tends to retard the growth of internal microcracking as it is the case in static tests. Ople and Hulsbos [3.149] conducted tests of cyclic compression with eccentricities and reported that the fatigue strength was increased by 15% to 18% due to stress gradient.

3.3.4.4 *Effect of Stress Reversal*

The great majority of fatigue tests have been conducted under pulsating stresses of tension, compression or flexure with constant amplitude. The stresses fluctuate within the tensile or compressive range. Very few tests have been conducted under alternating stresses. Such tests were carried out by Cornelissen [3.66] and the results indicated that alternating stresses (stress reversals) led to additional damages and greatly reduced the fatigue life of concrete. In addition, the number of cycles to failure for wet specimens was lower than that for dry ones.

3.3.4.5 *Effect of Impact Load Testing*

The strength of concrete under impact loading is generally higher than the static strength due to high stress rate. A test program on concrete under repeated unaxial impact tensile loading was conducted by Zielinski, et al. [3.214] and it was found that the uniaxial impact tensile strength of concrete was strongly and rapidly reduced by repeated loading. Even though the initial impact strength was 40% to 50% higher than the static splitting tensile strength, the tensile strength under 10 to 20 impact load cycles was reduced to values below the static splitting tensile strength. After 1,000 impact loading cycles with a stress rate of 2-6 $N/mm^2 \cdot ms$, the fatigue impact strength was reduced to 40% to 60% of the initial impact strength.

It was found that the relationship between the upper stress limit applied in fatigue testing and the number of impact load cycles could also be represented by the familiar S-N curve.

3.3.4.6 Effect of Air Entrainment

The effect of entrained air on fatigue strength of concrete was investigated by Lee, Klaiber, and Coleman [3.118]. In their tests, specimens with air content varying from 2.8% to 11.3% and a constant water-cement ratio of 0.41 were tested under cyclic one third-point loading. The familiar S-N curves were obtained from the test results. It was shown that air content had a definite effect on the fatigue strength of concrete in flexure. At the stress level of 65% of the flexural modulus, the anticipated fatigue life for concrete with 11.3% air was 200,000 cycles whereas the fatigue life for concrete with 2.8% air was 1,700.000 cycles.

3.3.4.7 Concluding Remark

Of all the fatigue studies found in the literature, virtually none covers the class of concrete that meets the criteria for high performance concrete as defined in this report. Fatigue tests were generally conducted when the concrete was 28 days of age or much older, with the compressive strength ranging from 3,000 to 6,000 psi (21 to 42 MPa). In some cases, the strength extended to the neighborhood of 8,000 psi (55 MPa). Thus there is a dearth of information regarding the behavior of high performance concrete subjected to fatigue loading at an early age as well as at higher stress and strength levels.

3.4 Durability

When properly designed and carefully produced with good quality control, concrete is inherently a durable material. However, under adverse conditions, concrete is potentially vulnerable to deleterious attacks such as frost, sulfate attack, alkali-aggregate reaction, and corrosion of steel. Each of these processes involves movement of water or other fluids, transporting aggressive agents through the pore structure of concrete. Therefore, porosity and permeability are important properties which affect the durability of concrete.

3.4.1 Porosity and Permeability

An excellent review of the pore structure and its influence on permeability of cement paste and concrete has been presented by Young [3.211]. It is generally agreed that for normal-weight concrete, its porosity resides principally in the cement paste. The pore structure of the paste can be classified into two types: (1) intrinsic pores in the cement gel resulting from hydration; and (2) capillary pores originating from the space initially filled with water. The size and distribution of these pores cover a very large range, from much less than 2.5 nm to 10,000 nm. Typically, the size of the gel pores is less than 10 nm whereas the size of the capillary pores is more than 10 nm. Pores of 10,000 nm or larger are classified as air voids [3.163].

3.4.1.1 Effect of W/C Ratio

The most important parameter that influences the pore structure of the paste is W/C ratio. As W/C ratio is reduced and hydration of the paste proceeds with moist curing, both capillary pore volume and pore size of the paste decrease significantly. Lower W/C ratio also increases concrete strength and thus improves its resistance to cracking from internal stresses, making concrete more impermeable. It was determined by Powers et al. [3.165] that for W/C ratio of 0.4 or less, there is virtually no permeability for cement paste as shown in Fig. 3.48. A similar curve for concrete [3.63] is also shown in the same figure. Note that the scale used for permeability coefficient of paste is 100 times larger than that of concrete. It is well known that the cement-aggregate interface is more porous than the bulk paste in all but well-cured systems. Thus the interfacial zone would be a more favorable passage for water movement, especially if there is bond breaking due to local stresses caused by differential thermal expansion between the paste and the aggregate or due to shrinkage of the paste restrained by the aggregate. Accordingly, the permeability coefficients for concrete can be as much as 100 times higher than for comparable pastes.

3.4.1.2 Effect of Curing

Porosity and permeability are also greatly affected by curing. It was shown by Powers et al. [3.164, 3.165] that for a given W/C ratio, the permeability of cement paste can be reduced significantly with increased time of moist curing as shown in Table 3.6. Well-cured pastes can achieve very low permeabilities, comparable to those of dense rocks, even though the total pore volumes of the pastes are high, see Table 3.7. This was attributed to the fact that the continuous capillary pore system through which water flows is blocked off by the deposition of hydration products.

More recently, Senbetta and Malchow [3.181] studied the effects of different curing methods on the various properties of concrete with a given mix design. They compared air cure with wax sealing, plastic cover, moist cure, and two different kinds of curing compound, all applied for 14 days. The results demonstrated that moist cure, wax sealing, and plastic cover were far superior (by several orders of magnitude) than the other three curing procedures with respect to abrasion resistance, shrinkage, resistance to corrosion of steel in concrete, chloride ion concentration in concrete, and absorptivity.

In a series of tests by Thomas et al. [3.198], the effect of curing on the strength and permeability of fly ash concrete was studied. Concrete specimens designed to have equal workability and 28 day compressive strength but with a range of fly ash contents were subjected to a range of moisture-curing periods prior to air storage. Compressive strength was then determined at various ages and permeability to oxygen and water was determined at 28 days. The results clearly indicated the importance of curing. Reductions in curing period produced lower-strength and more-permeable concrete. However, even though the strength of fly ash concrete was more sensitive to poor curing than that of the ordinary portland cement concrete, fly ash concretes moist-cured for only one day were in general no more permeable to water and much less permeable to oxygen than similarly cured concrete without fly ash.

3.4.1.3 Effect of Mineral Admixtures

The use of reactive mineral admixtures such as fly ash, slag, and silica fume reduces the total porosity and develops a finer pore structure of the cement paste. Thus the permeability is reduced and the durability of concrete is improved. The pozzolanic reaction enables a discontinuous pore system to be developed more readily [3.132]. It has been shown that higher curing temperature greatly increases the rate of pozzolanic reaction of fly ash and thus reduces waster flow [3.24]. On the other hand, the curing temperature has a much less effect on slag hydration. For the paste containing silica fume, there is a pronounced reduction in pore size because of its high pozzolanic reactivity and the very small particle size of silica fume packing efficiently between the cement grains [3.80].

3.4.1.4 Effect of Chemical Admixtures

Chemical admixtures also affect the pore size distributions and reduce permeability of the cement paste. The use of calcium chloride increases the volume of fine capillary pores and reduces that of large ones so that the paste becomes less permeable [3.131]. Water reducing agents should also reduce permeability since they are often used to lower W/C ratios. In addition, they promote a more uniform dispersion of cement grains and produce a more uniform pore structure with less coarse pores in a paste.

3.4.1.5 Measurement of Porosity

There are two methods generally used for the measurement of porosity for permeability predictions. Mercury intrusion porosimetry is used to measure the pore size distribution of capillary pores and the largest of gel pores while sorption techniques are required to investigate finer gel pores. Using mercury intrusion method, Mehta and Manmohan [3.135] predicted the permeability of hydrated cement paste as shown in Table 3.8.

Similarly, Perraton et al. [3.156] used a Carlo Erba mercury porosimeter to investigate the pore structure of silica fume concretes. Measurements were made on small concrete cores (20 x 100 mm) which, after a prescribed moist- and air-curing for 6 months, were oven-dried for 24 hours at 105°C before testing. Mercury was intruded in the sample up to a pressure of 150 MPa (21,750 psi), corresponding to an equivalent pore radius entrance of 5 nm. Fig. 3.49 shows the volume of intruded mercury in relation to pore entrance radius. The total volume of intruded mercury was slightly lower for W/C of 0.4 than for W/C of 0.5. It seemed to decrease slightly in both cases as the silica fume content increased. However, for the concrete with very low W/C of 0.24, a very low volume of mercury (23 mm^3/g) was intruded as opposed to 50 mm^3/g for the cases of W/C of 0.4 and 0.5.

As pointed out by Young [3.211], there are several drawbacks of the mercury intrusion method:

(1) Analysis of test results must use idealized assumptions of pore geometry which are not realistic;

(2) Restricted entries to large pores are a troublesome experimental problem;

(3) Paste or mortar must be thoroughly dried before mercury intrusion, thus causing significant changes of the pore structure;

(4) Drying can cause internal differential shrinkage of paste and aggregate, leading to the formation of internal microcracks;

(5) Permeability coefficient for a given paste or mortar will be different for different flow media, i.e., water, chloride ions, sulfate ions, and mercury;

(6) It takes a long time to conduct the experiments with inherently large scatter of results.

3.4.1.6 Measurement of Permeability

There is no recognized standard test method to measure the permeability of concrete. Different investigators have used different techniques and procedures. In general, there are three categories of methods: hydraulic permeability [3.34, 3.83, 3.105, 3.157, 3.195, 3.198, 3.205]; air (or gas) permeability [3.104, 3.157, 3.180, 3.195, 3.205]; and chloride ion permeability [3.45, 3.134, 3.138, 3.151, 3.157, 3.162, 3.205].

A. Hydraulic Permeability In their study to determine the water permeability of silica fume concretes under convergent flow, Perraton et al. [3.156] used a permeameter similar to what was normally used for rock samples. Using that permeameter, it was not necessary to dry the 150 x 300 mm (6 x 12 in.) specimens prior to the test at 28 days. The specimens were kept for 7 days in the permeameter cells while the water pressure was increased gradually to 7 MPa (1,000 psi). They found that the water permeability of the reference concrete with a W/C of 0.5 but without silica fume was 3×10^{-14} m/s. However, concrete with a W/C lower than 0.5 was practically impervious (with permeability coefficient less than 10^{-14} m/s) whether it contained silica fume or not.

Bisaillon and Malhotra [3.33] also found that water permeability test was not effective for concrete with W/C ratios of 0.22 and 0.27. When the tests were started at the age of 270 days, the concrete had attained a compressive strength exceeding 80 MPa (11,600 psi). Even after the concrete was placed under a pressure of 3.5 MPa (508 psi) in the permeability cell for 5000 hours, no outflow of water was observed. One test specimen with a W/C of 0.27 was broken in splitting tension and the average depth of water penetration was found to be 16 mm (0.63 in.).

Janssen [3.104] constructed a water permeameter from readily available parts and materials and utilized only standard laboratory air pressure and vacuum sources. Specimens were prepared first for saturation with de-aired water being drawn in by a vacuum of at least 45 cm (17.72 in.) mercury maintained for 24 hours. Then the permeability test was conducted with a driving pressure gradually increased to 40 psi (0.28 MPa). The test was continued for 33 days at which time the permeability of a concrete pavement core sample was found to be 420×10^{-14} m/s. The equipment has been used for permeabilities as low as 10×10^{-14} m/s.

Sullivan [3.194] described a computer-aided permeability testing system consisting of seven sample holders of the Hassler type which could handle cylindrical samples ranging from 1.5 in. to 4 in. (38 mm to 100 mm) in diameter, and from 4 to 11 in. (100 to 280 mm) in length. Confining and driving pressures could be varied independently up to 4,000 psi (28 MPa). Either liquid or gas, including brine, could be used as test medium since all tubing and containers were made of stainless steel.

Whiting [3.204] conducted water permeability tests on six different concrete mixtures with W/C ratio ranging from 0.26 to 0.75. Three concrete mixtures with the lowest W/C ratios

(0.26, 0.28, 0.40) contained water reducing agents and the one with W/C of 0.26 also contained silica fume. The 90 day compressive strength for the concrete with W/C of 0.26 and 0.28 was slightly over 15,000 psi (103 MPa) and 11,000 psi (76 MPa) respectively. Tests confirmed that permeability is a direct function of W/C ratio. The addition of silica fume would further reduce permeability. Concretes with W/C ratios less than 0.3, particularly when silica fume was utilized, were virtually impermeable to water. Permeability was greatly reduced by longer moist-curing period. For example, the permeability for the concrete with a W/C of 0.75 and 7 days moist curing was only one-fifth of that with one-day moist curing.

The above described investigations indicate that the water permeability test suffers several shortcomings. It usually needs a high driving pressure to force water to permeate through concrete and the test requires a long duration. Specimens for the test must be either oven-dried or pre-saturated. For concrete with a very low W/C ratio, the test is not effective. Furthermore, the test is not readily adaptable for field application. To overcome some of these shortcomings, several investigators introduced new techniques for permeability measurements.

Fagerlund [3.82] developed an absorption test based on the capillary absorption principle from which the resistance to water penetration, the coefficient of capillary absorption, and the effective porosity were determined. The resistance to water penetration was found to be a simple function of the capillary porosity.

Tanahashi et al. [3.197] developed a different type of water permeability apparatus which is suitable for either laboratory or field measurements. The apparatus consists of a pressure water feeding system and a pressure regulating system. When mounted on a wall or slab, the apparatus measures the permeability coefficient as the amount of water obtained from the wall or slab per unit area per unit time. The durability of field concrete is evaluated on the basis of its water-tightness which is derived from a comparison of the measured permeability coefficient with the computed coefficient from an empirical equation.

Recently, Roy [3.171] constructed a water-permeability cell based on a transient flow method. A cylindrical specimen is first placed in a flexible sleeve and connected to an upstream and downstream reservoir. At the start of a test, both reservoirs and the specimen are maintained at the same constant pressure. Fluid flow is initiated through the test specimen by rapidly establishing a pressure gradient between the upstream and downstream reservoirs. As the pressure begins to decay through the specimen, it is monitored and from this recorded pressure decay, the permeability is then calculated.

In yet another approach, Ludirdja et al. [3.123] developed a water permeameter in which a 0.5 in. thick concrete disk sample with its side sealed by a plexiglass ring is clamped between upper and lower plexiglass chambers. A pipet is mounted at the top of the upper chamber and a stainless tubing is attached to the lower chamber. Initially the lower chamber is fully filled with cold de-aired water and the upper chamber is partially filled with water. Vacuum is then applied to the upper chamber for 2 to 3 hours to remove air trapped in the specimen. After vacuum saturation is complete, the upper chamber is filled with more water extending into the pipet to maintain a 12 in. head. Cumulative flow of water through the disk sample is then measured at consecutive days. After 5 to 7 days, a steady state flow is established, and from the subsequent flow rate permeability coefficient is computed. If the lower chamber is kept empty of water so that the lower surface of the sample is exposed to air and the specimen is air-dried without vacuum saturation, the permeability coefficient would be 2 to 3 times higher due to capillary effects providing additional driving force. The tests performed with this equipment involved concretes with W/C ratios of 0.5 and 0.6. It is questionable whether this apparatus would be effective for concrete with very low W/C ratio.

B. Air Permeability In their study of concrete permeability, Perraton et al. [3.156] also conducted air permeability tests. A concrete core sample was placed in a permeability cell such that the side of the sample was surrounded by mercury which served as a sealer. The top side of the specimen was exposed to the atmospheric pressure and the bottom side exposed to a vacuum, thus drawing air through the specimen. The measured air permeability was considerably higher than the corresponding water permeability. For the reference concrete without silica fume and with a W/C ratio of 0.5, the air permeability was 5×10^{-8} m/s compared with its water permeability of 3×10^{-14} m/s. As one would expect, air permeability was found to decrease with decreasing W/C ratio. However, the air permeability was greatly affected by the method of drying the specimens. The oven-dried specimens were three times as permeable to air as the air-dried specimens.

Whiting [3.204] also conducted air permeability tests in his investigation, using standard American Petroleum Institute (API) procedures with the Hassler type permeameter [3.194]. The test results confirmed the observations discussed above with respect to his water permeability tests.

A relatively simple apparatus was used by Huovinen [3.103] for his study of air permeability of concrete. A single source of compressed air is supplied to three separate steel sample containers, each being regulated for a desired pressure. Test samples are sealed in the containers with bitumen except their top and bottom faces. Air volume passing through each sample from its top face is measured by a capillary tube at the bottom of the sample container. Using such an apparatus, Huovinen tested eleven different types of concrete with air pressures of 1, 3, and 5 bars. Other variables included temperature, length of sample, and age of concrete. The specific permeability coefficient was computed on the basis of measured air volume flow rate. The results indicated a wide range of the coefficient from 10^{-16} to 10^{-19} m^2.

In contrast to Huovinen's approach of using compressed air, Schonlin and Hilsdorf [3.179] applied vacuum to one side of a disk specimen placed inside a rubber ring with the other side of the disk exposed to the atmospheric pressure. The vacuum chamber is evacuated first to a stabilized pressure and the initial time and pressure are recorded. As the air flows through the concrete disk, the rising air pressure in the vacuum chamber is monitored until the rate of pressure increase becomes constant. Based on these pressure and time measurements, the permeability coefficient can be obtained from the following equation:

$$K = \frac{(p_1 - p_0)\, V_s L}{(t_1 - t_0)\left(p_a - \frac{p_1 + p_0}{2}\right) A} \tag{3.26}$$

where K = permeability coefficient in m^2/sec,

p_1, p_0 = pressure inside the vacuum chamber at the end and at the beginning, respectively, of the measurement in mbar

p_a = atmospheric pressure in mbar

t_1-t_0 = duration of measurement in sec

V_s = volume of vacuum chamber in m^3

L = thickness of specimen in m

A = cross-section of specimen in m^2

Schonlin and Hilsdorf's technique provides a rapid test method and requires no special devices to fix the test apparatus to the specimen. Their experience indicated that air permeability of the concrete can be measured within a period of about 15 minutes.

C. Chloride Ion Permeability Many investigators carried out studies of chloride ion permeability of concrete by using the standard procedures of AASHTO T 277 "Rapid Determination of the Chloride Permeability of Concrete". In this procedure, the specimens are conditioned first by one hour of air drying, three hours of vacuum (pressure < 1 mm Hg), one hour of additional vacuum with specimens under de-aired water, and followed by 18 hours of soaking in water. The test consists of monitoring the amount of electrical current passed through 102 mm (4 in.) diameter x 51 mm (2 in.) long specimen when one side of the specimen is immersed in a NaCl solution and the other side in a NaOH solution and a potential difference of 60V dc is maintained on the specimen for 6 hours. The total charge passed, in coulombs, is related to chloride permeability of the specimen.

Perraton et al. [3.156] observed that concrete with silica fume (dosage varying from 5% to 20% by weight of cement) was as effective in resisting chloride ion penetration as latex concrete for W/C ratios of 0.4 to 0.5 and as polymer-impregnated concrete for a W/C ratio of 0.24. They also showed that a silica fume dosage of 7.5% appeared to be the optimum for chloride ion penetration resistance. It should be noted that the silica fume concrete (6.3% dosage) with W/C ratio of 0.24 achieved a compressive strength of 71.5 MPa at 1 day , 80.4 MPa (11,660 psi) at 7 days, and 84.6 MPa (12,270 psi) at 28 days. These results and observations were corroborated by other investigators [3.136, 3.150, 3.161, 3.204].

In addition, fly ash and slag were also found to be an efficient partial replacement of cement for producing concrete almost impermeable to chloride ions [3.150, 3.161]. Whiting [3.204] also found that there were excellent correlations among the results of rapid chloride permeability tests, long-term ponding (AASHTO T 259) and hydraulic permeability tests for the same set of concrete.

Mobssher and Mitchell [3.136] conducted their study with the evaluation of the test procedure (AASHTO T 277) as one of its goals. Based on an interlaboratory test program carried out by 11 laboratories on specimens from four different concretes, they developed a precision statement which suggests that the coefficient of variation of a single test by a single operator is 12.3 percent and that the multi-laboratory coefficient of variation is 18.0 percent. They also recommended that for specimens with diameters other than the standard 3.75 in. (95 mm), a multiplying adjustment factor for the test results should be the ratio of the cross-sectional area to that of the nonstandard specimen. Their results also indicated that permeability increased with increasing entrained air content. A 1% increase in air content had the same impact on chloride permeability as a 0.03 increase in W/C ratio. Furthermore, permeability was also affected by the selection of aggregate. For a given aggregate source, concrete with densely-graded aggregates would have lower permeability than that of gap-graded aggregates. Permeability also decreased somewhat with decreasing maximum size of the aggregates.

Using a resistivity cell in which one face of a 100 mm (3.94 in.) diameter x 25 mm (1 in.) or 45 mm (1.75 in.) thick specimen is immersed in sea water and the other face immersed in saturated calcium hydroxide solution (lime water), Buenfeld and Newman [3.44] monitored the change in electrical resistance through the specimen as a measure of the chloride ion penetration into the specimen. (Note that this test setup is similar to that of AASHTO T 277 test apparatus, the only difference being that the resistance is measured rather than the current flowing through the specimen.) Their tests revealed that all specimens showed a fall in permeability (increase in resistance) on immersion in sea water. They attributed the decrease in permeability to "the formation of an aragonite-brucite layer on the surface of the mortar plus a more widespread progressive constriction of the cement paste pore system." It was suggested that "this effect also has a considerable influence upon the absorption capacity of concrete after a period of drying, which is important in the tidal and splash zones."

A series of studies dealing with chloride ion permeability of concrete made with various admixtures were summarized by Marusin [3.133]. In these studies, 10 cm (4 in.) concrete cube specimens were immersed in 15% NaCl solution for 21 days followed by an additional 21 days of air drying. Then 6 mm (0.25 in.) holes were drilled at the center of each of the six faces to obtain powder samples for chloride ion determination at four depth levels - 0 mm to 12 mm (0 in. to 0.5 in.), 12 to 25 mm (0.5 in. to 1 in.), 25 to 37 mm (1 to 1.5 in.), and 37 to 50 mm (1.5 in. to 2 in.). The chloride ion contents at these different levels were compared with the assumed corrosion threshold level chloride ion content of 0.03% for normal weight reinforced concrete. The test results indicated that for all the concrete tested, the vast majority of the absorbed chloride ion was found within the first 12 mm (0.5 in.) of depth. For concrete containing HRWR, polymer admixtures, or silica fume, the chloride ion content was greatly reduced within the depth level of 12 mm to 25 mm (0.5 in. to 1 in.) and it was mostly at the threshold level of 0.03%. So it was the portland cement concrete with W/C of 0.35. Within the depth level of 25 mm to 37 mm (1 in. to 1.5 in.), a chloride ion content below the threshold level of 0.03% was found in all cases.

In a study of permeability of concrete made with Pyrament blended cement, Carrasquillo [3.56] also used the rapid chloride permeability test (AASHTO T 277) and found that the concrete had a very low permeability in accordance with the guidelines of AASHTO T 277. The test results are summarized in Table 3.9.

3.4.2 Freeze-thaw

Damage of concrete under repeated cycles of freezing and thawing (frost attack) is a major problem of durability. It is well known that freezable water exists in the capillary pores of concrete paste, and the temperature at which the pore water freezes depends on the pore size. For instance, water in pores of 10 nm diameter will not freeze until the temperature reaches -5^{0}C. and the temperature at which water freezes in pores of 3.5 nm diameter is -20^{0}C.

When a saturated concrete is subjected to freezing, ice forms in a capillary. The volume increase of the ice causes the remaining water in the capillary to be compressed and thus a hydraulic pressure is generated. This pressure will increase as more capillary water is involved in freezing under progressively lowering temperature, unless the water can escape from the capillary to a free space by diffusing through unfrozen pores. Otherwise, the capillaries will tend to expand, causing internal stresses and microcracking, leading to severe damage of the concrete. If entrained air is used in the concrete, it provides empty space within the paste to which the excess capillary water can escape and freeze without causing damage.

Partially dry concrete is not vulnerable to frost damage for its larger capillaries are empty and provide the necessary free space throughout the paste. The critical degree of saturation is about 80% of the total freezable water. Entrained air is therefore required for protecting concrete against freezing and thawing only if the concrete is in a state of saturation or near saturation.

It is clear that the resistance of concrete to freezing and thawing depends on a number of factors. Among them are the permeability and the degree of saturation of the concrete, the amount of freezable water, the rate of freezing, and the distance from any point in the paste to a free space where water can freeze without causing any damages.

The effective use of entrained air in concrete as a defense against frost damage involves two important considerations: the total air content in the paste and the nature of the entrained air-void system.

Excessive air content has a detrimental effect in lowering the concrete strength. In general, for most air-entrained concretes 10% to 20% reduction in strength can be expected. The critical parameter of the air-void system is the spacing factor which is the average maximum distance from any point in the paste to the edge of a void. The spacing factor gives an indication of how far the freezable water in the capillary must travel to reach the air space before it freezes.

The recommended air content for the normal strength concrete is 4% to 8% by volume of concrete [3.2] and the exact amount is dependent on the maximum size of the coarse aggregate. The optimum spacing factor should be no more than 0.2 mm and the airvoids should be small with their diameter being in the range of 0.05 to 1.25 mm to ensure that the required spacing factor is obtained with low air contents.

In a study of permeability of silica fume concrete, Perraton et al. [3.156] found that there were no special problems in entraining the right amount of air in concretes containing up to 20% silica fume by weight, although the dosage of air-entraining agent had to be increased with increasing dosage of silica fume. In all cases, the spacing factors were found to be below the recommended limit of 0.2 mm. Sorensen [3.191] also reported that the frost resistance of conventional concrete was greatly affected by the drying and rewetting history of the concrete, whereas silica fume concrete was relatively unaffected. Air entrainment had equally beneficial effects on both conventional and silica fume concrete, although the latter with relatively low cement contents could be made frost resistant without air entrainment.

While the use of air entrainment for freeze-thaw protection of the normal strength concrete is a well established practice, the issue of whether air entrainment is needed for frost resistance of high strength concrete is not at all clear. Extensive discussions of the subject have been presented by Philleo [3.159] and in a FIP report [3.80]. As noted by Philleo, "The advent of this high-strength concrete has put requirements for strength and durability in conflict. Because entrained air reduces the strength of concrete, builders seek to eliminate or limit the use of entrained air. There are those who argue that high-strength concrete is of such a quality that entrained air is unnecessary." However, there are apparently conflicting research results.

Hooton [3.100] performed freeze-thaw tests according to ASTM C 666 on nonair-entrained concrete with W/(C+SF) ratio of 0.35. The cement replacement by silica fume varied from 0% to 20%. All the samples containing silica fume produced superior performance after 900 cycles of freezing and thawing, whereas the control failed only after 58 cycles. On the other hand, Malhotra et al. [3.128] also tested concretes with and without air entrainment by the same ASTM procedures. W/(C+SF) ratios from 0.25 to 0.36 with silica fume dosages of 0% to 20% were used. The results showed that all samples without air entrainment failed the test with durability factors below 12. Air-entrained concretes with 10% and 20% silica fume also failed to complete 300 cycles, probably due to the larger air void spacing factor which exceeded well over 0.2 mm.

It should be noted that for low W/C concrete, the addition of silica fume does alter the pore structure of the concrete and create more pores which are so small that water cannot freeze in them at temperature above -20^{0}C., hence the possibility of producing frost resistant concrete without entrained air. Philleo [3.159] recommended that when durability is important, silica fume should not be used in large quantities. An optimum amount is 5% to 10% by weight of cement.

Freeze and thaw studies using the ASTM C 666 procedures were performed by Carrasquillo [3.54] on concrete made with Pyrament blended cement. Three different W/C ratios of 0.25, 0.27, and 0.29 were used. Specimens for testing beginning at one day after casting were tested immediately upon removal from the forms. Specimens for testing beginning at 14 days after casting were demolded at 24 hours and stored in saturated lime water at $73.4^0F \pm 3^0F$ ($23^0C \pm 1.7^0C$) until the time of testing. Figures 3.50 and 3.51 show that for both 1 day and 14 day tests, the average relative dynamic modulus was well above 80% after more than 300 freeze-thaw cycles in all cases. It should be noted that the specimens tested starting at 1 day actually achieved a relative dynamic modulus of over 100%. This is reflective of the characteristics of Pyrament cement concrete gaining strength under freezing conditions.

One important point to recognize with respect to evaluation of frost resistance is that ASTM C 666 (AASHTO T 161) is a very severe test. Philleo [3.159] noted that it "exposes specimens to freezing at an intermediate level of maturity with no opportunity for drying before the test and exposes them to a very rapid freezing cycle. High strength specimens without air, which may ultimately become durable, cannot be expected to do well in the test." He suggested that while the test is appropriate for determining the frost resistance of young saturated specimens to severe exposure, the requirements on the test age and conditioning of specimen should be modified so that the frost resistance of more mature specimens might better be assessed under more realistic exposure conditions. Otherwise he would recommend a critical dilation test such as ASTM C 671. He further recommended that bubble-spacing factors for high strength concrete be established for different exposure conditions and that it be confirmed whether air may be entrained in high strength concrete without loss of strength.

3.4.3 Scaling

Scaling is another problem of durability. It is caused by repeated application of deicing salts. Concrete surface damaged by salt scaling becomes roughened and pitted as a result of spalling and flaking of small pieces of mortar near the surface. Even high-quality concrete with adequate air entrainment can still suffer scaling by deicing chemicals.

The exact cause of scaling is not well understood but it is recognized that when deicing chemicals are applied to melt ice, the heat consumption causes a rapid drop in the temperature of the concrete just below the surface resulting in damages from the effects of rapid freezing or differential thermal strains. Furthermore, deicing chemicals can accumulate in the surface layer of the concrete, forming relatively concentrated solutions. When water stays on the concrete surface, it flows towards the concentrated chemical solution causing an osmotic action accompanied by hydraulic pressures. These pressures may, in turn, cause salt scaling.

Scaling is most likely to occur where there is a weak layer of paste or mortar at or near the concrete surface. The best prevention of scaling is to eliminate the weak layer of material by proper mix design and good construction practice in placing, finishing, and curing. Over vibration, too much trowelling, and excessive bleeding should all be avoided. Well cured concrete pavements, allowed to dry for a period before deicing salts are applied, generally will have good scaling resistance.

Many recent studies [3.80, 3.84, 3.160] indicated that in general the scaling resistance of concrete was substantially improved by the addition of silica fume up to 16% by weight of cement. However, there were other surprising and contradicting results. It has also been reported [3.80] that certain tests with specimens containing 19% silica fume by weight and no entrained air (water/binder = 0.35) showed no scaling initially up to 110 cycles and the specimens then disintegrated rapidly. In another series of tests, a concrete with a W/C ratio of 0.45 and about 5% air content had minimal scaling but the same concrete disintegrated quickly when it was dried at 50^{0}C. and placed in water for a week just before testing. On the other hand, a concrete with water/binder ratio of 0.35, 7% silica fume, and 6% air performed well after similar treatment. These results suggest that curing history and moisture condition are important factors to field performance which can not be accounted for by the standard ASTM test procedures. Thus a need exists for new test procedures that will take into account these factors.

Scaling resistance of Pyrament-blended cement concrete was studied by Carrasquillo [3.55] according to the procedures of ASTM C 672. W/C ratios of 0.25, 0.27, and 0.29 were used. Specimens were air cured for tests started at 1 day but were moist cured for 14 days followed by 14 days of air cure for those tests started at 28 days. Three specimens were tested for each test age. As shown in Figs. 3.52 to 3.54, excellent scaling resistance was obtained in all cases. The maximum average rating of three specimens after 50 cycles of test was 2.5. The mix with W/C of 0.27 was far better than the other two mixes. The differences in performance were explained by the fact that the mix with W/C of 0.25 was more difficult to finish and that the mix with W/C of 0.29 had a higher water content.

Upon completion of 50 cycles of scaling test, Carrasquillo also examined the amount of chloride ion penetration in the test specimens at three different depths. Powder samples were taken from the depths of 0.25 in. to 0.50 in. (6 mm to 12 mm), 0.75 in. to 1.0 in. (19 mm to 25 mm), and 1.25 in. to 1.5 in. (32 mm to 38 mm). The results are shown in Figs. 3.55 to 3.57. The resistance to chloride ion penetration was excellent at depths below 1 in. (25 mm) in all cases. It is clear that because of better curing, the concrete for the 28 day tests was far more impermeable.

3.4.4 Abrasion

Abrasion is wearing due to repeated rubbing and friction. For pavements, abrasion results from traffic wear. Adequate abrasion resistance is important for pavements and bridge decks from the standpoint of safety. Excessive abrasion leads to an increase in accidents as the pavement becomes polished reducing its skid resistance.

There is no generally accepted criterion for evaluating the abrasion resistance of conventional concrete. The lack of an abrasion resistance criteria is due to the fact that surface wear normally is not a controlling factor in pavement performance. If the pavement surface is provided an adequate texture depth during construction, its design is dictated by other requirements. An exception is in areas where the use of studded tires is permitted.

Abrasion resistance of concrete is a direct function of its strength, and thus its constituent materials. High quality paste and strong aggregates are essential to produce an abrasion resistant concrete.

Mortars made with very low W/C ratio (<0.25) and high silica fume dosage ($>20\%$) are known to be highly resistant to abrasion and wear [3.80]. A new concrete code being developed in Norway will allow the use of 105 MPa (15,225 psi) concrete for structural applications. For concrete of grades above this level, studies have shown great potential of the concrete for applications requiring high abrasion resistance [3.146]. A laboratory study on abrasion-erosion was reported by Holland [3.99] in connection with a repair project using high strength silica fume concrete on the Kinzua Dam stilling basin. Figure 3.58 shows excellent abrasion resistance of silica fume concrete with Pennsylvania limestone aggregate in comparison with other types of concrete.

Recently reported research from Norway [3.147, 3.152] dealing with the studded tire wear resistance of concretes having compressive strengths ranging from 7,100 psi (49 MPa) to 14,300 psi (99 MPa) showed that abrasion resistance may be proportional to the compressive strength of concrete in these higher-strength ranges. This suggests that high performance concrete could be beneficial in improving abrasion resistance where studded tire usage is permitted.

In his studies of concrete made with Pyrament-blended cement, Carrasquillo [3.55] also investigated its abrasion resistance. Again three different W/C ratios were used: 0.25, 0.27, and 0.29. Tests were conducted according to the procedures of ASTM C 944 at 1 day and 7 days. Since the abrasion resistance can be affected by surface condition, the test surface of the specimens was given a light trowel finish initially and the specimens were tested first for flexural strength. After the flexural tests, the specimens were allowed to air dry for two hours before the start of the abrasion tests. Fig. 3.59 shows that the abrasion resistance at 1 day was greatly affected by the W/C ratio, and thus the concrete strength. However, Fig. 3.60 shows that at 7 days the abrasion resistance of all concretes was approximately equal, probably due to the fact that the concrete strength had reached a fairly high level in all three cases.

3.5 High Early Strength Effects

Traditionally, interest in the strength and other properties of concrete has been focused on those at 28 days and beyond. Recently, there has been an increasing interest in the strength and other properties of concrete at ages less than 28 days. There are at least three factors which have contributed to this increased interest in early strength: (1) the fast-paced construction schedules that expose concrete to significant structural loads at early ages, (2) the development of specialty cements or admixtures which enable the achievement of higher strength at early ages, and (3) the recognition that long-term performance of concrete is greatly affected by its early-age history.

At the present time, there is no generally accepted definition of early strength. Any strength measured at ages less than the standard 28 days is regarded as early strength. Since the properties of concrete depend closely on the degree of cement hydration, one definition of early strength could be the strength at the age corresponding to 50% hydration of cement. For concrete made with ordinary portland cement (ASTM Type I) and cured at a standard temperature of 20°C, approximately 50% of the cement will hydrate within 3 days. In a recent Engineering Foundation Conference on Properties of Concrete at Early Ages [3.48], it was recommended that the early age could possibly be defined as the period during which the properties of concrete undergo rapid change.

A total of seventeen papers were presented in the Engineering Foundation Conference [3.48]. The papers covered various topics including the following:

- Fresh concrete and early hydration
- Development of mechanical properties
- Test methods

- o Structural performance at early ages
- o Admixtures
- o Effects of early-age history on long-term properties

The Conference [3.48] presented four principal recommendations: (1) the influence of cement paste microstructure on long-term performance of concrete and the effects of early-age history on microstructure need to be understood; (2) codes and standards need to address concrete at early ages; (3) the importance of controlling the temperature rise in structures during early ages needs to be understood and methods for such control need to be implemented; and (4) increased efforts in education and technology transfer are required.

3.5.1 Effects on Mechanical Properties

Klieger in the 1950's [3.110, 3.112] defined mix proportion characteristics, consolidation techniques and curing conditions to develop one day compressive strength in excess of 2000 psi (14 MPa) for Type I cements and 4000 psi (28 MPa) for Type III cements. Accelerated curing at elevated temperatures provided one day cylinder strength up to 180% of that of equivalent moist-cured cylinders made from Type I cement. Based on his tests, Klieger recommended the following means of obtaining high quality high early strength concrete:

- o Use low W/C ratio mixes
- o Use Type III cement
- o Use mechanical vibration to permit more aggregate per unit volume
- o Use saturated steam at atmospheric pressure at temperatures below the boiling point of water, together with insulation
- o Control carefully aggregate gradation, batch weights, mixing, compaction, and curing
- o Use water curing during early hours of hydration

Recent developments in Blended Hydraulic cements, such as Pyrament-blended cement (PBC) and Pyrament-blended cement extended setting time (PBC-XT or PBC-XXT), have shown promise in developing very high early strengths. Pyrament-blended cements are complete cementitious systems including necessary functional additives and require only the addition of aggregates and water to produce the concrete mixture. It has been reported [3.168] that compressive strengths of 2000 psi to 3000 psi (14 MPa to 21 MPa) and flexural strengths of 550 psi (4 MPa) have been achieved in only 2 hours after the final set. The reported final setting time is 30-45 minutes for the PBC and 90-120 minutes for the PBC-XT type cement which compares to a setting time of 240 minutes for ASTM Type III cement. The concrete made from PBC also exhibits reduced drying shrinkage as compared to ordinary portland cement concrete [3.168].

Regulated Set cements have been used for patching due to their extremely rapid-setting and strength-gain characteristics. These materials are not particularly suited for high performance concrete applications, however. There is frequently a substantial trade-off between set and early strength characteristics. In order to attain VES strength levels, extremely short setting times are required (on the order of several minutes). Longer set times result in lower early strengths. Extremely high heat of hydration will make this material unsuitable for even moderately sized members, and low sulfate durability levels will cause the material to be unsuitable for many locations.

3.5.2 Effects on Long-Term Behavior

Klieger [3.110, 3.112] evaluated the creep and shrinkage characteristics as well as the freeze-thaw and deicer-scaling resistance of high early strength concretes. Air-entrained and nonair-entrained concretes with W/C ratios from 0.30 to 0.50, cement contents from 564 to 799 lbs/cu yd (355 to 474 kg/m^3) and compressive strengths (28-day moist-cured) up to 7630 psi (53 MPa) were tested. For air-entrained concretes, air contents ranged from 2.2 to 3% for higher cement content mixes, and 3.9 to 6% for lower cement content mixes. These tests indicated the following results:

- All concrete required intentionally entrained air for a high degree of freeze-thaw durability and deicing salt resistance.
- Concrete made with Type I and Type III are equally durable.
- Curing at elevated temperatures did not impair durability of air entrained concrete provided some drying followed prior to exposure.
- Richer mixes with lower W/C ratio showed lower creep strains than leaner mixes with a higher W/C ratio.

3.6 Interrelationships of Properties

Many of the mechanical properties of concrete discussed in the previous sections are interrelated and their relationships are expressed in quantitative terms. Some of the properties, however, may also be linked indirectly even though their relationships cannot be established explicitly. Some of these relationships will be discussed in the following sections.

3.6.1 Strength and Strain Capacity

The usable strain capacity is defined as the strain corresponding to the maximum, or peak, stress. The compressive strain capacity increases with increasing strength [3.10, 3.96, 3.109, 3.184, 3.185, 3.202, 3.207]. Based on a large number of data [3.10, 3.184], Ahmad and Shah [3.9] have suggested the following relationship to estimate the compressive strain capacity

$$\varepsilon_c' = 0.001648 + 1.14 \times 10^{-7} (f_c') \tag{3.15}$$

where f_c' is the compressive strength in psi.

It has been observed that the compressive strain capacity also increases for concrete subjected to very high rate of loading or strain rate [3.13, 3.23, 3.39, 3.75, 3.102, 3.126, 3.203]. Ahmad and Shah [3.13] have proposed the following relationship to account for the effect of strain rate.

$$(\varepsilon_c')_{\dot{\varepsilon}} = [938.46 + 11.138(\dot{\varepsilon}) + 0.272 f_c'] \beta \tag{3.27}$$

where $(\varepsilon_c')_{\dot{\varepsilon}}$ is strain capacity at fast strain rate,
$\dot{\varepsilon}$ is the strain rate ($\mu\varepsilon$/sec),
f_c' is in psi,
β is the shape factor to account for specimen size

β is given by

$$\beta = 0.80 + 0.143\,(d) - 0.033\,(h) \quad for\ \frac{h}{d} \le 5 \tag{3.28}$$

where d = diameter of the cylinder (in.),
h = height of the cylinder (in.), for eccentric compression.

Unpublished work at North Carolina State University [3.12] suggests that the strain capacity under uniaxial tension also increases with increasing strength of concrete. Since very little data is available, no recommended relationship has been proposed for estimating the tensile strain capacity.

It should be noted that under eccentric compression, concrete will generally exhibit a strain capacity considerably larger than the strain corresponding to the peak stress. However, due to brittleness, the higher the concrete strength, the smaller is the strain increment beyond the strain corresponding to the peak stress. For very high strength concrete, a conservative estimate of the usable strain capacity for eccentric compression is in the range of 0.003 to 0.004.

3.6.2 Strength and Permeability

Strength and durability are the two most important properties of high performance concrete. It is well known, that independent of all other factors, strength is greatly affected by the porosity of the concrete paste which is, in turn, dependent on W/C ratio and curing as reflected by the degree of hydration of the paste.

As for durability, perhaps the most important parameter is permeability. Concrete of low permeability resists penetration of liquids. Flow of water, gas, or chlorides mainly takes place in the open capillary pores and microcracks in the concrete. The degree of capillary porosity is primarily a function of W/C ratio and curing.

It is clear that the strength and the permeability of a concrete are interrelated through its porosity. Alternatively, W/C ratio and curing may be viewed as the common links between strength and permeability. Therefore, a high performance concrete is generally also a high quality, durable concrete of low permeability.

3.6.3 Fatigue and Tensile Strain Capacity

As discussed in section 3.3, concrete suffers damage resulting from progressive growth of internal microcracks under repeated loading. At failure, the fatigue strength of concrete is lower than its strength under a single static loading. However, the concrete strain is increased and the concrete modulus is reduced. As yet, no information is available on the limiting tensile strain value at failure due to fatigue, even though for static loading the tensile strain capacity is in the order of 100 to 200 microstrains.

For high performance concrete, with a much lower W/C ratio compared to ordinary concrete, the paste strength is much higher and microcracking in the interfacial zone between the paste and the aggregate is expected to be less. Thus the percentage increase in tensile strain at failure, for high performance concrete under fatigue loading may well be less than that for ordinary concrete.

3.6.4 Fatigue and Permeability

Recently reported fatigue studies [3.81, 3.138] have indicated that fatigue resistance of concrete is greatly influenced by the moisture condition of the test specimens. Air-dried specimens showed longer fatigue life than saturated specimens which had been submerged in water. The effect was observed mostly in fatigue with compressive loading. The phenomenon is true for both normal strength and high strength concrete. It was explained that the effect was due to the wedging action of water trapped in the microcracks and air voids of concrete that accelerated propagation of cracks. Repeated fatigue loading also increased the rate of capillary absorption.

Since the paste of high performance concrete with much lower W/C ratio will have considerably finer pore structure and the concrete will be less permeable, it is reasonable to expect that the moisture effect would be minimized for well cured high performance concrete.

4

Behavior of Fiber-Reinforced Concrete

4.1 Strength

4.1.1 Compression

The effect of fibers on the compressive properties of fiber-reinforced concrete (FRC) are expected to be less significant compared to tension and bending.

The influence of fibers in improving the compressive strength of the matrix depends on whether mortar or concrete (having coarse aggregate) is used and on the magnitude of compressive strength. Testing 6 x 12 in. (150 x 300 mm) cylinders, using steel fiber reinforcement with a volume fraction of the fiber $V_f = 2\%$, aspect ratio 100 and 3/4 inch (19 mm) maximum size aggregate, Williamson [4.61], reported an almost negligible increase in compressive strength for mortar mixtures, while an increase of about 23% was observed for concrete matrices. Fanella and Naaman [4.11] tested 3 x 6 in. (76 x 152 mm) cylinders and observed that except for the case of steel fibers, adding fibers (glass, polypropylene) to mortar matrices, does not improve their compressive strength. The increase in compressive strength with steel fibers ranged in their experiment between 0 to 15%. On the other hand, the strain at the peak stress (compressive strength) was observed to increase by the presence of any type of fibers.

Testing 4 x 8 in. (102 x 204 mm) cylinders, Otter and Naaman [4.40] reported that the use of steel fibers in lower strength concretes increases their compressive strength significantly compared to plain unreinforced matrices and is directly related to the volume fraction of steel fibers used. The compressive strength increased most using hooked steel fibers in comparison with straight steel fibers, glass, or polypropylene fibers. Strength increases of about 1.5 to 1.7 times that of plain concrete were observed for specimens with 1.4% and 2.1% volume fraction of fibers respectively.

The typical influence of fibers on the stress-strain curve of the concrete composites is illustrated in Figs. 4.1 and 4.2.

4.1.2 Flexure

Many factors influence the behavior and strength of FRC in flexure. These include: type of fiber; fiber length L; aspect ratio L/d_f (ratio of fiber length to its diameter); the volume fraction of the fiber V_f; fiber orientation and fiber shape; fiber bond characteristics (fiber deformation). Also, factors that influence the workability of FRC such as W/C ratio, density, air content and the like could also influence its strength. Depending on the volume fraction of the fibers, their length and bond characteristics, the ultimate strength could vary considerably, being either smaller or larger than the first cracking strength.

The behavior of FRC in flexure is perceived as being of primary importance in evaluating its strength and ductility of FRC composites. This is particularly true in pavement design.

Generally, three stages of load-deflection response characterize the load-deflection behavior of FRC specimens tested in flexure [4.51] as shown in Fig.4.3:

(1) A more or less linear ascending portion up to point A. The strengthening mechanism in this portion of behavior involves a transfer of stress from the matrix to the fibers by interfacial shear. The stress is shared between the matrix and fibers until the matrix cracks at what is called "first cracking strength" or "proportional limit".

(2) A transition nonlinear portion between point A and the maximum load capacity at point B (assuming the load at B is larger than the load at A). In this portion, and after cracking, the stress in the matrix is progressively transferred to the fibers. With increasing load, the fibers tend to gradually pull out from the matrix leading to a nonlinear load-deflection response until the ultimate flexural load capacity at point B is reached.

(3) A descending portion following the peak strength until complete failure of the composite. The load-deflection response in this portion of behavior and the degree at which loss in strength is encountered with increasing deformation is an important indication of the ability of the fiber composite to absorb large amounts of energy before failure and is a characteristic that distinguishes fiber-reinforced concrete from plain concrete. This characteristic is referred to as toughness and is discussed in section 4.2.3.

It should be pointed out that the nonlinear portion between A and B exists only if a sufficient volume fraction of fibers is present. For low volume fraction of fibers ($V_f < 0.5\%$), the ultimate flexural strength coincides with the first cracking strength and the load-deflection curve descends immediately following the cracking load (Fig. 4.4). Typical experimentally observed load-deflection curves of FRC beams for different types of fibers are shown in Fig. 4.5 and 4.6.

For the volume of fibers normally used (1% to 2%) and the properties normally encountered in plain concrete, the influence of fibers on the elastic properties of plain concrete, particularly the first cracking strength in tension and bending is not expected to be significant. However, while the volume fraction of fiber in the composite only slightly affects the proportional limit, it has a much greater influence on the ultimate flexural strength of the fiber composite. As shown in Table 4.1, while adding fibers in 4.6% by volume leads to a slight increase in the first cracking strength, it doubles the flexural strength of the matrix. It has been shown that, if segregation of fibers is avoided, increasing V_f results in almost a linear increase in the ultimate flexural strength of the composite [4.29]. However, for steel fibers, concentrations less than 0.5% by volume with low aspect ratio (less than 50) have negligible effect on the ultimate strength.

Increasing the aspect ratio (L/d_f) leads to an increase in the bond resistance or pull-out force and hence increases the ultimate flexural strength. Shah et al. [4.53] showed that increasing the aspect ratio of fibers up to 150, results in a linear increase in the ultimate flexural strength of the composite. Another important variable that affects the ultimate flexural strength is the orientation (distribution) of fibers. Aligned fibers (in the direction of stress) are expected, for the same fiber volume, to offer larger ultimate strength compared to randomly distributed fibers. Bergstorm [4.9] reported a flexural strength of 3,770 psi (26 MPa) for aligned deformed steel fibers of 1.2% by volume in comparison with 1,300 psi (9 MPa) flexural strength obtained using random fibers of the same volume fraction. The effect of fiber orientation on the pull-out behavior of steel fiber reinforced concrete was also studied by Naaman and Shah [4.33]. They reported that oriented fibers lead to a similar pull-out strength as aligned fibers because of additional resistance due to bending of the fibers during pull out. Crimped, indented and hooked fibers increase the ultimate strength. Fibers with hooked ends led to a flexural strength increase as high as 100% over plain concrete [4.21].

Two concepts are proposed in the literature for explaining the factors that affect the magnitude of the "first cracking strength" or proportional limit. One concept relates the "first cracking strength" to the spacing of the fibers in the composite [4.46, 4.47]. The other concept is based on the mechanics of the composite materials and relates the proportional limit to the volume fraction of the fiber, aspect ratio and fiber orientation.

In the fiber spacing concept, it is stipulated that the volume fraction of fibers and fiber aspect ratio must be such that there is a fiber overlap; however, except for this, the fiber aspect ratio L/d_f which has a significant effect on the flexural strength of FRC is not a parameter in the fiber spacing approach. Experimental results by some investigators [4.10, 4.58] tend to show that the fiber spacing concept does not accurately predict the first cracking strength of fiber-reinforced concrete. Additional discussion of the spacing concept is found in Hannant's book [4.16].

The law of composite materials is believed to be simple and is proven experimentally [4.53] to be more accurate for the prediction of first cracking strength in comparison with the fiber spacing concept. The composite materials approach is based on the assumptions that the fibers are aligned in the direction of the load, the fibers are bonded to the matrix, and the Poisson's ratio of the matrix is zero. In the law of composite materials, the effect of fibers on the cracking behavior of FRC composites can be viewed similarly to conventional reinforcing steel in concrete members. However, because the fibers are randomly distributed, an efficiency factor is commonly multiplied by the volume fraction of fibers to account for their random distribution. The efficiency factor was studied in the literature and was observed to vary between 40% [4.47] and 80% [4.39].

Because of the linear dependence of the ultimate flexural strength of FRC on the volume fraction of fibers and their aspect ratio, it could be stated that the ultimate flexural strength generally increases with the fiber reinforcing index, defined as the product of fiber volume fraction and aspect ratio ($V_f L/d_f$). Based on this observation, Shah et al. [4.53] proposed the following general equation for predicting the ultimate flexural strength of the fiber composite:

$$f_{cc} = A f_m (1 - V_f) + B\left(\frac{V_f L}{d_f}\right) \tag{4.1}$$

where f_{cc} is the ultimate strength of the fiber composite, f_m is the maximum strength of the plain matrix (mortar or concrete), A and B are constants which can be determined experimentally. For plain concrete A = 1 and B = 0. The constant B accounts for the bond strength of the fibers and randomness of fiber distribution. Swamy et al. [4.57] established values for the constants A and B as 0.97 and 4.94 for the ultimate flexural strength of steel fiber-reinforced concrete and 0.843 and 4.25 for its first cracking strength.

4.1.3 Tensile and Splitting Tensile

Cement-based matrices are known to fail in tension in a rather brittle manner and show extremely small tensile strains at failure. The addition of fibers to such matrices, whether in continuous or discontinuous form, leads to a substantial improvement in the tensile properties of the composite in comparison with the properties of the unreinforced matrix. Such properties include the maximum post cracking stress and the response of the post-peak portion of the stress-strain curve which is representative of the ductility and toughness of the composite.

Most investigations in the field of FRC derive tensile properties of the composite indirectly on the basis of observations from flexural tests or split cylinder tests. This is because there are difficulties associated with the interpretation of results obtained from direct tension tests. The difficulties are due to differences in specimen sizes, specimen shapes, instrumentations and methods of measurements. No standard test specimen is yet available for direct tension tests. As such, the observed stress-strain or force-elongation curve in direct tension is expected to vary depending on the size of the specimen, stiffness of the testing machine, gauge length used to calculate strains and the number of cracks developed within the gauge length. The primary difficulty in characterizing the tensile response of FRC composites is that the post cracking behavior is generally dominated by the widening of a single major crack as observed in several experimental tests [4.14, 4.60]. The concentration of deformation at the crack location leads to a nonuniform definition of strains in the cracked range which depends on the prescribed gauge length.

The stress-strain or load-elongation response of fiber composites in tension depends mainly on the volume fraction of fibers. In general, the response can be divided into two or three stages respectively depending on whether the composite is FRC (volume fraction less than about 3%) or Slurry Infiltrated (SIFCON) where the volume fraction of fibers normally varies between 5% and 25%. Typical stress-strain or load-elongation response for SIFCON and conventional FRC composites are depicted in Figs. 4.7 and 4.8.

Before cracking, the composite (both SIFCON and FRC) can be described as an elastic material with a stress-strain response very similar to that of the unreinforced matrix. Several approaches can be used to predict the main characteristics of the tensile stress-strain curve of fiber composites in the first linear stage before cracking. These include, the mechanics of composite materials, fracture mechanics, damage mechanics, and empirical approaches. Using the mechanics of composite materials, the tensile stress in the composite at cracking σ_{cc} can be predicted from the following equations [4.31]:

$$\sigma_{cc} = \sigma_{mu}(1 - V_f) + \alpha_1 \alpha_2 \tau V_f \frac{L}{d_f} \tag{4.2}$$

where σ_{mu} is the tensile strength of the unreinforced matrix, V_f and L/d_f are the volume fraction and aspect ratio of fibers respectively, α_1 is a bond coefficient representing the fraction of bond mobilized at matrix cracking strain, and α_2 is the efficiency factor of fiber orientation in the uncracked state of the composite. Equation (4.2) shows that a slight improvement in the first cracking strength is expected at low volume fraction of fibers.

After cracking and in bridging the cracked surface, the fibers tend to pull out under load resulting in a sudden change in the load-elongation or stress-strain curve. If the maximum post-cracking stress is larger than the cracking stress, such as in SIFCON (Fig. 4.7), then a second stage of behavior can be identified as the multiple cracking stage, and corresponds to the portion of the load-elongation curve that joins the cracking stress point to the maximum post-cracking stress point (peak point on the curve). Beyond the peak point, a third stage of behavior exists characterized by failure and/or pull-out of the fibers about a single critical crack. The corresponding descending branch of the load-elongation curve can be steep or of moderate slope depending on the fiber reinforcing parameters and whether a brittle or ductile failure occurs. Along stages I and II (Fig. 4.7), the elongation of the composite (assumed measured along a defined gage length) can be transformed into equivalent strain. However, along stage III, the elongation corresponds primarily to the opening of a single critical crack and cannot be transformed into strain since crack opening is independent of the gage length.

The multiple cracking stage described above occurs only if the maximum postcracking stress is larger than the cracking stress; otherwise, in the case of conventional FRC, with a relatively small volume fraction of fibers, the second portion of the curve vanishes and is replaced by a sudden drop in the load-elongation curve joining the cracking load to the post-cracking load. Hence the load-elongation response is reduced to two main parts (stages I and II) as illustrated in Figs. 4.8a and 4.8b. The curve of Fig. 4.8a is due to high modulus fibers such as steel fibers, while the curve of Fig. 4.8b is due to low modulus fibers such as polypropylene. A typical comparison of actual stress-elongation curves of steel fiber reinforced mortar and SIFCON is shown in Fig. 4.9.

The post cracking strength increases with increasing bond strength, aspect ratio and volume fraction of fibers. Several empirical equations were derived in the literature to calculate the ultimate strength of fiber composite in tension [4.12, 4.25, 4.31, 4.32]. Almost all equations expressed the ultimate tensile strength σ_{pc} in linear function of the fiber reinforcing index $V_f L/d_f$ and fiber bond strength τ_u as follows:

$$\sigma_{pc} = k\,\tau_u\,V_f\frac{L}{d_f} \tag{4.3}$$

where k is a constant (k<1.0) that takes into account the orientation, bond, and distribution characteristics of the fibers.

Experimental tests on splitting tensile strength of FRC are not as numerous as tests conducted in direct tension, flexure and compression. However, the same main factors that affect the behavior of FRC in direct tension, flexure and compression are expected to affect its behavior in splitting tensile mode; namely, the volume fraction, the aspect ratio, and the bond characteristics of fibers. Increasing the volume fraction of fibers and/or increasing their aspect ratio increases the splitting tensile strength of the fiber composite. Also, hooked and deformed fibers are expected to offer better splitting tensile resistance compared to straight or non-deformed fibers.

The effect of various fiber parameters on the splitting tensile strength and behavior of FRC can best be illustrated using the test results of Nanni [4.37] as shown in Table 4.2 and Fig. 4.10. It can be observed in Table 4.2 that while the fiber content has no significant effect on the first splitting-tensile cracking strength (as expected), increasing the volume fraction of fibers from 0.41% to 1.23% resulted in about 30% increase in the ultimate tensile strength. Also, for the same volume fraction of fibers, the ultimate splitting tensile strength increases with the aspect ratio of fibers. Hence the ultimate splitting tensile strength is expected to increase with increasing the fiber reinforcing index $V_f L/d_f$. Fig. 4.11 shows the type of relationship expected between the ratio of ultimate splitting tensile strength (ratio of reinforced to unreinforced matrix) and the fiber reinforcing index. The discrepancy in the data could be reduced if the reinforcing index is modified to include a bond coefficient assigned on the basis of experiments, which accounts for the different bonding characteristics of the fibers [4.38].

The load versus measured lateral deformation curves of the splitting tensile cylinders shown in Fig. 4.10, and the magnitude of toughness indices (in accordance with ASTM C 1018) given in Table 4.2, being comparable to elastic, perfectly plastic material behavior, is a clear indication of the beneficial effect of fibers on the ductility and toughness of the fiber composites under tensile loads.

4.2 Deformations

4.2.1 Modulus of Elasticity

The modulus of elasticity of a material, whether in tension, compression, or shear, is a fundamental property that is needed for modelling mechanical behavior in various structural applications. Tests have been devised to measure the moduli of elasticity of a given material. For pure materials, such as steel or glass, observed experimental values are tabulated once and for all, then used in practice. However, for composites made out of at least two different materials, the modulus of elasticity depends on various parameters.

Numerous studies have addressed the modulus of elasticity of composite materials. They lead to numerous models that range from the very simple to the very sophisticated. Among the simplest models for composites made out of two different materials, the upper-and lower-bound solutions or a combination of them (described below) only depend on the volume fraction and the modulus of each material. More-advanced models developed for fiber reinforced composites include, in addition, the properties of the interface between the two materials, whether the fibers are discontinuous or not, the distribution and orientation of the fibers, the aspect ratio (length to diameter) of the fiber, and the like.

The most common and the simplest models to predict the modulus of elasticity of FRC as a composite made out of two materials are the upper-and the lower-bound solutions or an arithmetic combination of both. They are described in details in many textbooks on composite materials and only the final solution is given below:

The upper-bound solution assumes that the fibers are continuous and oriented in the direction of loading along which the modulus of elasticity is needed. It leads to the following equation:

$$E_{cL} = E_f V_f + E_m (1 - V_f) \tag{4.4}$$

in which the subscripts ***c***, ***L***, ***f***, and ***m*** stand respectively for composite, longitudinal, fiber, and matrix.

The lower bound solution assumes that the fibers are lumped with their axis normal to the direction along which the modulus is measured. It leads to the following equation:

$$E_{cT} = \frac{E_f E_m}{(1 - V_f) E_f + V_f E_m} \tag{4.5}$$

in which the subscript ***T*** stands for transverse.

For a composite with randomly oriented fibers, Halpin and Tsai [4.15] suggested an equation based on a combination of equations (4.4) and (4.5). Although their predictions of longitudinal and transverse moduli were different from the above upper-and lower-bound solutions, their equation can be used as a first approximation with the above equations. It is given by:

$$E_c = \left(\frac{3}{8}\right) E_{cL} + \left(\frac{5}{8}\right) E_{cT} \tag{4.6}$$

Examination of Equations (4.4)-(4.6) shows that for the same volume fraction of fibers, steel fibers should improve the modulus of elasticity of the composite more than glass fibers ($E_{steel} = 3\ E_{glass}$). Also, polypropylene fibers having a modulus of elasticity lower than concrete should lead to a decrease in the elastic modulus of the composite. However, for the range of fiber volume V_f normally used in practice, the increase or decrease in E_c is expected to be of the same order as the variability in the experimental data. The same is also true of the flexural stiffness of FRC composites.

Experimental studies [4.11, 4.54] have shown that the addition of fibers have only a slight effect on the ascending branch (modulus of elasticity) of the stress-strain curve of the composite. Investigators have also observed that the effect of adding fibers in up to 4% by volume is small and linear for composites tested in flexure [4.10, 4.39, 4.53], direct tension [4.10, 4.39] and compression [4.28, 4.39]. Results showing the influence of steel fibers on the flexural stiffness of fiber composites is shown in Fig. 4.12.

A comprehensive investigation on the modulus of elasticity of fiber-reinforced cement based composites is underway at the University of Michigan at the time of this writing [4.34]. Preliminary results indicate that, although the factors suggested in Equations (4.4)-(4.6) above do influence the modulus of elasticity of the composite, other factors such as the length or aspect ratio of the fibers, their orientation, and the bond at the fiber matrix interface also have noticeable influence. It should be noted, however, that unless the fiber content is very large (more than 3% by volume), the approximate equation should give adequate results in all cases. Additional precision may not be warranted when compared to the variability usually encountered in the test results.

For the range of fiber volume normally used in practice, the dynamic modulus of fiber-reinforced concrete is little different from that of the plain, unreinforced concrete. Tests conducted by Swamy and Mangat [4.57] have shown that the dynamic modulus of FRC reinforced with up to about 2% by volume of steel fibers varied within 5% of the control unreinforced matrix. Hence, the conventional solutions for the static elastic modulus also apply for the dynamic modulus of fiber-reinforced concrete.

4.2.2 Creep and Shrinkage

Based on limited experimental data, the ACI committee 544 report [4.1] indicates that wire fiber reinforcement has no significant effect on the creep behavior of portland cement mortar. However, recent results on the creep characteristics of FRC appear to contradict the above statement.

Creep tests conducted by Balaguru and Ramakrishnan [4.6] in accordance with ASTM C 512 on steel fiber reinforced concrete (V_f = 0.6%, L/d_f = 100) subjected to a sustained load between 19% and 25% of the compression strength (stress to strength ratio between 0.19 and 0.25) showed that the creep strains were consistently higher than those of plain concrete. Also, creep tests conducted by Houde et al. [4.20] on polypropylene and steel fibers showed that the addition of fibers increases the creep strains of the fiber composite by about 20% to 30% in comparison with the unreinforced matrix.

Unlike the observation made in [4.6] and [4.20], Mangat and Azari [4.27] reported reduction in the creep strains with increasing content of steel fibers in comparison with plain concrete. For instance, at 3% by volume of fibers and at stress to strength ratio of 0.3, a reduction of about 25% in creep strain compared to plain concrete is achieved after 90 days. However, it was observed that the steel fibers were less effective in restraining the creep at high stress to strength ratio (equal to 0.55) in comparison with low stress to strength ratio (equal to 0.33). The low effectiveness of steel fibers in decreasing the creep strains at large stress to strength ratio was attributed to the reduced interfacial bond characteristics of the fibers under creep. Large stress to strength ratios increase the lateral strains and hence decrease the interfacial pressure between the fibers and the surrounding concrete. This in effect reduces the restraint to sliding action between the fibers and the concrete matrix and results in larger creep strains.

The same factors that influence the shrinkage strain in plain concrete influence also the shrinkage strain in fiber reinforced concrete; namely, temperature and relative humidity, material properties, the duration of curing and the size of the structure. The addition of fibers, particularly steel, to concrete has been shown to have beneficial effects in counterbalancing the movements arising from volume changes taking place in concrete, and tends to stabilize the movements earlier when compared to plain concrete.

The effect of fibers in restraining the free-drying shrinkage strains was found to be insignificant [4.26, 4.50] or to cause a slightly smaller shrinkage than that of plain concrete [4.6, 4.41]. If the purpose of fibers is only to restrain the free-drying shrinkage strain, then the use of short and randomly distributed fibers is more beneficial than long fibers because of the larger number of fibers available in a given volume [4.56].

The primary advantage of fibers in relation to shrinkage is their effect in reducing the adverse width of shrinkage cracks [4.26, 4.50, 4.56]. Shrinkage cracks arise when the concrete is restrained from shrinkage movements. The presence of steel fibers delays the formation of first crack, enables the concrete to accommodate more than one crack and reduces the crack width substantially [4.56]. Tests conducted on restrained shrinkage behavior of FRC have shown that the addition of small amounts of steel fibers (0.25% by volume) reduced the average crack widths by about 20% [4.50] and the maximum crack width by about 50% [4.26] in comparison with unreinforced plain concrete. Comparing the effect of different types of fibers on the restrained shrinkage characteristics, one finds that polypropylene fibers are much less effective in reducing crack widths than steel fibers [4.50].

Randomly distributed fibers could enhance the mechanical properties of shrinkage-compensating concrete by restraining the composite uniformly in all directions without adversely affecting the mechanical properties of such composites. Tests conducted by Paul et al. [4.41] on the effect of steel fibers on the expansion and drying shrinkage characteristics of expansive cement composites (Type K-conforming to ASTM C 845) have shown (Fig. 4.13) that the 7 day restrained expansion of the shrinkage-compensating concretes reinforced with straight fibers, crimped fibers and conventional steel bars were about 67%, 54% and 47% respectively of the expansion of unrestrained concrete.

4.2.3 Strain Capacity

The ability to withstand relatively large strains before failure, the superior resistance to crack propagation and the ability to withstand large deformations and ductility are characteristics that distinguish fiber-reinforced concrete from plain concrete. These characteristics are generally described by "toughness" which is the main reason for using fiber-reinforced concrete in most of its applications.

Unlike plain concrete specimens, the presence of fibers imparts considerable energy to stretch and debond the fibers before complete fracture of the material occurs. Toughness is a measure of the ability of the material to mobilize large amounts of post-elastic strains or deformations prior to failure. Typical load-deflection curves of FRC specimens in comparison with plain concrete specimens are shown in Fig. 4.14.

ASTM C 1018, provides Method A for evaluating the toughness of fiber reinforced composites through the use of a toughness index. The toughness index is calculated as the area under the load-deflection curve up to the prescribed service deflection divided by the area under the load-deflection curve up to the first cracking deflection. Three indexes are described in ASTM C 1018: I_5, I_{10} and I_{20} corresponding respectively to deflections of 3, 5.5 and 10.5 times the deflection at first cracking. These indices (computed as shown in Fig. 4.14) provide indications of the shape of the load-deflection response (post cracking) and available ductility. It should be pointed out that the value of I_5, I_{10} and I_{20} is unity for elastic, perfectly brittle material behavior and is equal to 5, 10 and 20 respectively for elastic, perfectly plastic material behavior. Indices higher than those defined above are possible (see Fig. 4.16) depending on the fiber deformation, aspect ratio and volume fraction.

The same variables that affect the ultimate flexural strength of FRC beams also influence the flexural toughness; namely, the type of fiber, volume fraction of fiber, the aspect ratio, the fiber's surface deformation, bond characteristics and orientation. Typical experimental results illustrating the effect of volume fraction, type of fibers and end anchorage on the load-deflection characteristics and Toughness Index are shown in Figs. 4.15 and 4.16. In Fig. 4.16, curves 1 and 2 correspond to specimens reinforced with 2 in. long and 0.02 in. diameter (50 x 0.5 mm) hooked-wire fibers with volume fraction of 0.75% and 0.5% respectively; curves 3 and 4 correspond to enlarged-end slit-sheet fibers of 0.71 x 0.12 x 0.24 in. (18 x 0.3 x 0.6 mm) with fiber concentration respectively of 1 and 0.5% by volume. All specimens were 4 x 4 x 14 in. long (102 x 102 x 355 mm) and tested in four point bending in accordance with ASTM C 1018.

Figure 4.15 shows that adding 1.25% fibers by volume resulted in a FRC composite having a toughness about 20 times that of the unreinforced matrix under similar loading and with similar matrix composition. Also, it can be observed from Fig. 4.16 that while only minor differences exist in the load-deflection curves up to the first cracking loads, differences in the post-cracking responses are pronounced reflecting the effect of change in fiber type and concentration on the ductility of FRC. Figure 4.16 clearly indicates that with improved fiber anchorage characteristics such as surface deformations, hooked ends or enlarged ends, a Toughness Index $I_5 > 5$ and $I_{10} > 10$ can be readily achieved with fiber volumes of more than 1%.

The same factors that affect the load-deformation response of fiber-reinforced concrete composites in the post-cracking range in the flexure tend to affect their behavior in the direct tension. In general, increasing the volume fraction and aspect ratio of fibers and enhancing their bond characteristics (hooked and crimped fibers) tend to increase the slope of the post cracking load-deformation response and hence increases the toughness of the composite fiber. The toughness of the fiber composite in direct tension (defined and measured in accordance with ASTM C 1018) can be one or two orders of magnitude higher than that of plain concrete. This is due to the large frictional-and fiber-bending energy developed during fiber pull-out on either side of the crack and due to larger deformation encountered as a result of multiple cracks (if they occur) in comparison with the single crack that normally develops in plain concrete.

Little information is available on modeling the descending branch of the stress-elongation curve of fiber-reinforced concrete composites (stage III in Fig. 4.7). However, for steel fiber reinforced concrete in which fiber pull-out occurs through a single crack (stage II of Fig. 4.8), prediction equations were proposed in [4.60] and [4.35] and are suggested for use when needed. Comparison of the analytical expression proposed in [4.60] with experimentally observed results (normalized to the maximum post cracking strength) is shown in Fig. 4.17.

Fibers are also known to increase significantly the strain capacity of concrete composites under compression loads. It can be seen from Figs. 4.1 and 4.2 that increasing the aspect ratio and/or increasing the volume fraction of fibers produces in general a less-steep descending portion, which results in a larger area under the stress-strain curve, higher ductility, and higher toughness of the composite compared to that of plain concrete. The improved toughness in compression due to fiber reinforcement is particularly useful in preventing sudden and explosive type failure under static loading and in absorbing energy under dynamic loading.

Tests conducted on steel fiber-reinforced mortar [4.11] have shown that the addition of fibers to plain mortar generally increases its toughness in compression (see Fig. 4.1). However, everything else being equal, steel fibers led to higher composite toughness than glass or polypropylene fibers. Also, for steel fiber-reinforced mortar, the toughness index was found to vary linearly with the fiber-reinforcing index.

Tests conducted on steel fiber-reinforced concrete [4.40] showed that the increase in toughness was directly related to the volume fraction of fibers with values of toughness index in compression of up to about 4 for specimens reinforced with 2.1% volume fraction of hooked steel fibers (see Fig. 4.2a). For concrete reinforced with straight, smooth fibers, increasing the aspect ratio of fibers from 45 to 80 resulted only in a minimal increase in compressive toughness (see Fig. 4.2b). The use of glass and polypropylene fibers led to low toughness values compared to steel fibers. Otter and Naaman [4.40] attributed in part the low performance of glass and polypropylene fibers to the high aspect ratios of the fibers used which led to difficult mixing and possibly higher porosity.

Considerable ductility and toughness can be achieved by using SIFCON. Experimentally observed stress-strain behavior of SIFCON in compression in comparison with plain concrete, fiber reinforced concrete, and mortar is given in Fig. 4.18.

4.2.4 Coefficient of Thermal Expansion

The authors are not aware of any investigation dealing with the thermal expansion of fiber-reinforced concrete. Since the coefficient of thermal expansion of steel is of the same order as that of concrete, it is expected that the coefficient of thermal expansion of steel fiber-reinforced concrete will be similar to that of the plain concrete matrix. When other fibers such as polypropylene or glass fibers are used in small volume fractions, the same conclusions can be drawn. However, for large volume fractions of fibers, it would be reasonable to use the simple rule of mixtures, as a first approximation, to determine the coefficient of thermal expansion, provided the temperature to which the composite is subjected does not affect significantly the properties of the fibers and their interfacial bond with the matrix.

4.2.5 Poisson's Ratio

Little information exists on the Poisson's ratio of fiber-reinforced concrete. In most analytical studies, the Poisson's ratio is generally assumed to be the same as that of concrete. This may be a reasonable assumption provided the composite remains in the elastic range of behavior. However, as soon as cracking develops, the confining effects of the fibers bridging the cracks will have a significant effect on the lateral deformation, thus the value of the measured Poisson's ratio. At the time of this writing, no investigation is known to have addressed this problem.

4.2.6 Fracture Toughness

Cementitious matrices such as mortar and concrete have low tensile strength relative to their compressive strength, and fail in a brittle manner. One way to improve their fracture properties is to reinforce them with randomly distributed fibers. There have been increasing attempts in recent years to characterize cementitious composites (i.e. concrete and fiber reinforced concrete) by their fracture properties. Both linear-elastic and elastic-plastic fracture mechanics techniques were applied. The crack growth mechanism in these materials is described in terms of three different zones: a stress-free zone, a pseudo-plastic zone, and a process zone [4.60]. The stress-free zone is the zone where the fibers have either completely pulled out or failed; the pseudo-plastic zone is the zone where the matrix has cracked but the fibers bridging the crack provide some resistance to pull-out; the process zone is the distributed region in front of an advancing crack due to the stress concentration field. The pseudo-plastic zone provides the main contribution to the fracture energy of fiber-reinforced cement composites. Apparent critical fracture energies observed [4.60] at stabilization of crack propagation were of the order of 50 lb-in/in^2 (8750 J/m^2) for fiber-reinforced mortar containing 1% fibers by volume, in comparison to 0.5 lb-in/in^2 (88 J/m^2) for plain mortar. However, the fracture toughness or the critical fracture energy cannot solely characterize fracture of fiber-reinforced concrete. The entire crack growth resistance energy is considered essential because it describes crack initiation, the slow stable crack growth process, and the crack extension prior to rapid propagation and fracture.

4.3 Fatigue

No standard test (specimen size, type of loading, loading rate, fatigue failure criteria) is currently available to evaluate the flexural fatigue performance of fiber reinforced concrete. However, several experimental fatigue studies have been conducted on steel fiber reinforced concrete and mortar in bending [4.7, 4.58, 4.62] using a testing procedure, specimen sizes, and loading conditions similar to those employed for static flexural tests of FRC or tests for conventional concrete with reversed and nonreversed type fatigue loading.

Fatigue strength can be described as the maximum flexural fatigue "stress" at which FRC composites can withstand a prescribed number of fatigue cycles before failure. Alternatively, it could be defined as the maximum number of fatigue cycles needed to fail a beam under a given maximum flexural stress level. However, the fatigue strength is often evaluated on the basis of endurance limit. The endurance limit of FRC in flexural bending is defined as the maximum flexural stress at which the beam could withstand a prescribed number of loading cycles (usually 2 million cycles), expressed as a percentage of either: 1) its virgin static flexural strength (first cracking strength or modulus of rupture), or 2) the maximum static flexural strength of plain similar unreinforced matrix (control).

The flexural fatigue strength of steel FRC was reported to be about 80% to 90% of its static flexural strength at 2 million cycles when nonreversed loading is used and about 70% of its static flexural strength when full reversed loading is used [4.1]. A conventional S-N diagram [4.7] showing the fatigue performance of steel FRC specimens with 4 x 6 in. (102 x 152 mm) cross section and 102 in. (2.6 m) span length tested under complete load reversal at a frequency of 3 Hz is shown in Fig. 4.19. The first cracking strength in this figure corresponds to that of the control fiber composite. Tests conducted by Ramakrishnan et al [4.43] at 20 Hz frequency of applied load have shown that the addition of twisted collated polypropylene fibers leads only to a slight improvement (18%) in the endurance limit (to achieve two million cycles) as compared to plain concrete.

In evaluating available fatigue data of steel FRC, Anderson [4.4] indicated that past investigations could have probably underestimated the fatigue resistance of steel FRC. This is because those investigations used the first cracking strength of the fiber composite as the reference strength. Since fiber addition modifies the cracking strength of plain concrete, Anderson pointed out that proper reference strength for fatigue evaluation of FRC beams should be taken as the unreinforced plain matrix beam strength. Using the proposed method of fatigue evaluation, Anderson showed that the fatigue resistance of already published fatigue data was much higher than reported.

Recent fatigue tests conducted on steel fiber-reinforced concrete by Ramakrishnan et al. [4.44] have shown that the addition of collated hooked-end steel fibers results in a considerable increase in the flexural fatigue strength of concrete. The flexural fatigue strength was increased by 200% to 250%, and endurance limit (to achieve two million cycles) was increased 90% to 95% compared to plain concrete.

From more recent tests of similar beam specimens with dimensions 6 x 6 x 21 in. (152 x 152 x 533 mm) in flexural fatigue under 20 Hz nonreversed loading with different types of fibers (hooked, straight, corrugated steel fibers and polypropylene fibers) and different volume fractions of fibers (0.5% and 1.0%), Ramakrishnan et al. [4.45] observed that the fatigue strength and endurance limit (to achieve two million cycles) increased with the addition of fibers and increasing volume fraction of fibers. For instance, expressed as a percentage of modulus of rupture of plain concrete, the endurance limit for mixes with corrugated end fibers was 71% for the 0.5% fiber content and 86% for the mix with 1% fiber content. This represents an increase of 9% and 32% respectively over the endurance limit of 65% observed for plain concrete. Also it was observed that the improved bond characteristics of fibers improves the fatigue strength of fiber composites. The highest increase in fatigue strength was with hooked-end steel fibers and the lowest increase was with straight steel fibers and polypropylene fibers. Ramakrishnan et al. also reported that, if expressed as percentage of its modulus of rupture rather than that of the plain unreinforced matrix, the improvement of endurance limit with increasing volume fraction of fibers is either only slight (hooked-end fibers) or unfavorable for the other types of fibers used (polypropylene). Hence the improvement in the endurance limit is only evident when expressed in relation to the unreinforced matrix. This is in support of the observation made by Anderson [4.4].

4.4 Durability

4.4.1 Abrasion Resistance

A review of abrasion studies of hydraulic structures undertaken by ACI Committee 544 [4.1-4.3], has shown that if erosion of the concrete surface is due to a gradual wearing as a result of small particles of debris rolling over the surface at low velocities, then the quality of aggregate and the hardness of the surface determine the rate of erosion. Hence fibers have no effect in this regard. On the other hand, when erosion is due to abrasion resulting from high velocity flow and impact of large debris, steel fiber concretes have provided significant erosion resistance.

Recent abrasion tests conducted by Nanni [4.36] in accordance with ASTM C 799, procedure C, on field-cut and laboratory-made specimens showed no significant difference between the abrasion resistance of plain concrete and steel or synthetic fiber-reinforced concrete. However, he found beneficial effects of steel fibers on scaling prevention of existing pavements [4.36]. As pointed out by ACI Committee 544 [4.1-4.3], abrasion as it relates to pavements, and slabs, wear under wheeled traffic is similar to the low velocity erosion in hydraulic structures where the presence of fibers is not expected to increase the abrasion resistance of concrete.

4.4.2 Freezing and Thawing

Exposure tests conducted on steel fiber-reinforced concrete [4.5] have shown that for fiber-reinforced concrete to be freezing and thawing-resistant, it must be air-entrained. However, as pointed out by ACI Committee 544 [4.1, 4.3], the addition of fibers themselves has no significant effect on the freezing-and thawing-resistance of concrete. That is, concretes that are not resistant to freezing and thawing will not have their resistance improved by the addition of fibers [4.18, 4.55]. Hence, the well-known practices for achieving durable concrete and the same air-entrainment criteria for plain concrete should be used also for fiber-reinforced concrete.

In a program to develop high-quality and durable concretes to resist chemical attack by seawater and water-borne ice, the Canada Center for Mineral and Energy Technology (CANMET) examined both the freeze-thaw resistance and abrasion resistance of FRC [4.8]. After 300 cycles of freeze-thaw (in accordance with ASTM C 666), little difference in the dynamic modulus of FRC was observed in comparison with the initial values, indicating excellent freeze-thaw resistance. It should be pointed out that all mixtures had high strengths, very low water-cementitious ratios, and an average air content of 4.5%.

Balaguru and Ramakrishnan [4.5] studied the influence of several parameters such as air content, fiber volume fraction, W/C and cement content on the freeze-thaw durability of FRC. Type I portland cement, natural sand fine aggregate and crushed limestone coarse aggregate were used. The air content was varied from 1.2% to 10.8%. Low-carbon hooked steel fibers, 2 in. (51 mm) long and 0.02 in. (0.5 mm) diameter in two contents of 75 pounds per cubic yard (pcy) (44.5 kg/m^3) and 100 pcy (59 kg/m^3) were used. Different cement contents of 611, 690 and 699 pcy (363, 409 and 415 kg/m^3) and W/C varying between 0.30 and 0.50 were investigated. For each mixture studied, six 4 x 4 x 14 in. (102 x 102 x 355 mm) specimens were tested at 300 cycles of freeze and thaw in accordance with ASTM C 666 procedure A.

They concluded that the addition of entrained air improves the freeze-thaw durability of FRC in a manner similar to that of plain concrete. It can be observed in Figs. 4.20 and 4.21 that the reduction in dynamic modulus decreases significantly by increasing the air content from 1.2% to 10.8 %. Also, for the same air entrainment, the freeze-thaw durability can be improved by increasing the cement and reducing the W/C (Fig. 4.21). Based on their experimental results, it was proposed that for a W/C of more than 0.4 (for most field applications) and cement content less than 700 pcy (415 kg/m^3), a minimum of 6% (preferably 8%) entrained air should be used to improve the freeze-thaw resistance of fiber reinforced concrete.

4.5 Applications for Pavements

Fiber-reinforced concrete has been used worldwide with and without conventional reinforcement in many field applications. These include bridge deck overlays, floor slabs, pavements and pavement overlays, refractories, hydraulic structures, thin shells, rock slope stabilization, mine tunnel linings and many precast products. The addition of fibers is known to improve most of the mechanical properties of concrete, namely, its static and dynamic tensile strength, energy absorption and toughness and fatigue resistance. Hence proper utilization of fiber-reinforced concrete depends on the skill of the engineer in taking advantage of its improved characteristics under a given loading for a given application. Many field applications in pavements have shown that FRC allows a reduction in pavement thickness of about 30 to 60% of that of conventional concrete pavement under a given load application.

The use of fiber-reinforced concrete in pavement applications started in the early 1970s. Many actual applications and experimental field studies of fiber concrete pavements and overlays have been reported [4.1-4.3, 4.19, 4.23, 4.49, 4.59] in several countries around the world. These pavement applications included bridge deck overlays, pavements and pavement overlays, airfields, taxiways, aircraft aprons, and industrial floor slabs. The size of applications (overlays and pavements) varied between those of small streets and bridge segments (in residential and rural areas) of 100 ft to 200 ft (30m to 60m) long to as large as 570,000 sq. ft (5,300 sq. m) at McCarren International Airport in Las Vegas, Nevada, 315,000 sq. ft (3,000 sq. m) at Norfolk Naval Air Station in Virginia, and about 600,000 sq.ft (5,600 sq.m) at Taoyuan Air Base in Taiwan. As reported in [4.23], 22 airport paving projects were completed in the United States as of 1983. Also, over 11 million square-feet (one million square meters) of fiber-reinforced concrete slabs were constructed as industrial floors in Europe since 1984 [4.59].

Almost all of the fiber-reinforced concrete pavement applications indicated above used steel fibers. Applications in which other commonly known types of fibers such as polypropylene, carbon, or glass fibers or a combination of fibers are almost nonexistent. The use of a combination of fibers such as steel and polypropylene to improve simultaneously the strength (using steel fibers) and ductility (using polypropylene fibers) of the concrete composite is one of the objectives of Task II of the SHRP C-205 project.

The amount of steel fiber used in experimental and actual pavement applications (bridge deck overlays, pavements and pavement overlays, airfields) varied from as low as 60 pcy (36 kg/m^3) to as high as 265 pcy (157 kg/m^3) with an average of about 175 pcy (104 kg/m^3). The cementitious content varied between as low as 550 pcy (326 kg/m^3) to as high as 970 pcy (575 kg/m^3).

Typical material properties of steel fiber-reinforced concrete used for pavements and overlays [4.2] are: flexural strength = 900 psi to 1,100 psi (6 MPa to 8 MPa), compressive strength > 6,000 psi (41 MPa), Poisson's ratio = 0.2, and modulus of elasticity = 4.0×10^6 psi (27,600 MPa). Recommended mix proportions for normal weight fiber-reinforced concrete can be found in the report of ACI Committee 544 [4.1].

Many of the early experimental and actual fiber-reinforced concrete pavements and overlays developed full-width transverse cracks within 24 to 36 hours after placing [4.19] and exhibited some degree of curling and corner cracking [4.48]. The amount of curl is typically 1/8 in. (3 mm) with a range of 0 to 5/8 in. (0 to 16 mm). Corner cracking generally begins to occur after 1 year of service and breaks in an arc of about 1 to 4 ft (0.3 to 1.2 m) radius around the corners where longitudinal and transverse joints meet.

Curling is a common problem of concern in concrete pavements and overlays and does not depend on whether FRC or conventional concrete is used. Although it is difficult to find a common denominator to the degree of curling or cracking, several recommendations have been presented [4.23, 4.24, 4.48] to minimize the level of curling and cracking in FRC pavements and overlays. These include: (1) reducing the cement content and increasing the aggregate content of the concrete, (2) replacing a portion of the cement content with fly ash, (3) using shrinkage compensating concretes, and (4) using water-reducing and set-retarding admixtures.

5

Applications of High Performance Concrete

5.1 Pavements

5.1.1 Potential Benefits for Pavements

To date, the use of high performance concrete in highway pavement applications has been limited. However, its use in other applications indicates that there is potential for significant benefits from its use in pavements. Possible benefits include reduced construction times, rapid pavement repairs, improved pavement durability, reduced studded-tire wear, and increased pavement life. The major benefit for new highways would be improved durability and a resultant increase in service life. However, the benefit that holds the greatest promise is likely the shortening of closure times for repair and rehabilitation efforts with no loss in future performance.

With the nation's highway network essentially complete, the emphasis for the foreseeable future will be on rehabilitation and reconstruction. Repair and construction times are extremely important aspects of this type of work. Disruption of traffic and reduced safety are major concerns which must be dealt with during any repair or construction effort. The use of high performance concrete offers potential for opening pavement patches, lane additions, and pavement overlays within a very short period of time. For example, the use of high early strength (HES) concrete could make it feasible to open newly constructed pavements and overlays to traffic within 24 hours. Very early strength (VES) concrete may offer even greater benefits. Its use presents the potential for overnight construction and repair. This would be particularly attractive for pavement overlays and lane additions where work requiring lane closures would be performed at night. Rehabilitation and reconstruction could be completed without disrupting traffic during heavy traffic periods.

The use of fast track paving can provide some of the benefits described above. The following examples illustrate the benefits of this approach. In 1987, a one-mile section of highway in Dallas County, Iowa was closed to traffic at 7:30 a.m., paved that same day, then reopened to traffic at 5:00 p.m. the following day [5.6]. A second project involved the reconstruction of nine busy intersections in Cedar Rapids, Iowa [5.5, 5.9]. Here, the contractor was allowed to close each intersection only between the hours of 6 p.m. and 6 a.m.. Each intersection could be closed only twice during the construction period. During the first closure, the contractor removed the existing pavement, prepared the grade, placed a base course and a temporary surfacing. The concrete overlay was placed during the second closure. Thus, the nine intersections were totally repaved without being closed during any high-traffic period. To date, the concretes used in fast track projects have not been high-performance concretes as defined earlier in this report. Combining the use of high-performance concretes with fast track paving techniques could provide even greater benefits.

High performance concrete also offers the potential for making permanent repairs during adverse weather conditions. Some very early strength concretes reportedly can be placed in sub-freezing weather without sacrificing strength or durability. This capability would eliminate the need to place temporary repairs under emergency conditions that must later be replaced with permanent repairs. This would be especially beneficial in repairing utility cuts made during the winter.

5.1.2 Reported Use of High Performance Concrete in Pavements

There is little actual use of high performance concrete in current pavement applications, judging from the lack of references available in the literature on this topic. In cases where higher strengths, improved durability, improved wear resistance, or reduced costs have been reported for pavements, these benefits can usually be attributed to a construction technique (such as roller-compacted concrete or fast track paving) more so than to the concrete itself. In cases where benefits have been shown to be directly related to the concrete, the material usually has not been high performance as defined earlier in this report. In addition, progress reports from research related to the long term study of high performance concrete in pavements are seriously lacking. There are reports regarding the mechanical properties of high performance concretes intended for use in pavements, but very few reports regarding their actual use and performance in the field. One area where high performance concretes have been used and their performance reported is patching [5.4, 5.13, 5.15, 5.17, 5.19, 5.20]. As noted previously, there is significant potential benefit for this application due to the very early and high early strength of high performance concretes permitting rapid repair and reducing lane closure times.

Research in the patching area has focused on various types of binding agents and their effects on many properties of concrete including compressive strength, flexural strength, early strength gain characteristics, set times, fatigue behavior, freeze/thaw durability, and bond to the existing material. In addition, the effects of extreme casting and curing temperatures and patch depths on performance have been examined. Many different types of binding agents have been evaluated for such applications. Consideration has been given to portland cement-based, polymer-based, and other nonportland cement-based concretes. The portland cement concretes are typically modified by the use of Type III cement, water-reducing agents, silica fume, or some combination of these materials. The polymer concretes utilize a polymer such as methyl methacrylate, which does not require water to be activated, as the binding agent. The nonportland cement concretes may be a high alumina cement, regulated set cement, gypsum, or a magnesium phosphate (MP) cement concrete. Magnesium phosphate cements may be water or nonwater activated.

El-Jazairi [5.19] investigated the properties and performance of one magnesium phosphate (MP) cement commercially known as Set-45. He reported that at normal temperatures MP mortars and concretes set up in 15 to 20 minutes and have compressive strengths of at least 2,900 psi (20 MPa) in one hour. The effects of extreme temperatures on set time can be offset by either controlling the temperature of the mixing water or using special admixtures. The MP concrete described by El-Jazairi was found to provide adequate strength at very early ages. Compressive strengths of 3,500 psi (24 MPa) were achieved in one hour with the 3 hour and 24 hour strengths being 5,000 psi (35 MPa) and 7,000 psi (48 MPa) respectively. Even at low temperatures, a one-hour strength of 2,000 psi (14 MPa) was achieved by adding an accelerator. The flexural and tensile strengths were reported to be similar to that of high strength concrete.

In addition to strength properties, El-Jazairi examined other properties that are important to successful pavement patching. These include shrinkage and thermal expansion characteristics, bonding strength, modulus of elasticity, and durability.

Shrinkage characteristics and the coefficient of thermal expansion are of concern because they influence cracking and debonding. The shrinkage potential should be small and the thermal coefficient should be close to that of the existing pavement (conventional concrete). El-Jazairi reported that the MP concrete has acceptable shrinkage and thermal properties. He also stated that the modulus of elasticity of MP concrete is similar to that of conventional concrete. The bonding shear strength of MP concrete was measured using a slant shear bond test, and bonding potential of MP concrete was found to be comparable to that of epoxy materials. Relative to durability, El-Jazairi reported that MP concrete has low permeability with its frost and salt-scaling resistance being similar to that of an air-entrained concrete.

Also, the presence of phosphates aid in preventing corrosion of reinforcement. He examined a number of patches placed in 1981 and 1982 and found no signs of material failure or deterioration in 1987.

Studies of patching materials for low temperature conditions (15°F to 20°F) were conducted by Nawy, Kudlapur, and others [5.13, 5.15]. In these studies, four methyl methacrylate (MMA) based polymer concretes, two magnesium phosphate based concretes, and a polyurethane polymer concrete were tested for various strength and durability properties. Three different patch depths, shallow, half, and full, were considered. All of the patch materials, except the polyurethane, had one-day compressive strengths in the range of 4,600 psi to 9,700 psi (38 MPa to 67 MPa). The plain MMA concretes showed a loss of strength at 7 days while all other concretes showed a gain. Compressive slant shear tests for patch to pavement bond showed the MMA-based concretes to be superior with strengths at 1 day equal to the strengths of other materials at 7 days. Results from static and fatigue flexure tests proved highly variable. The freeze-thaw durability of all materials, except the water-activated MP concrete, was better than the parent concrete which was a standard mix with Type III cement with an air content of 5.5 to 7 percent. Overall, the nonwater activated MP concrete was recommended as a good compromise material while the polyurethane was found inferior in all respects.

A similar study was conducted by Popovics and Rajendran [5.17]. They examined the early age properties of magnesium phosphate based cements under a range of temperature conditions. The laboratory testing centered on set times and strength development in the first 24 hours. No data on the long term properties was reported. Three magnesium phosphate cement formulations, one for normal to cold conditions (MP-C), another for hot conditions (MP-H), and a 50-50 blend of the two (MP-CH) were used. A total of 35 different mixes were tested. The material, mixing water, and curing temperatures all ranged from 32°F to 100°F (0°C to 38°C) in eight different combinations to simulate different weather conditions. Initial and final set times along with compressive strengths at 1, 3, and 24 hours were recorded. The set times for all MP cements were found to be much less than that for standard portland cements. Set times ranged from less than 5 minutes to nearly 2 hours. Most mortars had compressive strengths of at least 2,000 psi (14 MPa) at 1 hour regardless of the temperature conditions. Compressive strengths at 3 hours were around 3,000 psi (21 MPa). In general, the hot weather cement formulation (MP-H) had the highest early strengths for all material and temperature combinations considered. This cement reached 90% to 95% of its 24-hour strength in the first hour. The MP-H formulation also proved to have the best potential under the various temperature conditions considered.

5.1.3 Parameters of Concern for Pavement Design and Performance

Despite the lack of extensive information regarding the use of high performance concrete in pavements, the properties that need to be studied can be identified. Those properties of concrete which influence the performance of conventional concrete pavements can be expected to have similar effects on pavements constructed of high performance concrete. An understanding of those effects would indicate the information needed to effectively utilize high performance concrete in pavements.

5.1.3.1 Pavement Strength, Thickness, and Fatigue

The main emphasis of most pavement design procedures is the determination of the required pavement thickness. Typically, these procedures use some type of fatigue-based approach. The pavement thickness is selected, at least in part, on the basis of a stress ratio and the number of load repetitions. The two most commonly used design procedures for rigid highway pavements are the PCA [5.22] and the AASHTO Guide [5.2] procedures, both of which incorporate fatigue considerations.

The PCA design procedure directly incorporates a fatigue analysis as part of the pavement thickness selection process. The fatigue analysis involves a relationship between an allowable number of load repetitions and a ratio of the load induced flexural stress and concrete flexural strength. The fatigue relationship is based on the 28-day flexural strength of the concrete and assumes a normal rate of strength gain. In other words, it accounts for the fact that the stress ratio will decrease for a given flexural stress as the concrete gains strength.

Unlike the PCA procedure, the AASHTO Guide procedure does not directly include a fatigue analysis. The AASHTO procedure is empirical and based on data collected from the AASHO Road Test [5.1]. A fatigue approach was employed in extrapolating this procedure to concrete and soil strengths other than those used in the Road Test. The extrapolation involved the addition of a stress ratio term to the original design equation. Because of its empirical nature, the AASHTO procedure also includes the effects of concrete strength gain, at least for the two years of the Road Test.

In order to account for fatigue in pavements constructed of high performance concrete, it will be necessary to understand the fatigue behavior of the concrete as well as its long term strength gain characteristics. Additional consideration will also need to be given to the fact that high performance concrete pavements will normally be opened to traffic very quickly. Even if their compressive strengths are comparable at the time of opening to traffic, the effect of very early loads on the high performance concrete may be different from that of conventional concrete.

5.1.3.2 Load Transfer and Pavement Thickness

The traditional emphasis on fatigue analysis for pavement thickness design might suggest that the higher strengths of high performance concrete would justify a reduction in the required thickness. However, the stress-strength ratio is not the sole determinant of thickness.

Joint faulting and the erosion of subsurface materials (subgrade and base) play an important role in the performance of most concrete pavements. The previous version of the PCA design procedure based thickness selection solely on the stress ratio and fatigue cracking. In recognition of the influence of faulting and erosion, the current PCA procedure includes an erosion analysis. Concrete strength does not enter into the erosion analysis but thickness does. For pavements with heavy traffic, the design thickness is usually controlled by the erosion analysis [5.16]. Thus, a reduced pavement thickness may not be warranted simply because of higher strengths or improved fatigue properties.

Load transfer is another factor influencing erosion and faulting. For plain concrete (non-reinforced) pavements, aggregate interlock alone is sometimes relied upon for load transfer. However, most concrete pavements include smooth, round steel dowels at the joints for load transfer. The long term efficiency of these dowels is believed to be a function of the bending moment in the bar and the bearing stress between the bars and the concrete when a load passes over the joint. Because the strength properties of high performance concrete differ from those of conventional concrete, the allowable bearing stress may also differ.

5.1.3.3 Modulus of Elasticity

The modulus of elasticity of concrete is a necessary parameter in pavement stress analysis. Thus, it is needed for fatigue analysis and any rational design procedure.

The modulus of elasticity is needed explicitly in the AASHTO Guide design procedure. This is not the case for the PCA procedure. However, the modulus has been accounted for indirectly since typical modulus values for normal concrete were used in developing the procedure. If a similar procedure was developed for pavements with high performance concrete, the modulus of elasticity of the concrete would need to be known.

5.1.3.4 Shrinkage and Thermal Contraction

Both shrinkage and thermal contraction have a significant influence on the performance of concrete pavements. They also have a considerable bearing on pavement design. A major element of pavement design is the design of the joints. The factors that control the joint design are shrinkage, thermal contraction, and the amount of reinforcement. For plain concrete pavement (no reinforcement) the joints are designed to prevent random cracking due to forces generated in the concrete as it shrinks and contracts. When the concrete is reinforced, the amount of reinforcement and spacing of the joints are selected so that the steel can withstand these forces without rupturing.

Thermal gradients also influence the performance of the pavement by causing differential contraction and expansion between the outside surfaces of the slab. This creates warping that results in stresses in the slab and temporary loss of slab support. The combination of warping stresses and reduced support adds to the effects of load induced stresses and contributes significantly to pavement cracking. The typical pavement lane joint is used to control this type of cracking in the longitudinal direction.

A knowledge of the shrinkage and thermal contraction behavior of the high performance concrete is essential in order to account for these parameters in design. Of the two, the shrinkage is probably the more critical since it is controlled by the mortar fraction of the concrete. The thermal contraction is also influenced by the mortar fraction but not to the extent that it is affected by the aggregate fraction. Therefore, the thermal contraction of high performance concrete would be expected to differ little from the behavior of conventional concrete.

5.1.3.4 Durability

Concrete pavements are typically designed for an initial service life of 20 or more years. They are also expected to serve as a sound rehabilitation base for an additional 20 or more years. To achieve this longevity, the concrete must be durable.

Common durability problems with conventional concrete are surface scaling, alkali aggregate reaction, and D-cracking. Surface scaling is controlled through the use of air entrainment, proper curing, and mix quality. Alkali aggregate reaction and D-cracking are associated with the type of aggregate. These problems are controlled through aggregate selection and, in the case of alkali aggregate reaction, the type of cement.

Similar durability problems may exist for high performance concretes. The potential for such problems must be investigated in order to use these concretes in pavements with confidence.

5.1.3.6 Wear Resistance

Wear resistance refers to the ability of the pavement to resist surface wear due to the abrasive action of vehicle tires. As the surface wears, the surface texture is altered and becomes polished. This results in a reduction in skid resistance and increases the potential for accidents. Where studded tires are used, wear resistance is especially critical.

With conventional concrete, wear resistance is considered to be controlled primarily by the hardness of the sand fraction. However, research has demonstrated that the wear resistance of high strength concrete [5.8] can be significantly greater than that of conventional concrete. The degree of improvement is a function of the concrete's compressive strength and the type of aggregate. This suggests that the use of high performance concretes could be especially beneficial in improving the wear resistance of pavements. Additional research is needed in this area.

5.1.4 Critical Research Needs for Use in Pavements

Of the various parameters discussed above, the one most critical to the beneficial use of high performance concrete in pavements is durability. Pavements are subjected to adverse environmental and loading conditions and expected to provide good service for extended periods, typically 20 or more years. To use these materials with confidence, the engineer needs to know whether this length of service can be realized.

The second most critical need is an understanding of the shrinkage and thermal contraction behavior of the concrete. These properties govern the selection and design of joints and joint spacings. Since joint deterioration is the predominant mode of pavement failure, knowledge is definitely needed to assure that the joint design is appropriate.

Fatigue behavior is the third most critical research need. This property is needed for the rational determination of the required thickness of overlays and pavements. Closely allied with fatigue is the long-term strength gain characteristics. These characteristics should be taken into consideration in any pavement fatigue analysis.

At present, wear resistance appears to be of secondary importance. However, for states which permit the use of studded tires, wear-resistance research could be quite important.

5.2 Bridge Members

5.2.1 High Strength Concrete

As proposed by ACI Committee 363 [5.3], high strength concrete is defined as having a minimum 28-day compressive strength of 6,000 psi (41 MPa). Concrete of this level of specified minimum strength has been used widely for standard AASHTO precast, prestressed concrete bridge girders in the United States since the 1950s. With few exceptions, concrete strength for these girders rarely exceeded 7,000 psi (48 MPa) even though concrete of considerably higher strength has been used increasingly in recent years for columns of high-rise buildings [5.7]. A number of the examples are listed in Table 5.1.

Several recent studies have examined the potential uses of high strength concrete for highway bridges. Jobse and Moustafa [5.11] analyzed the structural efficiency and cost effectiveness of many different bridge components and conducted tests for verifications. Their results indicated that by increasing the concrete strength from 6,000 psi (41 MPa) to 10,000 psi (69 MPa), a significant increase in girder span (for a given spacing) or increase in girder spacing (for a given span length) could be achieved. One example showed that 9 girders could be reduced to 4 if concrete strength were increased from 6,000 psi (41 MPa) to 10,000 psi (69 MPa). Their results also demonstrated the considerable economic advantages of using high strength concrete for struts and bridge piers. Similar studies were also conducted by Rabbat and Russell [5.18] from which they developed recommendations for optimizing the sections of standard AASHTO girders.

In their recent report, Zia et al. [5.23] concluded that the optimum concrete strength was 8,000 psi (55 MPa) for the prestressed concrete-cored slabs being used by the NCDOT and the optimum concrete strength for the current AASHTO girders was about 10,000 psi (69 MPa).

In the United States, concrete of higher-specified design strength has been used in several recently completed long-span bridges such as East Huntington Bridge in West Virginia [5.21]. However, the concrete strength is only in the range of 8,000 psi (55 MPa).

The use of high strength concrete for bridges has received much wider acceptance in Europe and Japan. Some of the examples as reported by FIP-CEB [5.7] are listed in Table 5.2.

The increasing trend of using high strength concrete for bridges is quite clear. Since durability of bridge is also a major concern, bridge designs will call for the use of concrete with low permeability (i.e., low W/C ratio, use of silica fume, etc.) which will naturally lead to the use of higher strength concrete.

5.2.2 High Early Strength Concrete

For the fabrication of precast and pretensioned AASHTO bridge girders and piles, high early strength concrete is required to expedite the daily production cycle. Concrete strength required for detensioning is specified generally in the range of 3,500 psi (24 MPa) to 4,500 psi (31 MPa) in 18 to 20 hours. These strength levels are usually achieved by accelerated curing of the concrete with heat.

Very limited information has been reported on bridges using high early strength (HES) concrete as defined in this report, i.e., 5,000 psi (34 MPa) in 24 hours. One such application is a prestressed concrete railroad bridge in North Dakota [5.10]. The 72 ft. (22 m) single-span replacement structure carries the Burlington Northern railroad (Cooper E-80 loading) over four lanes of highway traffic plus an 8 ft. (2.44 m) pedestrian walkway on each side of the highway. Twenty-five AASHTO Type IV prestressed concrete girders, each 54 in. (1.4 m) deep, were used to carry four railroad tracks, one mainline and three spur tracks, for a total width of 81 ft. (24.7 m). Because of the tight construction schedule and the need for not delaying the train traffic, the prestressed girders had to be produced and delivered on a rather rigid schedule. Thus the detensioning strength of the concrete, 5,500 psi (38 MPa) attained overnight, controlled the design.

The strength was achieved by using a Type III cement with superplasticizer. The average strength obtained after 1 day was 6,280 psi (43 MPa), and the average strength at 21 days was 7,110 psi (49 MPa).

5.2.3 High Strength Fiber-Reinforced Concrete

Applications of high strength fiber-reinforced concrete for bridge members have been mainly in two areas: bridge deck overlays and bridge repairs. A general discussion of fiber-reinforced concrete used for overlays of pavements and bridge decks has been presented in section 4.5.

In a recent report, Matala [5.14] described the experience of using steel fiber-reinforced concrete for a 70 mm (2.75 in.) bridge deck overlay on the Karhiniemi bridge in Finland.

The length of the overlay was 202 m (221 yd) and the area 1,500 m^2 (1,794 sq yd). The concrete mix proportion was reported as follows:

Cement	390 kg/m^3	(657 pcy)
Water	184 kg/m^3	(310 pcy)
Coarse Aggregate	1,690 kg/m^3	(2,848 pcy)
Fine Aggregate	467 kg/m^3	(787 pcy)
Steel Fiber	75 kg/m^3	(126 pcy)
Air Entraining Agent	0.1% of Cement by Wt.	
HRWR	1.2% of Cement by Wt.	
Air	5%	

The concrete was batched at a ready-mix plant and delivered to the site 40 km (25 miles) away by a rotating drum truck mixer. The average slump of the concrete was 4.75 cm (1.75 in.) and its 28-day average compressive strength was 46 MPa (6,690 psi). The concrete was placed at a speed of 10 m^3 (13 cu yd) per hour.

Based on the results of laboratory studies and site experience, Matala concluded that when compared to the conventional concrete overlay, use of steel fibers would improve the abrasion resistance by 20% to 30%, increase the salt frost resistance to 2 to 3-fold, and enhance the service life of the overlay to 1.3 to 1.4-fold. Both the dosage of HRWR and the batching cost were increased because of the use of steel fibers. With sufficient slump, the field procedures were not different from the conventional methods. To prevent excessive segregation, it was recommended that the slump should not exceed 10 cm to 15 cm (4 in. to 6 in). It was estimated that the service life cost of bridge overlays could be reduced by 15% to 20% with steel fiber-reinforced concrete.

Since 1984, steel fiber-reinforced concrete has been used by the Alberta Transportation Department for bridge deck overlays and bridge repairs in Canada. Johnston and Carter [5.12] reported recently that between 1984 and 1988, 26 fiber-reinforced concrete bridge overlay projects have been completed in Alberta, totaling 11,402 m^2 (13,637 sq yd). Approximately 12 more projects were scheduled for 1989. In addition, 19 bridge repair projects with fiber-reinforced shotcrete have also been completed involving piers, abutments, precast girders, and curb parapets. These shotcrete projects totaled 201 m^3 (263 cu yd) in volume. Detailed specifications have been developed for prebagged concrete used for overlays and shotcrete. A 28-day compressive strength of 35 MPa (5,000 psi) but no less than 27.5 MPa (4,000 psi) is specified for overlays, and a compressive strength in the range of 55 MPa (8,000 psi) to 75 MPa (11,000 psi) at 28 days is specified for shotcrete.

Based on the experience with these projects, the use of fiber-reinforced concrete for bridge deck overlays and shotcrete repairs has been judged technically and economically successful. Fiber reinforcement improves resistance to cracking; and even if cracking does occur in overlays, the spalling tendency of the concrete is reduced by the ability of the fibers to bridge cracks and maintain continuity. Silica fume used in the mix improves strength and durability with respect to chloride penetration, but a proper air-void system is still required for freeze-thaw resistance. The combination of steel fiber and silica fume permits the use of thinner overlays, thus reducing the added dead load on the bridges.

For shotcrete repairs, there have been no durability problems due, in part, to the elimination of potential sources of problems such as leakage and poor drainage before shotcreting. The technique costs only 60 to 70% of that of the latex-modified concrete used previously, needs less mesh, and is easier in finishing. It has also been found that bid prices are more competitive because there are more qualified contractors.

6

Conclusions

An extensive search [6.1] and review of available literature on the mechanical properties of concrete has been conducted with particular reference to high performance concrete for highway applications. Pertinent information has been summarized in the previous chapters. Based on the results of the review, the following conclusions can be drawn:

1. There is no generally accepted definition of high performance concrete. In fact, it is not possible to provide a unique definition. To define such a term, one must consider the performance requirements of the intended use of the concrete. For the purpose of this study, high performance concrete is defined by the following three requirements:

(1) A maximum W/C ratio of 0.35
(2) A minimum durability factor of 80% as determined by ASTM C 666, Method A (AASHTO T 161, Method A)
(3) A minimum strength criteria of either
  (a) 3,000 psi (21 MPa) within 4 hours after placement (VES), or
  (b) 5,000 psi (34 MPa) within 24 hours (HES), or
  (c) 10,000 psi (69 MPa) within 28 days (VHS)

2. It is crucial that criteria for the selection of raw materials for the manufacture of high performance concrete are carefully established. In general, there are more varieties of materials available for VHS concrete production, but in terms of cementitious materials and admixtures, only limited choices for VES and HES concretes are possible.

3. The use of admixtures should be carefully controlled. For VES concrete, special cements (such as Pyrament-blended cement) are usually required and no admixtures should be used. For HES concrete, conventional pozzolans will provide no strength advantage. In addition, there are usually limitations on the type and quantity of the chemical admixtures used. For VHS concrete, many different kinds of admixtures may be used advantageously where set times are not critical and longer hydration periods are possible. Entrained air of appropriate amount and distribution is usually needed to ensure durability. The effects of other admixtures on frost durability of concrete with low W/C ratios has not been fully established.

4. In view of its rapid chemical reaction, adequate working time is critical for VES concrete.

5. More information is needed on all aspects of short-term and long-term mechanical properties of VES concrete. These include modulus of elasticity, strength and strain capacity, creep, shrinkage, and fatigue.

6. For HES concrete, ensuring adequate workability and an adequate entrained air-void system at the time of placement is a critical consideration. Balancing set time, rate of strength gain and workability requirements will incur extra care in raw materials selection and methods of production.

7. Much is already known about the various mechanical properties of concrete with a strength range comparable to that of HES concrete. However, most of the existing data are based on tests at 28 days. Since HES concrete achieves its expected strength in only 24 hours, there is a need to confirm the mechanical properties of HES with the existing data.

8. For VHS concrete, more information on its mechanical properties at 28 days is needed since most of the existing data are based on tests conducted at older ages such as 56 or 90 days. In addition, data on durability, fatigue, and brittleness of VHS concrete is needed.

9. For high performance concrete, there is insufficient information on the effects of vibration and curing on the subsequent mechanical properties of the concrete.

10. The present freeze-thaw durability test procedure, ASTM C666 (AASHTO T161), is far more severe than what is actually encountered in the field since it requires a much higher rate of freezing with almost fully saturated specimens. The primary value of the test method is to evaluate the relative freeze-thaw behavior of different concretes. A more realistic test procedure should be developed to measure the concrete durability under an environment more similar to the service condition. Additional research is needed to establish more realistically the freeze-thaw durability of high performance concrete and its entrained air requirements.

11. With respect to fiber-reinforced concrete, there is ample information on the mechanical properties under short-time loading except thermal expansion and Poisson's ratio after cracking. However, more research is needed for different aspects of long-term effects.

12. Current research results are contradictory regarding the creep characteristics of fiber-reinforced concrete when compared to plain concrete. Some results suggest that the addition of fiber reduces the amount of creep while others indicate the opposite.

13. In pavement applications, steel fibers have been used almost exclusively. Use of other types of fibers is practically non-existent.

14. Mixed fibers, such as a combination of steel and polypropylene fibers, may enhance both strength and ductility of concrete. Virtually no research has been conducted in this area.

15. There is little evidence that high performance concrete is used in current pavement applications. However, for such applications, one can anticipate significant potential benefit. The use of VES and HES concretes will permit rapid repair and construction of pavements so that the interruption of traffic can be substantially minimized, while at the same time providing adequate long term performance at a reasonable cost.

16. Most rigid pavement design methods rely heavily on empirically developed relationships. The data on which these empirical formulas were based do not include any of the high performance concrete. Therefore, research data on durability, shrinkage, thermal properties, fatigue, and long-term strength gain of the high performance concrete are critically needed. Field trials will also be required to establish its performance record.

References

Chapter 1

1.1 ACI Committee 363. State-of-the-Art Report on High Strength Concrete (ACI 363R-84). American Concrete Institute, 1984, 48 pp.

1.2 ACI Committee 363. Research Needs for High-Strength Concrete. ACI Materials Journal, Vol. 84, No. 6, November-December 1987, pp. 559-561.

1.3 ACI Committee 548. Guide for Mixing and Placing Sulfur Concrete. ACI Materials Journal, Vol. 85, No. 4, July-August 1988, pp. 314-325.

1.4 Robert E. Philleo. Freezing and Thawing Resistance of High-Strength Concrete. National Cooperative Highway Research Program, Synthesis of Highway Practice 129, Transportation Research Board, Washington, D.C., December 1986, 31 pp.

Chapter 2

2.1 ACI Committee 212. Chemical Admixtures for Concrete (ACI 221.3R-89), ACI Materials Journal, Vol. 86, No. 3, May-June 1989, pp. 297-237.

2.2 ACI Committee 226. Silica Fume in Concrete (ACI 226.3R-87), ACI Materials Journal, Vol. 84, No. 2, March-April 1987, pp. 158-166.

2.3 ACI Committee 226. Ground Granulated Blast-Furnace Slag as a Cementitious Constituent in Concrete, (ACI 226.1R-87). ACI Materials Journal, Vol. 84, No. 4, July-August 1987, pp 327-342.

2.4 ACI Committee 226. Use of Fly Ash in Concrete, (ACI 226.3R-87). ACI Materials Journal, Vol. 84, No. 5, September-October 1987, pp 381-409.

2.5 ACI Committee 318. Building Code Requirements for Reinforced Concrete, (ACI 363-89) and Commentary -- ACI 318R-89. American Concrete Institute, 1989, 353 pp.

2.6 ACI Committee 363. State-of-the-Art Report on High-Strength Concrete, (ACI 363R-84). American Concrete Institute, 1984, 48 pp.

2.7 ACI Committee 544. State-of-the-Art Report on Fiber Reinforced Concrete (ACI 544.1R-82). Concrete International, Vol. 4, No. 5, May 1982, pp. 9-30.

2.8 ACI Committee 544. Guide for Specifying, Mixing, Placing, and Finishing Steel Fiber Reinforced Concrete (ACI 544.3R-84). ACI Manual of Concrete Practice, Part 5, American Concrete Institute, Detroit, 1987, 8 pp.

2.9 P. C. Aitcin and P. K. Mehta. Effect of Coarse-Aggregate Characteristics on Mechanical Properties of High-Strength Concrete. ACI Materials Journal, Vol. 87, No. 2, March-April 1990, pp. 103-107.

2.10 P. C. Aitcin, S. L. Sarkar and P. Laplante. Long-Term Characteristics of a Very High Strength Concrete. Concrete International: Design and Construction, Vol. 12, No. 1, January 1990, pp. 40-44.

2.11 J. G. Asselanis, P. C. Aitcin and P. K. Mehta. Effect of Curing Conditions on the Compressive Strength and Elastic Modulus of Very High-Strength Concrete. Cement, Concrete, and Aggregates, Technical Note, Vol. 11, Summer 1989, pp. 80-83.

2.12 A. Bentur and A. Goldman. Curing Effects, Strength and Physical Properties of High Strength Silica Fume Concretes. Journal of Materials in Civil Engineering (ASCE), Vol. 1, No. 1, February 1989, pp. 46-58.

2.13 R. L. Blick. Some Factors Influencing High-Strength Concrete. Modern Concrete, Vol. 36, No. 12, April 1973, pp. 38-41.

2.14 G. G. Carette and V. M. Malhotra. Mechanical Properties, Durability and Drying Shrinkage of Portland Cement Concrete Incorporating Silica Fume. Cement, Concrete, and Aggregates, Vol. 5, No. 1, Summer 1983, pp. 3-13.

2.15 R. L. Carrasquillo. Freeze/Thaw Resistance of Pyrament Blended Cement; Deicer Scaling Resistance, Resistance to Chloride Ion Penetration, and Abrasion Resistance of Pyrament Blended Cement; Permeability and Time to Corrosion of Pyrament Blended Cement; Alkali-Aggregate Reaction of Pyrament Blended Cement; Resistance of Sulfate Attack of Pyrament Blended Cement; Creep, Shrinkage and Coefficient of Thermal Expansion of Pyrament Blended Cement. Fergusun Structural Engineering Laboratory, University of Texas, Austin.

2.16 J. E. Cook. 10,000 psi Concrete. Concrete International: Design and Construction, Vol. 11, No. 10, October 1989, pp. 67-75.

2.17 J. E. Cook. Research and Application of High-Strength Concrete Using Class C Fly Ash. Concrete International: Design and Construction, Vol. 4, No. 7, July 1982, pp. 72-80.

2.18 W. A. Cordon and H. A. Gillespie. Variables in Concrete Aggregates and Portland Cement Paste Which Influence the Strength of Concrete. ACI Journal, Proceedings, Vol. 60, No. 8, August 1963, pp. 1029-1052.

2.19 R. J. Detwiler and P. K. Mehta. Chemical and Physical Effects of Silica Fume on the Mechanical Behavior of Concrete. ACI Materials Journal, Vol. 86, No. 9, November-December 1989, pp. 609-614.

2.20 E. R. Dunstan, Jr. A Possible Method for Identifying Fly Ashes That Will Improve the Sulfate Resistance of Concretes. Cement, Concrete, and Aggregates, Vol. 2, No. 1, Summer 1980, pp 20-30.

2.21 FIP Commission on Concrete. Condensed Silica Fume in Concrete. State of Art Report, Federation Internationale de la Precontrainte, 1988, 37 pp.

2.22 J. M. Gaidis and A. M. Rosenberg. The Inhibition of Chloride-Induced Corrosion in Reinforced Concrete by Calcium Nitrite. Cement, Concrete, and Aggregates, Vol. 9, No. 1, Summer 1987, pp. 30-33.

2.23 S. Gebler and P. Klieger. Effect of Fly Ash on the Air-Void Stability of Concrete. Fly Ash, Silica Fume, Slag and Other Mineral By-Products in Concrete, SP-79, American Concrete Institute, 1983, pp. 103-142.

2.24 A. Goldman and A. Bentur. Bond Effects in High-Strength Silica-Fume Concretes. ACI Materials Journal, Vol. 86, No. 5, September-October 1989, pp. 440-447.

2.25 F. J. Hogan and J. W. Meusel. Evaluation for Durability and Strength Development of a Ground Granulated Blast-Furnace Slag. Cement, Concrete, and Aggregates, Vol. 3, No. 1, Summer 1981, pp. 40-52.

2.26 C. Y. Huang and R. F. Feldman. Hydration reactions in Portland Cement - Silica Fume Blends. Cement and Concrete Research, Vol. 15, No. 4, July 1985, pp. 585-592.

2.27 M. L. Leming. Investigation of High Strength Concrete Characteristics using Material in North Carolina. Report No. FHWA/NC/88-006, North Carolina State University, July 1988, 195 pp.

2.28 D. Manmohan and P. K. Mehta. Influence of Pozzolanic, Slag, and Chemical Admixtures on Pore Size Distribution and Permeability of Hardened Cement Pastes. Cement, Concrete, and Aggregates, Vol. 3, No. 1, Summer 1981, pp. 63-67.

2.29 P. K. Mehta and O. E. Gjorv. Properties of Portland Cement Concrete Containing Silica-Fume. Cement and Concrete Research, Vol. 12, No. 5, September 1982, pp. 587-595.

2.30 R. C. Meininger. Use of Fly Ash in Air-Entrained Concrete--Report of Recent NSGA-NRMCA Research Laboratory Studies. National Ready Mixed Concrete Association, February 1981, 32 pp.

2.31 K. Okkenhaug and O. E. Gjorv. Influence of Condensed Silica Fume on the Air-Void System in Concrete. FCB/SINTEF, Norwegian Institute of Technology, Report STF65 A82044.

2.32 C. Ozyildirim. Laboratory Investigation of Concrete Containing Silica Fume for Use in Overlays. ACI Materials Journal, Vol. 84, No. 1, January-February 1987, pp. 3-7.

2.33 W. F. Perenchio and P. Klieger. Further Laboratory Studies of Portland Pozzolan Cements. Research and Development Bulletin No. RD041-01T, Portland Cement Association, 9 pp.

2.34 R. E. Philleo. Freezing and Thawing Resistance of High-Strength Concrete. National Cooperative Highway Research Program, Synthesis of Highway Practice, N 129, Transportation Research Board, December 1986, 38 pp.

2.35 M. Pigeon, P. Plante and M. Plante. Air-Void Stability Part I: Influence of Silica Fume and Other Parameters. ACI Materials Journal, Vol. 86, No. 5, September-October 1989, pp. 482-490.

2.36 V. Randall and K. Foot. High-Strength Concrete for Pacific First Center. Concrete International: Design and Construction, Vol. 11, No. 4, April 1989, pp. 14- 16.

2.37 M. Regourd. Microstructure of High Strength Cement Paste Systems. Materials Research Society Symposium Proceedings, Vol. 42, 1985, pp. 3-17.

2.38 E. K. Schrader. Fiber Reinforced Concrete Pavements and Slabs. Steel fiber concrete, US-Sweden joint seminar (NSF-STU) Stockholm, June 1985, pp. 109-131.

2.39 E. K. Schrader and A. V. Munch. Deck Slab Repaired by Fibrous Concrete Overlay. Proceedings, ASCE, Vol. 102, CO1, March 1976, pp. 179-196.

2.40 R. K. Smutzer and A. R. Zander. A Laboratory Evaluation of the Effects of Retempering Portland Cement Concrete with Water and a High-Range, Water-Reducing Admixture. Transportation Research Record No. 1040, Transportation Research Board, pp. 34-39.

2.41 Y. P. Virmani. Time-to-Corrosion of Reinforcing Steel in Concrete Slabs, Vol. VI: Calcium Nitrite Admixture. Report No. FHWA-RD-88-165, September 1988, 45 pp.

2.42 V. Yogendran, B. W. Langan, M. N. Haque and M. A. Ward. Silica Fume in High-Strength Concrete. ACI Materials Journal, Vol. 84, No. 2, March-April 1987, pp. 124-129.

Chapter 3

3.1 M. S. Abrams. Compressive Strength of Concrete at Temperatures to 1600° F. Temperature and Concrete, SP 25, American Concrete Institute, 1971, pp. 33-58.

3.2 ACI Committee 201. Guide to Durable Concrete. Manual of Concrete Practice, Part 1, American Concrete Institute, 1990, pp. 201.2 R-1 to 201.2 R-37.

3.3 ACI Committee 209. Prediction of Creep, Shrinkage and Temperature Effects in Concrete Structures. Manual of Concrete Practice, Part 1, American Concrete Institute, 1990, pp. 209R-1 to 209R-92.

3.4 ACI Committee 214. Simplified Version of the Recommended Practice for Evaluation of Strength Test Results. ACI Materials Journal, July-Aug 1988, pp. 272-279.

3.5 ACI Committee 215. Considerations for Design of Concrete Structures Subjected to Fatigue Loading. Manual of Concrete Practice, Part 1, American Concrete Institute, 1990, pp. 215 R-1 to 215 R-25.

3.6 ACI Committee 318. Building Code Requirements for Reinforced Concrete. American Concrete Institute, 1989, 111 pp.

3.7 ACI Committee 363. State-of-the-Art Report on High Strength Concrete. ACI Journal, Vol. 81, No. 4, July-Aug 1984, pp. 364-411.

3.8 ACI Committee 363. Research Needs for High-Strength Concrete. ACI Materials Journal, Nov-Dec 1987, pp. 559-561.

3.9 S. H. Ahmad and S. P. Shah. Structural Properties of High Strength Concrete and Its Implications for Precast Prestressed Concrete. PCI Journal, Vol. 30, No. 6, Nov-Dec 1985, pp. 91-119.

3.10 S. H. Ahmad. Properties of Confined Concrete Subjected to Static and Dynamic Loading. PhD Thesis, University of Illinois, Chicago, March 1981, 375 pp.

3.11 S. H. Ahmad and S. P. Shah. Stress-Strain Curves of Concrete Confined by Spiral Reinforcement. ACI Journal, Vol. 79, No. 6, Nov-Dec 1982, pp. 484-490.

3.12 S. H. Ahmad. Optimization of Mix Design for High Strength Concrete. Report No. CE 001-82, Department of Civil Engineering, North Carolina State University, Raleigh, NC, 1982, 21 pp.

3.13 S.H. Ahmad and S.P. Shah. Behavior of Hoop Confined Concrete under High Strain Rates. ACI Journal, Vol. 82, No. 5, Sept-Oct 1985, pp. 634-647.

3.14 S. H. Ahmad and S. P. Shah. Complete Stress-Strain Curves of Concrete and Nonlinear Design. Non-Linear Design of Concrete Structures, University of Waterloo Press, 1980, pp. 222-230.

3.15 P. C. Aitcin. CONDENSED SILICA FUME. University of Sherbrooke, Sherbrooke, Quebec, 1983.

3.16 P. C. Aitcin, S. L. Sarkar and P. Laplante. Long-Term Characteristics of A Very High Strength Concrete. Concrete International, Vol. 12, No. 1, Jan 1990, pp. 40-44.

3.17 P. C. Aitcin and P. K. Mehta. Effect of Coarse-Aggregate Characteristics on Mechanical Properties of High-Strength Concrete. ACI Materials Journal, Vol. 87, No. 2, March-April 1990, pp. 103-107.

3.18 P. C. Aitcin, M. S. Cheung and V. S. Shah. Strength Development of Concrete Cured Under Arctic Sea Conditions. Temperature Effects on Buildings, STP-858, ASTM, Philadelphia, 1985, pp. 3-20.

3.19 K. M. Alexander, G. M. Bruere and I. Ivanusec. The Creep and Related Properties of Very High-Strength Super-plasticized Concrete. Cement and Concrete Research, Vol. 10, No. 2, 1980, pp. 131-137.

3.20 J. A. Almudaiheem and W. Hansen. Prediction of Concrete Drying Shrinkage from Short-Term Measurements. ACI Materials Journal, Vol. 86, No. 4, July-Aug 1989, pp. 401-408.

3.21 American Society of Testing Material, Annual Book of ASTM Standards, Vol 04.02 (Concrete and Mineral Aggregates), 1983.

3.22 F. Ansari. Stress-Strain Response of Microcracked Concrete in Direct Tension. ACI Materials Journal, Vol. 84, No. 6, Nov-Dec 1987, pp. 481-490.

3.23 B. L. Atchley and H. L. Furr. Strength and Energy Absorption Capabilities of Plain Concrete Under Dynamic and Static Loadings. ACI Journal, Vol. 64, No. 11, Nov 1967, pp. 745-756.

3.24 R. F. M. Bakker. Permeability of Blended Cement Concrete. Fly Ash, Silica Fume, Slag and Other Mineral By-Products in Concrete, SP 79, Vol. 1, American Concrete Institute, 1983, pp. 589-605.

3.25 P. B. Bamforth. In Situ Measurements of the Effect of Partial Portland Cement Replacement Using Either Fly Ash Or Granulated Blast-Furnace Slag On the Performance of Mass Concrete. Proceedings of Institution of Civil Engineers, Vol. 69, Part 2, 1980, pp. 777-800.

3.26 Z. P. Bazant, and J. C Chern. Log Double Power Law for Concrete Creep. ACI Journal, Vol. 82, No. 5, Sept-Oct 1985, pp. 665-675.

3.27 Z. P. Bazant, J. K. Kim, F. H. Wittman and F. Alou. Statistical Extrapolation of Shrinkage Data - Part II: Bayesian Updating. ACI Materials Journal, Vol. 84, No. 2, Mar-Apr 1987, pp. 83-91.

3.28 Z. P. Bazant and L. Panula. Practical Prediction of Creep and Shrinkage of High Strength Concrete. Materiaux et Constructions (RILEM, Paris), Vol. 17, No. 101, Sept-Oct 1984, pp. 375-378.

3.29 Z. P. Bazant, F. H. Wittmann, J. K. Kim and F. Alou. Statistical Extrapolation of Shrinkage Data - Part I: Regression. ACI Materials Journal, Jan-Feb 1987, pp. 20-34.

3.30 Z. P. Bazant and L. Panula. Practical Prediction of Time-Dependent Deformations of Concrete. Materiaux et Constructions (RILEM, Paris), Vol. 11, No. 65, No. 66, Vol. 12, No. 69, Sept-Oct 1978, Nov-Dec 1978, May-June 1979, pp. 307-328, pp. 415-434, pp. 169-183.

3.31 Z. P. Bazant and L. Panula. Creep and Shrinkage Characterization for Analyzing Prestressed Concrete Structures. PCI Journal, Vol. 25, No. 3, May-June 1980, pp. 86-122.

3.32 Z. P. Bazant and L. Panula. New Model for Practical Prediction of Creep and Shrinkage. Designing for

Creep and Shrinkage in Concrete Structures, SP 76, American Concrete Institute, 1982, pp. 7-23.

3.33 A. Bisaillon and V. M. Malhotra. Permeability of Concrete Using a Uniaxial Water-Flow Method. Permeability of Concrete, SP 108, American Concrete Institute, 1988, pp. 175-193.

3.34 A. G. Bishara, J. D. Rose and A. R. Y. Mahmoud. Shrinkage and Creep Characteristics of Latex-Modified Concrete. ACI Journal, Vol. 75, No. 5, May 1978, pp. 204-208.

3.35 R. Blundell. Superplasticizers - Testing and Proving Experience. Lecture presented at the Cement and Concrete Association, Fulmer Grange, 1976.

3.36 D. E. Branson, B. L. Myers, and K. M. Kripanarayanan. Loss of Prestress Camber and Deflection of Non Composite and Composite Structures Using Different Weight Concrete. Final Report No. 70-6, Iowa Highway Commission, Ames, Aug 1970, 292 pp.

3.37 D. E. Branson and M. L. Christiason. Time Dependent Concrete Properties Related to Design-Strength and Elastic Properties, Creep, and Shrinkage. Designing for Effects of Creep, Shrinkage and Temperature in Concrete Structures, SP-27, American Concrete Institute, Detroit, 1971, pp. 257-277.

3.38 D. E. Branson. DEFORMATION OF CONCRETE STRUCTURES. Mcgraw Hill Book Co., New York, 1979, 546 pp.

3.39 B. Bresler and V. V. Bertero. Influences of High Strain Rate and Cyclic Loading on Behavior of Unconfined and Confined Concrete in Compression. Proceedings, Second Canadian Conference on Earthquake Engineering, MacMaster University, Hamilton, Ontario, Canada, June 1975.

3.40 J. J. Brooks and P. J. Wainwright. Properties of Ultra-High-Strength Concrete Containing A Superplasticizer. Magazine of Concrete Research, Vol. 35, No. 125, Dec 1983, pp. 205-213.

3.41 J. J. Brooks, P. J. Wainwright and A. M. Neville. Time-Dependent Properties of Concrete Containing A Superplasticizing Admixture. Superplasticizers in Concrete, SP 62, American Concrete Institute, 1979, pp. 293-314.

3.42 J. J. Brooks, P. J. Wainwright and A. M. Neville. Superplasticizer Effect on Time-Dependent Properties of Air-Entrained Concrete. Concrete, Vol. 13, No. 6, June 1979, pp. 35-38.

3.43 A. H. Bryant and C. Vadhanavikkit. Creep and Shrinkage-Size, and Age at Loading Effect. ACI Materials Journal, Vol. 84, No. 2, Mar-Apr 1987, pp. 117-123.

3.44 N. R. Buenfeld and J. B. Newman. The Permeability of Concrete in a Marine Environment. Magazine of Concrete Research, Vol. 36, No. 127, June 1984, pp. 67-80.

3.45 M. Buil and P. Acker. Creep of A Silica Fume Concrete. Cement and Concrete Research, Vol. 15, No. 3, May 1985, pp. 463-466.

3.46 T. A. Burge. High Strength Lightweight Concrete with Condensed Silica Fume. Fly Ash, Silica Fume, Slag and Other Mineral By-Products in Concrete, SP-79, Vol. II, American Concrete Institute, 1983, pp. 731-745.

3.47 T. A. Burge. Densified Cement Matrix Improves Bond With Reinforcing Steel. Proceedings, International Conference on Bond in Concrete, Edited by Bartos P., Applied Science Publishers, London, 1982, pp. 273-281.

3.48 N. J. Carino, H. M. Jennings, and L. M. Snell. Properties of Concrete at Early Ages. Summary of Engineering Foundation Workshop. Concrete International, Vol. 11, No. 4, April 1989, pp. 51-54.

3.49 R. L. Carrasquillo, A. H. Nilson and F. O. Slate. Properties of High Strength Concrete Subject to Short-Term Loads. ACI Journal, Vol. 78, No. 3, May-June 1981, pp. 171-178.

3.50 R. L. Carrasquillo, F. O. Slate and A. H. Nilson. Microcracking and Behavior of High Strength Concrete Subjected to Short Term Loading. ACI Journal, Vol. 78, No. 3, May-June 1981, pp. 179-186.

3.51 P. M. Carrasquillo. Pull out Tests on Straight Deformed Bars Embedded in Superplasticized Concrete, ACI Materials Journal, Vol. 85, No. 2, March-April 1988, pp. 90-94.

3.52 P. M. Carrasquillo and R. L. Carrasquillo. Effect of Using Unbonded Capping Systems on the Compressive Strength of Concrete Cylinders. ACI Materials Journal, Vol. 85, No. 3, May-June 1988, pp. 141-147.

3.53 P. M. Carrasquillo and R. L. Carrasquillo. Evaluation of the Use of Current Concrete Practice in the Production of High-Strength Concrete. ACI Materials Journal, Vol. 85, No. 1, Jan-Feb 1988, pp. 49-54.

3.54 R. L. Carrasquillo. Freeze/Thaw Resistance of Pyrament Blended Cement. Industrial report furnished by Pyrament, Division of Lone Star Industries, Inc., Houston, Texas, 1989, 21 pp.

3.55 R. L. Carrasquillo. Deicer Scaling Resistance, Resistance to Chloride Ion Penetration, and Abrasion Resistance of Pyrament Blended Cement. Industrial report furnished by Pyrament, Division of Lone Star Industries, Inc., Houston, Texas, 1989, 30 pp.

3.56 R. L. Carrasquillo. Permeability and Time to Corrosion of Pyrament Blended Cement. Industrial Report furnished by Pyrament, Division of Lone Star Industries, Inc., Houston, Texas, 1989, 25 pp.

3.57 C. Castillo and A. J. Durrani. Effect of Transient High Temperature on High-Strength Concrete. ACI Materials Journal, Vol. 87, No. 1, Jan-Feb 1990, pp. 47-53.

3.58 CEB-FIP Model Code for Concrete Structures, 3rd Ed. Comite European du Beton Federation Internationale de la Precontrainte, Paris, 1978, 348 pp.

3.59 L. Cedolin, S. D. Poli and I. Iori. Tensile Behavior of Concrete. Journal of Engineering Mechanics, ASCE, Vol. 113, No. 3, March 1987, pp. 431-449.

3.60 R. A. Chapman and S. P. Shah. Early-Age Bond Strength in Reinforced Concrete. ACI Materials Journal, Vol. 84, No. 6, Nov-Dec 1987, pp. 501-510.

3.61 L. Chung and S.P.Shah. Effect of Loading Rate on Anchorage Bond and Beam-Column Joints. ACI Structural Journal, Vol. 86, No. 2, March-April 1989, pp. 132-142.

3.62 T. M. Collins. Proportioning High-Strength Concrete to Control Creep and Shrinkage. ACI Materials Journal, Vol. 86, No. 6, Nov-Dec 1989, pp. 576-580.

3.63 Concrete Manual, 8th Ed. U. S. Bureau of Reclamation, Denver, Colorado, 1975.

3.64 D. J. Cook and P. Chindaprasirt. Influence of Loading History Upon the Tensile Properties of Concrete. Magazine of Concrete Research, Vol. 33, No. 116, Sept 1981, pp. 154-160.

3.65 J. E. Cook. Research and Application of High-Strength Concrete: 10,000 PSI Concrete. Concrete International, Oct 1989, pp. 67-75.

3.66 H. A. W. Cornelissen. Fatigue Failure of Concrete in Tension. Heron, Vol. 29, No. 4, 1984, pp. 1-68.

3.67 H. A. W. Cornelissen and A. J. M. Siemes. Plain Concrete Under Sustained Tensile or Tensile and Compressive Fatigue Loadings. Behaviour of Offshore Structures, Elsevier Science Publishers, Amsterdam, 1985, pp. 487-498.

3.68 H. A. W. Cornelissen and H. W. Reinhardt. Uniaxial Tensile Fatigue Failure of Concrete Under Constant-Amplitude and Programme Loading. Magazine of Concrete Research, Vol. 36, No. 129, Dec 1984, pp. 216-226.

3.69 J. I. Daniel. Investigation of High Strength Concrete at Chicago Mercantile Exchange. Report to ACI Chicago Chapter, Chicago Committee in High-Rise Buildings, Concrete Reinforcing Steel Institute, Material Service Corporation, and Structural Engineering Association of Illinois, Construction Technology Laboratory, Skokie, Illinois, Jan 1983, 6 pp.

3.70 DESIGN AND CONTROL OF CONCRETE MIXTURES, 11th Ed. Portland Cement Association, Skokie, Ill, 1968, 121 pp.

3.71 R. J. Detwiler and P. K. Mehta. Chemical and Physical Effects of Silica Fume on the Mechanical Behavior of Concrete. ACI Materials Journal, Vol. 86, No. 6, Nov-Dec 1989, pp. 609-614.

3.72 J. D. Dewar. The Indirect Tensile Strength of Concrete of High Compressive Strength. Technical Report, No. 42.377. Cement and Concrete Association, Wexham Springs, England, March 1964.

3.73 R. K. Dhir and A. W. F. Yap. Superplasticized Flowing Concrete: Strength and Deformation Properties. Magazine of Concrete Research, Vol. 36, No. 129, Dec 1984, pp. 203-215.

3.74 U. Diederichs, U-M. Jumppanen and V. Penttala. Behaviour of High Strength Concrete at High Temperatures. Report 92, Department of Structural Engineering, Helsinki University of Technology, Espoo, Finland, 1989, 76 pp.

3.75 W. H. Dilger, R. Koch and R. Andowalczyk. Ductility of Plain and Confined Concrete Under Different Strain Rates. ACI Journal, Vol. 81, No. 1, Jan-Feb 1984, pp. 73-81.

3.76 J. F. Dixon and V. K. Sunley. Use of Bond Coats in Concrete Repair. Concrete, Vol. 17, No. 8, London, Aug 1983, pp. 34-35.

3.77 P. L. Domone. Uniaxial Tensile Creep and Failure of Concrete. Magazine of Concrete Research, Vol. 20, No. 88, Sept 1974, pp. 144-152.

3.78 A. Elzedin and P. N. Balaguru. Bond Behavior of Normal and High-Strength Reinforced Concrete. ACI Materials Journal, Vol. 86, No. 5, Sept-Oct 1989, pp. 515-524.

3.79 R. H. Evans and M. S. Marathe. Microcracking and Stress-Strain Curves for Concrete In Tension. Materials and Structures, Research and Testing, (RILEM, Paris), Vol. 1, No. 1, Jan-Feb 1968, pp. 61-64.

3.80 FIP Commission on Concrete. Condensed Silica Fume in Concrete. State of Art Report, Federation Internationale de la Precontrainte, London, 1988, 37 pp.

3.81 FIP-CEB Working Group on HSC. High Strength Concrete, State of the Art, Draft 5. Federation Internationale de la Precontrainte, London, Feb 1990, 190 pp.

3.82 G. Fagerlund. On the Capillarity of Concrete. Nordic Concrete Research, No. 1, The Nordic Concrete Federation, 1982, pp. 6.1-6.20.

3.83 A. E. Fiorato. PCA Research on High-Strength Concrete. Concrete International, Vol. 11, No. 4, April 1989, pp. 44-50.

3.84 C. Foy, M. Pigeon et al. Freeze-Thaw Durability and Deicer Salt Scaling Resistance of a 0.25 Water-Cement Ratio Concrete. Cement and Concrete Research, Vol. 18, No. 4, July 1988, pp. 604-614.

3.85 S. Freedman. High Strength Concrete. Modern Concrete, Vol. 34, No. 6, Oct 1970, pp. 29-36; No. 7, Nov 1970, pp. 28-32, No. 8, Dec 1970, pp. 21-24, No. 9, Jan 1971, pp. 15-22, and No. 10, Feb 1971, pp. 16-23.

3.86 N. J. Gardner. Effect of Temperature on Early-Age Properties of Type I, Type II, and Type I/Fly Ash Concretes. ACI Materials Journal, Vol. 87, No. 1, Jan-Feb 1990, pp. 68-78.

3.87 N. J. Gardner, P. L. Sau and M. S. Cheung. Strength Development and Durability of Concretes Cast and Cured at 0^{0} C. ACI Materials Journal, Vol. 85, No. 6, Nov-Dec 1988, pp. 529-536.

3.88 R. S. Ghosh and J. Timusk. Creep of Fly Ash Concrete. ACI Journal, Vol. 78, No. 5, Sept-Oct 1981, pp. 351-357.

3.89 O. E. Gjorv et al. Effect of Condensed Silica Fume on the Steel-Concrete Bond. Report BML 86.201, Norwegian Institute of Technology, 1986.

3.90 A. Goldman and A. Bentur. Bond Effects in High-Strength Silica-Fume Concretes. ACI Materials Journal, Vol. 86, No. 5, Sept-Oct 1989, pp. 440-447.

3.91 V. S. Gopalaratham and S. P. Shah. Softening Response of Concrete in Direct Tension. ACI Journal, Vol. 82, No. 3, May-June 1985, pp. 310-323.

3.92 W. E. Grieb and G. Werner. Comparison of Splitting Tensile Strength of Concrete with Flexural and Compressive Strengths, Public Roads, Vol. 32, No. 5, Dec 1962.

3.93 Z-H. Guo and X-Q. Zhang. Investigation of Complete Stress-Deformation Curves for Concrete in Tension. ACI Materials Journal, Vol. 84, No. 4, July-Aug 1987, pp. 278-285.

3.94 D. J. Hannant. Effects of Heat on Concrete Strength. Engineering (London), Vol. 203, No. 21, 1964, p. 302.

3.95 T. Hatano. Dynamic Behavior of Concrete Under Impulsive Tensile Load. Technical Report, No. C-6002, Central Research Institute of Electric Power Industry, Tokyo, 1960, pp. 1-15.

3.96 S. Helland et al. Höyfast betong. Presented at Norsk Betongdag, Trondheim, Oct. 1983. (In Norwegian).

3.97 High-Strength Concrete in Chicago, High-Rise Buildings. Task Force Report No. 5, Chicago Committee on High-Rise Buildings, Feb 1977, 63 pp.

3.98 K. Hindo. In Place Bond Testing and Surface Preparation of Concrete. Concrete International, Vol. 12, No. 2, April 1990, pp. 46-48.

3.99 T. C. Holland. Abrasion-Erosion Evaluation of Concrete Mixtures for Stilling Basin Repairs, Kinzua Dam, Pennsylvania. Miscellaneous Paper, SL-83-16, US Army Engineer Waterways Experiment Station, Structures Laboratory, Vicksburg, 1983.

3.100 R. D. Hooton. Some Aspects of Durability with Condensed Silica Fume in Pastes, Motars and Concretes. Proceedings, International Workshop on Condensed Silica Fume in Concrete, CANMET, Montreal, May 1987.

3.101 H. Houk. Concrete Aggregates and Concrete Properties Investigations. Design Memorandum, No.16, Dworshak Dam and Reservoir, U.S. Army Engineer District, Walla, WA, 1965.

3.102 B. P. Hughes and R. Gregory. Concrete Subjected to High Rates of Loading and Compression. Magazine of Concrete Research, Vol. 24, No. 78, London, March 1972.

3.103 P. Huovinen. Air-Permeability of Concrete. Nordic Concrete Research, No. 1, The Nordic Concrete Federation, 1982, pp. 10.1-10.17.

3.104 D. J. Janssen. Laboratory Permeability Measurement. Permeability of Concrete, SP 108, American Concrete Institute, 1988, pp. 145-158.

3.105 M. R. Jerome. Tensile Strength of Concrete. ACI Journal, Vol. 81, No. 2, March-April 1984, pp. 158-165.

3.106 R. Johansen. Silicastov Iabrikksbetong. Langtidseffekter. Report STF65 F79019, FCB/SINTEF, Norwegian Institute of Technology, Trondheim, 1979 (In Norwegian).

3.107 R. Johansen. Report 6: Long-Term Effects. Report STF65 A81031, FCB/SINTEF, Norwegian Institute of Technology, Trondheim, 1981.

3.108 A. Johansson and A. Petersons. Flowing Concrete. Advances in Concrete Slab Technology. Pergamon Press, Oxford, 1979, pp. 58-65.

3.109 P. H. Kaar, N. W. Hanson and H. T. Capell. Stress-Strain Characteristics of High Strength Concrete. Research and Development Bulletin, RD051-01D, Portland Cement Association, Skokie, Illinois, 1977, 11 pp. Also Douglas McHenry International Symposium on Concrete and Concrete Structures, SP 55, American Concrete Institute, 1978, pp. 161-185.

3.110 P. Klieger. Early High-Strength Concrete for Prestressing. Proceedings of World Conference on Prestressed Concrete, San Francisco, July 1957, pp. A5-1 to A5-14. Also Research Department Bulletin No. 91, Portland Cement Association, 1957.

3.111 P. Klieger. Effect of Mixing and Curing Temperatures on Concrete Strength. ACI Journal, V. 54, No. 12, June 1958, pp. 1063-1081.

3.112 P. Klieger. Some Aspects of Durability and Volume Change of Concrete for Prestressing. Research Department Bulletin, No. 118, Portland Cement Association, Skokie, Nov 1960, 12 pp.

3.113 S. A. Klink. Actual Elastic Modulus of Concrete. ACI Journal, Vol. 82, No. 5, Sept-Oct 1985, pp. 630-633.

3.114 M. D. Kotsovos. Effect of Testing Techniques on the Post-Ultimate Behaviour of Concrete in Compression. Materiaux et Constructions (RILEM, Paris), Vol. 16, No. 91, pp. 3-12.

3.115 J. D. Kreigh. Arizona Slant Shear Test: A Method to Determine Epoxy Bond Strength. ACI Journal, Vol. 73, No. 7, July 1976, pp. 372-373.

3.116 D. R. Lankard, D. L. Birkimer, F. F. Fondfriest and M. J. Snyder. Effects of Moisture Content on the Structural Properties of Portland Cement Concrete Exposed to Temperatures up to 500 F. Temperature and Concrete, SP 25, American Concrete Institute, 1971, pp. 59-102.

3.117 F. C. Lea. The Effect of Temperature on Some of the Properties of Materials. Engineering (London), V. 110, 1920, pp. 293-298.

3.118 D. Lee, F. W. Klaiber, and J. W. Coleman. Fatigue Behavior of Air-Entrained Concrete. Transportation Research Record, No. 671, National Research Council, Washington, D. C., 1978, pp. 20-23.

3.119 G. C. Lee, T. S. Shih and K. C. Chang. Mechanical Properties of High-Strength Concrete at Low Temperature. Journal of Cold Regions Engineering, Vol. 2, No. 4, Dec 1988, pp. 169-179.

3.120 M. L. Leming. Properties of High Strength Concrete: An Investigation of High Strength Concrete Characteristics Using Materials in North Carolina. Research Report FHWA/NC/88-006, Department of Civil Engineering, North Carolina State University, Raleigh, N.C., July 1988, 202 pp.

3.121 A. D. Liniers. Microcracking of Concrete Under Compression and Its Influence on Tensile Strength. Materiaux et Constructions (RILEM, Paris), Vol. 20, No. 116, Mar 1987, pp. 111-116.

3.122 K. E. Loland and O. E. Gjorv. Silikabetong. Nordisk Betong, No. 6, 1981, pp. 1-6 (In Norwegian).

3.123 D. Ludirdja, R. L. Berger, and J. F. Young. Simple Method for Measuring Water Permeability of Concrete. ACI Materials Journal, Vol. 86, No. 5, Sept-Oct 1989, pp. 433-439.

3.124 M. D. Luther and W. Hansen. Comparison of Creep and Shrinkage of High-Strength Silica Fume Concretes With Fly Ash Concretes of Similar Strengths. Fly Ash, Silica Fume, Slag, and Natural Pozzolans in Concrete, SP 114, Vol. 1, American Concrete Institute, 1989, pp. 573-591.

3.125 M. Maage and T. A. Hammer. Modifisert Portlandsement. Detrapport 3. Fasthetsutvikling Og E-Modul. Report STF65 A85041, FCB/SINTEF, Norwegian Institute of Technology, Trondheim, 1985 (In Norwegian).

3.126 R. J. Mainstone. Properties of Materials at High Rates of Straining or Loading. Materiaux et Constructions (RILEM, Paris), Vol. 8, No. 44, March-April 1975.

3.127 H. L. Malhotra. The Effect of Temperature on the Compressive Strength of Concrete. Magazine of Concrete Research, Vol. 8, No. 23, Aug 1956, pp. 85-94.

3.128 V. M. Malhotra, K. A. Painter, et al. Mechanical Properties and Freezing and Thawing Resistance of High-Strength Concrete Incorporating Silica Fume. Cement, Concrete and Aggregates, ASTM, Vol. 9, No. 2, 1987, pp. 65-79.

3.129 V. M. Malhotra, editor. Fly Ash, Silica Fume, Slag and Other Mineral By-Products in Concrete, SP 79, Vols. 1 & 2, American Concrete Institute, 1983, 1176 pp.

3.130 V. M. Malhotra, editor. Fly Ash, Silica Fume, Slag and Natural Pozzolans in Concrete, SP 91, Vols. 1 & 2, American Concrete Institute, 1986, 1601 pp.

3.131 D. Manmohan and P. K. Mehta. Influence of Pozzolanic, Slag, and Chemical Admixtures on Pore Size Distribution and Permeability of Hardened Cement Pastes. Cement, Concrete, and Aggregates, ASTM, Vol. 3, No. 1, 1981, pp. 63-67.

3.132 B. K. Marsh, R. L. Day, and D. G. Bonner. Pore Structure Characteristics Affecting the Permeability of Cement Paste Containing Fly Ash. Cement and Concrete Research, Vol. 15, No. 6, Nov. 1985, pp. 1027-1038.

3.133 S. L. Marusin. Influence of Superplasticizers, Polymer Admixtures, and Silica Fume in Concrete on Chloride Ion Permeability. Permeability of Concrete, SP 108, American Concrete Institute, 1988, pp. 19-34.

3.134 P. K. Mehta. Concrete Structures, Properties and Materials. Prentice Hall, Inc, Englewood Cliffs, New Jersey, 1986, 450 pp.

3.135 P. K. Mehta and D. Manmohan. Pore Size Distribution and Permeability of Hardened Cement Paste. Proceedings, 7th International Congress on the Chemistry of Cement, Vol. III, Paris, 1980, pp. VII-1 to VII-5.

3.136 B. Mobasher and T. M. Mitchell. Laboratory Experience with the Rapid Chloride Permeability Test. Permeability of Concrete, SP 108, American Concrete Institute, 1988, pp. 117-144.

3.137 J. Moreno. The State of the Art of High-Strength Concrete in Chicago: 225 W. Wacker Drive. Concrete International, Vol. 12, No. 1, Jan 1990, pp. 35-39.

3.138 H. Mugurama. Low-Cycle Fatigue Behavior of Concrete under Submerged Conditions. International Experience with Durability of Concrete in Marine Environment. Proceedings of a Symposium honoring Professor Ben C. Gerwick, Jr., Department of Civil Engineering, University of California, Berkeley, Jan 1989, pp. 187-212.

3.139 E. G. Nawy. REINFORCED CONCRETE: A FUNDAMENTAL APPROACH, Second edition, Prentice Hall, New Jersey, 1990, 701 pp.

3.140 A. M. Neville. PROPERTIES OF CONCRETE, Third edition, Pittman Publishing Ltd., London, 1981, 351 pp.

3.141 A. S. Ngab, A. H. Nilson and F. O. Slate. Shrinkage and Creep of High Strength Concrete. ACI Journal, Vol. 78, No. 4, July-Aug 1981, pp. 255-261.

3.142 A. H. Nilson and F. O. Slate. Structural Design Properties of Very High Strength Concrete. Second Progress Report, NSF Grant ENG 7805124, School of Civil and Environmental Engineering, Cornell University, Ithaca, New York, 1979.

3.143 B. H. Oh. Fatigue Analysis of Plain Concrete in Flexure. Journal of Structural Engineering, ASCE, Vol. 112, No. 2, Feb 1986, pp. 273-288.

3.144 B. H. Oh. Behavior of Concrete Under Dynamic Tensile Loads. ACI Materials Journal, Vol. 84, No. 1, Jan-Feb 1987, pp. 8-13.

3.145 R. P. Ojdrovic, A. L. Stojimirovic and H. J. Petroski. Effect of Age on Splitting Tensile Strength and Fracture Resistance of Concrete. Cement and Concrete Research, Vol. 17, No. 1, Jan. 1987, pp. 70-76.

3.146 O. E. Ojorv. High Strength Concrete. Nordic Betong, Vol. 32, No. 1, Stockholm, 1988, pp. 5-9.

3.147 O. E. Ojorv, T. Baerland and R. R. Heinrich. Abrasion Resistance of High Strength Concrete Pavements. Concrete International, Vol. 12. No. 1, Jan 1990, pp. 45-48.

3.148 A. Omojola. The Effect of Cormix SPI Super Workability Aid on Creep and Shrinkage of Concrete. Research and Development Report No. 014J/74/1683, Taylor Woodrow (London), June 1974.

3.149 F. S. Ople and C. L. Hulsbos. Probable Fatigue Life of Plain Concrete with Stress Gradient. ACI Journal, Vol. 63, No. 1, Jan 1966, pp. 59-82.

3.150 C. Ozyildirim and W. Halstead. Resistance to Chloride Ion Penetration of Concretes Containing Fly Ash, Silica Fume, or Slag. Permeability of Concrete, SP 108, American Concrete Institute, 1988, pp. 35-61.

3.151 L. J. Parrot. The Properties of High-Strength Concrete. Technical Report No. 42.417, Cement and Concrete Association, Wexham Springs, 1969, 12 pp.

3.152 N. Pedersen. Wear Resistance Concrete for Pavements. Concrete International, Vol. 10, No. 10, Aug 1988, pp. 53-58.

3.153 V. Pentalla. Mechanical Properties of High Strength Concretes Based on Different Binder Compositions. Proceedings, Symposium on Utlization of High Strength Concrete, Norway, June 15-18, 1987, pp.123-134.

3.154 W. F. Perenchio. An Evaluation of Some of the Factors Involved in Producing Very High-Strength Concrete. Research and Development Bulletin, No. RD014.01T, Portland Cement Association, Skokie, 1973, 7 pp.

3.155 W. F. Perenchio and P. Klieger. Some Physical Properties of High Strength Concrete . Research and Development Bulletin, No. RD056.01T, Portland Cement Association, Skokie, IL, 1978, 6 pp.

3.156 D. Perraton, P. C. Aitcin, and D. Vezina. Permeabilities of Silica Fume Concrete. Permeability of Concrete, SP 108, American Concrete Institute, 1988, pp. 63-84.

3.157 D. W. Pfeifer, D. D. Magura et al. Time Dependent Deformations in a 70 Story Structure. Designing for Effects of Creep, Shrinkage, Temperature in Concrete Structures, SP 37, American Concrete Institute, Detroit, 1971, pp.159-185.

3.158 R. E. Philleo. Comparison of Results of Three methods for Determining Young's Modulus of Elasticity of Concrete. ACI Journal, Vol. 26, No. 5, Jan. 1955, pp. 461-469.

3.159 R. E. Philleo. Freezing and Thawing Resistance of High-Strength Concrete. NCHRP Synthesis of Highway Practice 129, TRB, National Research Council, Washington, D.C., December 1986, 31 pp.

3.160 M. Pigeon, R. Pleau et al. Freeze-Thaw Durability of Concrete with and without Silica Fume in ASTM C 666 (Procedure A) Test Method: Internal Cracking versus Scaling. Cement, Concrete, and Aggregates, ASTM, Vol. 8, No. 2, 1986, pp. 76-85.

3.161 P. Plante and A. Bilodeau. Rapid Chloride Ion Permeability Test: Data on Concretes Incorporating Supplementary Cementing Materials. Fly Ash, Silica Fume, Slag, and Natural Pozzolans in Concrete, SP 114, Vol. 1, American Concrete Institute, 1989, pp. 625-644.

3.162 S. Popovics. Verification of Relationships between Mechanical Properties of Concrete-Like Materials. Materials and Structures, (RILEM, Paris), Vol. 8, No. 45, May-June 1975, pp. 183-191.

3.163 T. C. Poweres and T. L. Brownyard. Studies of the Physical Properties of Hardened Portland Cement Paste, Part VII. ACI Journal, Vol. 43, April 1947, pp. 933-992.

3.164 T. C. Powers, L. E. Copeland and H. M. Mann. Capillary Continuity or Discontinuity in Cement Pastes. Journal, PCA Research and Development Labs, Vol. 2, May 1959, pp. 38-48.

3.165 T. C. Powers, L. E. Copeland, J. C. Hayes and H. M. Mann. Permeability of Portland Cement Paste. ACI Journal, Vol. 26, No. 8, April 1955, pp. 285-298.

3.166 E. Pramono. Numerical Simulation of Distributed and Localized Failure in Concrete. Structural Research Series, No. 88-07, C.E.A.E. Department, University of Colorado, Boulder, 1988.

3.167 W. H. Price. Factors Influencing Concrete Strength. ACI Journal, Vol. 47, No. 6, Feb 1951, pp. 417-431.

3.168 Pyrament Technical Bulletins, Lone Star Industries, Houston, Texas, May 1988, pp. 4.

3.169 H. W. Reinhardt. Concrete Under Impact Loading - Tensile Strength and Bond. HERON, Vol. 27, No. 3, 1982, 48 pp.

3.170 M. Ronne. Effect of Condensed Silica Fume and Fly Ash on Compressive Strength Development of Concrete, Fly Ash, Silica fume, Slag, and Natural Pozzolans in Concrete, SP 114, American Concrete Institute, 1987, pp. 175-189.

3.171 D. M. Roy. Concrete Microstructure. Second Quarterly Report, Contract No. SHRP-87-C201, Strategic Highway Research Program, National Research Council, Washington, D.C., July 17, 1989.

3.172 H. G. Russell and W. G. Corley. Time-Dependent Behavior of Columns in Water Tower Place. Douglas McHenry International Symposium on Concrete and Concrete Structures, SP 55, American Concrete Institute, 1978, pp. 347-373.

3.173 M. Saito. Characteristics of Microcracking in Concrete Under Static and Repeated Tensile Loading. Cement and Concrete Research, Vol. 17, No. 2, March 1987, pp. 211-218.

3.174 K. Sakata, K. Yamura and S. Nishibayashi. Study of Fatigue Properties of Concrete Under Variable Repetitive Compressive Loading. Transactions of the Japan Concrete Institute, Vol. 7, 1985, pp. 257-262.

3.175 M. Sargin. Stress-Strain Curves Relationships for Concrete and Analysis of Structural Concrete Sections. Study No. 4, Solid Mechanics Division, University of Waterloo, Ontario, Canada, 1971.

3.176 K. L. Saucier. High Strength Concrete for Peacekeeper Facilities. Final Report, Structures Laboratory, U.S. Army Engineer Waterways Experimental Station, March, 1984.

3.177 K. L. Saucier, W. O. Tynes and E. F. Smith. High Compressive Strength Concrete - Report 3, Summary Report. Miscellaneous Paper No. 6-520, U.S Army Engineer Waterways Experiment Station, Vicksburg, Sept 1965, 87 pp.

3.178 U. Schneider. Behavior of Concrete Under Thermal Steady State and Non-Steady State Conditions. Fire and Materials, Vol. 1, 1976, pp. 103-115.

3.179 K. Schonlin and H. K. Hilsdorf. Permeability as a Measure of Potential Durability of Concrete - Development of a Suitable Test Apparatus. Permeability of Concrete, SP 108, American Concrete Institute, 1988, pp. 99-115.

3.180 E. J. Sellevold and F. F. Radjy. Condensed Silica fume (microsilica) in Concrete : Water Demand and Strength Development. Fly Ash, Silica Fume, Slag & Other Mineral By-Products in Concrete, SP-79, American Concrete Institute, 1983, Vol. II, pp. 677-694.

3.181 E. Senbetta and G. Malchow. Studies on Control of Durability of Concrete through Proper Curing. Concrete Durability, SP 100, Vol. 1, American Concrete Institute, 1987, pp. 73-87.

3.182 S. P. Shah. Predictions of Cumulative Damage for Concrete and Reinforced Concrete. Materiaux et Construction (RILEM, Paris), Vol. 17, No. 97, Jan-Feb 1984, pp. 65-68.

3.183 S. P. Shah, U. N. Gokos and F. Ansari. An Experimental Technique for Obtaining Complete

Stress-Strain Curves for High Strength Concrete. Cement, Concrete and Aggregates, CCAGDP, Vol. 3, Summer 1981.

3.184 S. P. Shah, A. Fafitis and R. Arnold. Cyclic Loading of Spirally Reinforced Concrete. Journal of Structural Engineering, ASCE, Vol. 109, No. ST7, July 1983, pp. 1695-1710.

3.185 S. P. Shah and R. Sankar. Internal Cracking and Strain Softening Response of Concrete Under Uniaxial Compression. ACI Materials Journal, Vol. 84, No. 3, May-June 1987, pp. 200-212.

3.186 M. R. Sharma and B. L. Gupta. Sonic Modulus as Related to Strength and Static Modulus of High Strength Concrete. Indian Concrete Journal, Vol. 34, No. 4, pp. 139-141.

3.187 S. T. Shirley, R. G. Burg and A. E. Fiorato. Fire Endurance of High-Strength Concrete Slabs. ACI Materials Journal, Vol. 85, No. 2, Mar-Apr 1988, pp. 102-108.

3.188 J. Skalny and L. R. Roberts. High-Strength Concrete. Ann. Rev. Mater. Sci., Vol. 17, 1987, pp. 35-56.

3.189 M. M. Smadi, F. O. Slate and A. H. Nilson. Shrinkage and Creep of High-, Medium-, and Low-Strength Concretes, Including Overloads. ACI Materials Journal, Vol. 84, No. 3, May 1987, pp. 224-234.

3.190 S. S. Smith, J. W. Kasper, K. H. Gerstle and S. Sture. Concrete Over the Top, or: Is There Life after Peak ? ACI Materials Journal, Vol. 86, No. 5, Sept-Oct 1989, pp. 491-497.

3.191 E. V. Sorensen. Freezing and Thawing Resistance of Condensed Silica Fume (Microsilica) Concrete Exposed to Deicing Chemicals. Fly Ash, Silica Fume, Slag & Other Mineral By-Products in Concrete, SP 79, Vol. 2, American Concrete Institute, 1983, pp. 709-718.

3.192 E. C. M. Su and T. T. C. Hsu. Biaxial Compression Fatigue and Discontinuity of Concrete. ACI Materials Journal, Vol. 85, No. 3, May 1988, pp. 178-188.

3.193 W. Suaris and S. P. Shah. Properties of Concrete Subjected to Impact. Journal of Structural Engineering, ASCE, Vol. 109, No. 7, July 1983, pp. 1727-1741.

3.194 B. R. Sullivan. Permeability Testing System for Grout, Concrete, and Rock. Permeability of Concrete, SP 108, American Concrete Institute, 1988, pp. 159-174.

3.195 R. N. Swamy and K. L. Anand. Shrinkage and Creep of High Strength Concrete. Civil Engineering and Public Works Review (London), Vol. 68, No. 807, Oct 1973, pp. 859-865, 867-868.

3.196 R. N. Swamy and H. B. Mahmud. Shrinkage and Creep Behaviour of High Fly Ash Content Concrete. Fly Ash, Silica Fume, Slag, and Natural Pozzolans in Concrete, SP 114, Vol. 1, American Concrete Institute, 1989, pp. 453-475.

3.197 I. Tanahashi, S. Ohgishi, H. Ono, and K. Mizutani. Evaluation of Durability for Concrete in Terms of Watertightness by "Permeability Coefficient Test Results". Concrete Durability, SP 100, Vol. 1, American Concrete Institute, 1987, pp. 187-206.

3.198 M. D. A. Thomas, J. D. Matthews, and C. A. Haynes. The Effect of Curing on the Strength and Permeability of PFA Concrete. Fly Ash, Silica Fume, Slag, and Natural Pozzolans in Concrete, SP 114, Vol. 1, American Concrete Institute, 1989, pp. 191-217.

3.199 S. Walker and D. L. Bloem. Effects of Aggregate Size on Properties of Concrete. ACI Journal, Vol. 32, No. 3, Sept 1960, pp. 283-298.

3.200 J. S. Wall, N. G. Shrive and B. R. Gamble. Testing of Bond Between Fresh and Hardened Concrete. Proceedings, RILEM Symposium on Adhesion Between Polymers and Concrete (Aix-en-Provence, Sept 1986), Chapman and Hall Ltd., London, 1986, pp. 335-344.

3.201 J. S Wall and N. G. Shrive. Factors Affecting Bond between New and Old Concrete. ACI Materials Journal, Vol. 85, No.2, March-April 1988, pp. 117-125.

3.202 P. T. Wang, S. P. Shah and A. E. Naaman. Stress-Strain Curves of Normal and Lightweight Concrete in Compression. ACI Journal, Vol. 75, No. 11, Nov 1978, pp. 603-611.

3.203 D. Watstein. Effect of Straining Rate on the Compressive Strength and Elastic Properties of Concrete. ACI Journal, Vol. 49, No. 8, April 1953, pp. 729-744.

3.204 D. Whiting. Permeability of Selected Concretes. Permeability of Concrete, SP 108, American Concrete Institute, 1988, pp. 195-222.

3.205 D. Whiting. Durability of High-Strength Concrete. Concrete Durability - Katharine and Bryant Mather International Conference, SP 100, American Concrete Institute, 1987, pp. 169-186.

3.206 D. Whiting. Effects of High-Range Water Reducers on Some Properties of Fresh and Hardened Concretes. Research and Development Bulletin, No. RD061.01T, Portland Cement Association, Skokie, 1979, 15 pp.

3.207 G. Wischers. Application and Effects of Compressive Loads on Concrete. Betontechnische Berichte, Betonverlag Gmbh, Dusseldorf, 1979, pp. 31-56.

3.208 J. Wolsiefer. Ultra High-Strength Field Placeable Concrete with Silica Fume Admixture. Concrete International, Vol. 6, No. 4, April 1984, pp. 25-31.

3.209 T. Yamato and H. Sugita. Fly Ash, Silica Fume, Slag and Other Mineral By-Products in Concrete. Fly Ash, Silica Fume, Slag and Other Mineral By-Products in Concrete, SP 79, Vol. 1, American Concrete Institute, 1983, pp. 87-102.

3.210 V. Yogenendran, B. W Langan and M. A. Ward. Utilization of Silica Fume in High Strength Concrete. ACI Materials Journal, Vol. 84, No. 2, Mar-Apr 1987, pp. 85-97. Also Proceedings, Symposium on Utilization of High Strength Concrete, Norway, June 15-18, 1987, pp. 85-97.

3.211 J. F. Young. A Review of the Pore Structure of Cement Paste and Concrete and Its Influence on Permeability. Permeability of Concrete, SP 108, American Concrete Institute, 1988, pp. 1-18.

3.212 Z. A. Zielinski and I. Spiropoulos. An Experimental Study on the Uniaxial and Biaxial Flexural Tensile Strength of Concrete. Canadian Journal of Civil Engineering, Vol. 10, 1983, pp. 104-115.

3.213 A. J. Zielinski, H. W. Reinhardt and H. A. Kormeling. Experiments on Concrete Under Uniaxial Impact Tensile Loading. Materiaux et Constructions (RILEM, Paris), Vol. 14, No. 80, Mar-Apr 1981, pp. 103-112.

3.214 A. J. Zielinski, H. W. Reinhardt, and H. A. Kormeling. Experiments on Concrete Under Repeated Uniaxial Impact Tensile Loading. Materiaux et Constructions (RILEM, Paris), Vol. 14, No. 81, May-June 1981, pp. 163-169.

Chapter 4

4.1 ACI Committee 544. State-of-the-Art Report on Fiber Reinforced Concrete. (ACI 544.1R-82). Concrete International, Vol. 4, No. 5, May 1982, pp. 9-30.

4.2 ACI Committee 544. Design Considerations for Steel Fiber Reinforced Concrete. (ACI 544.4R-88). ACI Manual of Concrete Practice, Part 5, American Concrete Institute, Detroit, 1988, 18 pp.

4.3 ACI Subcommittee 544.01. State-of-the-Art Report of FRC- Steel Fiber Reinforced Concrete. In preparation, 1990.

4.4 W. E. Anderson. Proposed Testing of Steel-Fibre Concrete to Minimize Unexpected Service Failures. Testing and Test Methods of Fibre Cement Composites, RILEM Symposium, 1978, The Construction Press, Lancaster, England, pp. 223-232.

4.5 P. N. Balaguru and V. Ramakrishnan. Freeze-Thaw Durability of Fiber Reinforced Concrete. ACI Journal, Vol. 33, No.3, May-June 1986, pp. 374-382.

4.6 P. N. Balaguru and V. Ramakrishnan. Properties of Fiber Reinforced Concrete: Workability, Behavior Under Long-Term Loading, Air-Void Characteristics. ACI Materials Journal, Vol. 85, No. 3, May-June 1988, pp. 189-196.

4.7 G. Batson, C. Ball, L. Bailey and J. Hooks. Flexural Fatigue Strength of Steel Fiber Reinforced Concrete. ACI Journal, Vol. 69, No. 11, Nov 1972, pp. 673-677.

4.8 C. Bedard, G. C. Carette and V. M. Malhotra. Development of Air-Entrained, High Strength Concrete:

Mechanical Properties and Resistance to Freezing and Thawing. CSCE/CANMET International Workshop on Concrete for Offshore Structures, Sept 10-11, 1986, St. John's, Newfoundland, Canada, 23 pp.

4.9 S. G. Bergstorm. A Nordic Research Project on Fibre Reinforced, Cement Based Materials. Proceedings, RILEM Symposium on Fibre Reinforced Cement and Concrete (Sept 1975), Construction Press, Lancaster, Vol. 2, 1976, pp. 595-600.

4.10 J. Edington, D. J. Hannant and R. I. T. Williams. Steel Fiber Reinforced Concrete. Paper No. CP 69174, Building Research Establishment, Garston, Waterford, 1974, 17 pp.

4.11 D. A. Fanella and A. E. Naaman. Stress-Strain Properties of Fiber Reinforced Concrete in Compression. ACI Journal, Vol. 82, No. 4, July-Aug 1985, pp. 475-483.

4.12 D. A. Gasparini, D. Verna and A. Abdallah. Post Cracking Tensile Strength of Fiber Reinforced Concrete. ACI Materials Journal, Jan-Feb 1989, pp. 10-15.

4.13 V. S. Gopalaratnam, S. P. Shah and R. John. A Modified Instrumented Charpy Test for Cement Based Composites. Experimental Mechanics, Vol. 24, No. 2, June 1984, pp. 102-110.

4.14 V. S. Gopalaratnam and S. P. Shah. Tensile Failure of Steel Fiber Reinforced Mortar. Journal of Engineering Mechanics, ASCE, Vol. 113, No. 5, May 1987, pp. 635-652.

4.15 J. C. Halpin, and S. W. Tsai. Effects of Environmental Factors on Composite Materials. AFML-TR 67-423, June 1969.

4.16 D. J. Hannant. FIBRE CEMENTS AND FIBRE CONCRETES, John Wiley and Sons, Chichester, 1978, 219 pp.

4.17 H. H. Haynes. Investigation of Fiber Reinforcement Methods for Thin Shell Concrete. Technical Report No. 979, Naval Civil Engineering Laboratory, Port Hueneme, Calif., 1968, 47 pp.

4.18 G. C. Hoff. Durability of Fiber Reinforced Concrete in Severe Marine Environment. Proceedings, Katherine and Bryant Mather International Symposium on Concrete Durability, American Concrete Institute, Detroit, SP-100, 1987, Vol. 1, pp. 997-1041.

4.19 G. C. Hoff. Use of Steel Fiber Reinforced Concrete in Bridge Decks and Pavements. STEEL FIBER CONCRETE, US-Sweden joint seminar (NSF-STU), Stockholm, June 1985, pp. 67-108.

4.20 J. Houde, A. Prezeau and R. Roux. Creep of Concrete Containing Fibers and Silica Fume. Fiber Reinforced Concrete Properties and Applications, SP 105, American Concrete Institute, 1987, pp. 101-118.

4.21 C. D. Johnston. Properties of Steel Fiber Reinforced Mortar and Concrete. Proceedings, International Symposium on Fibrous Concrete (C1-80), Construction Press, Lancaster, 1980, pp. 29-47.

4.22 C. D. Johnston. Definition and Measurement of Flexural Toughness Parameters for Fiber Reinforced

Concrete. Cement, Concrete, and Aggregates, CCAGDP, Vol. 4, No. 2, Winter 1982, pp. 53-60.

4.23 D. R. Lankard and E. K. Shrader. Inspection and Analysis of Curl in Steel Fiber Reinforced Concrete Airfield Pavement. Bekaert Steel Wire Corp., Pittsburg, Apr 1983, 9 pp.

4.24 D. R. Lankard and A. J. Walker. Pavement Applications for Steel Fibrous Concrete. Transportation Engineering Journal, ASCE, Vol. 101, No. TE1, Feb 1975, pp. 137-153.

4.25 T. Y. Lim, P. Paramavisam and S. L. Lee. Analytical Model for Tensile Behavior of Steel Fiber Concrete. ACI Materials Journal, Vol. 84, No. 4, July-Aug 1987, pp. 286-298.

4.26 B. Malmberg and A. Skarendahl. Method of Studying the Cracking of Fibre Concrete Under Restrained Shrinkage. Testing and Test Methods of Fibre Cement Composites, RILEM Symposium, Construction Press, Lancaster, England, 1978, 545 pp.

4.27 P. S. Mangat and A. M. Azari. A Theory for the Creep of Steel Fibre Reinforced Cement Matrices Under Compression. Journal of Materials Science, 1985, pp. 1119-1133.

4.28 D. C. McKee. Properties of an Expansive Cement Mortar Reinforced with Random Wire Fibers. Ph.D Thesis, University of Illinois, Urbana 1969.

4.29 G. E. Monfore. A Review of Fiber Reinforcement of Portland Cement Paste, Mortar and Concrete. Journal, PCA Research and Development Laboratories, Vol. 10, No. 3, Sept 1968, pp. 36-42. Also, Research Development Bulletin No. 226, Portland Cement Association.

4.30 A. E. Naaman. High Strength Fiber Reinforced Cement Composites. Materials Research Society Symposium on the Potential of Very High Strength Cement-Based Materials, J. Francis Young, Editor, MRS, Vol. 42, Pittsburgh 1985, pp. 217-229.

4.31 A. E. Naaman. High Performance Fiber Reinforced Cement Composites. Concrete Structures for the Future, IABSE Symposium, Paris 1987, pp. 371-376.

4.32 A. E. Naaman, F. Moavenzadeh and F. McGarry. Probabilistic Analysis of Fiber Reinforced Concrete. Journal of Engineering Mechanics, ASCE, Vol. 100, No. EM2, April 1974, pp. 397-413.

4.33 A. E. Naaman and S. P. Shah. Pull-out Mechanisms in Steel Fiber-Reinforced Concrete. Journal of Structural Engineering, ASCE, Vol. 102, No. ST8, Aug 1976, pp. 1537-1548.

4.34 H. Najm and A. E. Naaman. Elastic Modulus of High Performance Cement-Based Composites. Research in progress, University of Michigan. NSF Center for Advanceed Cement Based Materials.

4.35 G. C. Nammur and A. E. Naaman. Strain Rate Effects on Tensile Properties of Fiber Reinforced Concrete. Proceedings of MRS Symposium on Cement Based Composites, Materials Research Society, Vol. 64, Pittsburgh, 1986, pp. 97-118.

4.36 A. Nanni. Abrasion Resistance of Roller Compacted Concrete. ACI Materials Journal, Vol. 86, No. 6, Nov-Dec 1989, pp. 559-565.

4.37 A. Nanni. Splitting-Tension Test For Fiber Reinforced Concrete. ACI Materials Journal, Vol. 81, No.4, July-Aug 1988, pp. 229-233.

4.38 R. Narayanan and A. S. Kareen-Palanjian. Factors Influencing the Strength of Steel Fiber Reinforced Concrete. Proceedings of RILEM Symposium FRC 86, University of Sheffield, July 1986.

4.39 L. E. Nielsen and P. E. Chen. Young's Modulus of Composites Filled with Randomly Oriented Fiber. Journal of Materials, Vol. 3, No. 2, June 1968, pp. 352-358.

4.40 D. E. Otter and A. E. Naaman. Fiber Reinforced Concrete Under Cyclic and Dynamic Compression Load. Research Report, No. UMCE 88-9, Department of Civil Engineering, the University of Michigan, Ann Arbor, Oct 1988, 178 pp.

4.41 B. K. Paul, M. Polivka and M. K. Mehta. Properties of Fiber Reinforced Shrinkage-Compensating Concrete. ACI Journal, Vol. 78, No. 6, Nov-Dec 1981, pp. 488-492.

4.42 M. E. Patton and W. L. Whittaker. Effects of Fiber Content and Damaging Load on Steel Fiber Reinforced Concrete Stiffness. ACI Journal, Vol. 80, No. 1, Jan-Feb 1983, pp. 13-16.

4.43 V. Ramakrishnan, S. Gallapudi and R. Zelles. Performance Characteristics and Fatigue Strength of Polypropylene Fiber Reinforced Concrete. Fiber Reinforced Concrete Properties and Applications, SP 105, American Concrete Institute, 1987, pp. 159-177.

4.44 V. Ramakrishnan, G. Oberling and P. Tatnall. Flexural Fatigue Strength of Steel Fiber Reinforced Concrete. Fiber Reinforced Concrete Properties and Applications, SP 105, American Concrete Institute, 1987, pp. 225-245.

4.45 V. Ramakrishnan, Y. W. George and G. Hosalli. Flexural Fatigue Strength, Endurance Limit, and Impact Strength of Fiber Reinforced Concretes. Transportation Research Board, 68th Annual Meeting, Jan 1989, Washington, D.C.

4.46 J. P. Romualdi and G. B. Batson. Mechanics of Crack Arrest in Concrete. Journal of Engineering Mechanics, ASCE, Vol. 89, No. EM3, June 1963, pp. 147-168.

4.47 J. P. Romualdi and J. A. Mandel. Tensile Strength of Concrete Affected by Uniformly Distributed Closely Spaced Short Lengths of Wire Reinforcement. ACI Journal, Vol. 61, No. 6, June 1964, pp. 657-671.

4.48 E. K. Schrader. Design Methods for Pavements With Special Concretes. FIBER REINFORCED CONCRETE, SP 81, American Concrete Institute, 1984, pp. 197-212.

4.49 E. K. Schrader. Fiber Reinforced Concrete Pavements and Slabs. Steel Fiber Concrete, US-Sweden joint seminar (NSF-STU) Stockholm, June 1985, pp. 109-131.

4.50 S. P. Shah and M. Grzybowski. Shrinkage Cracking of Fiber Reinforced Concrete. NSF Center for Science and Technology of Advanced Cement-Based Materials, private communication, 1989.

4.51 S. P. Shah and A. E. Naaman. Mechanical Properties of Glass and Steel Fiber Reinforced Mortar. ACI Journal, Vol. 73, No. 1, Jan 1976, pp. 50-53.

4.52 S. P. Shah and B. V. Rangan. Effects of Reinforcement on Ductility of Concrete. Journal of Structural Engineering, ASCE, Vol. 96, No. ST6, June 1970, pp. 1167-1184.

4.53 S. P. Shah and B. V. Rangan. Fiber Reinforced Concrete Properties. ACI Journal, Vol. 68, No. 2, Feb 1971, pp. 126-135.

4.54 S. P. Shah, P. Stroeven, D. Dalhuisen and P. Van Stekelenburg. Complete Stress-Strain Curves for Steel Fiber Reinforced concrete in Uniaxial Tension and Compression. Testing and Test Methods of Fibre Cement Composites, RILEM Symposium, Construction Press, Lancaster, 1978, pp. 399-408.

4.55 M. Schupack. Durability of Steel Fiber Reinforced Concrete Exposed to Severe Environments. STEEL FIBER CONCRETE, US-Sweden joint seminar (NSF-STU), Stockholm, June 1985, pp. 479-496.

4.56 R. N. Swamy. Steel Fibre Concrete for Bridge Deck and Building Floor Applications. STEEL FIBER CONCRETE, US-Sweden joint seminar (NSF-STU), Stockholm, June 1985, 520 pp.

4.57 R. N. Swamy and P. S. Mangat. Influence of Fibers Geometry on the Properties of Steel Fiber Reinforced Concrete. Cement and Concrete Research, Vol. 4, No. 3, 1974, pp. 451-465.

4.58 R. N. Swamy, P. S. Mangat and C. V. S. K. Rao. The Mechanics of Fiber Reinforcement of Cement Matrices. Fiber-Reinforced Concrete, SP 44, American Concrete Institute, 1974, pp. 1-28.

4.59 M. P. Vandenberghe and D. E. Nemegeer. Industrial Flooring With Steel Fiber Reinforced Concrete. Concrete International, Vol. 7, No. 32, Mar 1985, pp. 54-57.

4.60 K. Visalvanich and A. E. Naaman. Fracture Model for Fiber Reinforced Concrete. ACI Journal, Vol. 80, No. 2, Mar-Apr 1983, pp. 128-138.

4.61 G. R. Williamson. The Effect of Steel Fibers on the Compressive Strength of Concrete. Fiber Reinforced Concrete, SP 44, American Concrete Institute, 1974, pp. 195-207.

4.62 R. F. Zollo. Wire Fiber Reinforced Concrete Overlays for Orthotropic Bridge Deck Type Loading. ACI Journal, Vol. 72, No. 10, Oct 1972, pp. 576-582.

Chapter 5

5.1 The AASHO Road Test: Report 5 - Pavement Research. Special Report 61E, HRB, National Research Council, Washington, D.C., 1962.

5.2 AASHTO Guide for Design of Pavement Structures. American Association of State Highway and Transportation Officials, Washington, D.C., 1986.

5.3 ACI Committee 363. State-of-the-Art Report on High Strength Concrete. ACI Journal, Vol. 81, No. 4, July-Aug 1984, pp. 364-411.

5.4 B. El-Jazairi. The Properties of Hardened MPC Mortar and Concrete Relevant to the Requirements of Rapid Repair of Concrete Pavements. Concrete, Vol. 21, No. 9, Sept. 1987, pp. 25-31.

5.5 Fast Track Concrete - The Construction Material with a Conscience. Special Report SR-809.3 FT, American Concrete Pavement Association.

5.6 Fast Track - Fast Pay. Special Report No. 1, American Concrete Pavement Association, May 1987.

5.7 FIP-CEB Working Group on HSC. High Strength Concrete, State of the Art, Draft 5. Federation Internationale de la Precontrainte, London, Feb 1990, 190 pp.

5.8 O. E. Gjorv, T. Baerland and R. R. Heinrich. Abrasion Resistance of High Strength Concrete Pavements. Concrete Internationa, Vol. 12, No. 1, Jan 1990.

5.9 J. D. Grove, K. B. Jones, K. Bharil, A. Abdulshafi and W. Calderwood. Fast Track and Fast Track II, Cedar Rapids, Iowa. Paper Presented at 69th Annual Meeting, TRB, National Research Council, Washington, D. C., 1990.

5.10 J. K. Jennings. A Prestressed Concrete Railroad Bridge on the Prairie. PCI Journal, Vol. 34, No. 3, May-June 1989, pp. 26-35.

5.11 H. J. Jobse and S. E. Moustafa. Applications of High Strength Concrete for Highway Bridges. PCI Journal, Vol. 29, No. 3, May-June 1984, pp. 44-73.

5.12 C. D. Johnston and P. D. Carter. Fiber Reinforced Concrete and Shotcrete for Repair and Restoration of Highway Bridges in Alberta. Transportation Research Record 1226, Transportation Research Board, National Research Council, Washington, D. C., 1989, pp. 7-16.

5.13 S. Kudlapur, et al. Evaluation of Cold-Weather Concrete Patching Materials. ACI Materials Journal, Vol. 86, No. 1, Jan 1989, pp. 36-44.

5.14 S. Matala. Bridge Overlay of Steel Fiber Concrete. Concrete and Silicate Laboratory, Technical Research Center of Finland, Espoo, Finland, April 1988, 17 pp.

5.15 E. G. Nawy, et al. Early Strength of Concrete Patching Materials at Low Temperatures. Transportation Research Record 1110, Transportation Research Board, National Research Council, Washington, D. C., 1987, pp. 24-34.

5.16 Pavement Design, Principles and Practices. National Highway Institute, Federal Highway Administration, Washington, D. C., 1987.

5.17 S. Popovics and N. Rajendran. Early Age Properties of Magnesium-Based Cements under Various Temperature Conditions. Transportation Research Record 1110, Transportation Research Board, National Research Council, Washington, D. C., 1987, pp. 34-45.

5.18 B. G. Rabbat and H. G. Russell. Optimized Sections for Precast Prestressed Bridge Girders. PCI Journal, Vol. 27, No. 4, July-Aug 1982, pp. 88-104.

5.19 G. E. Ramey and A. M. Strickland. An Experimental Evaluation of Rapid-Setting Patching Materials Used in the Repair of Concrete Bridges and Pavements. FHWA/AL-88/97B, HPR 97B, Federal Highway Administration, Washington, D. C., 1984.

5.20 K. G. Smith, et al. Laboratory and Field Evaluation of Rapid-Setting Materials Used for Repair of Concrete Pavements. FHWA-TX-85-20+311-4, Federal Highway Administration, Washington, D. C., 1984.

5.21 M. C. Tang. Construction of East Huntington Bridge. PCI Journal, Vol. 32, No. 6, Nov-Dec 1987, pp. 32-48.

5.22 Thickness Design for Concrete Highway and Street Pavements. Portland Cement Association, Skokie, Illinois, 1984.

5.23 P. Zia, J. J. Schemmel and T. E. Tallman. Structural Applications of High Strength Concrete. Report No. FHWA/NC/89-006, Center for Transportation Engineering Studies, North Carolina State University, Raleigh, N. C., June 1989, 330 pp.

Chapter 6

6.1 M. L. Leming et al. High Performance Concretes, An Annotated Bibliography, 1974-1989. SHRP-C/WP-90-001, Strategic Highway Research Program, National Research Council, Washington, D.C., 1990, 403 pp.

Tables

Table 2.1 Recommended combined aggregate gradations for steel fiber reinforced concrete [4.3]

U.S. STANDARD SIEVE SIZE		Percent Passing For Maximum Size Of 3/8" (10 mm)	1/2" (13 mm)	3/4" (19 mm)	1" (25 mm)	1-1/2" (38 mm)
2	(51 mm)	100	100	100	100	100
1-1/2	(38 mm)	100	100	100	100	85-100
1	(25 mm)	100	100	100	94-100	65-85
3/4	(19 mm)	100	100	94-100	76-82	58-77
1/2	(13 mm)	100	93-100	70-88	65-76	50-68
3/8	(10 mm)	96-100	85-96	61-73	56-66	46-58
# 4	(5 mm)	72-84	58-78	48-56	45-53	38-50
# 8	(2.4 mm)	46-57	41-53	40-47	36-44	29-43
# 16	(1.1 mm)	34-44	32-42	32-40	29-38	21-34
# 30	(0.6 mm)	22-33	19-30	20-32	19-28	13-27
# 50	(0.3 mm)	10-18	8-15	10-20	8-20	7-19
# 100	(0.15 mm)	2-7	1-5	3-9	2-8	2-8
# 200	(0.08 mm)	0-2	0-2	0-2	0-2	0-2

Note: Aggregates shall be well graded from the largest to the smallest size. Aggregate shall not vary from near the maximum allowable percent passing one sieve to near the minimum allowable percent passing the next sieve size.

Table 2.2 Recommended mix proportions for normal weight fiber reinforced concrete [2.7]

	Mortar	3/8 in. Maximum Sized Aggregate	3/4 in. Maximum Sized Aggregate
Cement (lb per cu yd)	700-1200	600-1000	500-900
W/C ratio	0.30-0.45	0.35-0.45	0.40-0.50
Percent of fine to coarse aggregate	100 percent	45 percent to 60 percent	45 percent to 55 percent
Entrained air content	7 percent to 10 percent	4 percent to 7 percent	4 percent to 6 percent
Fiber Content (Volume percent)			
Deformed steel fiber	0.5 to 1.0	0.4 to 0.9	0.3 to 0.8
Smooth steel fiber	1.0 to 2.0	0.9 to 1.8	0.8 to 1.6
Glass fiber	2 to 5	0.3 to 1.2	

1 lb per cu yd = 0.5933 kg/m^3
1 in. = 25.4 mm

Table 2.3 Recommended mix proportions for steel fiber reinforced concrete in airfield pavement applications [2.8]

*	Mixture Number 1, ⅜ in. (9 mm) aggregate with pozzolan or fly ash	Mixture Number 2, ¾ in. (19 mm) aggregate with pozzolan or fly ash
Cement	500 lb/yd^3 (296 kg/m^3)	525 lb/yd^3 (311 kg/m^3)
Fly ash or pozzolan	235 lb/yd^3 (139 kg/m^3)	250 lb/yd^3 (148 kg/m^3)
Steel fibers†		
Coarse aggregate‡		
[⅜ in. (9 mm) max]	1470 lb/yd^3 (872 kg/m^3)	
[¾ in. (19 mm) max]		1330 lb/yd^3 (789 kg/m^3)
Sand	1370 lb/yd^3 (812 kg/m^3)	1440 lb/yd^3 (854 kg/m^3)
Water§	255 lb/yd^3 (151 kg/m^3)	283 lb/yd^3 (168 kg/m^3)
Additives		
Water reducers (normal or high range)	Per manufacturer's instructions.	
Air-entraining agent	Per manufacturer's recommendation for 6 percent air when subject to freezing and thawing conditions.	

*These mixture proportions are given as examples. The exact mixture proportions required to produce 1 yd^3 (or 1 m^3) for any given project will depend on a number of factors, such as the specific gravity of the materials and the water and air content of the mixture. Each mixture should be designed to yield correctly. These mixtures have been placed by slipform pavers.

†Fiber content of these airfield paving mixtures varied from 83 lb/yd^3 to 140 lb/yd^3 (49 to 83 kg/m^3). Flexural strengths ranged from 1050 to 1100 psi (7.2 to 7.6 MPa) at 28 days.

‡Aggregates larger than ¾ in. (19 mm) are not generally used in steel fiber concrete. If larger aggregates are used, the use of longer fibers should be considered.

§Water content varies depending upon amount and type of water reducer, workability achieved with the aggregates used, and other factors. Field adjust to optimum for strength and workability.

Table 3.1 Approximate relative strength of concrete as affected by cement type.

Type of portland cement		Compressive strength (percent of strength of Type I or normal portland cement concrete)			
ASTM	Description	1 day	7 days	28 days	90 days
I	Normal or general purpose	100	100	100	100
II	Moderate heat of hydration and moderate sulfate resisting	75	85	90	100
III	High early strength	190	120	110	100
IV	Low heat of hydration	55	65	75	100
V	Sulfate resisting	65	75	85	100

Source: Adapted from *Design and Control of Concrete Mixtures, 11th Edition,* Portland Cement Association, Skokie, Ill., 1968.

Table 3.2 Effect of drying on compressive strength [3.49]

Moist cured, days	Drying period, days	Test age, days	$\frac{\text{Strength attained after drying}^{*}}{\text{Strength attained when moist cured until test age}}$			
			Compressive strength, f_c'		Modulus of rupture, f_r'	
			Normal strength	High strength	Normal strength	High strength
0-7	8-28	28	0.98	0.91	0.83	0.74
0-7	8-28	28	0.94	0.89	0.86	0.74
0-7	8-28	28	0.95	0.88	0.88	0.74
0-28	29-95	95	0.99	0.95	0.97	0.91
0-28	29-95	95	1.01	0.96	0.96	0.93
0-28	29-95	95	0.99	0.96	0.99	0.91

Normal strength: f_c' = 3330 psi @ 28 days; f_c' = 3750 psi @ 95 days
High strength: f_c' = 10,210 psi @ 28 days; f_c' = 11,560 psi @ 95 days
*Average of three tests

Table 3.3 Comparison of compressive strength test results of 12,000 psi (83 Mpa) concrete at 56 days as obtained by 6x12 in. (152x304 mm) and 4x8 in. (102x203 mm) cylinders [3.137]

Cylinder size	6 x 12 in.	4 x 8 in.
Mean	13,444	13,546
Standard deviation	463	515
Coefficient of variation, percent	3.4	3.8
Number of tests	29	29

Table 3.4 Column core strengths versus 6x12 in. (152x304 mm) cylinders* [3.65]

Test age	7-Days		28-Days		56-Days		180-Days		1-Year	
Maximum size stone	¾ in	1 in	¾ in	1 in	¾ in	1 in	¾ in	1 in	¾ in	1 in
Compressive strength of 6 X 12 in. cylinders, psi										
Field-cured	8,596	8,139	10,177	10,204	10,775	10,542	11,514	11,546	12,444	11,772
Moist-cured	9,228	9,277	11,522	11,236	12,376	12,448	13,852	13,776	14,060	13,951
Compressive strength of cores, psi										
West face	9,407	9,312	11,118	10,743	11,598	10,964	12,970	12,400	15,080	13,775
Middle	8,660	8,959	9,674	9,724	9,833	9,656	11,635	10,720	13,404	13,003
East face	9,180	9,706	10,584	10,575	10,756	10,603	11,626	11,589	14,088	13,695
All cores	9,083	9,326	10,459	10,347	10,729	10,408	12,077	11,570	14,190	13,490
Cores/6 X 12 in. moist-cured cylinders, percent										
West face	102	101	97	96	94	88	94	90	107	99
Middle	94	97	84	87	79	78	84	78	95	93
East face	99	105	92	94	87	85	87	84	100	98
All cores	98	101	91	92	87	84	87	84	101	97

*Reported strengths are average of two specimens.

Table 3.5 Factors affecting concrete creep and shrinkage and variables considered in the recommended prediction method [3.3]

Factors			Variables Considered	Standard Conditions
Concrete (Creep & Shrinkage)	Concrete Composition	Cement Paste Content Water-Cement Ratio Mix Proportions Aggregate Characteristics Degree of Compaction	Type of cement	Type I and III
			Slump	2.7 in, (70 mm)
			Air Content	$\leq$ 6 percent
			Fine Aggregate Percentage	50 percent
			Cement Content	470 to 752 lb/cu yd (279 to 446 kg/m^3)
	Initial Curing	Length of Initial Curing	Moist Cured	7 days
			Steam Cured	1-3 days
		Curing Temperature	Moist Cured	73.4 $\pm$ 4°F (23 $\pm$ 2°C)
			Steam Cured	$\leq$ 212°F, ($\leq$ 100°C)
		Curing Humidity	Relative Humidity	$\geq$ 95 percent
Member Geometry & Environment (Creep & Shrinkage)	Environment	Concrete Temperature Concrete Water Content	Concrete Temperature	73.4 $\pm$ 4°F, (23 $\pm$ 2°C)
			Ambient Relative Humidity	40%
	Geometry	Size and Shape	Volume-Surface Ratio, (v/s)	v/s = 1.5 in (v/s = 38 mm)
			or Minimum Thickness	6 in, (150 mm)
Loading (Only Creep)	Loading History	Concrete Age at Load Application	Moist Cured	7 days
			Steam Cured	1-3 days
		Duration of Loading Period	Sustained Load	Sustained Load
		Duration of Unloading Period Number of Load Cycles	-	-
	Stress Conditions	Type of Stress and Distribution Across the Section	Compressive Stress	Axial Compression
		Stress/Strength Ratio	Stress/Strength Ratio	$\leq$0.50

Table 3.6 Effect of curing time on permeability of cement paste (W/C = 0.51) [3.166]

Curing Time (Days)	1	3	7	14	28	90
Permeability Coeff. (in 10^{-14} m/s)	10^6	10^5	10^3	10^2	10	0.01

Table 3.7 Comparison of permeability and capillary porosity between well-hydrated cement paste and natural rocks [3.166]

Cement Paste		**Permeability Coeff.**	**Rock**	
W/C	**Porosity (%)**	**(in 10^{-14} m/s)**	**Porosity (%)**	**Type**
0.38	6	0.35	0.6	Dense Trap
0.48	15	3.30	1.8	Fine-grained Marble
0.66	28	80	3.1	Limestone
0.71	30	1700	4.3	Sandstone

Table 3.8 Permeability of hydrated cement paste estimated by Mehta and Manmohan based on measured porosity using mercury intrusion method [3.137]

W/C	0.4	0.5	0.6	0.7	0.8	0.9
Permeability Coeff. (in 10^{-14} m/s)	10	30	230	2200	9600	41000

Table 3.9 Chloride ion permeability of Pyrament blended cement concrete [3.57]

	W/C RATIO BY WEIGHT		
	0.25	0.27	0.29
Pyrament cement, lbs.	752	752	752
River sand, SSD, lbs.	1382	1365	1348
River gravel, SSD, lbs.	1690	1668	1647
Water, lbs.	188	203	218
Slump, in.	2	7	9
Concrete temperature, deg. F.	81	80	78
Compressive strength @ 7 days, psi	8530	7700	7650
Permeability tested @ 28 days, Coulombs	723	1025	1688
Permeability tested @ 91 days, Coulombs	314	392	399

Table 4.1 Flexural strength of fiber reinforced concrete [Ref. 4.17].

Volume of fibers, percent	Proportional limit, psi	Maximum load, psi
0.0	920	920
4.60	1060	1930
5.32	1200	2290
7.80	1600	3140
8.80	1860	3960

Specimen size = 1.5x6.0x22 in.beams. Fibers were 0.017 in. in diameter and 1.5 in. long.

Table 4.2 Splitting tensile results of FRC [Ref. 4.37].

Fiber type	Fiber volume, percent	Fiber L/D ratio	First crack load, kips	Ultimate load, kips	I_5	I_{10}	I_{30}	I_{10}/I_5
	0.00	—	14.75	14.75	—	—	—	—
B (deformed wire)	0.41	60.00	16.29	16.29	5.00	9.90	27.30	1.98
	0.82	60.00	14.51	17.02	5.20	10.60	31.50	2.04
	1.23	60.00	16.06	21.30	5.40	12.20	33.80	2.26
F (slit sheet)	0.41	59.80	14.30	14.30	4.90	9.80	—	1.97
	0.82	59.80	15.46	16.12	5.10	10.20	—	2.02
	1.23	59.80	13.20	18.84	5.70	12.40	—	2.17
H (mill cut)	0.41	30.00	14.23	14.23	5.00	10.00	—	2.00
	0.82	30.00	15.65	15.70	5.00	10.00	28.80	2.00
	1.23	30.00	14.08	15.40	5.30	10.30	—	1.95

Note: 1.0 kip = 4.49 kN.

Table 5.1 List of recent buildings using high strength concrete [5.7]

Building	Year	Total stories	Design Concrete Strength (MPa)
Midcontinental Plaza (Chicago)	1972	50	62
Frontier Towers (Chicago)	1973	55	62
Water Tower Place (Chicago)	1975	79	62
River Plaza (Chicago)	1976	56	62*
Mercantile Exchange (Chicago)	1982	40	62#
Columbia Center (Seattle)	1983	72	66
Interfirst Plaza (Dallas)	1983	72	69
900 N. Mich. Annex (Chicago)	1986	15	97
S. Wacker Tower (Chicago)	1989	79	83
Gateway Tower (Seattle)	1989	62	94
Two Union Square (Seattle)	1989	58	115
Pacific First Center (Seattle)	1989	44	115

* Includes two experimental columns of 76 MPa concrete

Includes two experimental columns of 97 MPa concrete

(1 MPa = 145 psi)

Table 5.2 List of recent bridges using high strength concrete [5.7]

Bridge	Year	Max. Span (m)	Design Concrete Strength (MPa)
Ootanabe Railway Bridge (Japan)	1973	24	79
Fukamitsu Highway Bridge (Japan)	1974	26	69
Akkagawa Railway Bridge (Japan)	1976	46	79
Deutzer Bridge (West Germany)	1978	185	69*
Tower Road Bridge (Washington)	1981	49	62
Pont du Pertuiset (France)	1988	110	65
Pont de Joigny (France)	1988	**	60
Arc sur la Rance (France)	1989	**	60
Boknasundet (Norway)	1990	190	60*
Helgelandsbrua (Norway)	1990	425	65

* Lightweight concrete
(1 m = 39 in., 1 MPa = 145 psi)

** Information not reported

Figures

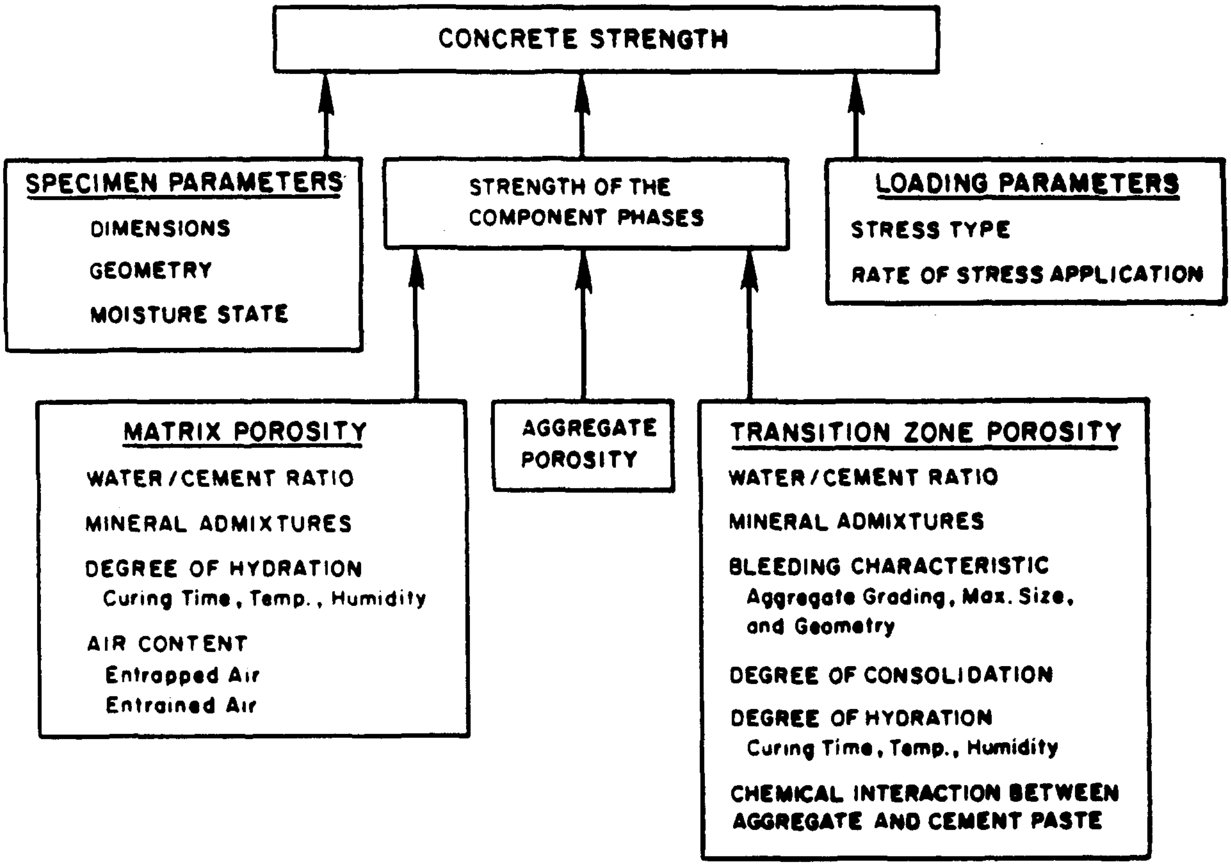

Fig. 3.1 An oversimplified view of factors influencing strength of plain concrete [3.134]

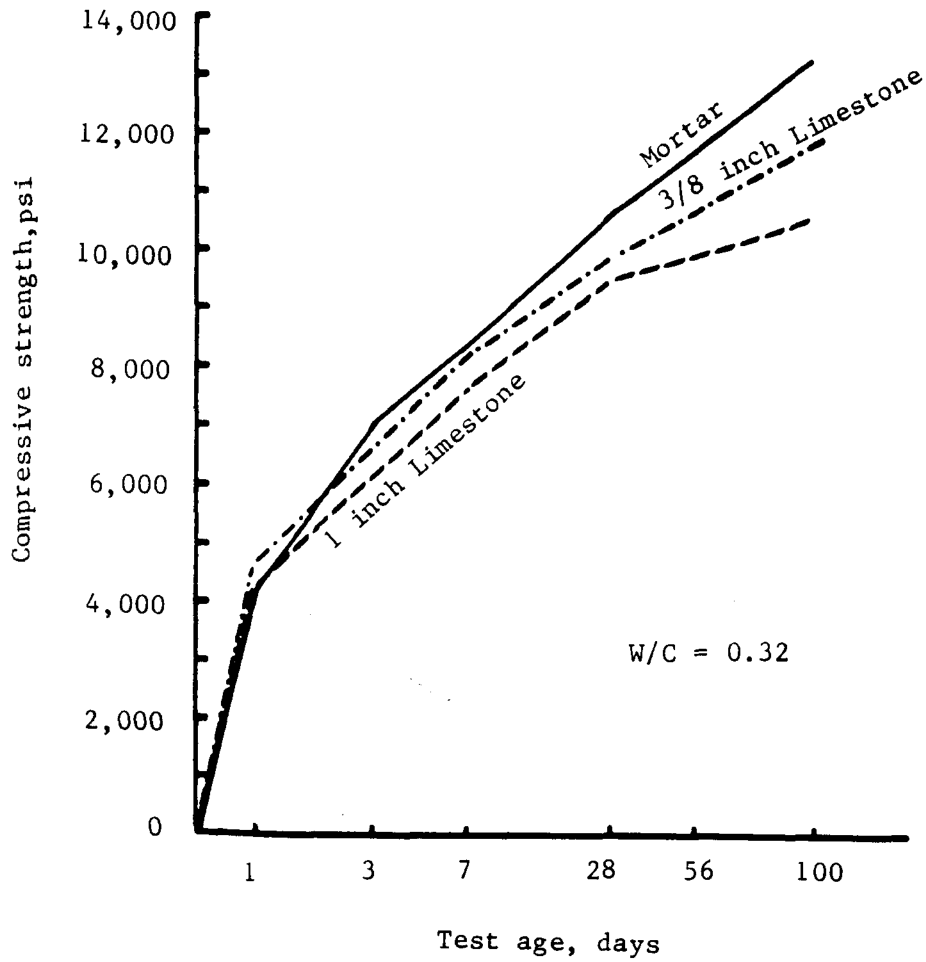

Fig. 3.2 Effect of aggregate type on strength at different ages for a constant water-cementitous materials ratio, without superplasticizer [3.65]

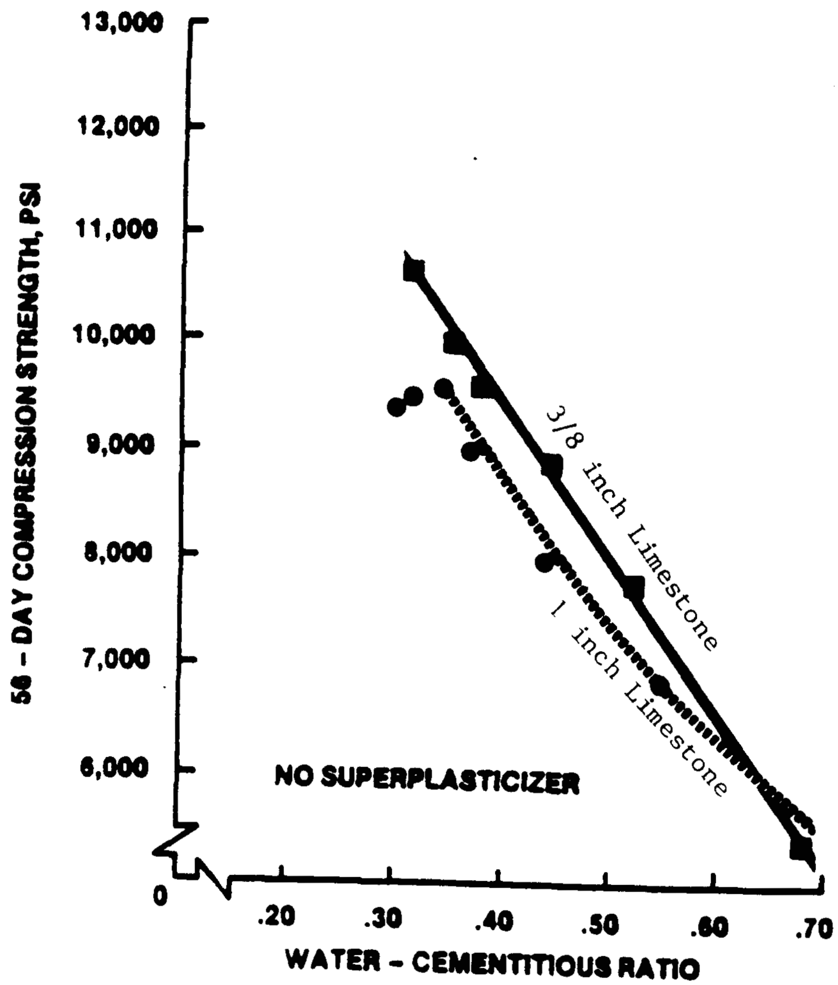

Fig. 3.3 Effect of aggregate type on 56 day concrete strength for different water-cementitous materials ratios [3.65]

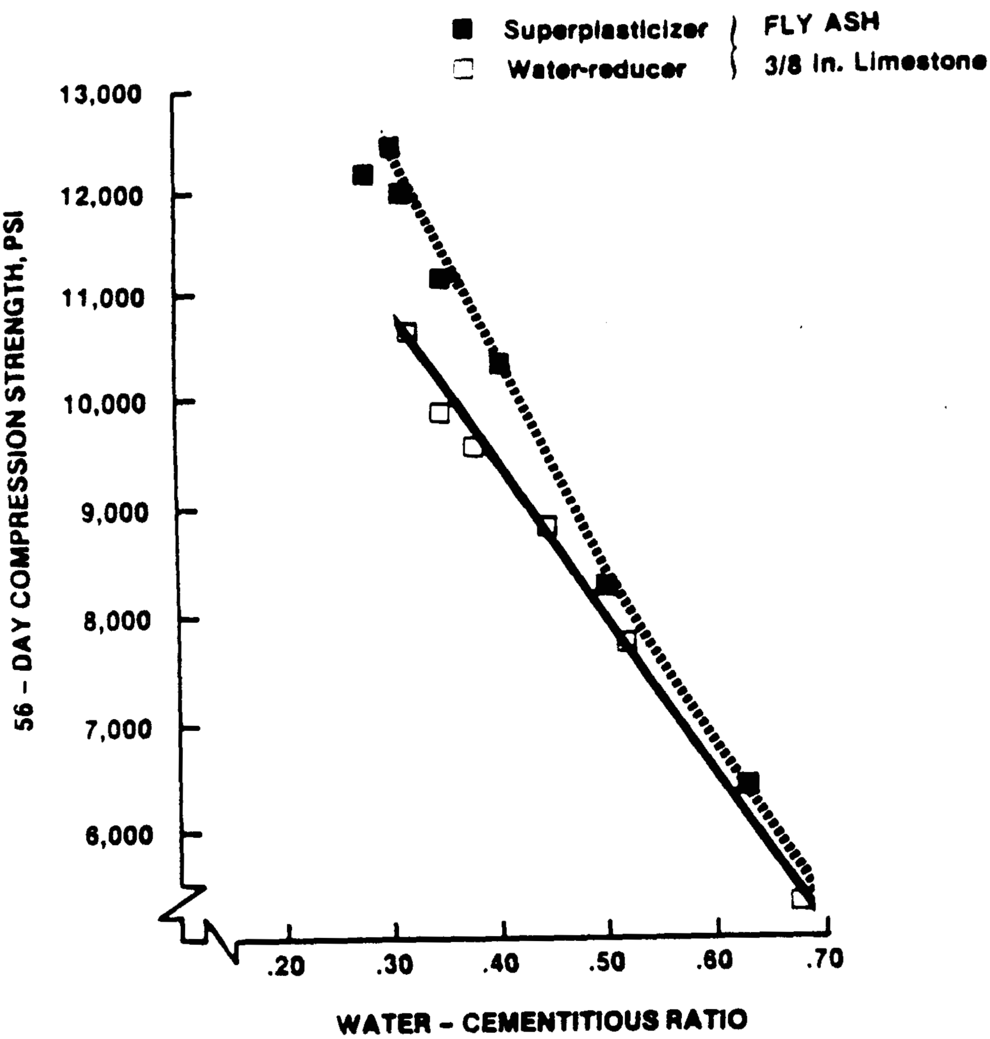

Fig. 3.4 Relationship of water-cementitious materials ratio with and without a high range water-reducing admixture for coarse aggregate size not exceeding 3/8 in. (10 mm) [3.65]

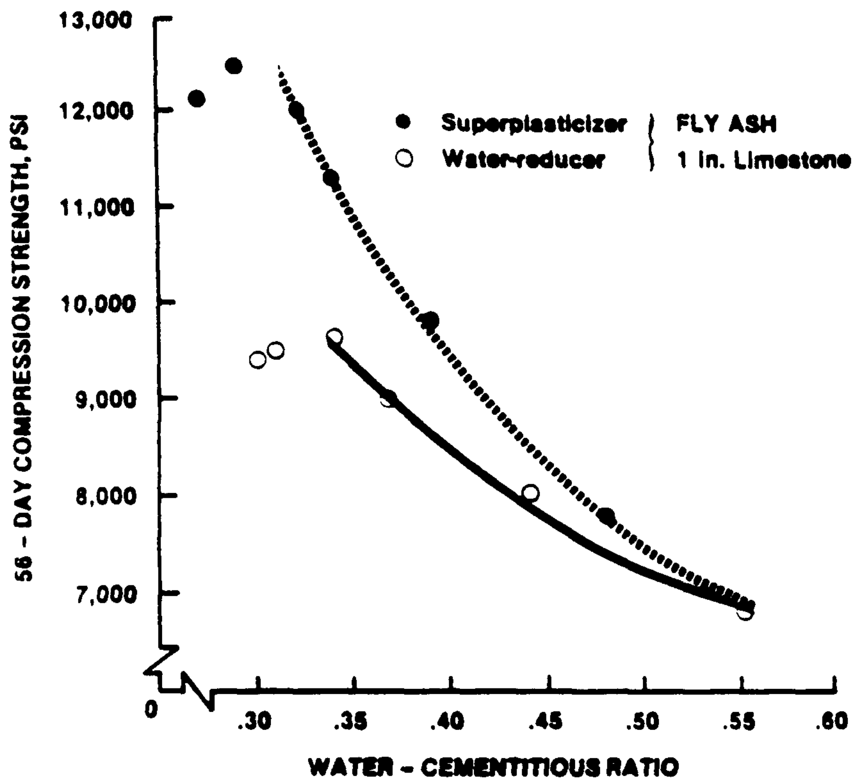

Fig. 3.5 Relationship of water-cementitious materials ratio with and without a high range water-reducing admixture for coarse aggregate size not excceding 1 in. (25 mm) [3.65]

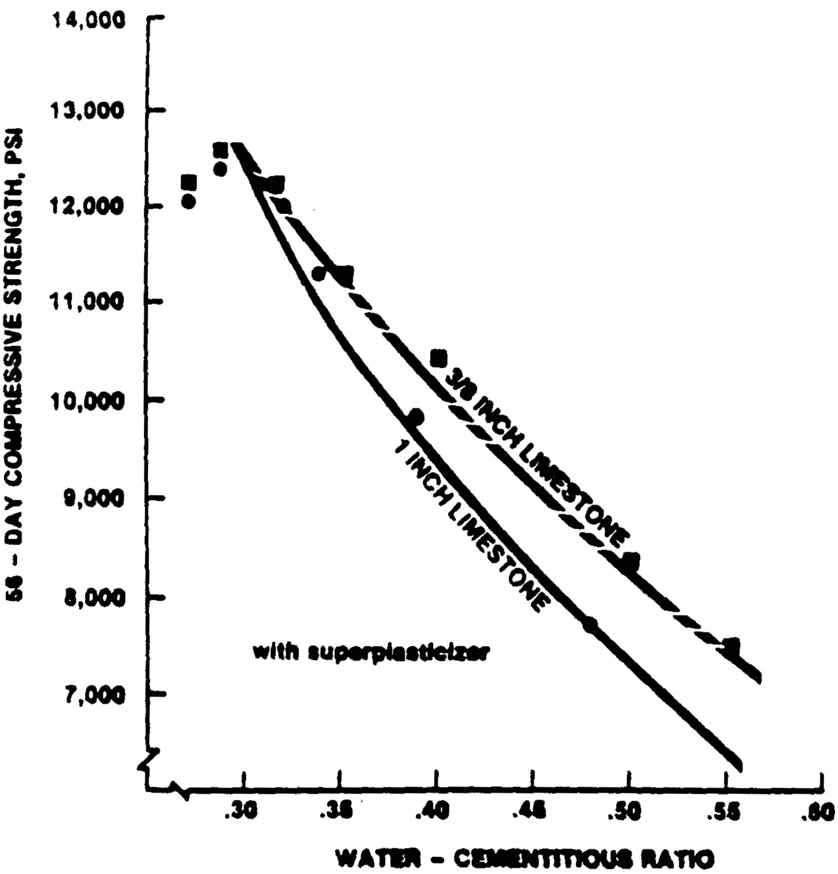

Fig. 3.6 Effect of aggregate type on strength at different ages for a constant water-cementitious materials ratio, with superplasticizer [3.65]

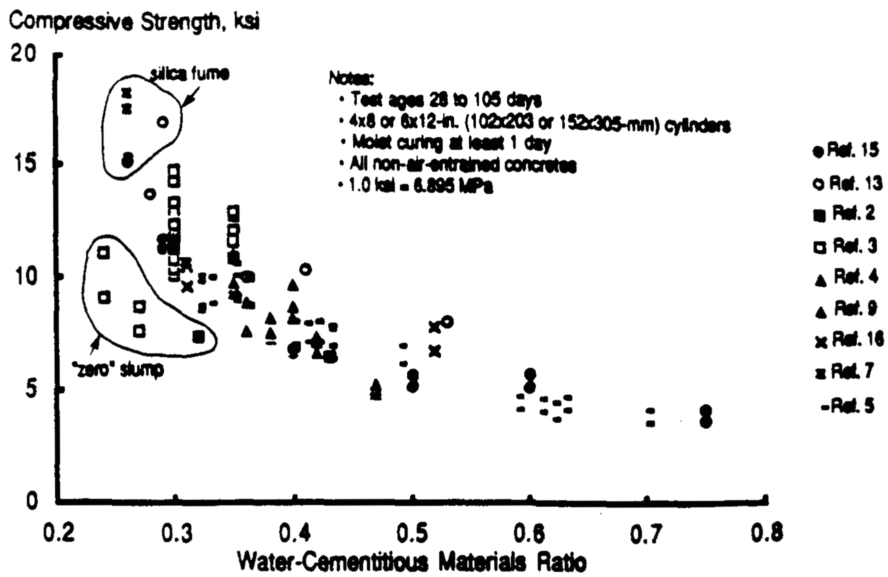

Fig. 3.7 Summary of strength data as a function of water-cementitious materials ratio [3.83]

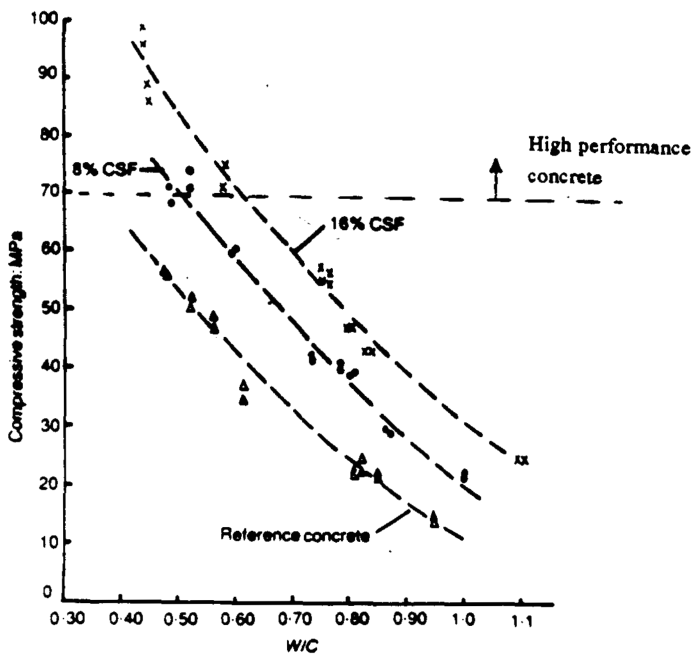

Fig. 3.8 28 day compressive strength versus water-cementitious materials ratio for concrete with different condensend silica fume contents [3.180]

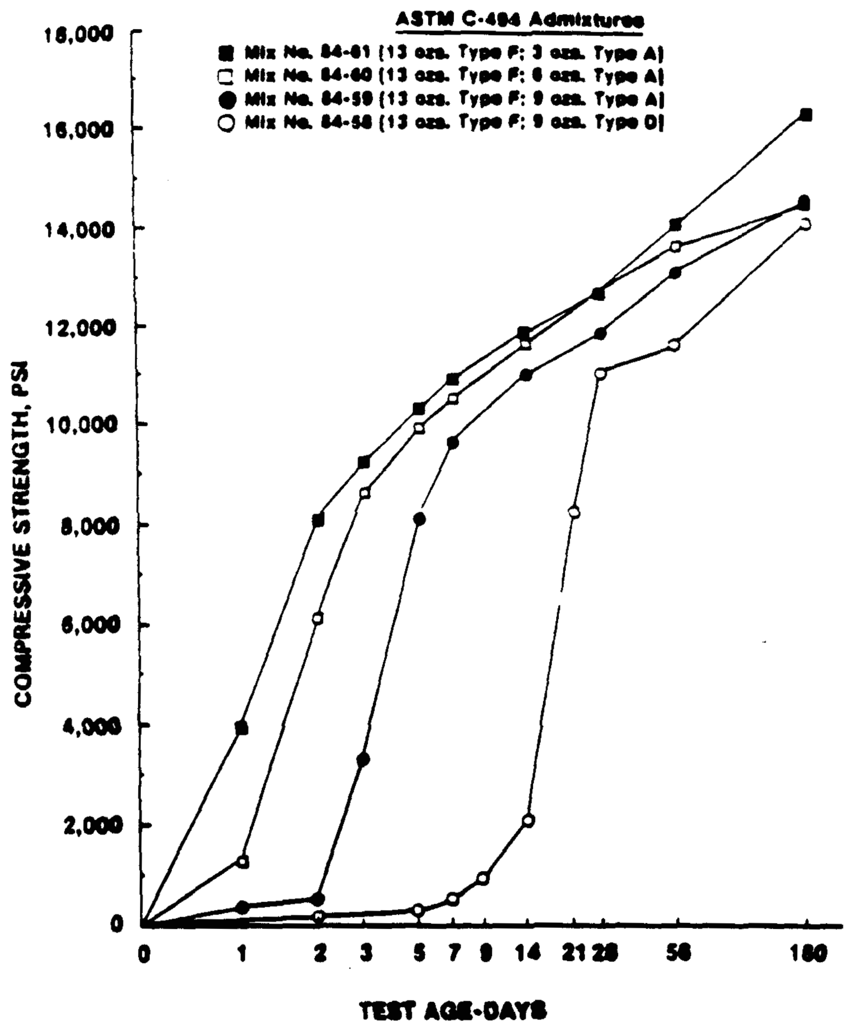

Fig. 3.9 Effect of varying dosage rates of a normal retarding water-reducing admixtures on the strength development of concrete [3.65]

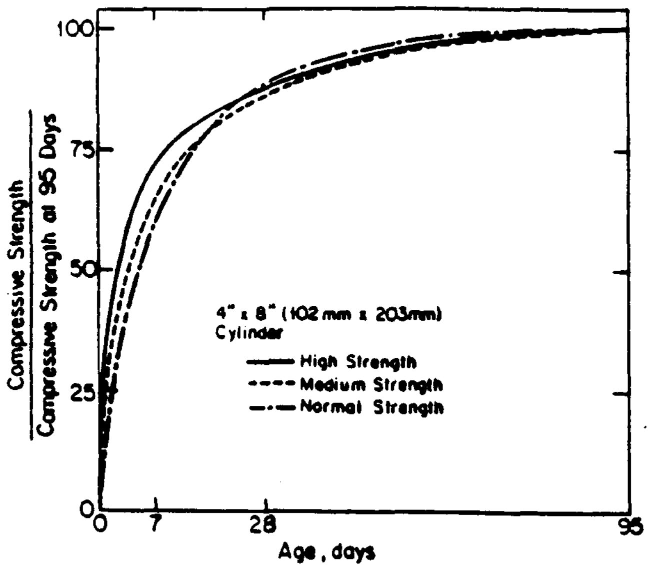

Fig. 3.10 Normalized strength gain with age for limestone concretes moist-cured until testing [3.49]

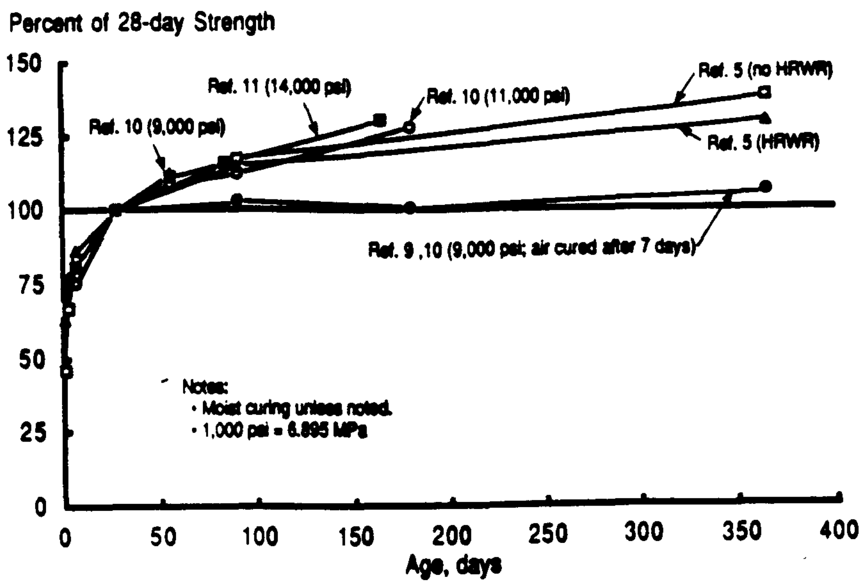

Fig. 3.11 Compressive strength development for concretes with and without high range water reducers [3.83]

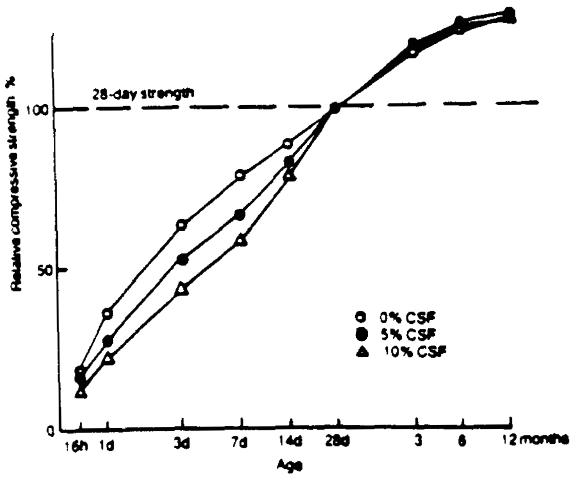

Fig. 3.12 Compressive strength development of concrete cured at 20^{0}C with different dosages of condensed silica fume [3.125]

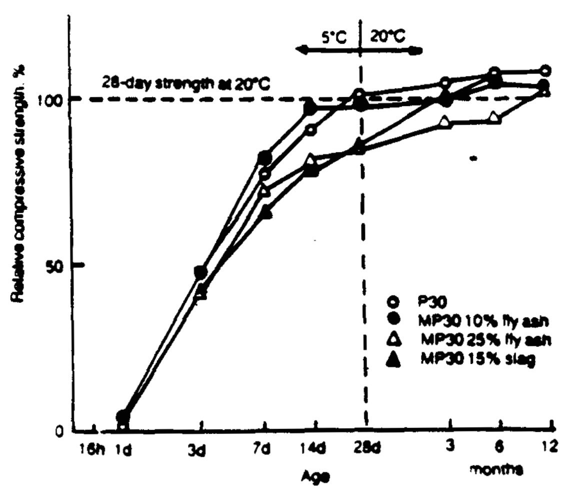

Fig. 3.13 Development of compressive strength in reference concrete cured in water at 5^{0}C for 28 days then at 20^{0}C. 100 percent represents 28-day strength at 20^{0}C for each cement type [3.125]

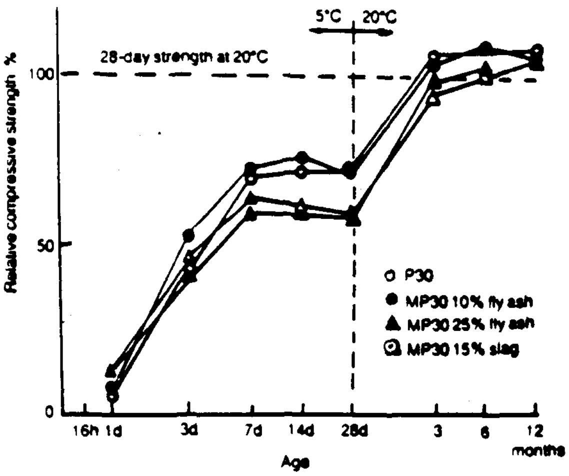

Fig. 3.14 Development of compressive strength in concrete containing 10% condensed silica fume and cured in water at 5^{0}C for 28 days then at 20^{0}C. 100 percent represents 28-day strength at 20^{0}C for each cement type (with 10% CSF) [3.125]

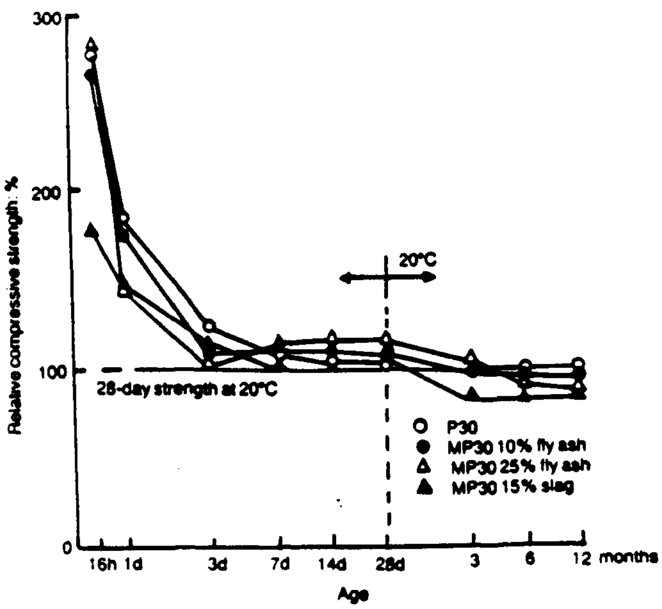

Fig. 3.15 Development of compressive strength in reference concrete cured in water at 35^{0}C for 28 days then at 20^{0}C. 100 percent represents 28-day strength at 20^{0}C for each cement type [3.125]

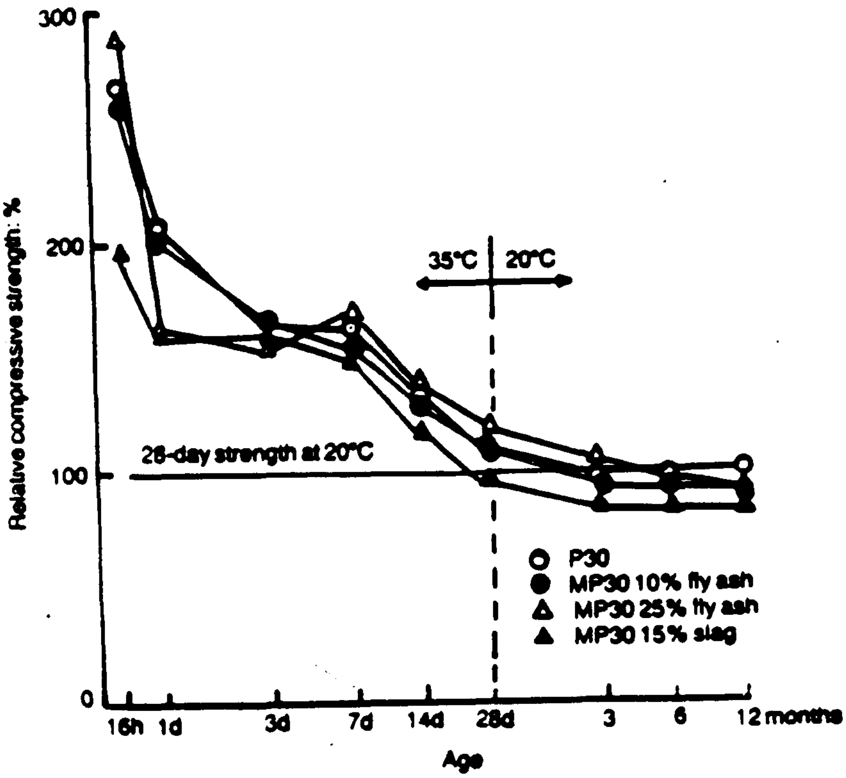

Fig. 3.16 Development of compressive strength in concrete containing 10% condensed silica fume and water-cured at 35^{0}C for 28 days then at 20^{0}C. 100 percent represents 28-day strength at 20^{0}C for each cement type [3.125]

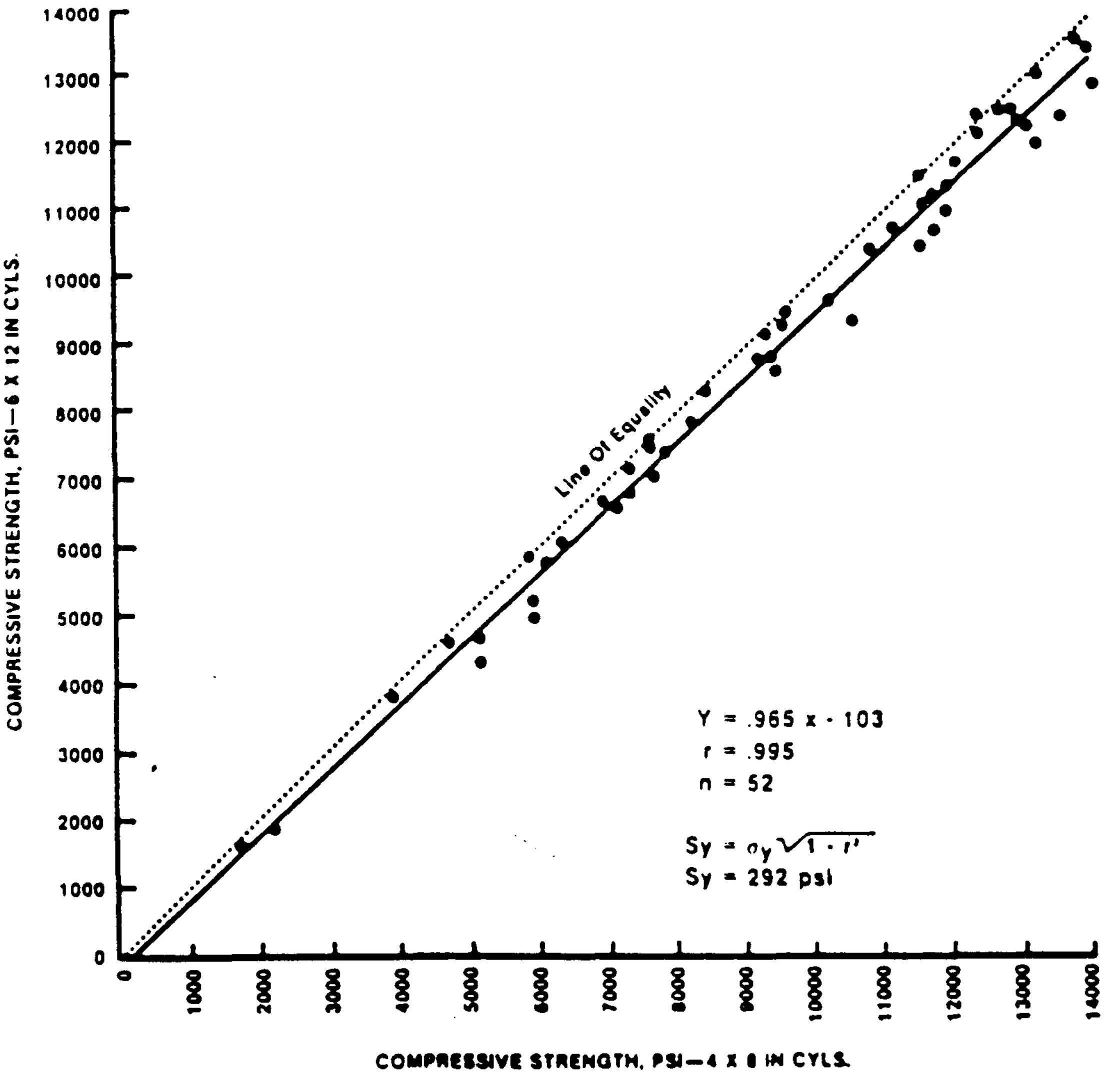

Fig. 3.17 Relationship between the compressive strength of 4 x 8 in. (102 x 203 mm) cylinders and 6 x 12 in. (152 x 304 mm) cylinders [3.65]

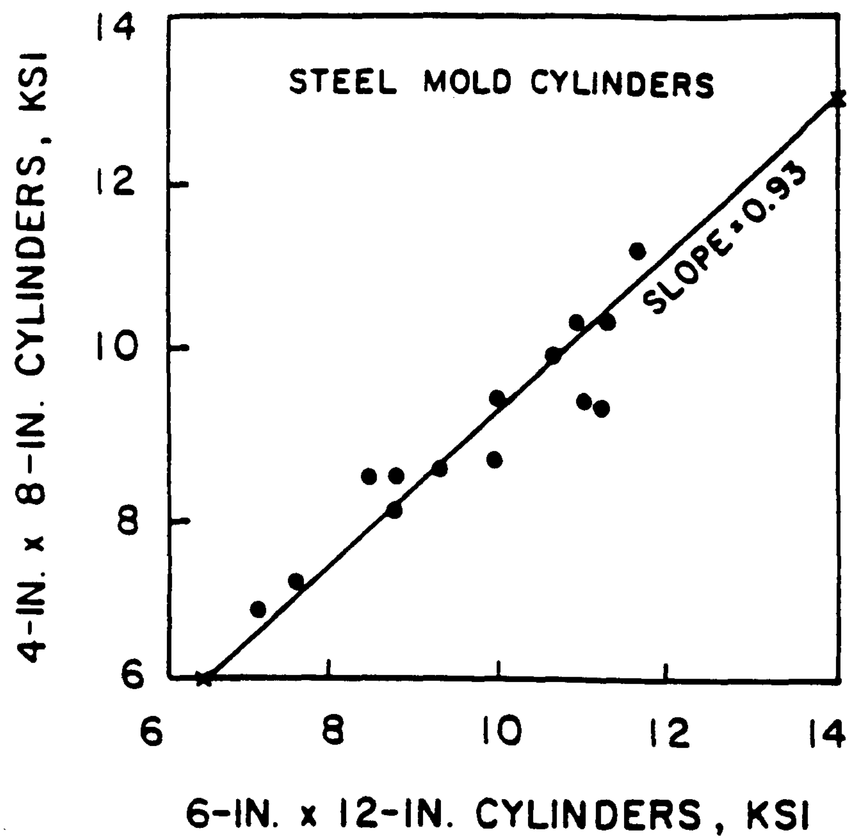

Fig. 3.18 Compressive strength of concrete cylinders cast in 4 x 8 in. (102 x 203 mm) steel molds versus 6 x 12 in. (152 x 304 mm) steel molds [3.53]

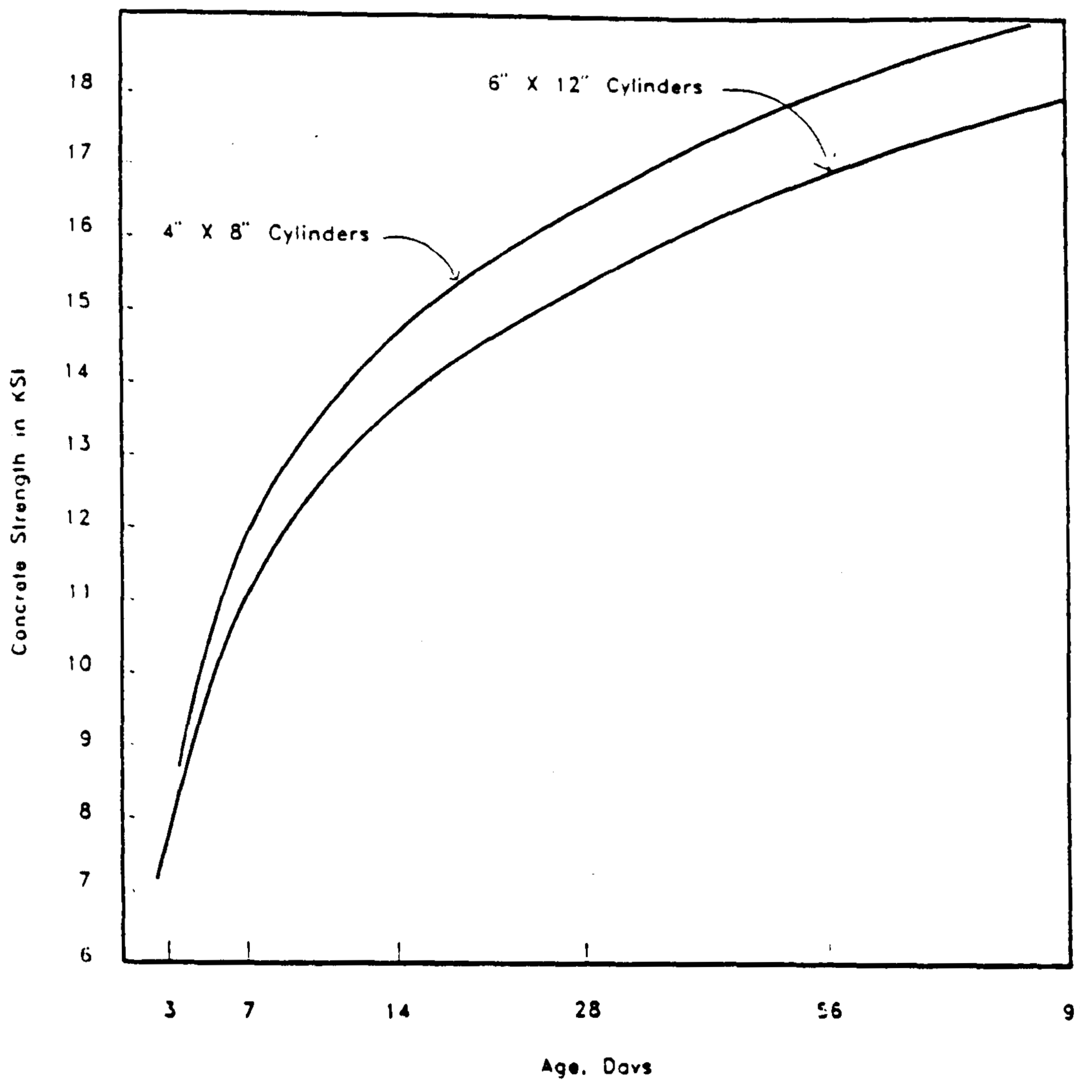

Fig. 3.19 Compressive strength development for 17,000 psi (117 MPa) concrete [3.137]

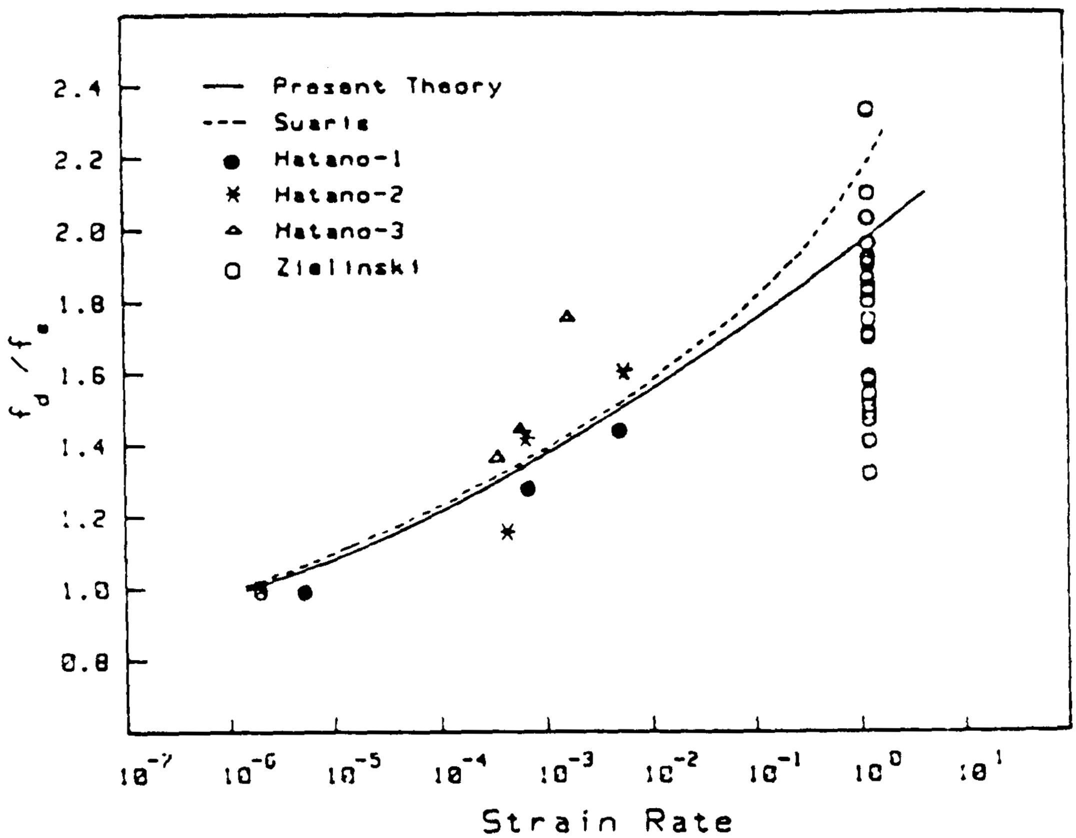

Fig. 3.20 Effect of strain rate on tensile strength of concrete [3.144]

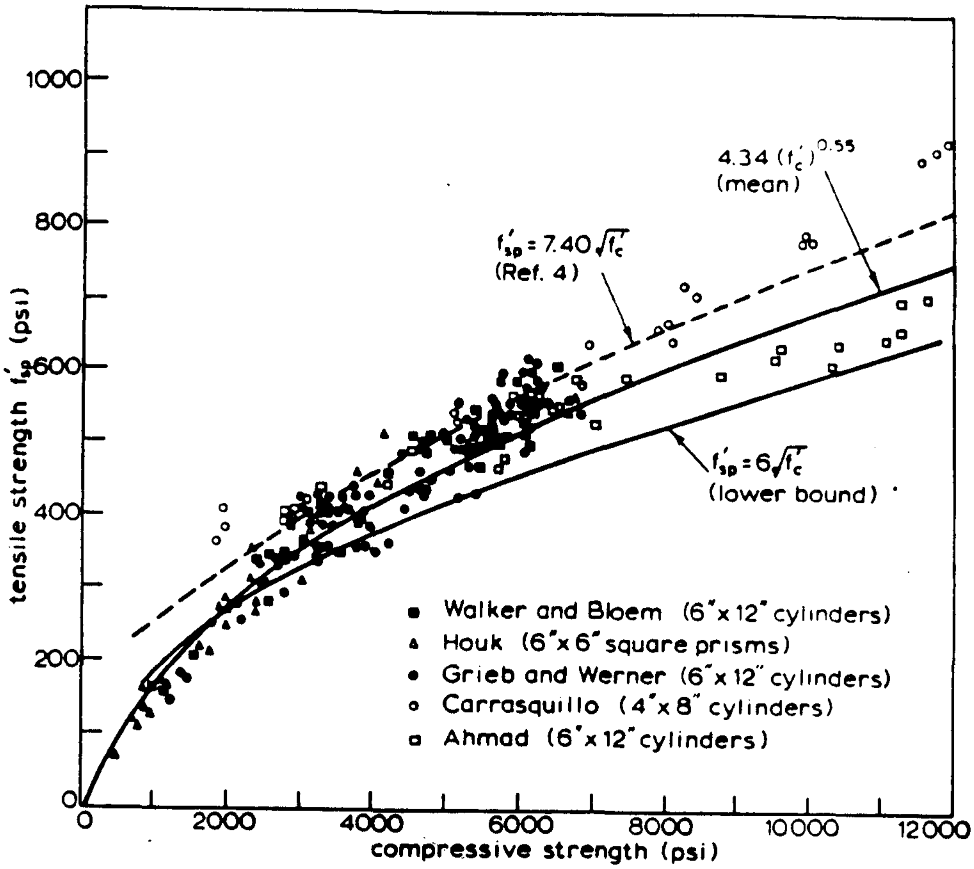

Fig. 3.21 Variation of splitting tensile strength of normal weight concrete with the compressive strength [3.9]

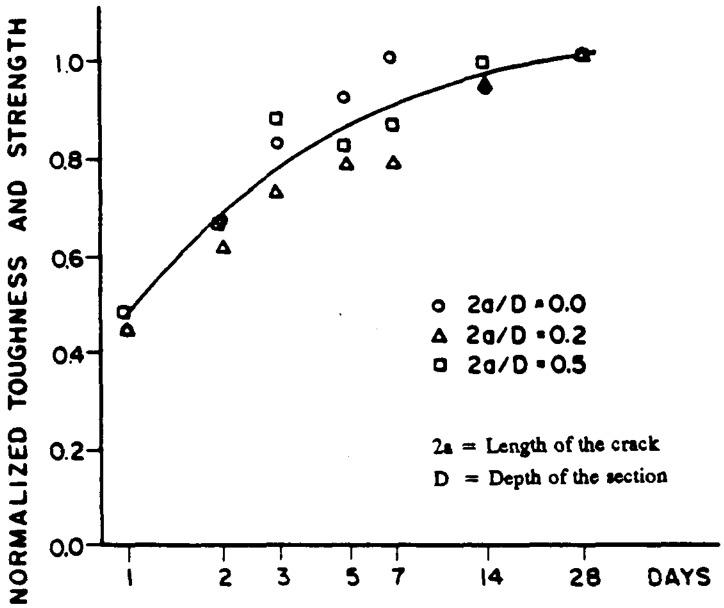

Fig. 3.22 Normalized splitting tensile strength as a funtion of the age at testing [3.145]

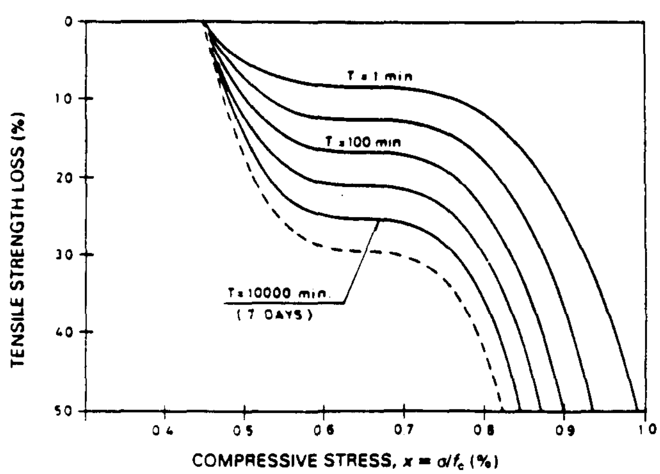

Fig. 3.23 Tensile strength loss as a function of compressive stress fraction for different duration of loading [3.121]

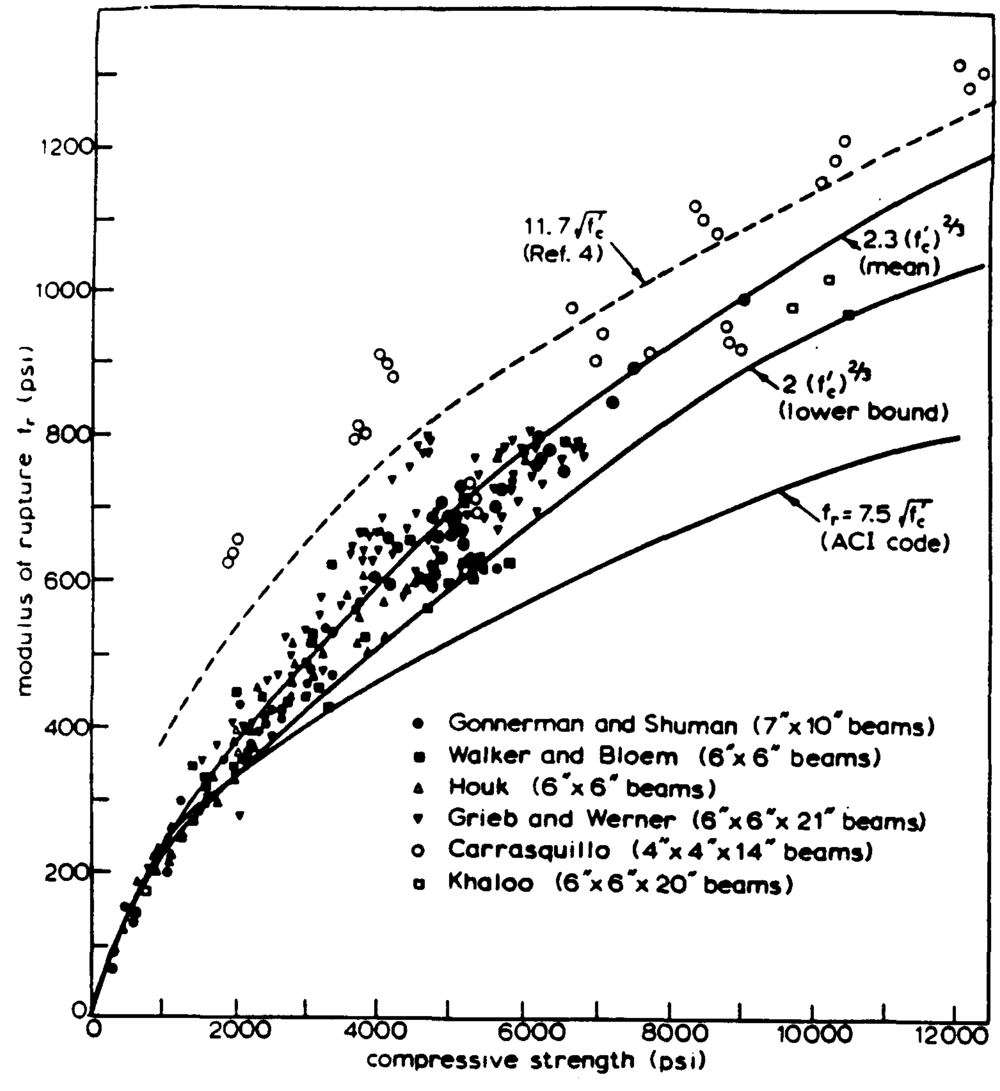

Fig. 3.24 Variation of modulus of rupture with the compressive strength [3.9]

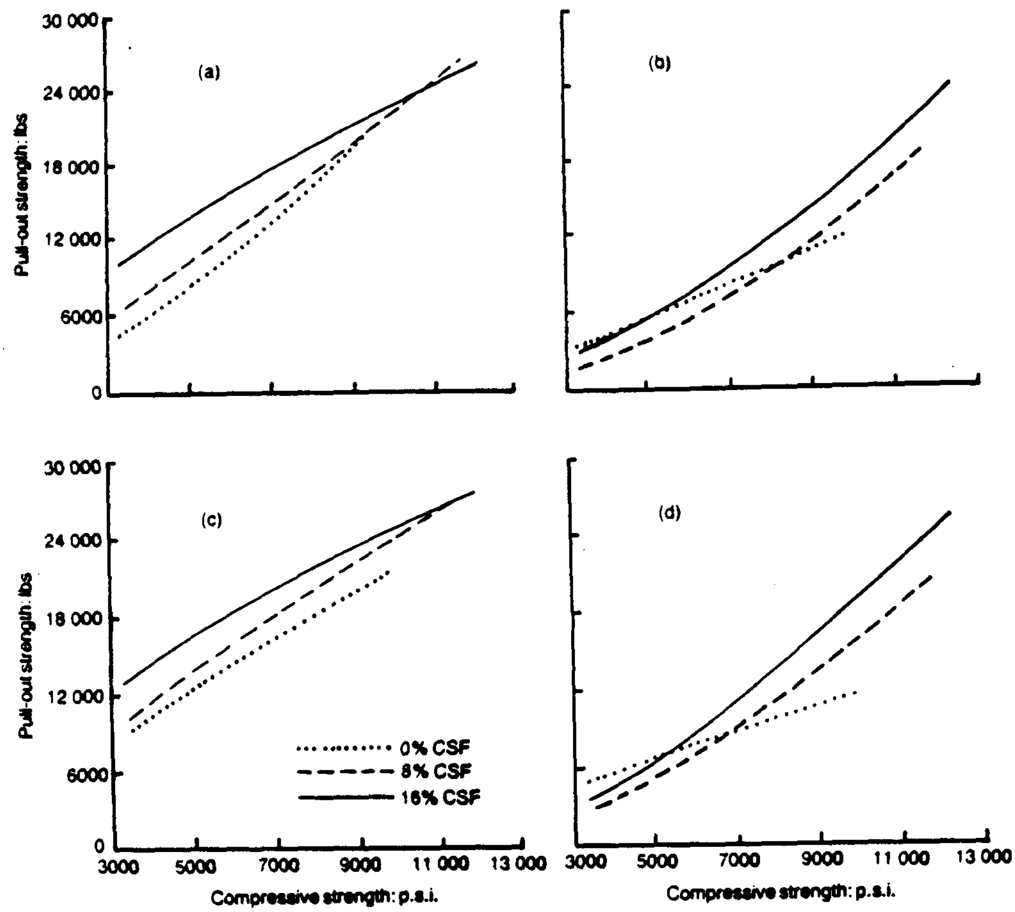

Fig. 3.25 Pull-out strengths versus concrete compressive strengths; (a) deformed bars (upper position); (b) plain bars (upper position); (c) deformed bars (lower position); (d) plain bars (lower position) [3.89]

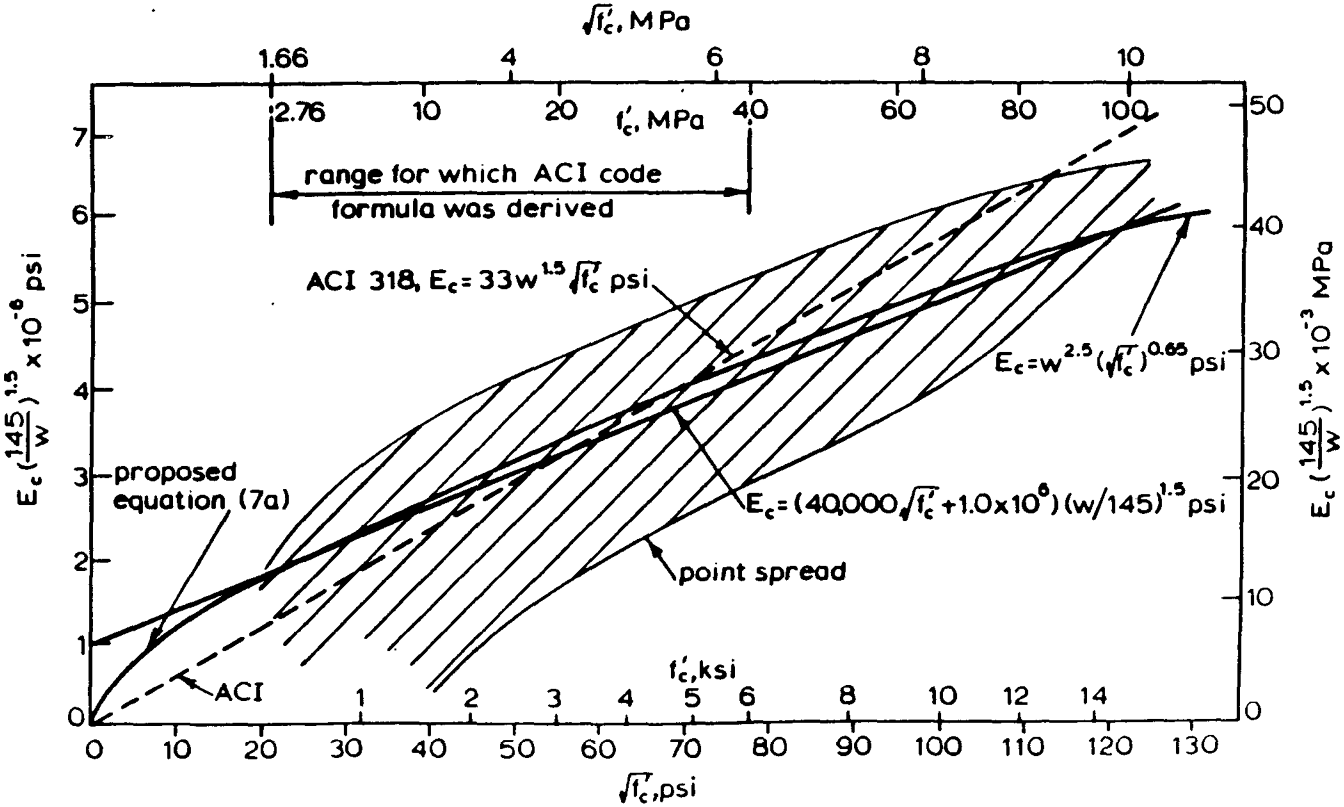

Fig. 3.26 Secant modulus of elasticity versus concrete strength [3.9]

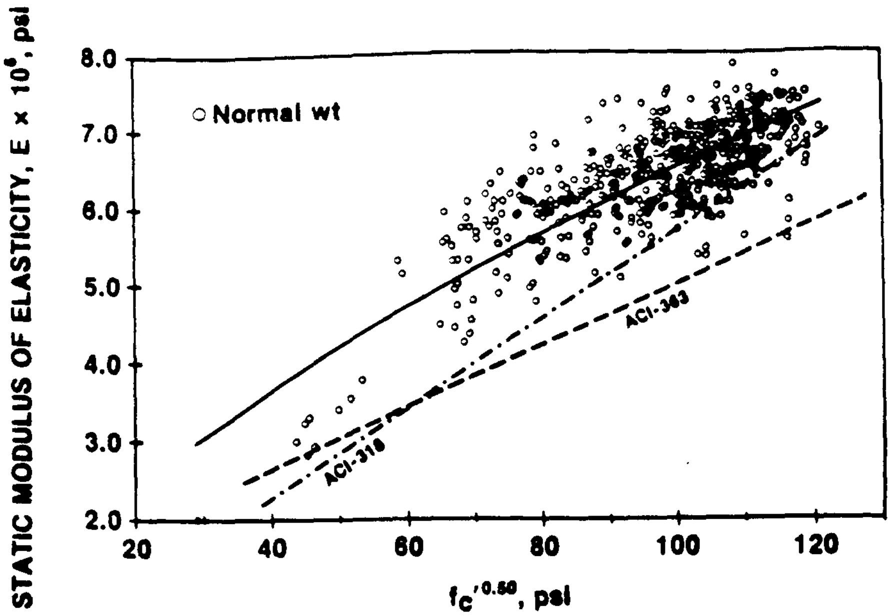

Fig. 3.27 Secant modulus of elasticity versus concrete strength for normal weight concrete [3.65]

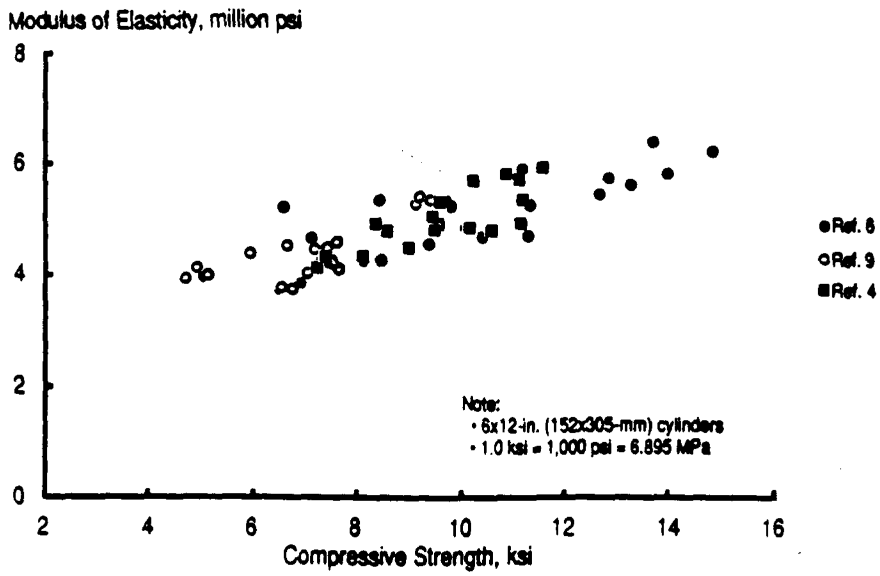

Fig. 3.28 Secant modulus of elasticity as a function of strength [3.83]

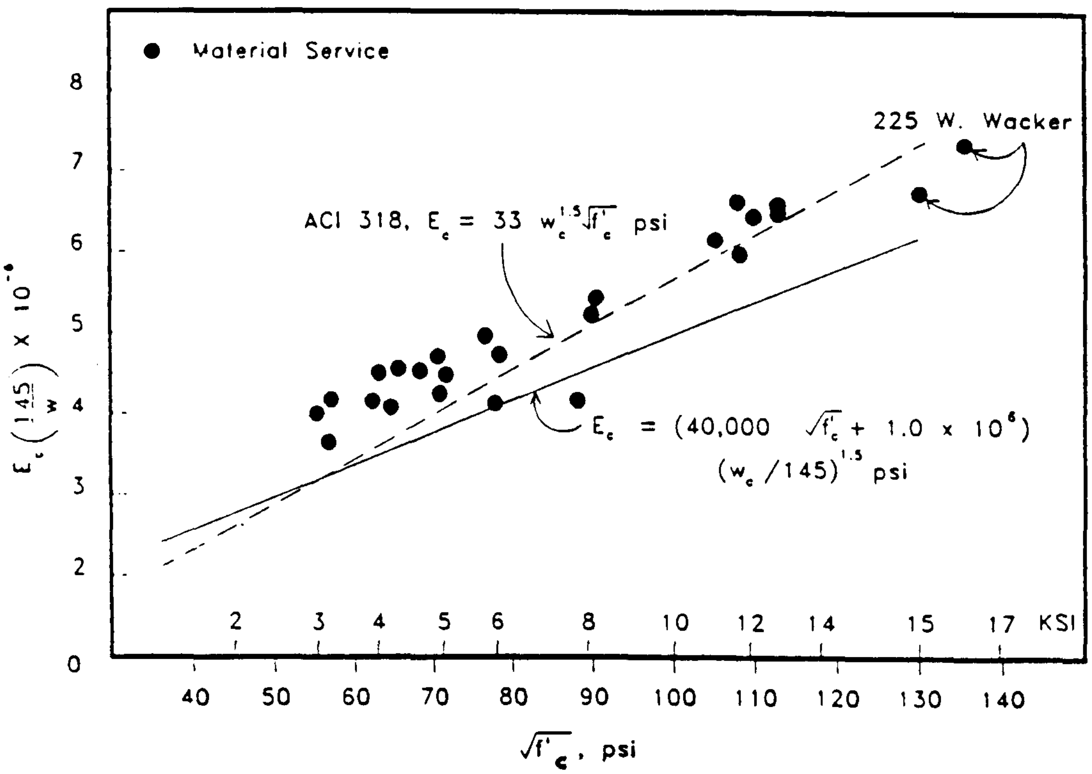

Fig. 3.29 Secant modulus of elasticity variation with $\sqrt{f_c'}$ [3.137]

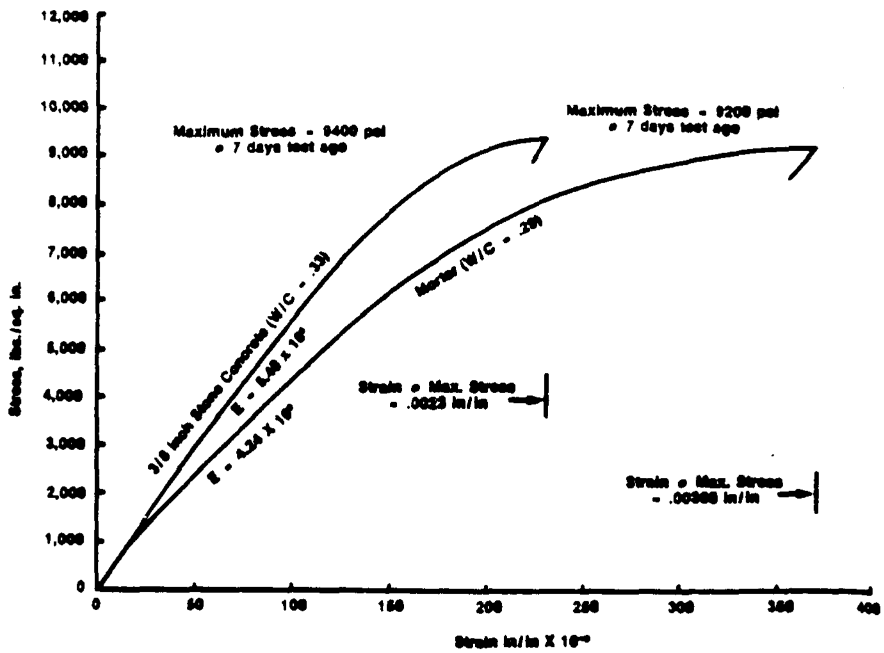

Fig. 3.30 Effect of coarse aggregate and mix proportions on the modulus of elasticity [3.65]

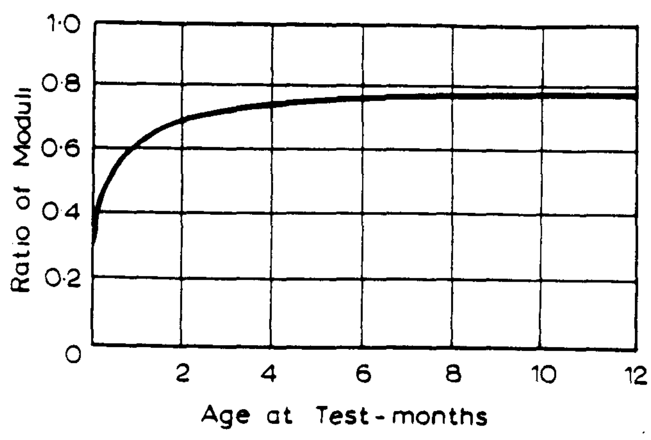

Fig. 3.31 Ratio of static and dynamic modulus of elasticity of concrete at different ages [3.158]

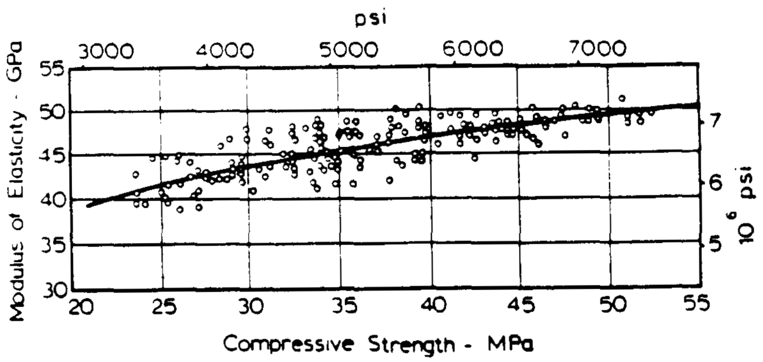

Fig. 3.32 Relation between the dynamic modulus of elasticity, determined by transverse vibration of cylinders, and their compressive strengths [3.186]

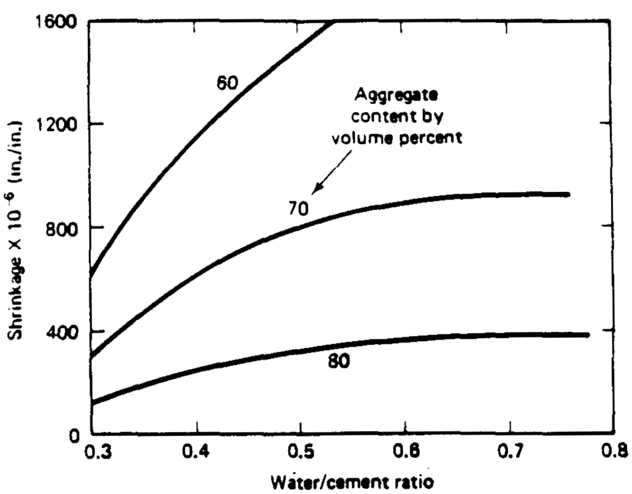

Fig. 3.33 Effect of water-cementitious materials ratio and aggregate content on shrinkage [3.139]

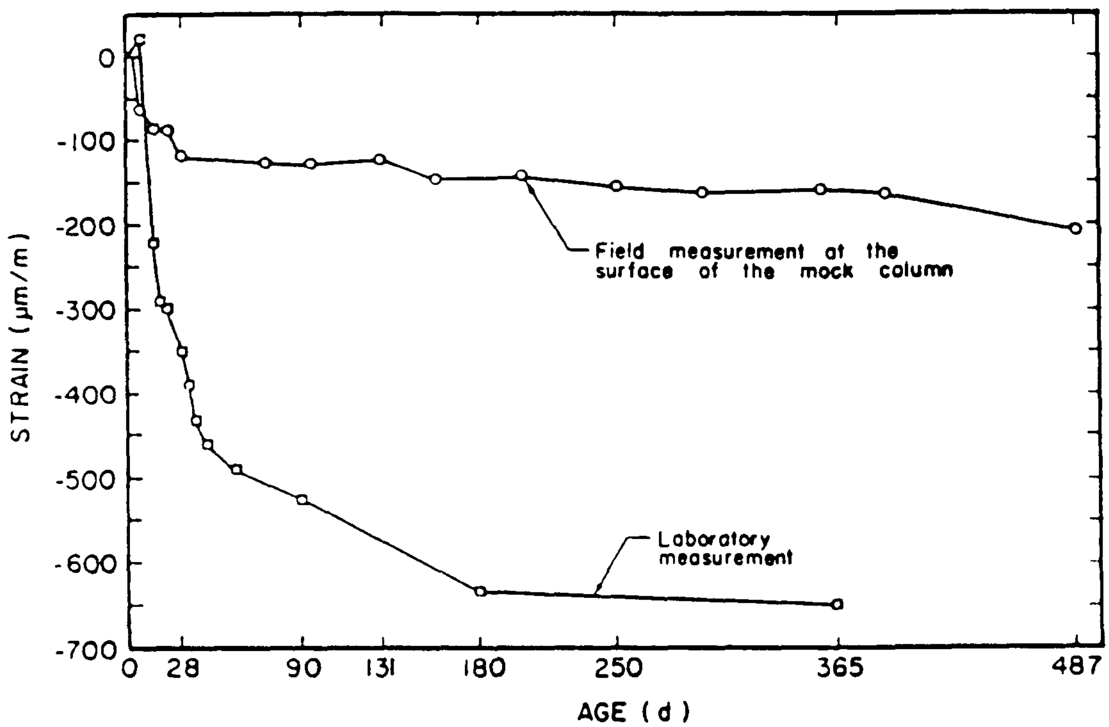

Fig. 3.34 Comparison of field and laboratory drying shrinkage [3.16]

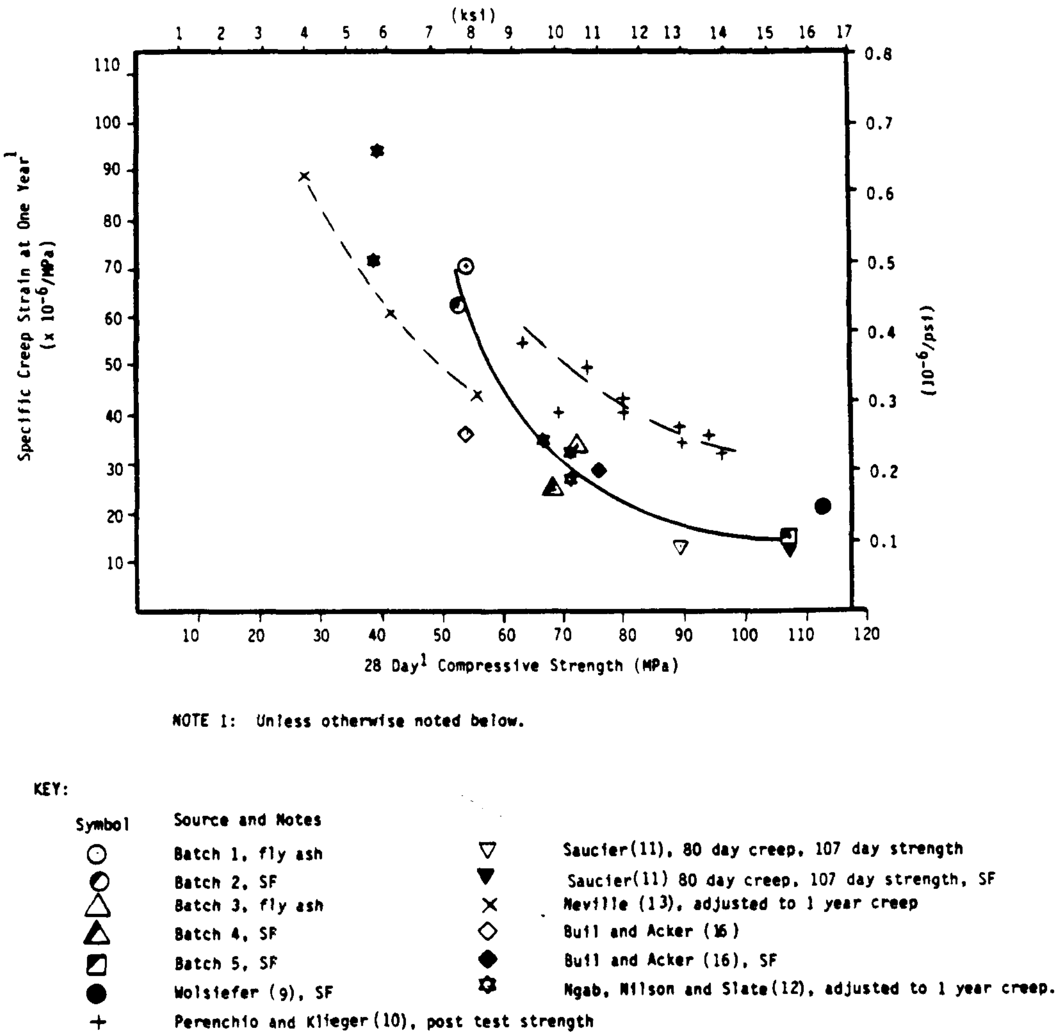

Fig. 3.35 Relationship between specific creep and compressive strength [3.124]

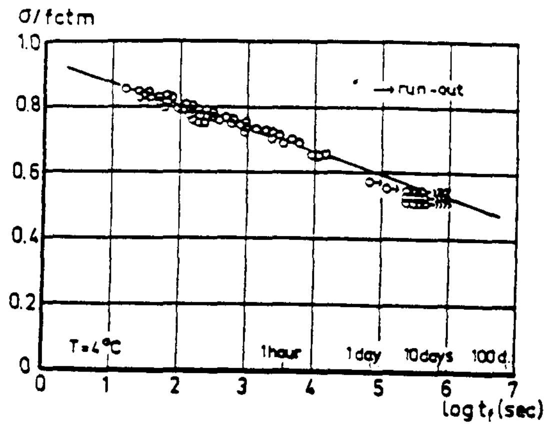

Fig. 3.36 Relative stress versus time to failure under unaxial tensile fatigue [3.67]

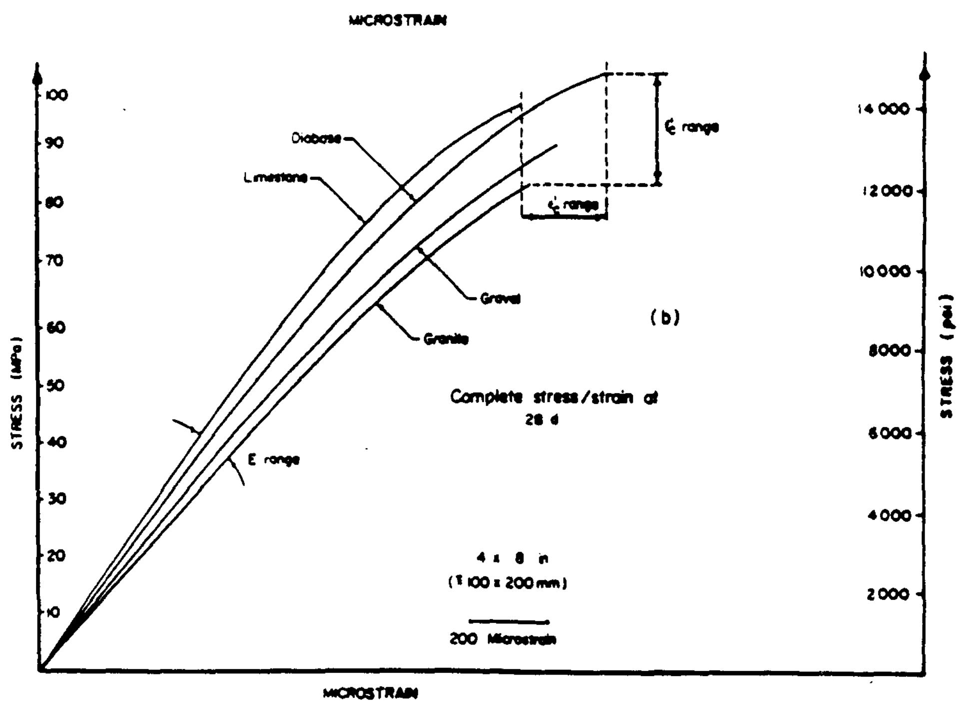

Fig. 3.37 Effect of the aggregate type on the ascending portion of the stress-strain curves of concrete at 28 days [3.17]

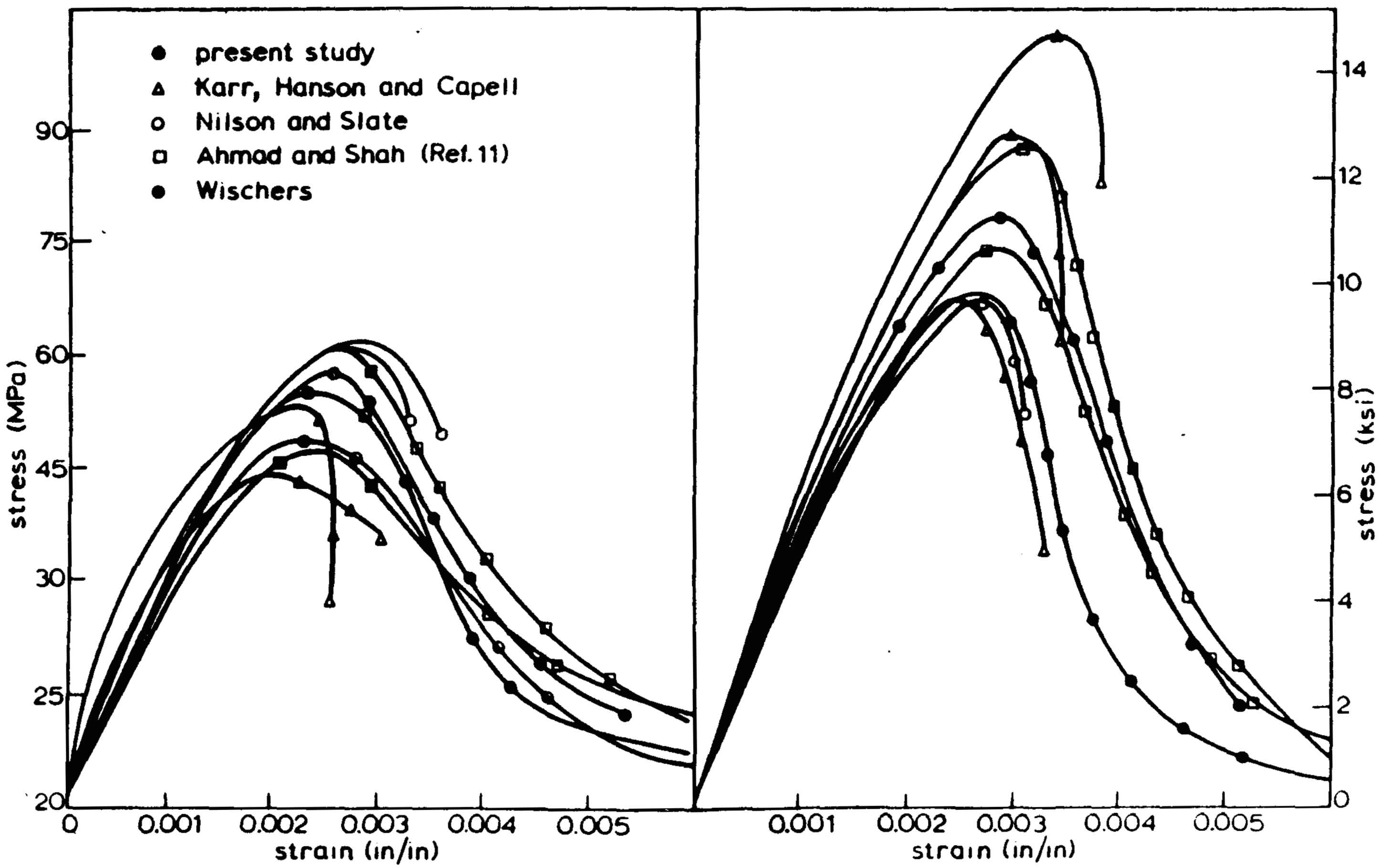

Fig. 3.38 Different stress strain curves reported for high strength concrete under uniaxial compression [3.9]

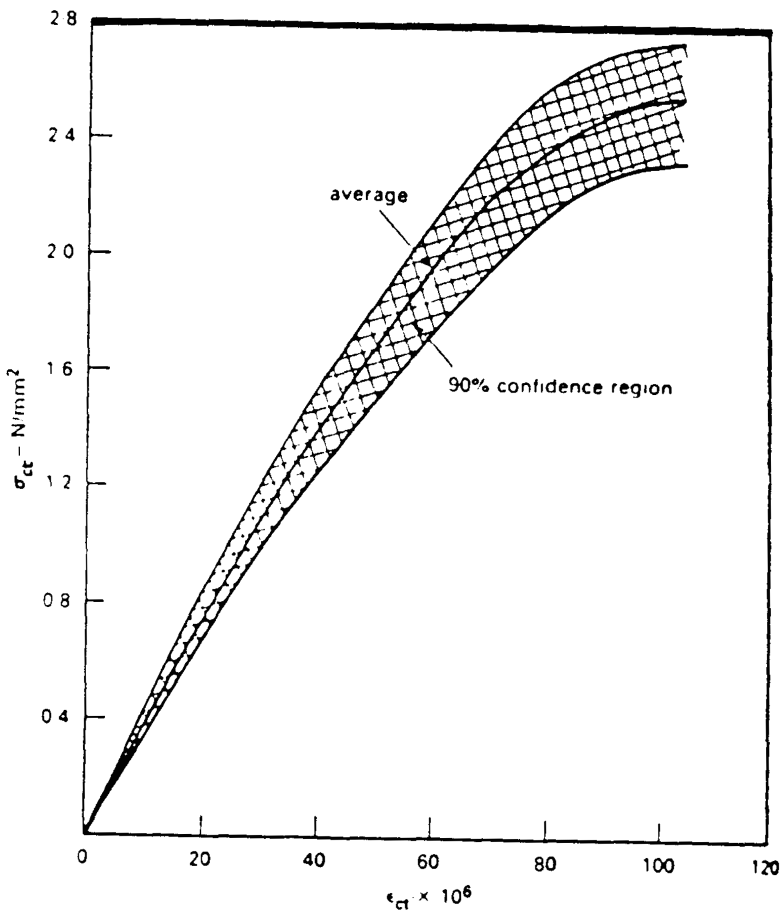

Fig. 3.39 A typical stress strain curve for concrete under uniaxial tension determined under static load controlled tests [3.68]

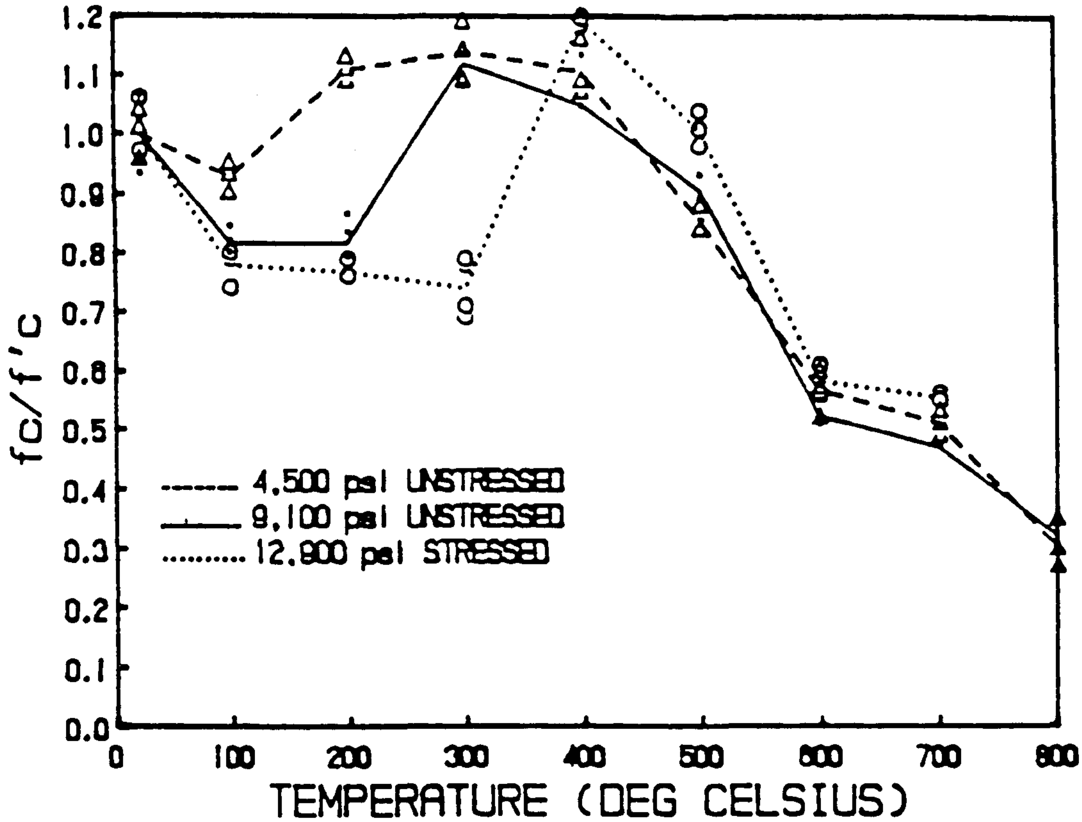

Fig. 3.40 Variation of compressive strength with increase in temperature [3.57]

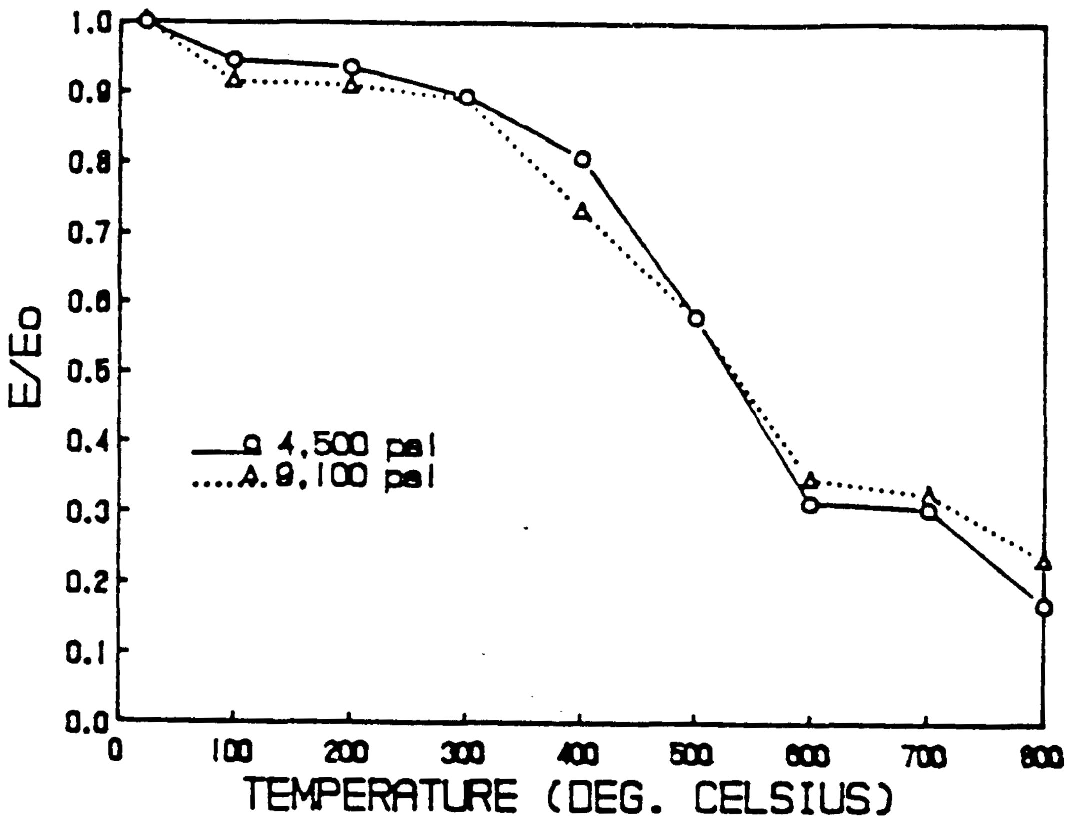

Fig. 3.41 Variation in modulus of elasticity of normal and high- strength concrete with increase in temperature [3.57]

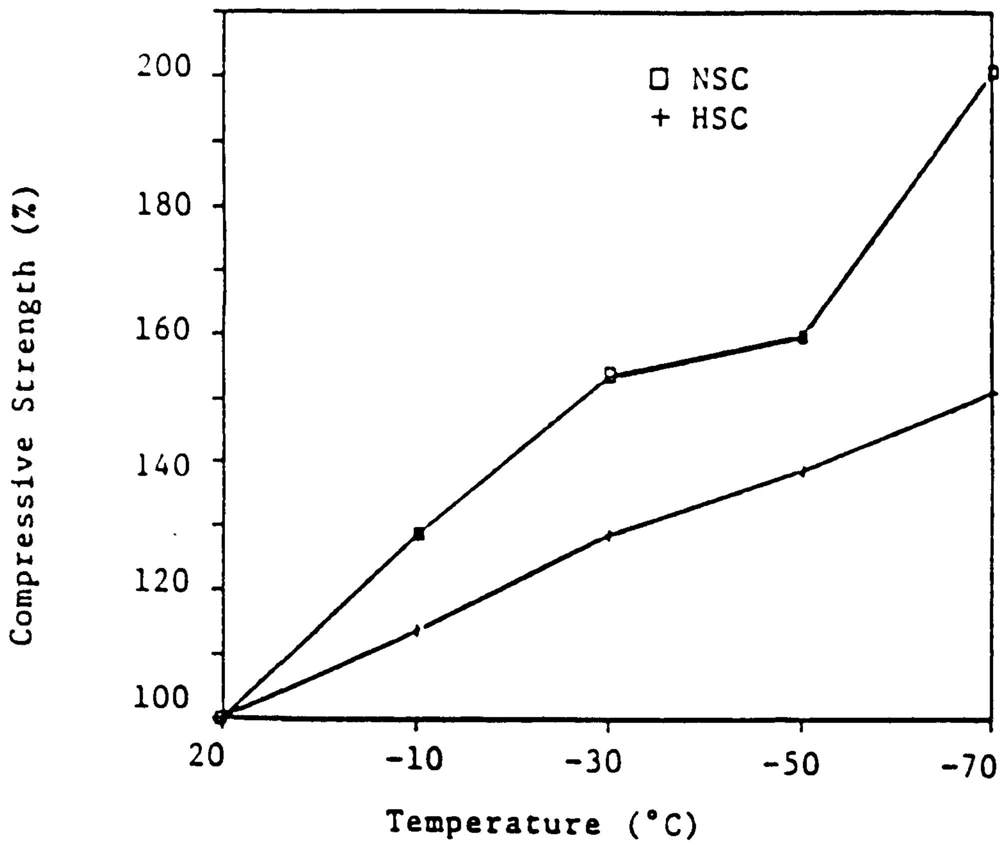

Fig. 3.42 Effect of low temperature variation on the percentage of compressive strength increase for normal and high-strength concrete [3.119]

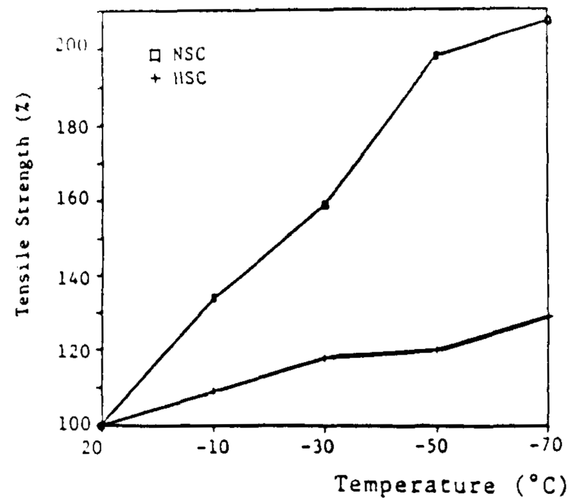

Fig. 3.43 Effect of low tempreture on the percentage of tensile strength increase for normal and high-strength concrete [3.119]

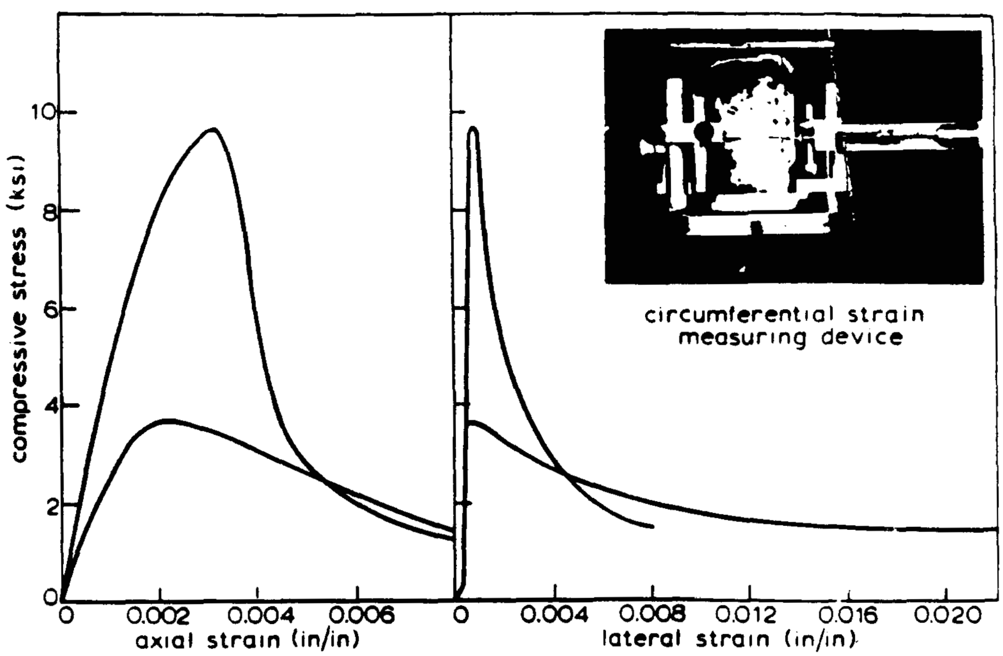

Fig. 3.44 Axial stress versus axial strain and lateral strain for normal and high-strength concrete [3.9]

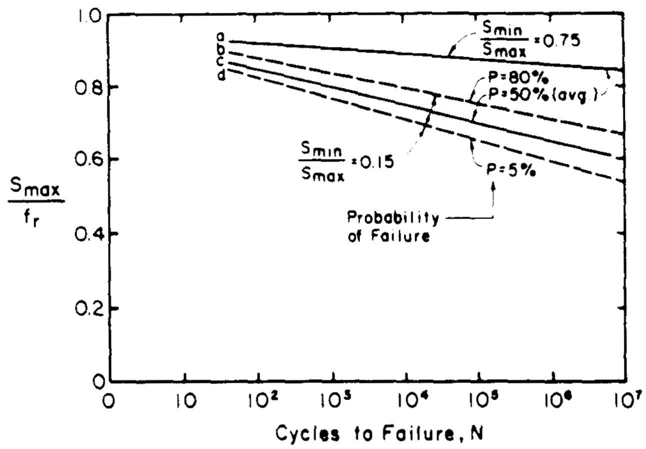

Fig. 3.45 Fatigue strength of plain concrete beams [3.5]

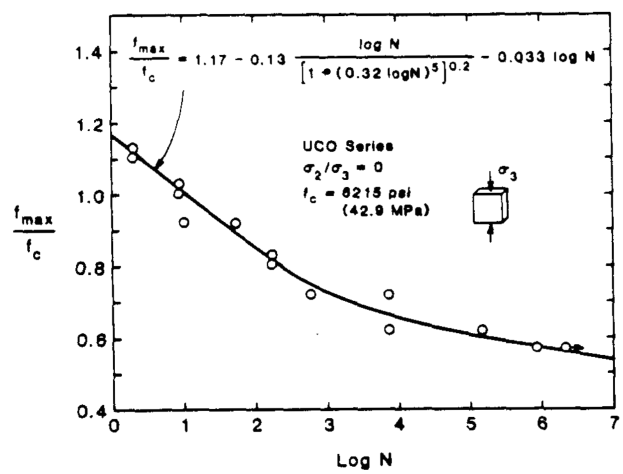

Fig. 3.46 S-N curve for uniaxial test of concrete [3.193]

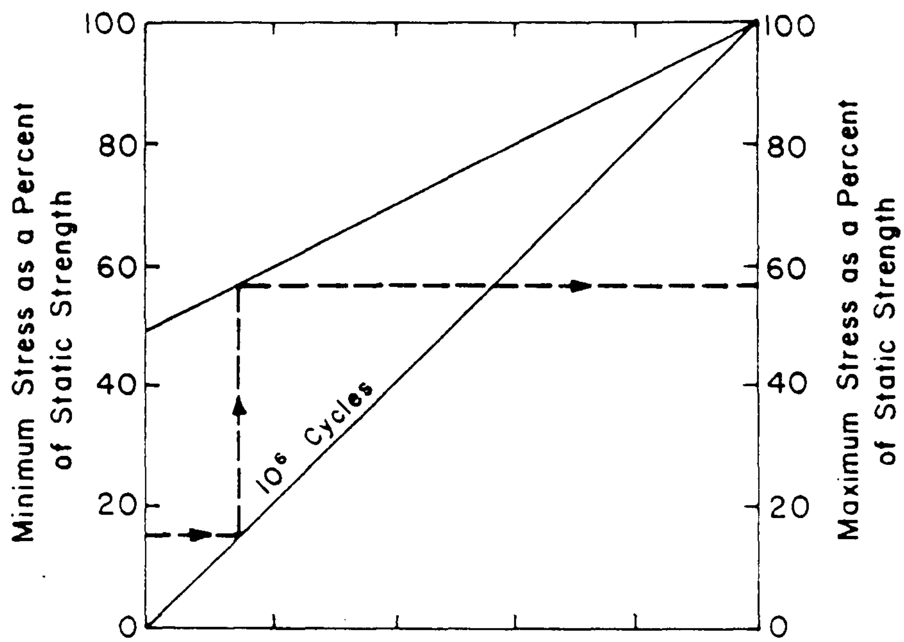

Fig. 3.47 Fatigue strength of plain concrete in tension, compression, or flexure [3.5]

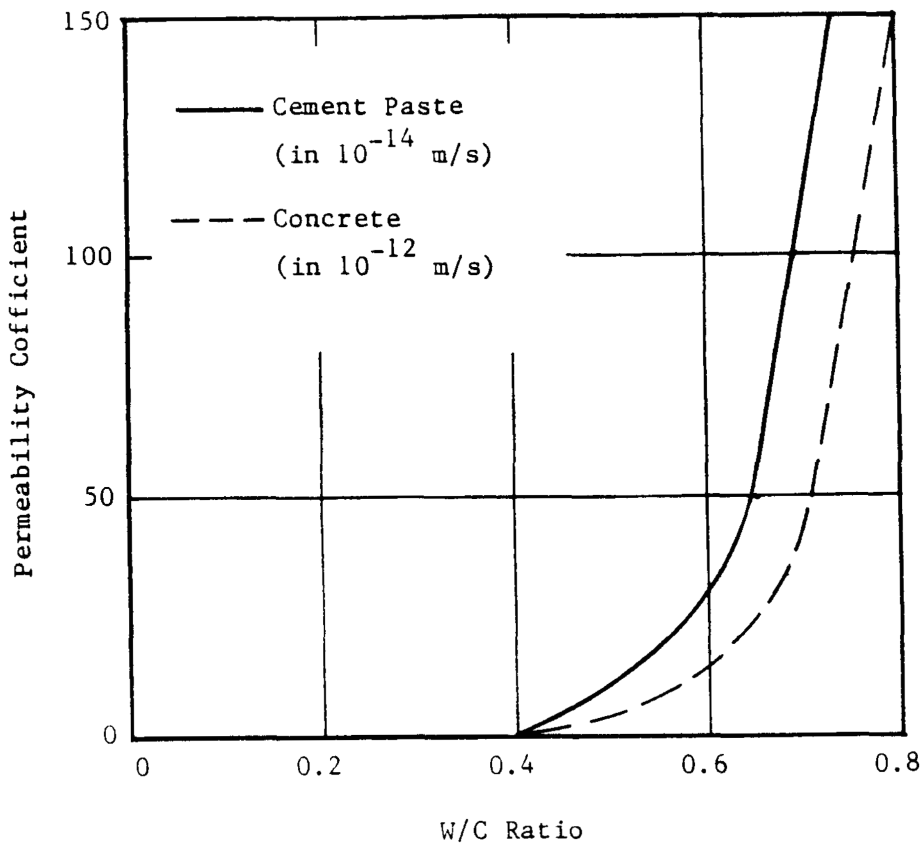

Fig. 3.48 Effect of W/C ratio on permeability of cement paste [3.212]

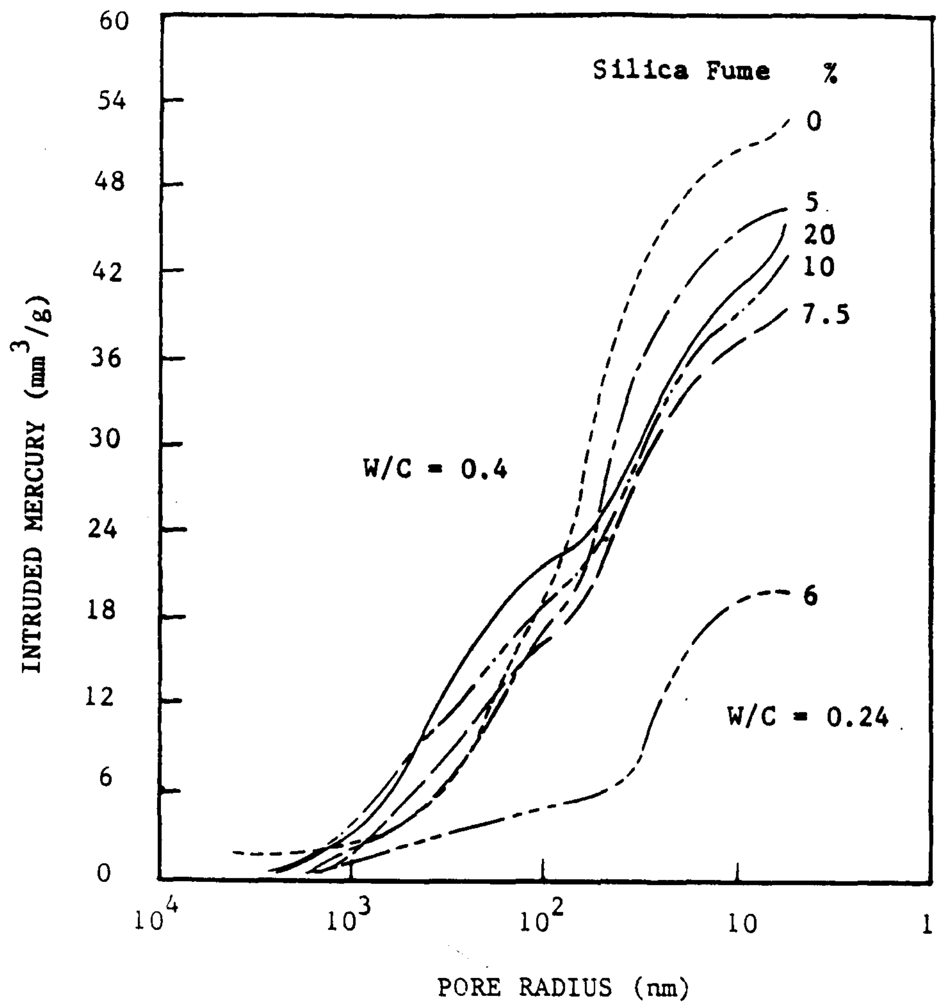

Fig. 3.49 Effect of pore radius on intruded mercury [3.157]

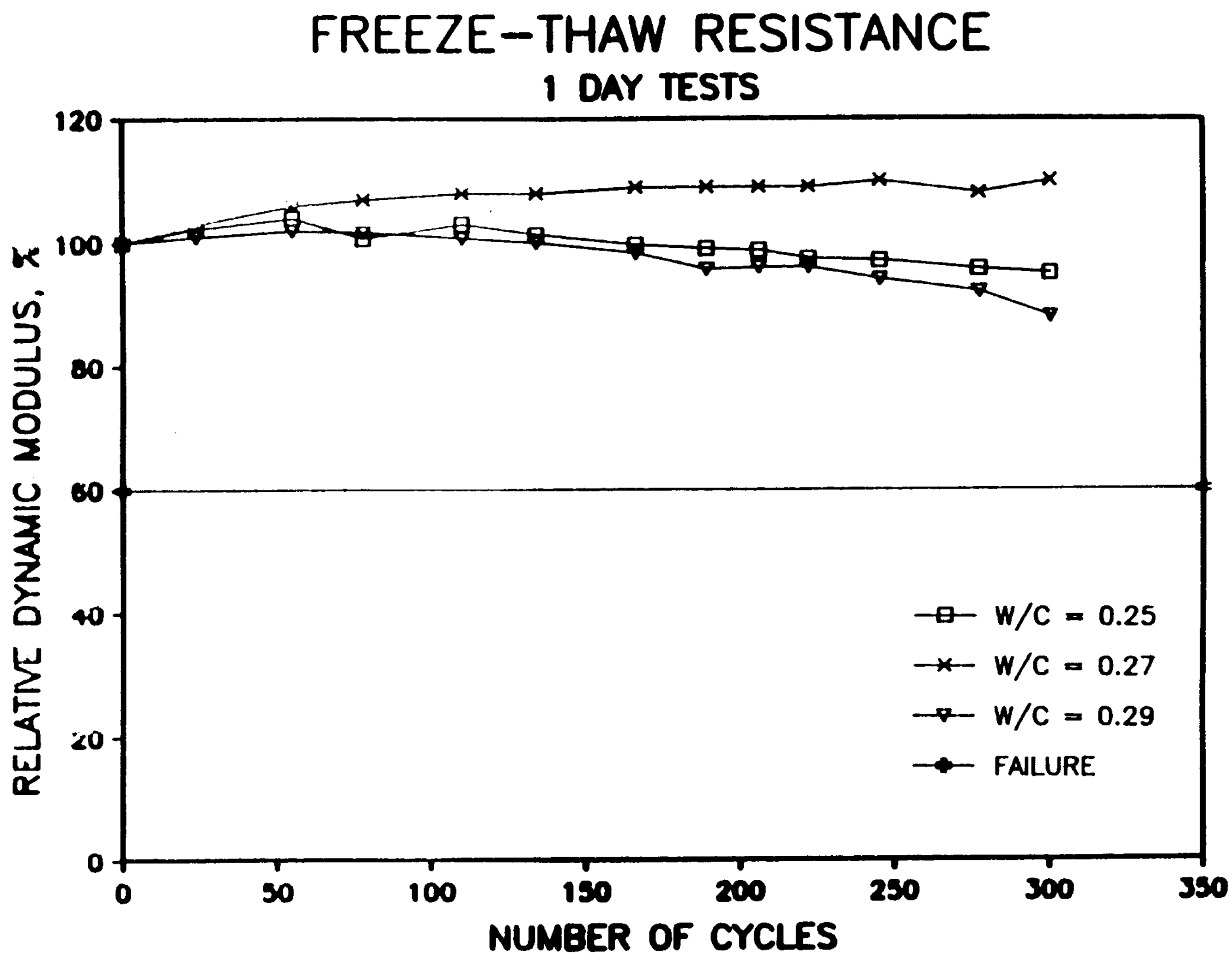

Fig. 3.50 Freeze-Thaw resistance of concrete made with Pyrament blended cement tested at one day after casting [3.55]

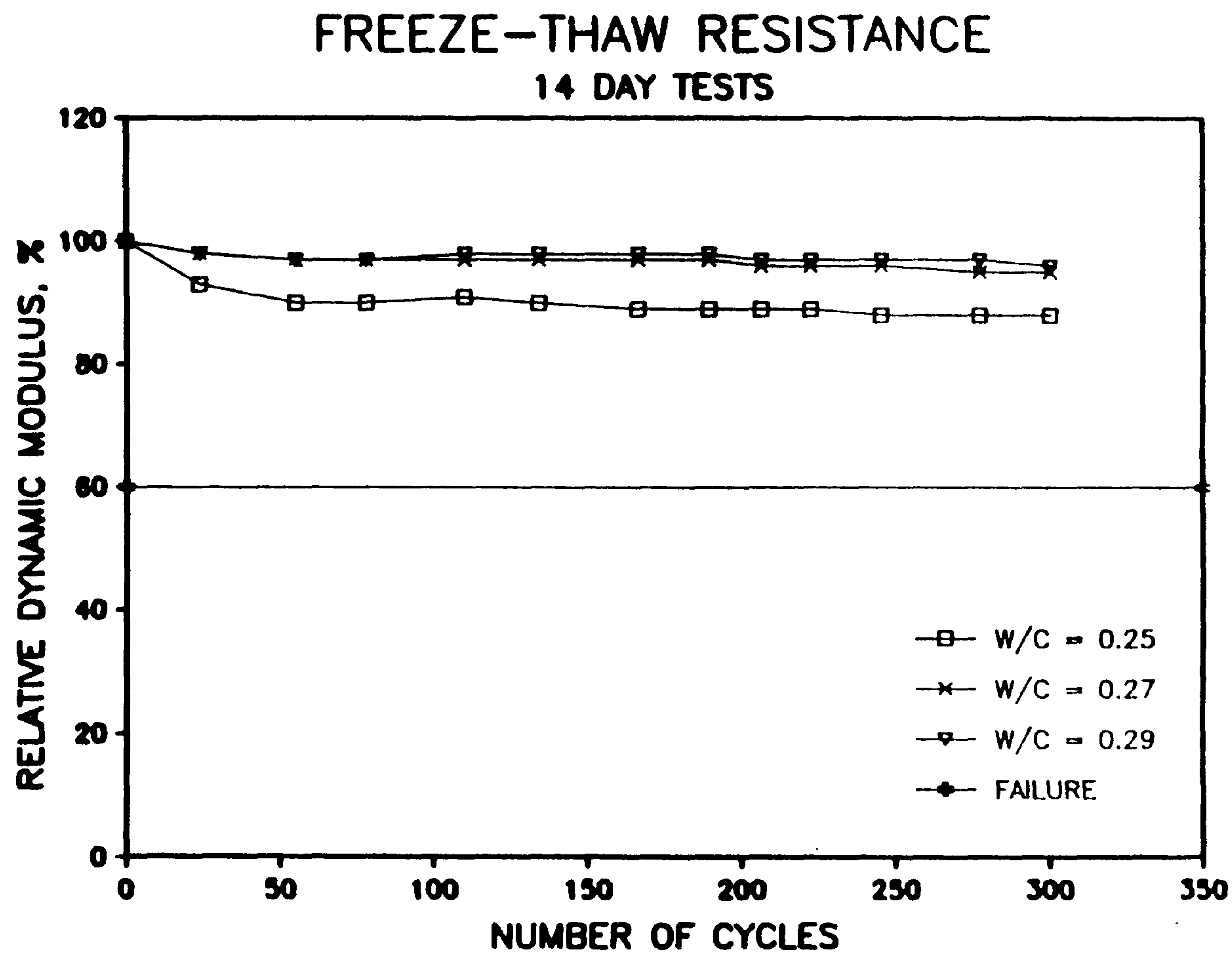

Fig. 3.51 Freeze-Thaw resistance of concrete made with Pyrament blended cement tested at 14 days after casting [3.55]

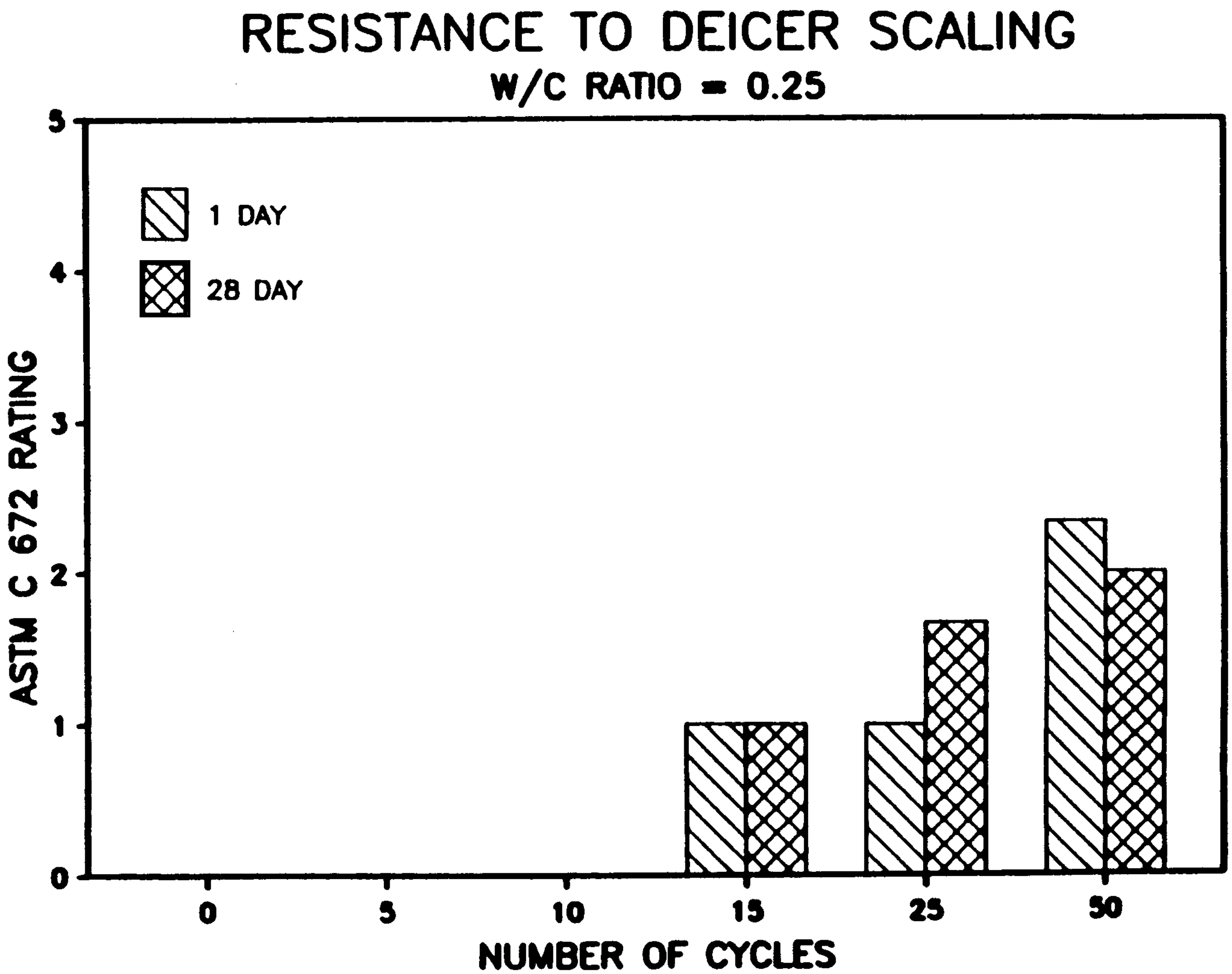

Fig. 3.52 Scaling resistance of concrete (W/C = 0.25) made with Pyrament blended cement tested starting at 1 and 28 days [3.56]

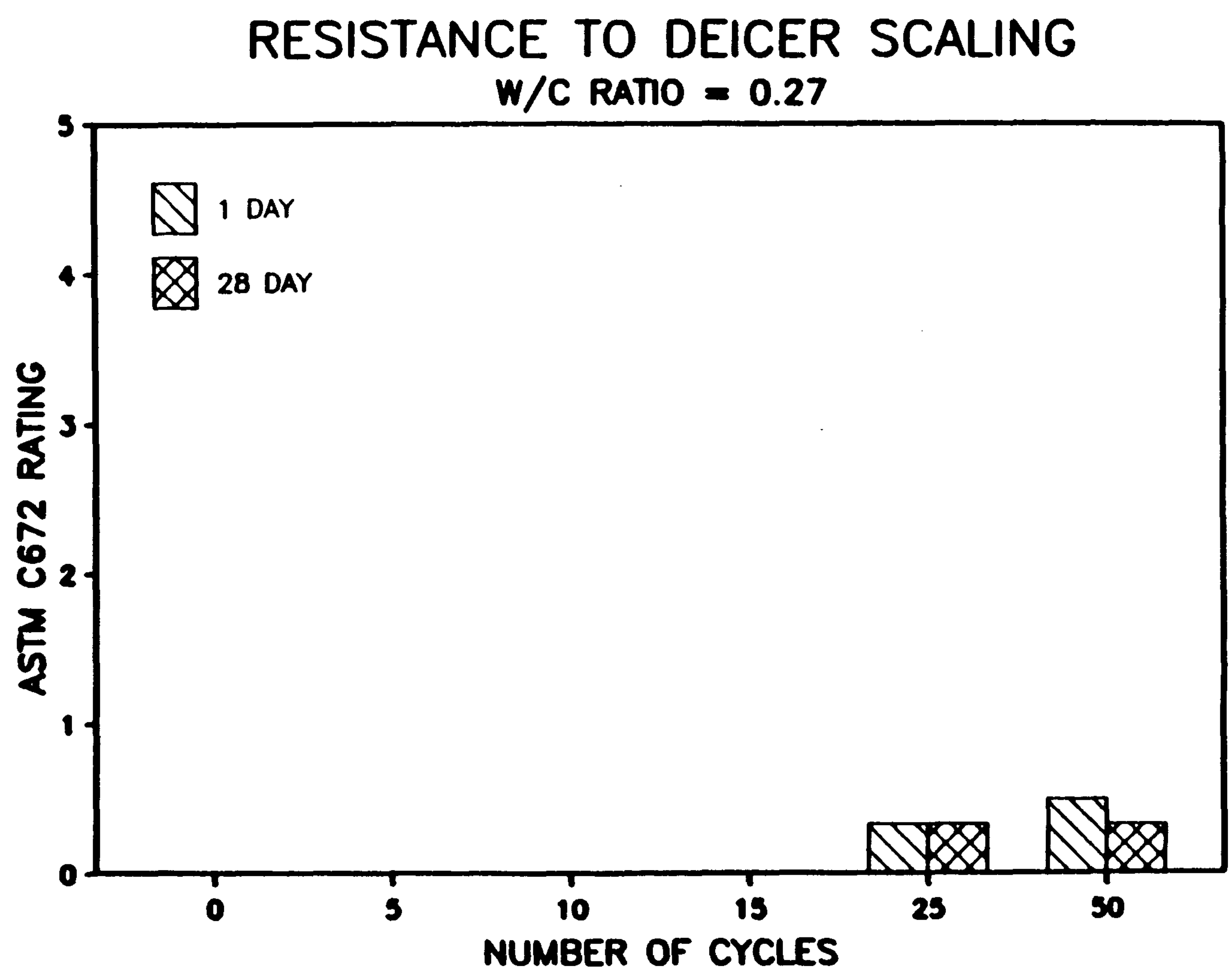

Fig. 3.53 Scaling resistance of concrete (W/C = 0.27) made with Pyrament blended cement tested starting at 1 and 28 days [3.56]

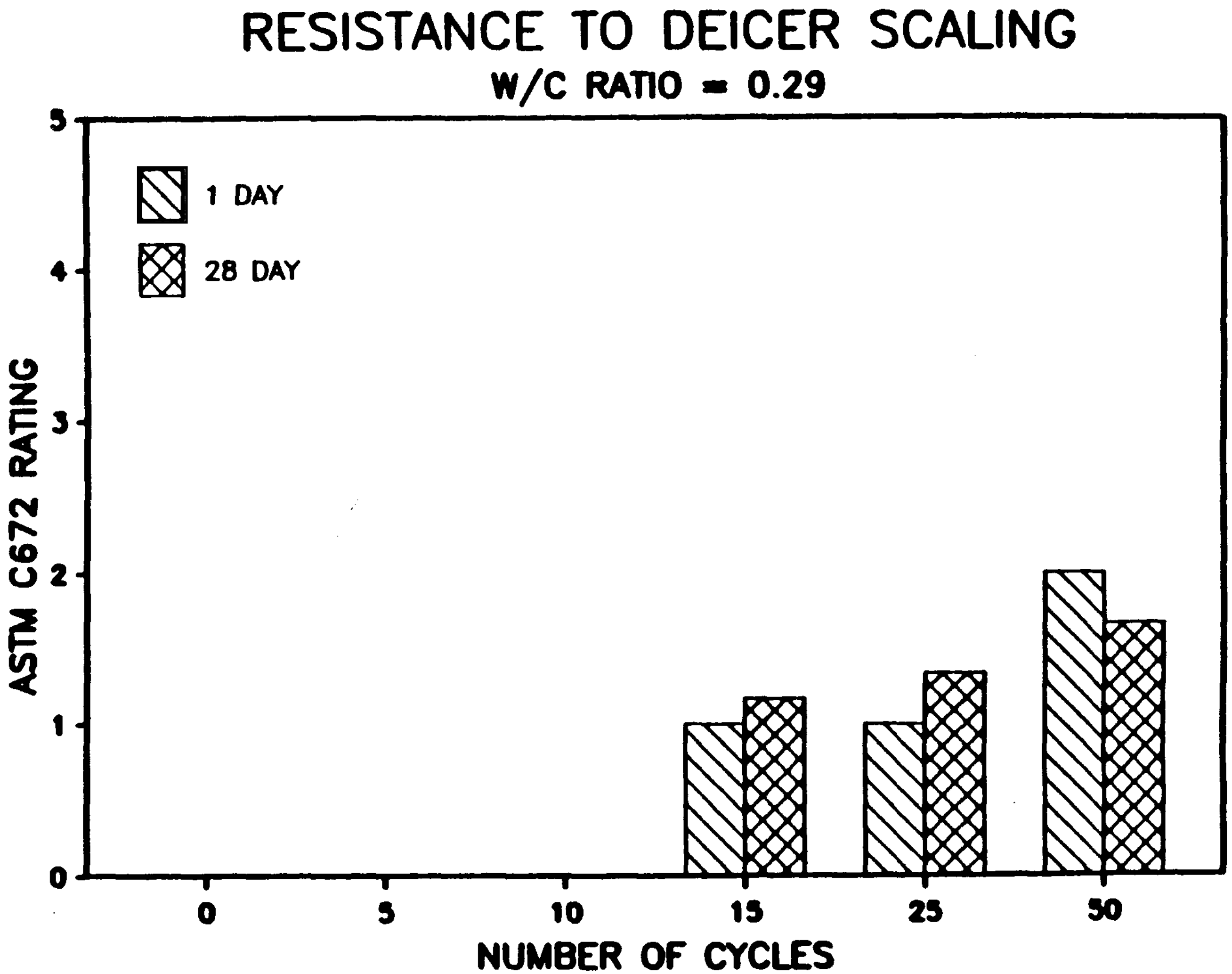

Fig. 3.54 Scaling resistance of concrete (W/C = 0.29) made with Pyrament blended cement tested starting at 1 and 28 days [3.56]

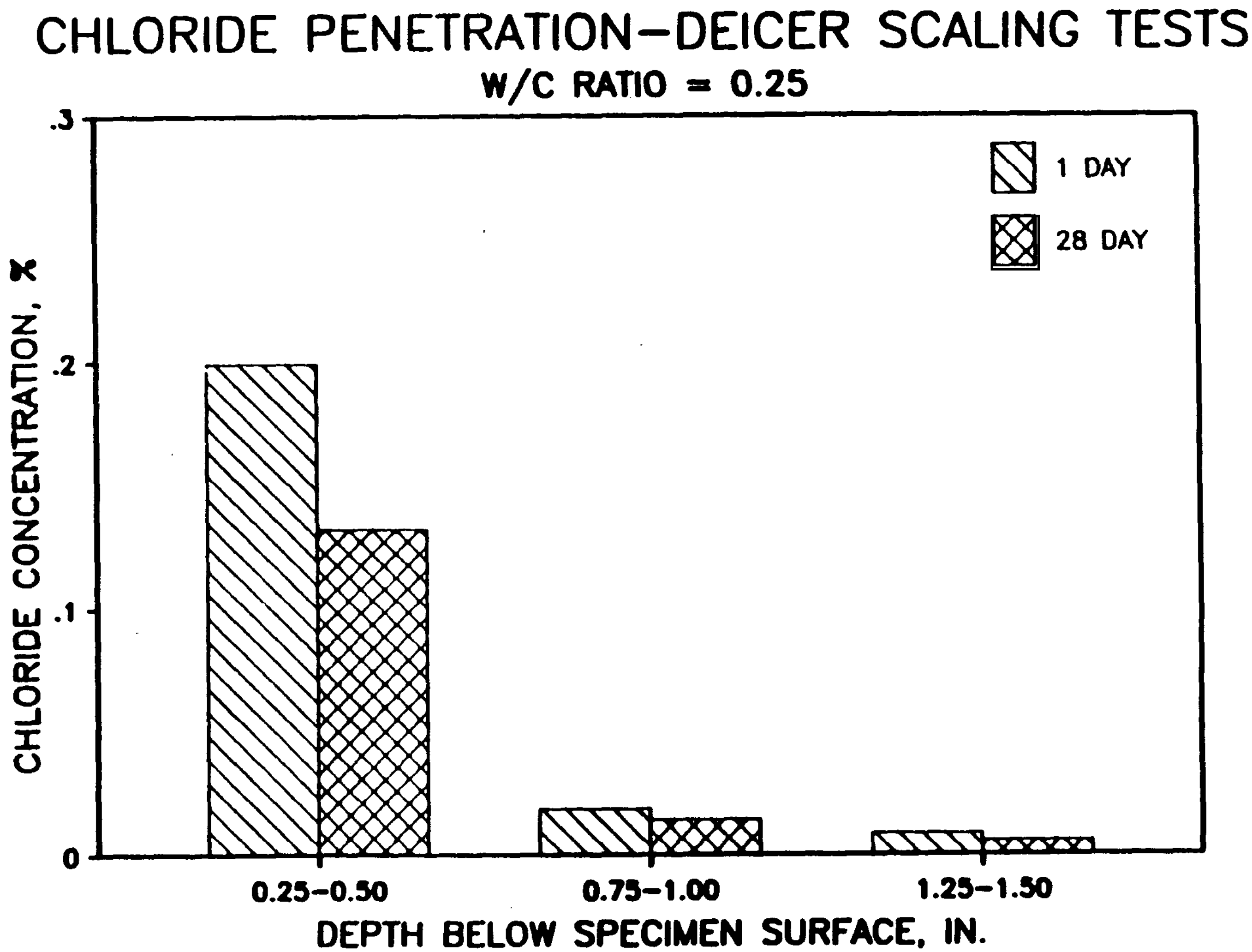

Fig. 3.55 Chloride penetration of concrete (W/C = 0.25) made with pyrament blended cement tested after 1 and 28 days of curing [3.56]

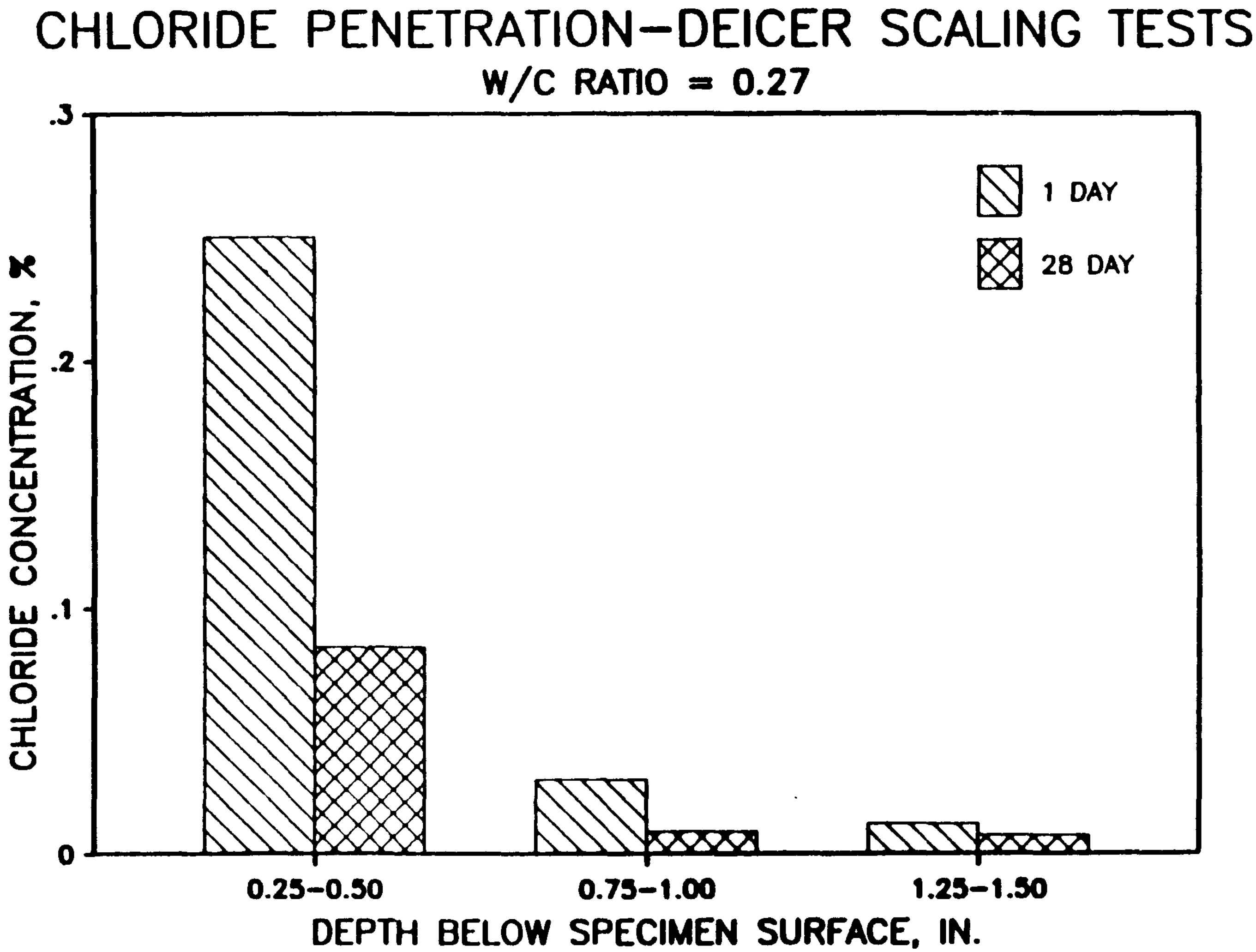

Fig. 3.56 Chloride penetration of concrete (W/C = 0.27) made with pyrament blended cement tested after 1 and 28 days of curing [3.56]

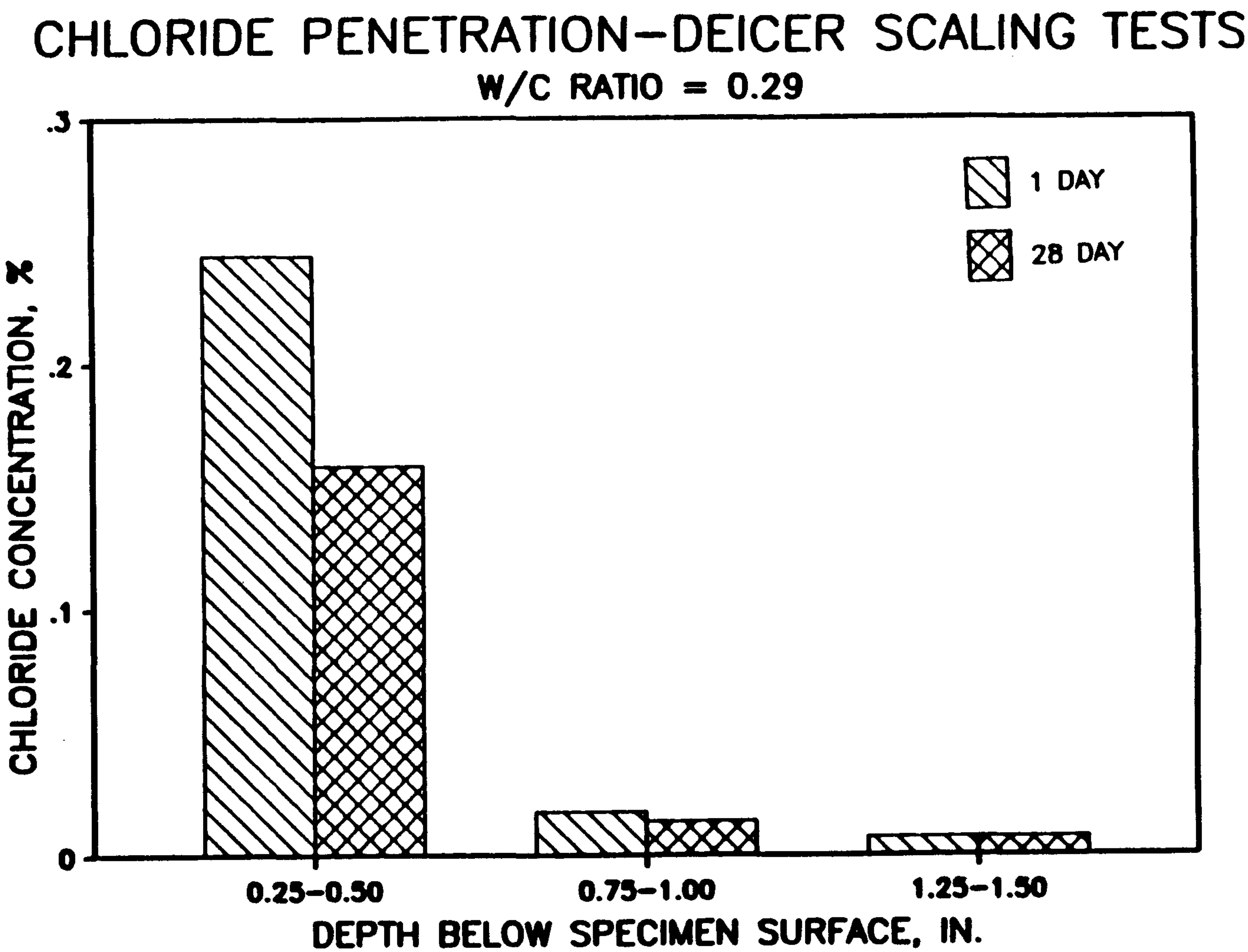

Fig. 3.57 Chloride penetration of concrete (W/C = 0.29) made with pyrament blended cement tested after 1 and 28 days of curing [3.56]

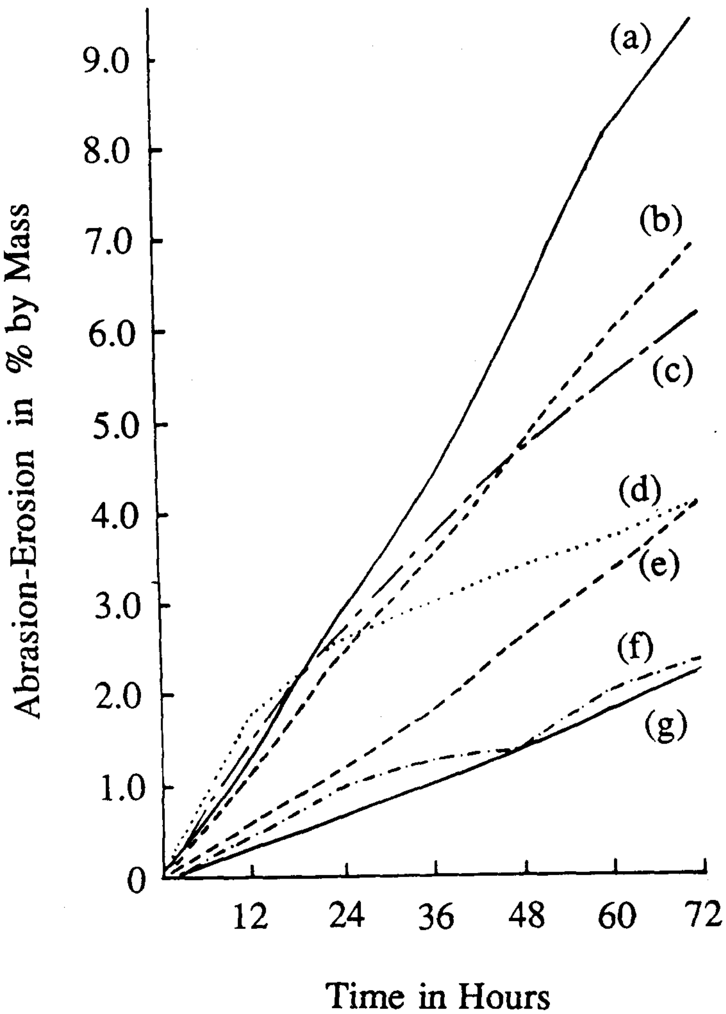

(a) Fiber-reinforced concrete from Kinzua stilling basin
(b) Conventional concrete with Pennsylvania limestone aggregate
(c) Conventional concrete with Virginia diabase aggregate
(d) Conventional concrete with Mississippi chert aggregate
(e) Average of silica fume concrete specimens prepared during actual construction
(f) Silica fume concrete with Virginia diabase aggregate
(g) Silica fume concrete with Pennsylvania limestone aggregate

Fig. 3.58 Abrasion-Erosion test data for various concretes from laboratory tests [3.100]

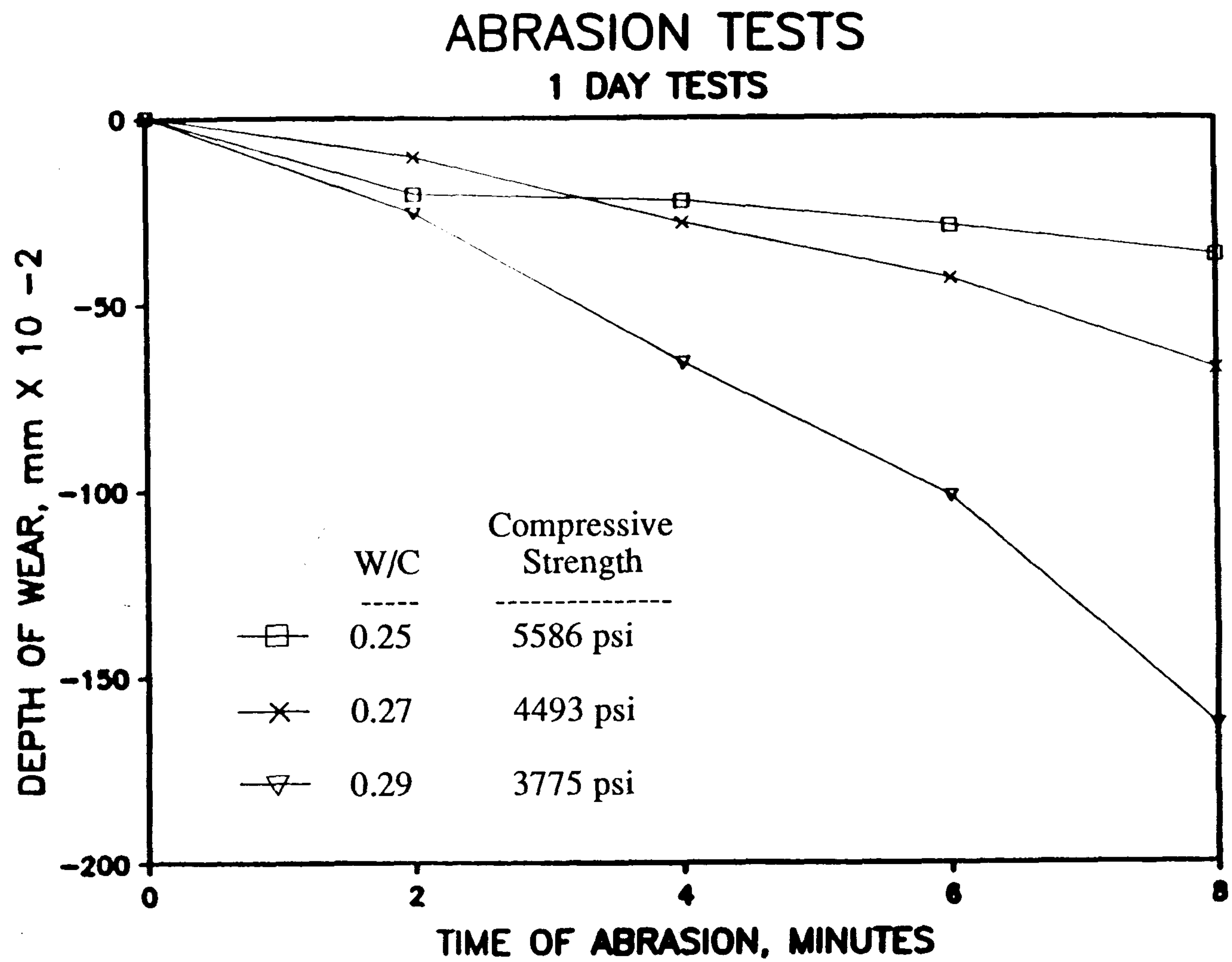

Fig. 3.59 Abrasion tests of concrete made with Pyrament blended cement at 26 hours [3.56]

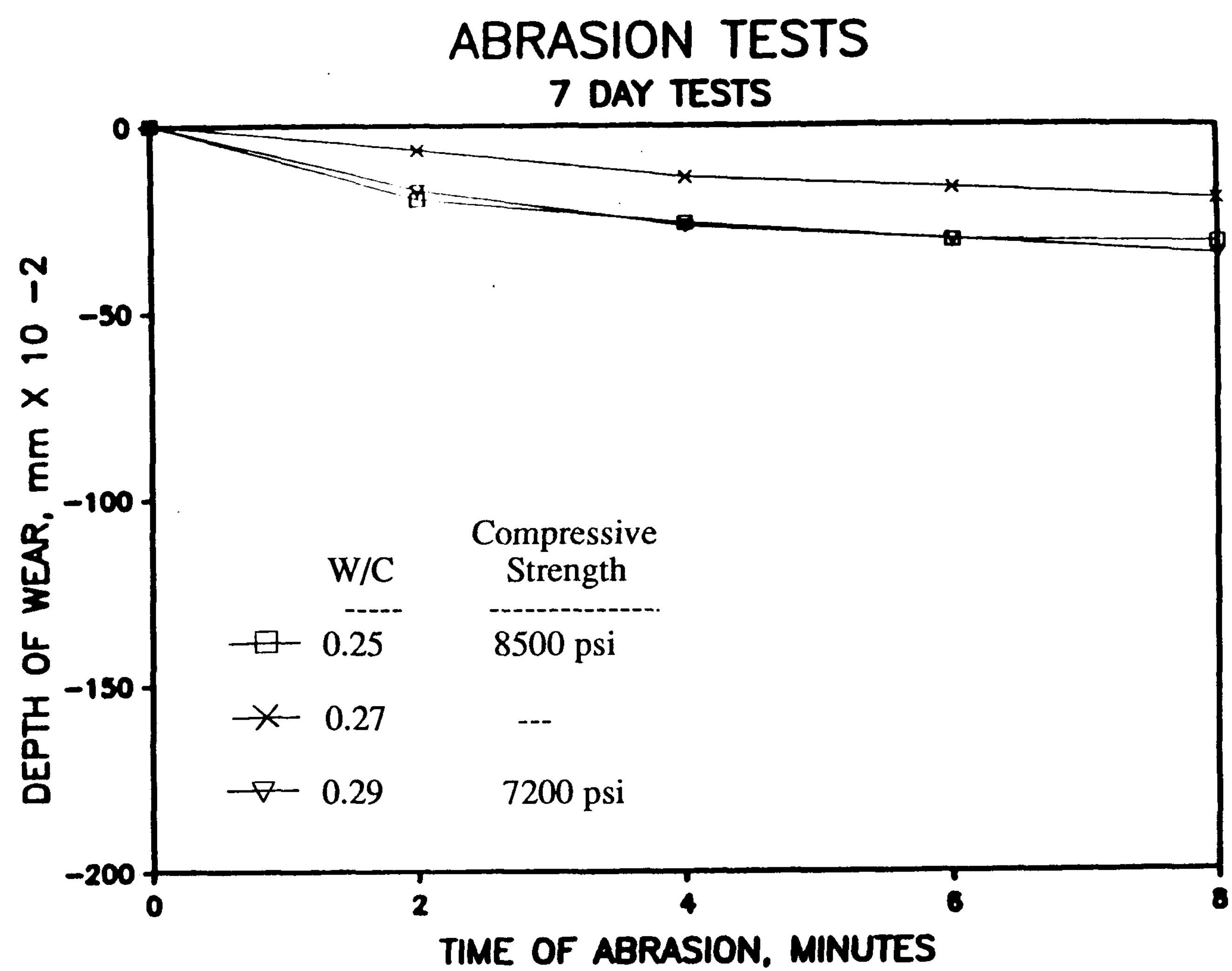

Fig. 3.60 Abrasion tests of concrete made with Pyrament blended cement at 7 days plus 2 hours [3.56]

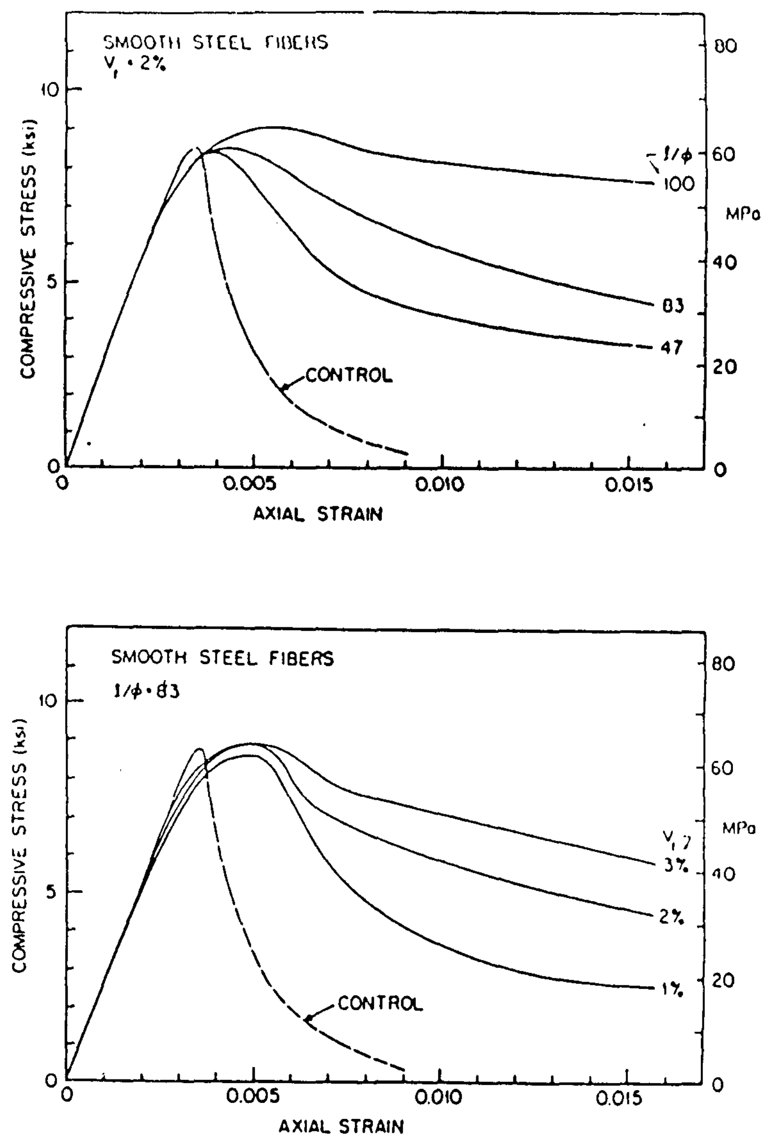

Fig. 4.1 Typical effects of volume fraction and aspect ratio of fibers on the stress-strain curve of mortar [Ref. 4.13].

(a)

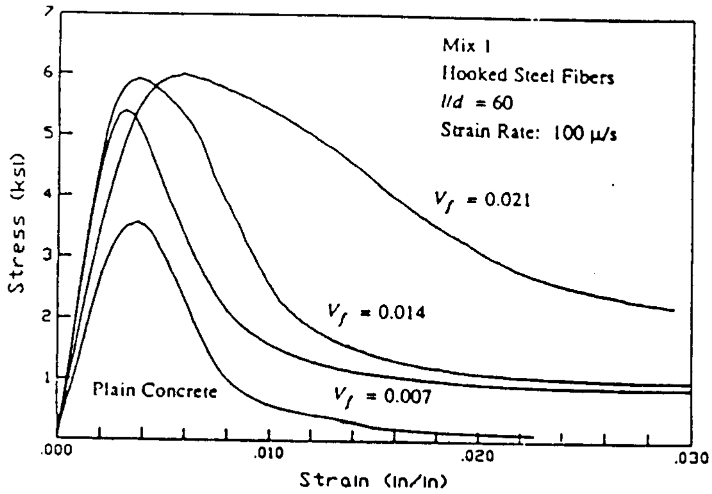

(b)

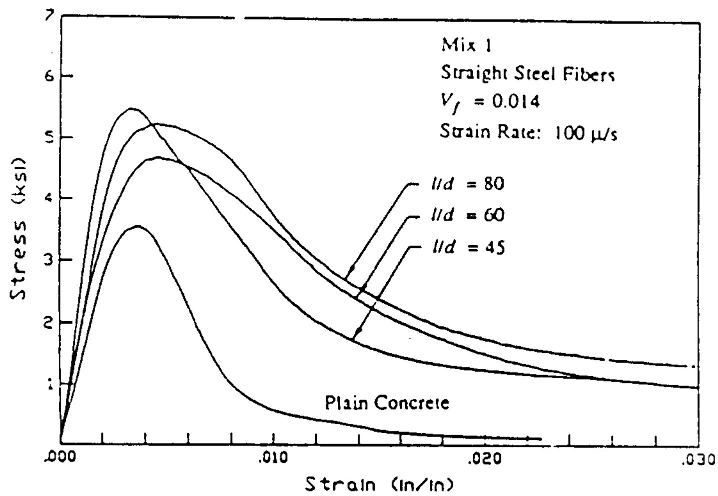

Fig. 4.2 Stress-strain response of FRC under compression. (a) hooked steel fibers; (b) straight steel fibers [Ref. 4.40].

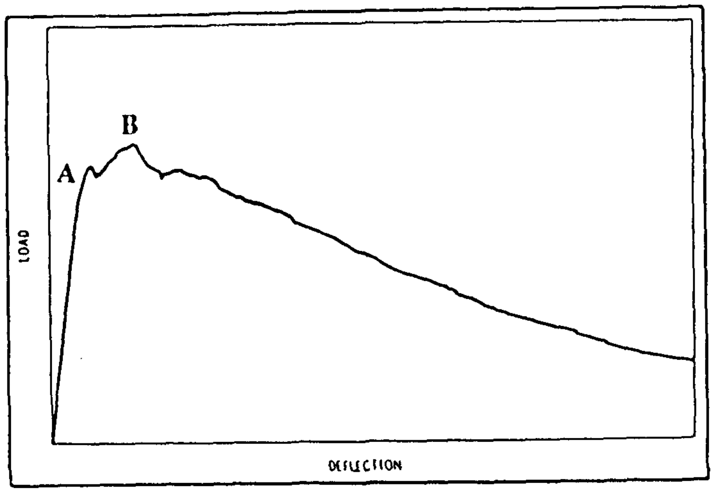

Fig. 4.3 Schematic load-deflection diagrams of FRC.

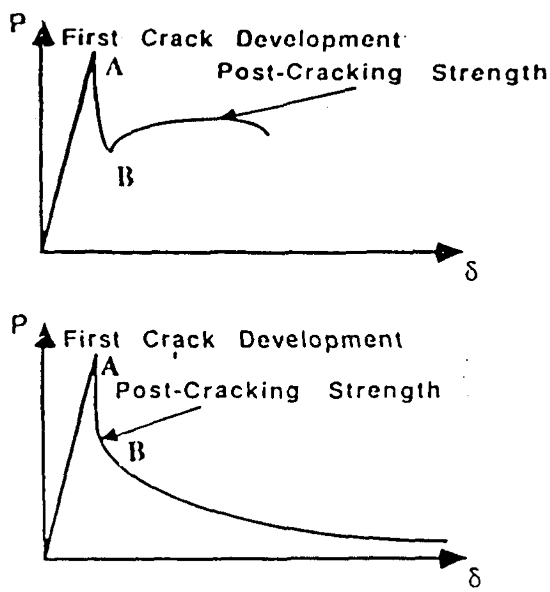

Fig. 4.4 Typical load-deflection curves of FRC beams with low volume fraction of fibers.

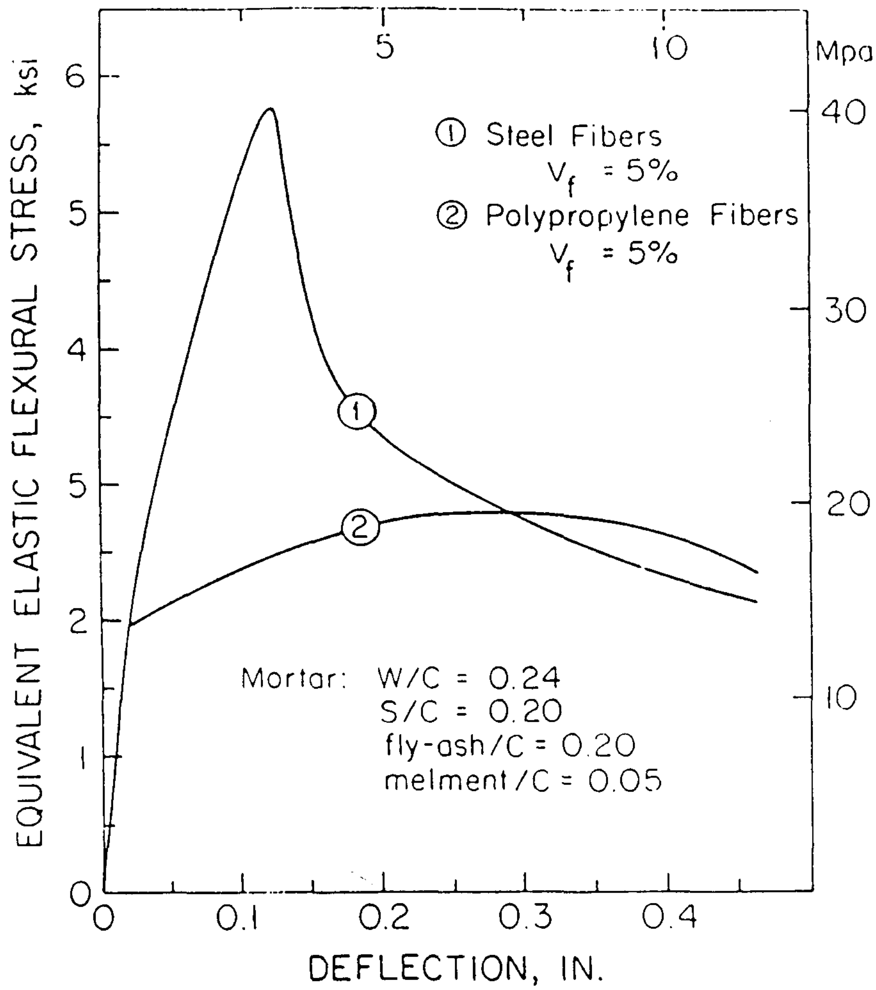

Fig. 4.5 Experimentally observed load-deflection curves of steel and polypropylene fiber reinforced concrete beams [Ref. 4.30].

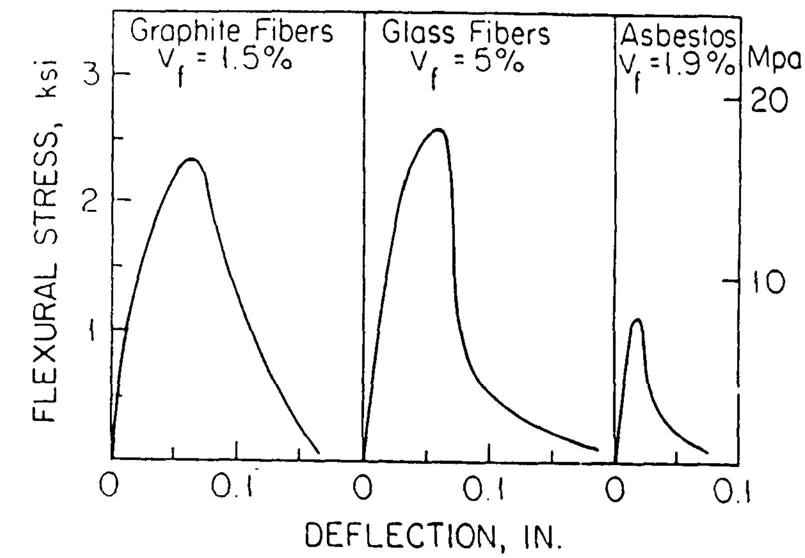

Fig. 4.6 Experimentally observed load-deflection curves for different types of fibers [Ref. 4.30].

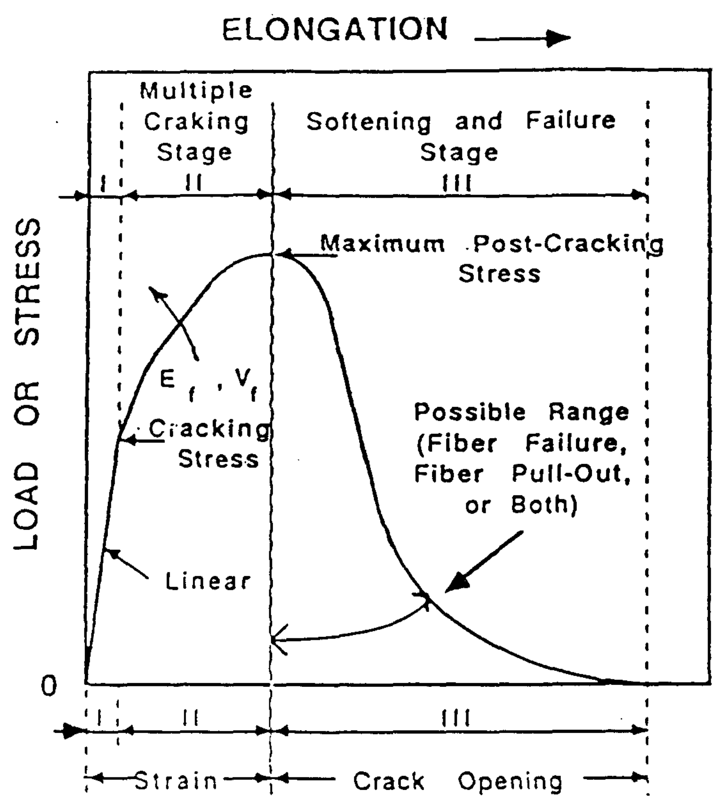

Fig. 4.7 Typical load-elongation response in tension of high performance FRC composite as SIFCON [Ref. 4.30].

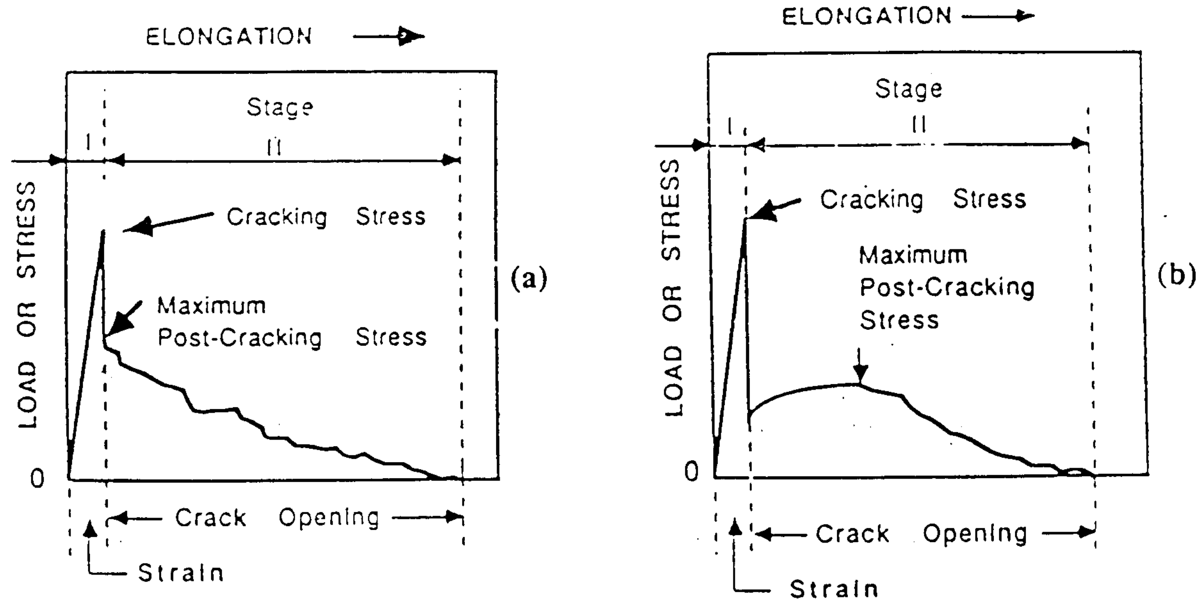

Fig. 4.8 Typical load-elongation response in tension of fiber reinforced concrete: a) using premixed steel fibers, and b) using premixed polypropylene fibers [Ref. 4.30].

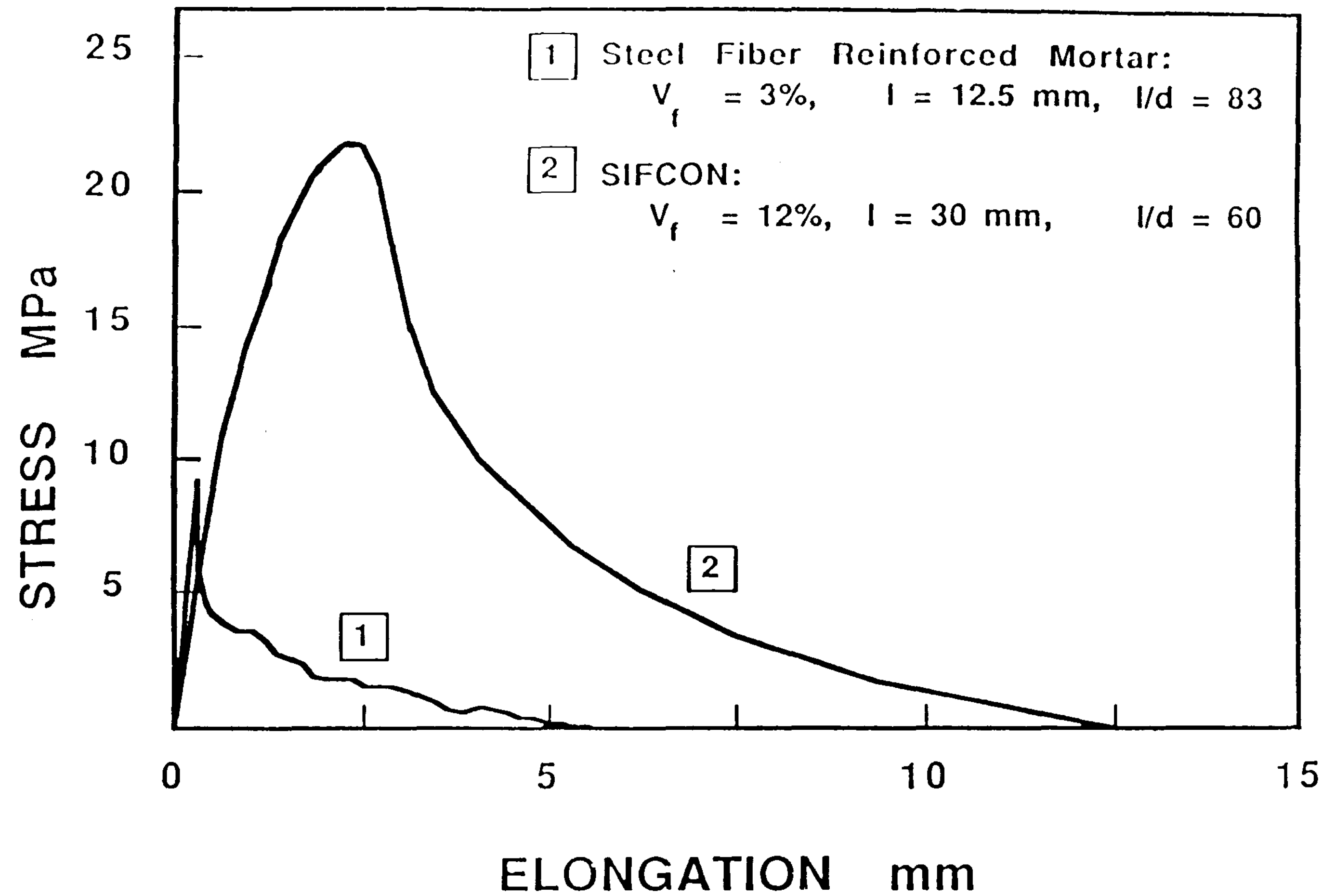

Fig. 4.9 Comparison of experimentally observed stress-elongation curves of steel fiber reinforced mortar and SIFCON [Ref. 4.30].

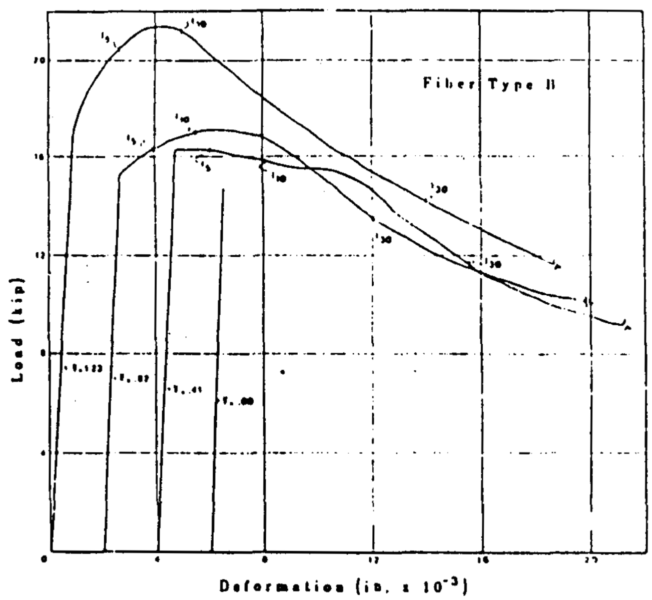

Fig. 4.10 Load-deformation curves under splitting tensile stress [Ref. 4.37].

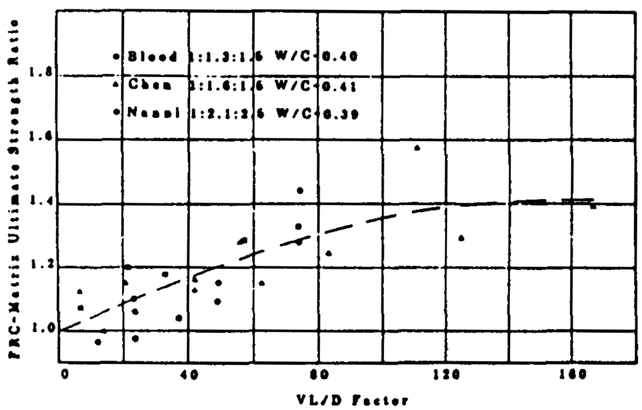

Fig. 4.11 Variation of ultimate splitting tensile strength ratio of FRC with fiber reinforcing index [Ref. 4.37].

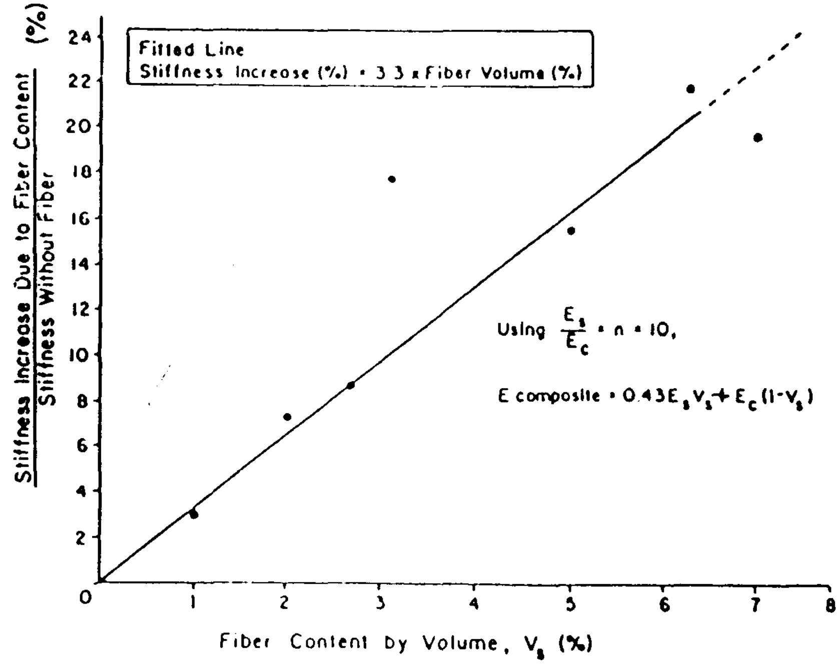

Fig. 4.12 Increase of undamaged stiffness versus steel fiber content [Ref. 4.42].

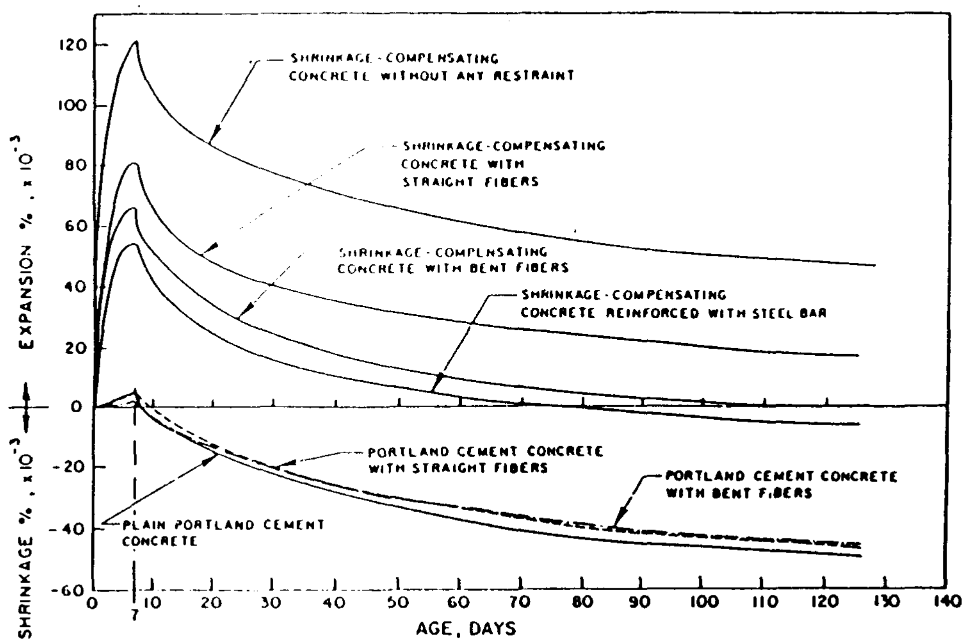

Fig. 4.13 Expansion and shrinkage behavior of shrinkage-compensating and portland cement concrete [Ref. 4.41].

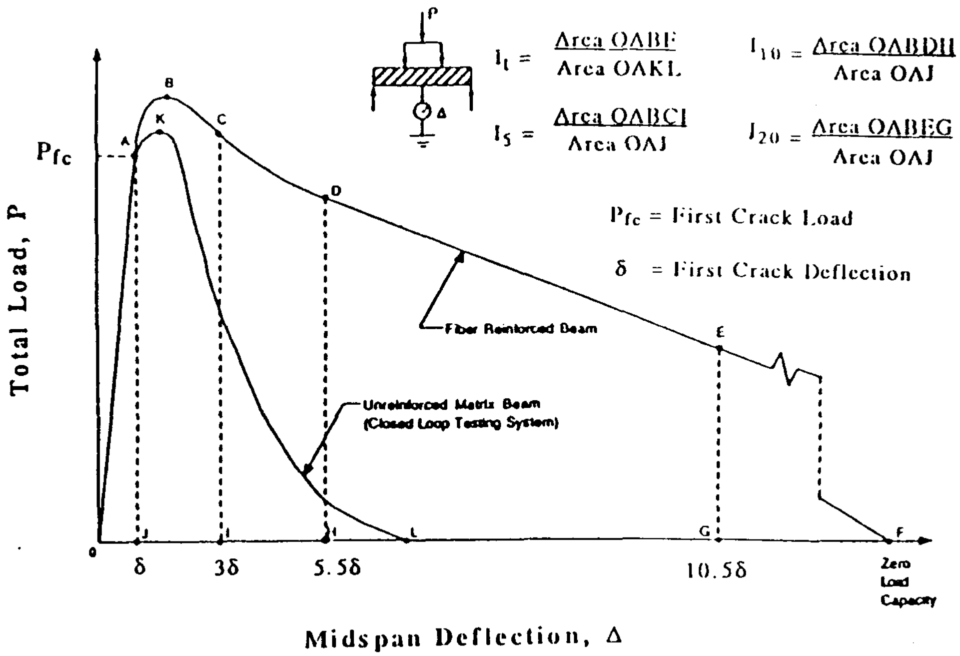

Fig. 4.14 Toughness indexes from flexural load-deflection diagram.

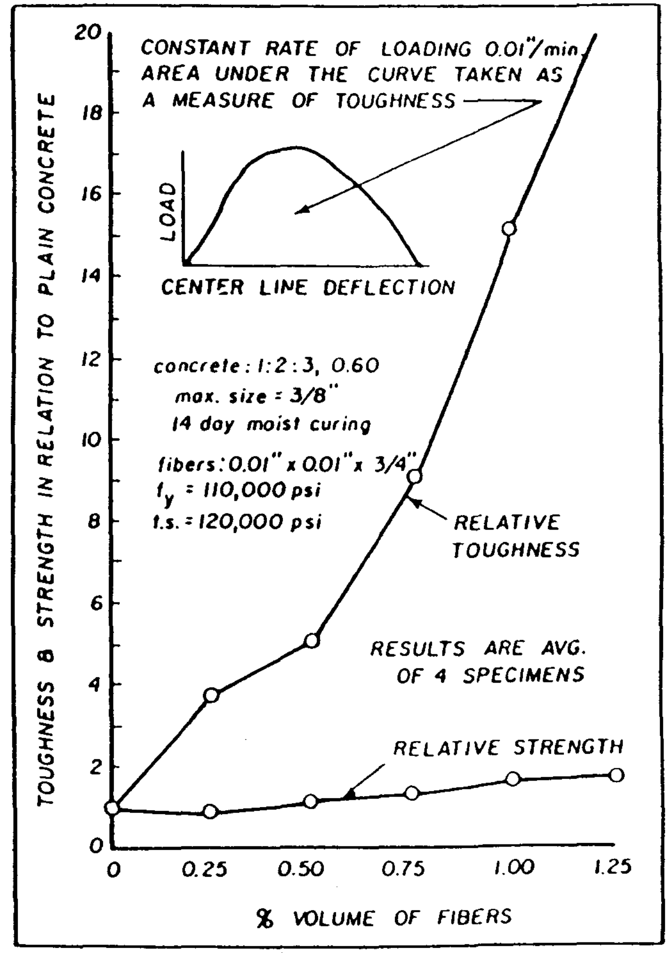

Fig. 4.15 Effect of volume of fiber on toughness in flexure [Ref. 4.52].

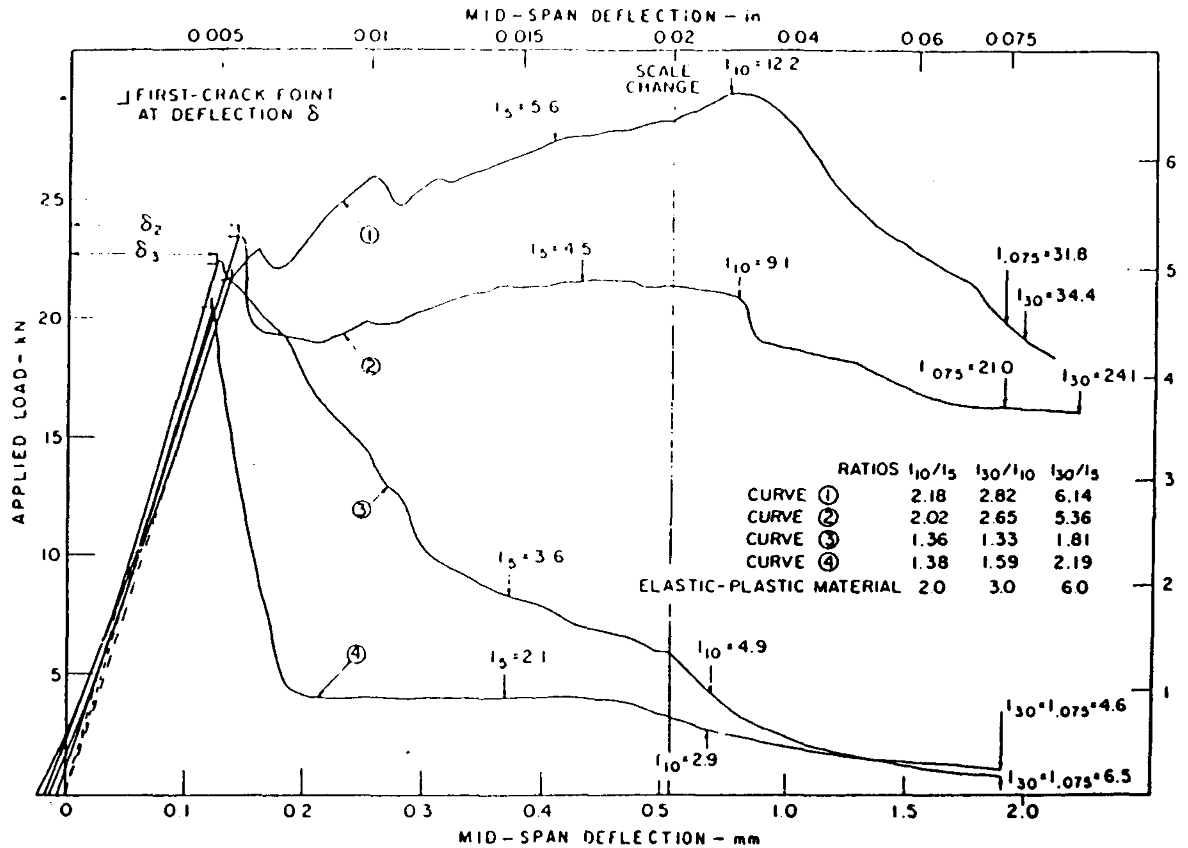

Fig. 4.16 Load-deflection curves illustrating the range of material behavior possible for four mixes containing various amounts and types of fibers [Ref. 4.22].

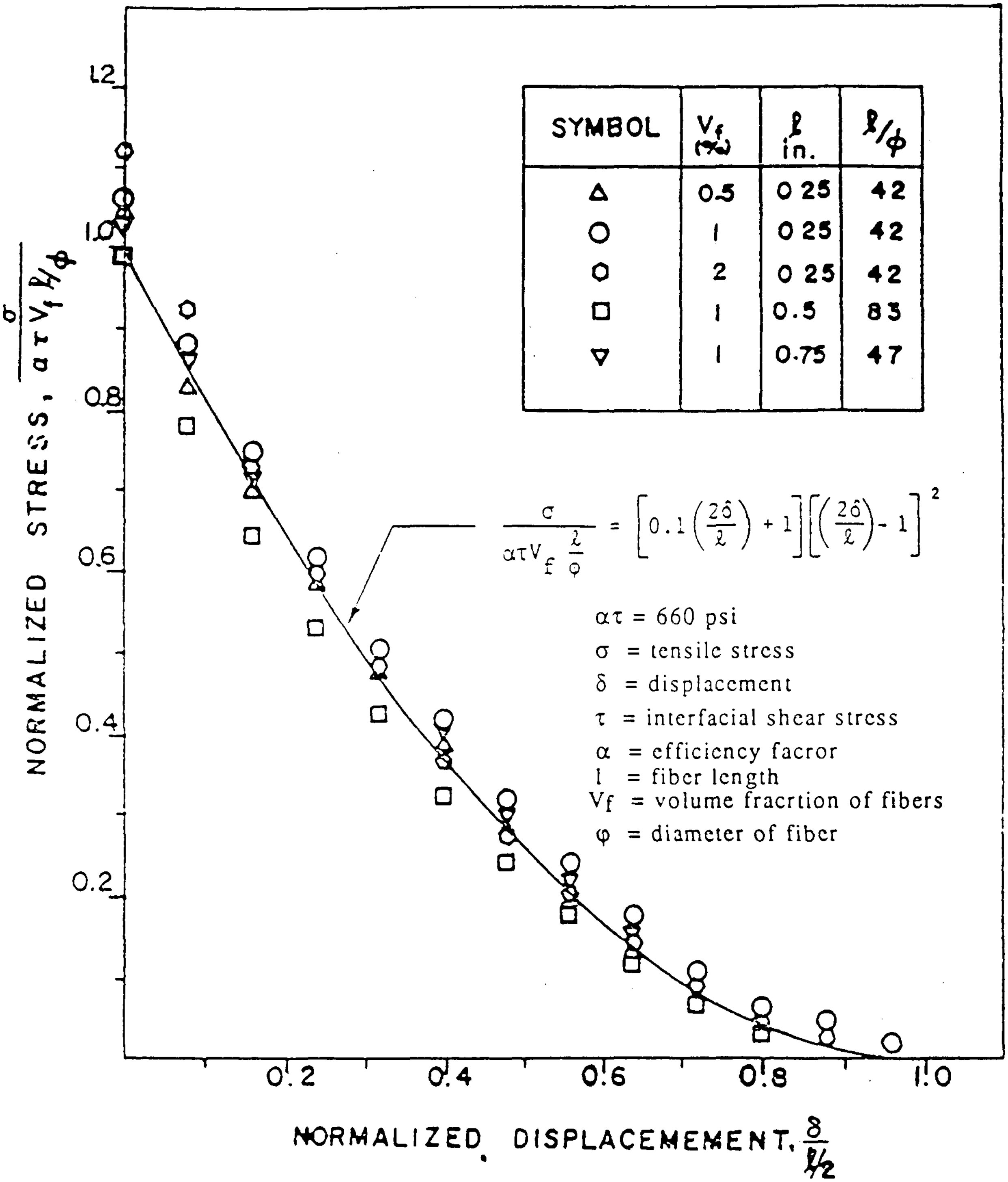

Fig. 4.17 Normalized stress-displacement law of steel fiber reinforced mortar (all cases) [Ref. 4.60].

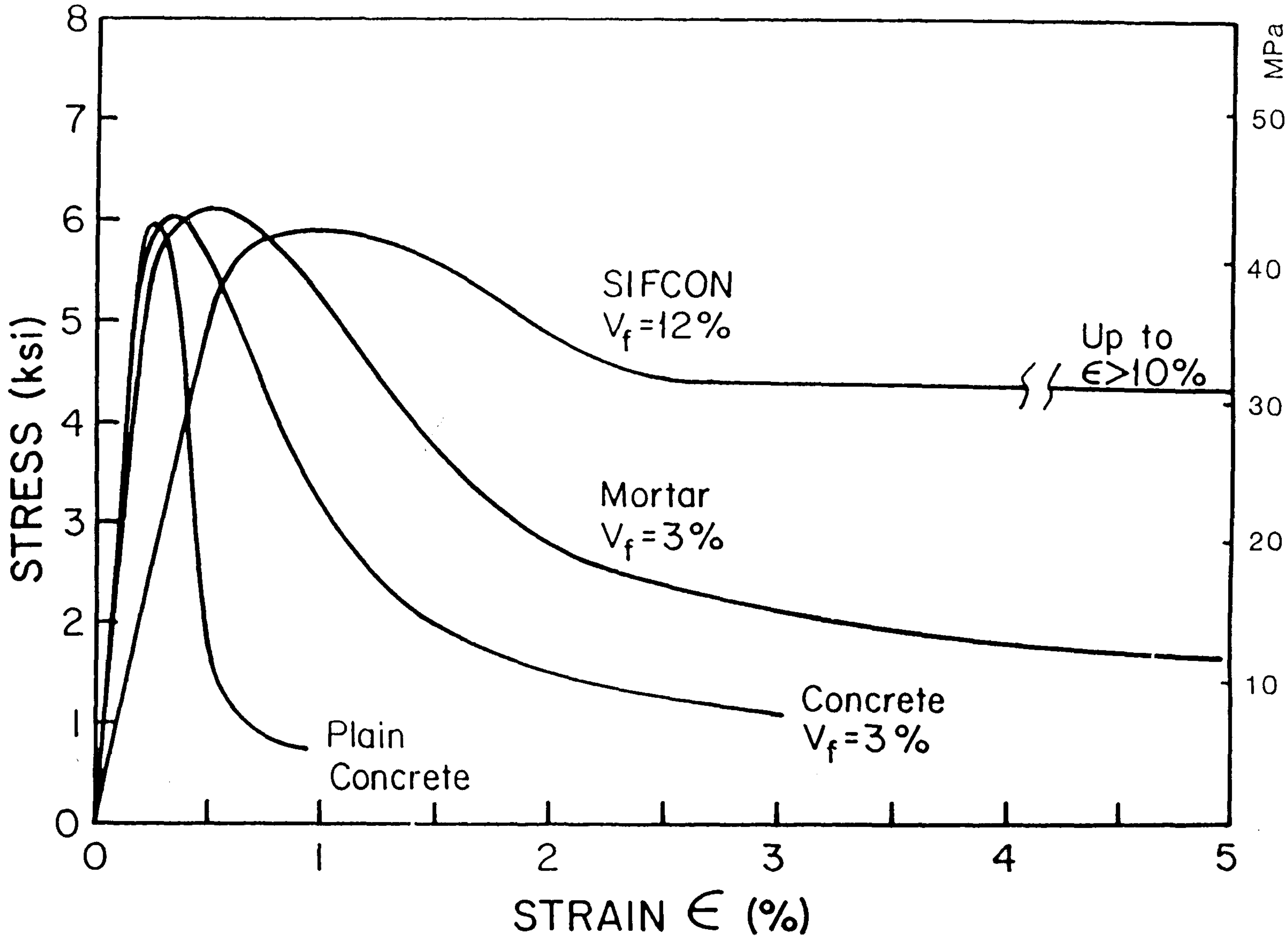

Fig. 4.18 Comparison of experimentally observed stress-strain curves of plain concrete, fiber reinforced concrete and mortar, and SIFCON.

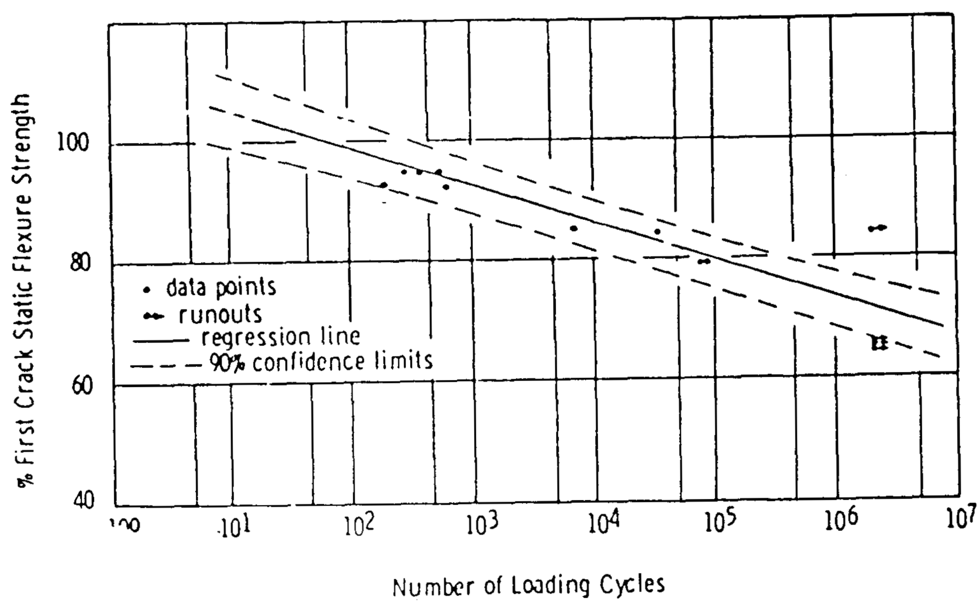

Fig. 4.19 Fatigue strength for complete reversal of loading using 2.98% by volume of 0.5x0.0066in. fibers [Ref. 4.7].

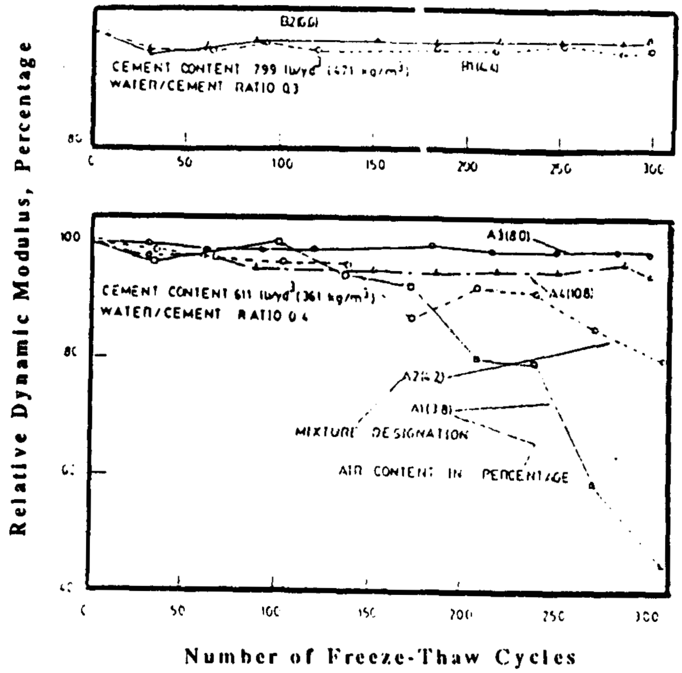

Fig. 4.20 Influence of air content on relative dynamic modulus, fiber content 75 pcy (45.5 kg/m³) [Ref. 4.5].

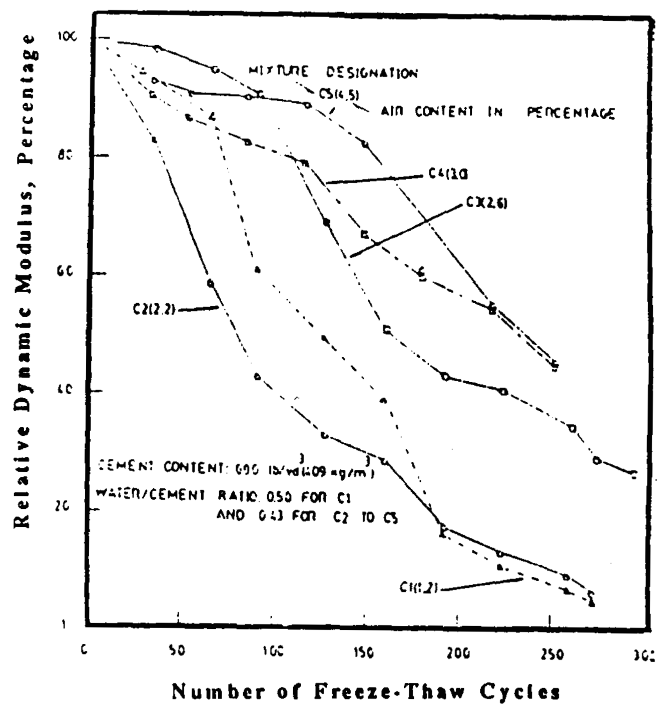

Fig. 4.21 Influence of air content on relative dynamic modulus, fiber content 100 pcy (59 kg/m³) [Ref. 4.5].